

## Durham E-Theses

---

### *The measurement of the earth tide and regional heterogeneity due to the ocean tide*

Bower, Donald R.

#### How to cite:

---

Bower, Donald R. (1971) *The measurement of the earth tide and regional heterogeneity due to the ocean tide*, Durham theses, Durham University. Available at Durham E-Theses Online:  
<http://etheses.dur.ac.uk/8660/>

#### Use policy

---

The full-text may be used and/or reproduced, and given to third parties in any format or medium, without prior permission or charge, for personal research or study, educational, or not-for-profit purposes provided that:

- a full bibliographic reference is made to the original source
- a [link](#) is made to the metadata record in Durham E-Theses
- the full-text is not changed in any way

The full-text must not be sold in any format or medium without the formal permission of the copyright holders.

Please consult the [full Durham E-Theses policy](#) for further details.

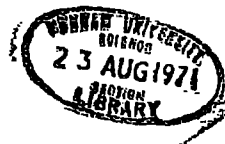
THE MEASUREMENT OF THE EARTH TIDE  
and  
REGIONAL HETEROGENEITY DUE TO THE OCEAN TIDE

A thesis submitted for the degree of Doctor of Philosophy in the  
University of Durham

Donald R. Bower

The Graduate Society

July 1971



## SUMMARY

The tide-producing force is derived as a sum of harmonic terms and directly as a function of time. The Love Numbers are then introduced to relate the tide-producing forces to the earth tide and in particular to changes in the amplitude and direction (tilt) of gravity as measured at the surface of the earth. The classical problem of earth-tide research, the determination of the Love Numbers, is complicated by the surface and body-force effects of the ocean tide. The present thesis is concerned with evaluating these effects with a view to: 1. Determining true values of the earth tide uncontaminated by ocean-tide effects. 2. Investigating the use of the ocean tide as a probe for determining the mechanical characteristics of the crust and mantle.

A method is introduced for representing the ocean tide by  $n$ -sided surface polygons of constant tidal amplitude and phase, and for determining the gravitational attraction of these polygons at any point on a spherical earth. The Boussinesq solution for elastic yielding of an infinite halfspace is then used with this ocean-tide representation to predict the ocean tide loading effect on tilt throughout Western Europe. These predictions confirm the main features of observed spatial variations and encourage a more accurate treatment. The Slichter-Caputo solution for a 2-shell earth is then adapted to the problem and preliminary results are obtained for the effect on tilt of distant ocean tides including the body-force components of the effect. The

Longman solution for a Gutenberg earth is dealt with next and a method of extrapolation for determining results in the range  $0-30^\circ$  is introduced. A computer program is described for implementing the prediction of world-wide tilt and gravity tides when provided with the Longman solution, or any other solution expressed as a Green's function, and ocean-tide data in the form of polygons. In general, predictions are found to be consistent with world-wide coastal observations and with inland observations in North America. Predictions for the gravity effect at mid-European and mid-Asian sites are not consistent with observations; likely due to inaccurate ocean tide data for the Arctic and Indian Oceans. Observations of tilt throughout the same area show marked regional variations which can not be due to ocean-tide effect and may reflect local hydrological effects.

The establishment of a tiltmeter site is described and several computer programs used in the analyses are presented. The development and testing of a new type, sensitive hydrostatic tiltmeter is described.

## ACKNOWLEDGEMENTS

I wish to thank Professor G. M. Brown for providing facilities for this research at the University. I would also like to acknowledge the support of the Earth Physics Branch of the Dept of Energy, Mines and Resources (Canada) and in particular that of Dr M.J.S. Innes, Chief of the Gravity Division, who encouraged me to undertake this study.

I am especially grateful to my supervisor Dr M.H.P. Bott for his expert advice and his kind cooperation in all matters. His method of evaluating magnetic anomalies due to finite three dimensional bodies is the basis of the method used here for determining the gravitational attraction of the ocean tide.

I am indebted to the Weardale Lead Co. Ltd. for the underground facilities in the Redburn Mine at Rookhope. The manager Mr H. Green facilitated the preparation of a suitable tiltmeter site and tolerated the inconveniences brought about because of its presence. The tiltmeter installation could not have been kept operating throughout the two year period of use, without the active assistance and cooperation of individual miners, too numerous to mention, and in particular of the foreman Mr T.I. Martin.

Several members of the technical staff of the department were particularly helpful. Mr Dave Asbery carried out repairs on much of the electronic equipment. Mr W. Teasdale did the machine work in adapting the water-tube tiltmeters to transducers. I am very much indebted to Mr M.S. Macconachie, who worked closely with me during my

entire period at the University, for much hard work during the installation phase and for many helpful suggestions.

Finally, I would like to express my appreciation for the stimulation provided by close association with Dr A. Lambert and Mr C.R. Beaumont during the last few months of this study. Chris Beaumont kindly made available to me his results for the Green's function near the load calculated on the basis of a finite-element model of the crust.

I am grateful for financial assistance from the Government of Canada during my stay at Durham, and for a grant provided by the Royal Society for the purpose of developing the water-tube tiltmeter.

CONTENTS

CHAPTER 1	INTRODUCTION
CHAPTER 2	THE THEORETICAL EARTH TIDE
2-1	The Tide-Producing Force
2-1-1	Calculation By The Harmonic Method
2-1-2	Calculation By The Direct Method
2-2	The Love Numbers and the Gravimetric and Diminishing factors
CHAPTER 3	THE OCEAN-TIDE EFFECT
3-1	Introduction
3-2	The Effect On An Infinite Half-Space Earth
3-2-1	The Attraction Of The Ocean Tide
3-2-2	Program PRESS
3-2-3	Discussion and Results
3-3	The Effect On A 2-Shell Earth
3-3-1	Program CAPS
3-4	The Effect On A Gutenberg-Model Earth
3-4-1	Program LONG
3-5	Discussion
3-6	Effects Within 30 Degrees of the Load
3-6-1	The Burmister Problem
3-6-2	Comparison with other results
CHAPTER 4	PREDICTION OF THE OCEAN-TIDE EFFECT
4-1	Introduction
4-2	The Ocean-Tide Data
4-3	Program GLOBL
4-3-1	Refinement for Computing Local Effects

CHAPTER 5 THE MEASUREMENTS

5-1 The Horizontal Pendulum

5-2 Recording the Pendulum Measurement

5-3 Preparation of the Rookhope Site

5-4 Operation of the Rookhope Site

5-4-1 Initial Setting Up

5-4-2 Summary

CHAPTER 6 DATA ANALYSIS

6-1 Editing the Data

6-2 The Fourier Method

6-3 The Least Squares Method

6-3-1 Program JANET

6-4 Results

6-4-1 Rookhope Results

6-4-2 Ottawa Results

CHAPTER 7 SPATIAL VARIATIONS IN WORLD-WIDE OBSERVATIONS

7-1 Introduction

7-2 Gravity and Tilt Measurements in Britain

7-2-1 Bidston

7-2-2 Winsford

7-2-3 Llanrwst

7-2-4 Rookhope

7-2-5 A Suggested Site

7-3 Tilt Measurements in Belgium

7-3-1 The Influence of Hydrology

7-4 Gravity Measurements in Western Europe



(iii)

7-5 North American Measurements

7-5-1 Gravity Along a Trans-U.S.A  
Profile

7-5-2 Gravity at Ottawa

7-5-3 Tilt Measurements

7-6 Measurements in Africa, Asia and India

CHAPTER 8 DEVELOPMENT OF A SENSITIVE HYDROSTATIC TILTMETER

8-1 Introduction

8-2 Description of the Apparatus

8-3 Laboratory Tests and Modifications.

8-4 Results

8-5 Conclusions

CHAPTER 9 CONCLUSIONS

APPENDIX I Program JANET

APPENDIX II Program ROBIN

APPENDIX III Program PRESS

APPENDIX IV Program CAPS

APPENDIX V Program LONG

APPENDIX VI Program GLOBL

APPENDIX VII Program BETTY

APPENDIX VIII World-wide Tidal Data File

APPENDIX IX Deformation due to the  $n=1$  term in the series  
representing a surface or body force

REFERENCES

LIST OF ILLUSTRATIONS

- 2-1 Construction for deriving the expression for the attraction of the Moon
- 3-1 The function  $\epsilon$  near the load.
- 3-2 Ocean-tide contours near Britain (region 0)
- 3-3 Construction for determining the attraction of n-sided polygon
- 3-4 Elastic depression due to ocean-tide loading round Britain
- 3-5 The function  $T_2/T_3$  for three models
- 3-6 Comparison of elastic depression on Boussinesq and CAPS models
- 3-7 The surface-load function for  $p=0.99$
- 3-8 The load-deformation coefficients  $H_n'$  and  $K_n'$  showing the extrapolation used for  $n>40$
- 3-9 Comparison of elastic depression for three models
- 3-10 Comparison of gravity perturbation for three models
- 3-11 Elastic depression near the load: results for CAPS and LONG
- 3-12 Comparison of total tilts near the load: results for CAPS and LONG
- 3-13 Comparison of tilt ratios near the load: results for CAPS and LONG
- 3-14 Depression near the load: results for CAPS, LONG and Beaumont
- 3-15 Tilt ratio (Green's function) near the load: comparison of several results
- 3-16 Gravity perturbation ratio (Green's function) near the load

- 4-1 The Green's function for tilt (Beaumont's preliminary solution)
- 4-2 Ocean-tide polygons for the N. Atlantic (region 1)
- 4-3 The ocean tide of the N. Atlantic
- 4-4 Ocean-tide polygons for N. Atlantic (region 2)
- 4-5 Ocean-tide polygons for the Pacific (region 3 and 4)
- 4-6 Ocean-tide polygons for E. Canada (part of region 6)
- 4-7 Ocean-tide polygons for Hudson Straits and Bay (6)
- 4-8 Ocean-tide polygons for Davis Strait (6)
- 4-9 Ocean-tide polygons for U.S. East Coast (6)
- 4-10 Ocean-tide polygons for Gulf of Mexico (6)
- 4-11 Tidal charts for the Pacific (summarized by Munk et al)
- 4-12 Tidal charts for the Pacific (summarized by Munk et al)
- 4-13 Ocean-tide polygons for the Pacific to fit M.S.W results of\* fig 4-12
- 4-14 Ocean-tide polygons for the Mediterranean Area (7)
- 5-1 Plan of the Rookhope mine showing the instrument sites
- 7-1 Ocean-tide polygons near Rookhope, England
- 7-2 Coamplitude-Cophase chart of the global ocean tide (Tiron et al)
- 7-3 Trans-U.S.A earth-tide profile (Kuo et al)
- 7-4 Confined and unconfined aquifers
- 7-5 Geologic section through the Sclaigneaux site
- 7-6 Ocean-tide polygons near Bidston, England
- 8-1 Records of tilt measured by the water tube tiltmeter and by the horizontal pendulum
- 8-2 Record from the water-tube tiltmeter showing detail

LIST OF TABLES

- 2-1 The Love Numbers
- 3-1 Elastic deformation of W. Europe due to ocean-tide loading
- 3-2 Influence values for surface displacements
- 3-3 Properties of the Gutenberg earth model
- 3-4 Data for homogeneous-shell earth (1-30°)
- 3-5 Data for homogeneous-shell earth (35-175°)
- 3-6 Data for Gutenberg-model earth (1-30°)
- 3-7 Data for Gutenberg-model earth (35-175°)
- 4-1 Values of the Green's function
- 6-1 Diminishing factors for Holland Mills, 1967,68
- 6-2 Diminishing factors for Rookhope, 1968 and 1969
- 6-3 Gravimetric factor for Ottawa, 1969
- 6-4 Diminishing factor for Rookhope determined by water-tube tiltmeter
- 7-1 Comparison of observed and calculated gravity tide
- 7-2 Bidston: contribution to gravity tide by global zones
- 7-3 Bidston: calculated effects due to local polygons
- 7-4 Comparison of observed and calculated tidal tilts, Bidston etc
- 7-5 Comparison of observed and calculated tidal tilts, Warmifontaine etc
- 7-6 Comparison of observed and corrected gravity tide in Western Europe
- 7-7 Calculated gravimetric factors and ocean-tide effect for Trans-USA profile

(vii)

- 7-8 Calculated ocean-tide effect on tidal gravity: Reno
- 7-9 Calculated ocean-tide effect on tidal gravity: Carlisle
- 7-10 Observed and calculated tidal gravity at Ottawa
- 7-11 Calculated ocean-tide effect on gravity at Ottawa
- 7-12 Observed and calculated tidal tilts at Holland Mills
- 7-13 Observed and calculated gravimetric factors: Africa etc

(viii)

LIST OF PLATES

- 5-1 Preparation of the Rookhope Site: The levelled base from which the holes for the support pins were drilled
- 5-2 Preparation of the Rookhope Site: drilling the holes for the support pins
- 5-3 Preparation of the Rookhope site: The base plate for the Spot follower installed on solid rock.
- 5-4 Preparation of the Rookhope site: The completed moisture-sealed pendulum case
- 5-5 The Sefram 2-channel Spot Follower and light source
- 5-6 Representative records of tilt from the Holland Mills site
- 8-1 The measuring pot of the water-tube tiltmeter

CHAPTER 1

INTRODUCTION

The classical aim of earth-tide research is to verify the theory of earth tides proposed by Love (1909). According to this theory there are two numbers which can be determined by measurements of the earth tide and which characterize the elastic behaviour of a spherically-symmetric earth without regard to any assumed density law or physical state of the earth. The significance of this theory is best appreciated when theories prior to Love's are considered: Kelvin (1890) for example assumed a uniform earth and obtained an expression connecting the deformation of the surface due to tidal forces with 'the rigidity of the Earth'. Kelvin's 'rigidity' however is not real but rather depends on the law of rigidity assumed and on the particular earth-tide phenomenon observed. Love's numbers on the other hand, for a spherically-symmetric and oceanless earth, are physical constants independent of any hypothesis on the interior of the earth. Given the tide-producing forces they are sufficient to determine such earth-tide phenomena as: deviations of the vertical with respect to the crust; deviations of the vertical with respect to the axis of the earth; variations in the speed of rotation of the earth; variations in gravity, elastic linear strain and cubical expansions.

The two principal means of observing the earth-tide are by recording gravimeter and by horizontal pendulum. The



latter measures the deviation of the gravity vertical with respect to the local surface. Love numbers determined during the last few decades by both these methods however have been found to exhibit regional variations far beyond those which might be due to the Earth not being spherically symmetric. Some of these apparent regional variations have been due simply to measurement errors but this cause has become steadily less important as better instruments, better methods of installations and, most important, better means of calibration have been developed. Regional differences have persisted in spite of these improvements however and as a result the Love numbers determined from observations are uncertain within  $\pm 1$  or 2 percent. Since, in order to be useful for evaluating various present-day earth models, the Love numbers should be known with an uncertainty of less than  $\pm 0.1$  percent it is important to account for regional variations. This is the purpose of the present thesis.

The problem is approached here on a broad front because many of the methods in use for investigating the earth tide when this work began are ill-suited to the study of regional variations and required some attention. This includes methods of data analysis and methods of making the measurements. The principal 'legitimate' cause of regional variations however is surface loading effects of the ocean tide and the main research effort is concentrated on the problem of predicting this effect in terms of earth structure. Western Europe is the logical place to begin a



study of this type because of the concentration of earth-tide measurements in Belgium and France and because the neighboring ocean tides are particularly well known. This data is supplemented here by British measurements from Liverpool and from a new site which we established at Rookhope. For treating global effects data from diverse sources is considered. Original data from Ottawa, including tiltmeter data from nearby Holland Mills, is particularly useful as being representative of midcontinental measurements.

CHAPTER 2

THE EARTH TIDE

2-1 The Tide-producing Force

Tide-producing stresses are set up in the Earth because the gravitational attraction of the Moon (Sun) is not the same everywhere throughout the body of the Earth. At the center of the Earth the gravitational attraction must provide the centripetal force necessary because of rotation of the Earth-Moon system about its center of mass. Elsewhere within the Earth, and at its surface, the gravitational attraction will be different and the consequent stresses will cause a deformation which we call the Earth tide.

The tide-producing potential is the difference between the potential due to rotation of the Earth-Moon system and the potential due to gravitational attraction. This is given by:

$$V = GM[ (1/\rho) - (1/R) - (r \cos\theta)/R^2 ] \quad (2-1)$$

where  $G$  is the gravitational constant;  $M$  is the mass of the Moon;  $\rho$  is the distance from the observing point to the Moon;  $R$  is the distance between the center of the Earth and the center of the Moon;  $r$  is the distance from the center of the Earth to the observing point and  $\theta$  is the geocentral zenith distance to the Moon. The distance  $\rho$  can be written as:

$$(1/\rho) = (1/R) [ 1 - (2r \cos\theta/R) + (r^2/R^2) ]^{-1/2} \quad (2-2)$$

Since  $r < R$  this can be represented by an expansion in Legendre polynomials:

$$(1/\rho) = (1/R)[P_0(\cos\theta) + P_1(\cos\theta) + P_2^2(\cos\theta) + \dots] \quad (2-3)$$

Substituting this in (2-1) yields the tide-producing potential:

$$V = (GMr^2/R^3) [P_2(\cos\theta) + P_3(\cos\theta)(r/R) + \dots] \quad (2-4)$$

The third order and higher terms are generally ignored.

It is necessary next to express the geocentral distance  $\theta$  in terms of a coordinate system which is fixed with respect to the celestial sphere.

#### 2-1-1 Calculation Of The Theoretical Tide, Harmonic Method.

Doodson (1921) shows that the tide-producing potential due to both the Moon and the Sun can be expressed as a sum of harmonic terms each of whose arguments is a linear function of six astronomical coordinates with integer coefficients. The astronomical coordinates, with their periodicities are:

- T = The mean lunar time. (1 day)
- S = The mean longitude of the Moon. (1 month)
- H = Mean longitude of the Sun.. (1 year)
- P = Longitude of lunar perigee. (8.85 years)
- N = -n, where n is the longitude of the ascending node of the Moon. (18.61 y)
- Ps = longitude of the perihelion. (20900 years)

The mean lunar time expressed in terms of Greenwich Mean Time is:

$$T = 15 t + H - S - L$$

where L is the longitude west of Greenwich, and t is Greenwich Mean Time. A convenient notation for each of the

possible harmonic terms results if the number five is added to each of the coefficients in the linear function of astronomic coordinates, except the first. Each term can then be written in the form:

$$V_{abcdef} = C_{abcdef} G_j \cos[aT + (b-5)S + (c-5)H + (d-5)p + (e-5)N + (f-5)Ps]$$

where  $a$ ,  $b$ ,  $c$ ,  $d$ ,  $e$  and  $f$  are integers,  $C_{abcdef}$  is a numerical coefficient and  $G_j$  is a geodetic coefficient involving the radius of the Earth at the point in question and the latitude.

The most fundamental classification of the harmonic terms is on the basis of the long period, diurnal, semi-diurnal and the ter-diurnal species formed when  $a=0, 1, 2$  and  $3$  respectively. Within each species the terms are classified according to the group number  $b$  with neighboring groups differing in frequency by one cycle per month. The waves within each group can be further subdivided according to the constituent member with neighboring constituents differing by one cycle per year. In Doodson's four schedules values for  $C_{abcdef}$  and for  $G_j$  are given for 99 long period terms, 158 diurnal terms, 115 semi-diurnal terms and 14 ter-diurnal terms. Also noted in the schedules is whether the cosine or the sine term is to be used.

To facilitate the determination of horizontal tidal forces from the potential given in the schedules it is best to retain in the formula for  $G$  the radius  $\rho$  which Doodson has replaced by the mean radius  $a$ . For the unprimed values

G0, G1 and G2 found in the schedules substitute  $G(\rho/a)^2$  and for the primed values substitute  $G(\rho/a)^3$ . For G itself use: (Melchior, 1965, p 19)

$$G = 3Mga^4/4Ec^3 = 26.206 \text{ cm}^2/\text{sec}^2$$

The numerical coefficients have been adjusted by Doodson so that the same G factor can be used for all.

To illustrate the notational scheme consider the principal component of the N2 group given in Doodson's schedule 2. This is:

$$V^{245655} = .17387 G\rho^2 \text{Cos}^2\lambda \text{Cos}(2T-S+P)/a^2$$

A minor component of this same group involves the primed geodetic coefficient G2' and it becomes:

$$V^{245555} = .00567(2.59808) G\rho^3 \text{Sin}\lambda \text{Cos}^2\lambda \\ \text{Sin}(2T-S+P+2n)/a^3$$

The vertical and horizontal components of the tide producing force are determined by differentiating as follows:

$$F_v = -\delta V/\delta\rho \quad F_n = -\delta V/\rho\delta\lambda \quad F_w = -\delta V/\rho\text{Cos}\lambda\delta L$$

When this is done it is found that the tidal gravity, and the north and west components of tilt can each be determined from the schedule of numerical coefficients by determining a new series of geodetic coefficients for use as multiplying factors. These new geodetic coefficients can be found in quite a straight forward manner by differentiating the several kinds of terms found in the schedules. This has been done by Melchior (1965, p64) and his results have been presented together with a shorter and easier to use version

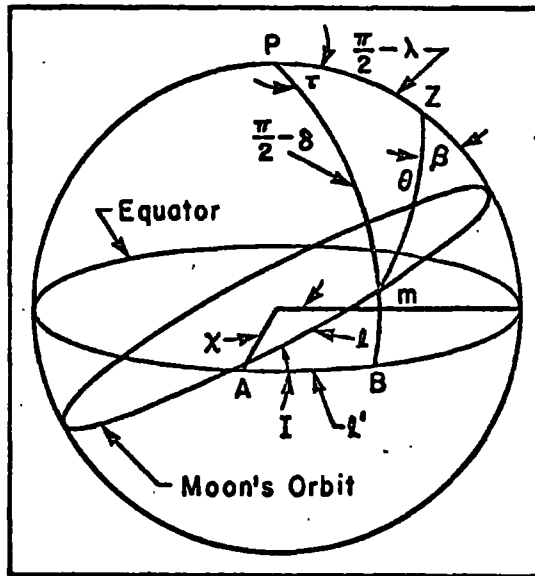


FIGURE (2-1) Construction for deriving the expression for the attraction of the Moon. (See text for definition of the symbols)

of Doodson's schedules. Melchior omits from his table terms whose amplitude is less than .001 relative to the amplitude of the largest term leaving a total of 79 terms. Melchior's table has been used in the analysis program JANET, which is documented in the appendix and will be described later.

2-1-2 Calculation Of The Theoretical Tide, Direct Method. Longman (1959) has presented a summary of the formulas used in developing a closed expression for the vertical component of tidal acceleration as a function of time for any given place on the Earth's surface. His summary does not include formulas for determining the north-south and east-west components of the horizontal tidal acceleration therefore these formulas are developed here. In addition to the symbols used by Longman we will use the symbols  $\beta$ ,  $\delta$  and  $t$  respectively for the azimuth, declination and hour angle of the attracting body. Referring to Figure (2-1), the letters P, Z and m denote the position on the celestial sphere of the north pole, the zenith and the attracting body. The angular distance  $l'$  is the projection of  $l$  on the equator. Expressions derived for the Moon are immediately applicable to the Sun after the obvious substitutions. According to Longman the horizontal tidal acceleration due to the Moon is given by:

$$H = C \sin 2\theta + [Cr(5\cos^2\theta)\sin\theta]/d \quad (2-5)$$

where:  $C = 3\omega Mr/2d^3$

From the figure, the south and west components of H are given by:

$$H_s = 2C \cos\theta \sin\theta \cos\beta + (Cr/d) (5\cos^2\theta - 1) \sin\theta \cos\beta \quad (2-6)$$

$$H_w = 2C \cos\theta \sin\theta \sin\beta + (Cr/d) (5\cos^2\theta - 1) \sin\theta \cos\beta \quad (2-7)$$

using the following relations for  $\Delta mpz$ :

$$\cos\theta = \sin\lambda \sin\delta + \cos\lambda \cos\delta \cos T \quad (2-8)$$

$$\sin\theta \cos\beta = \cos\lambda \sin\delta + \sin\lambda \cos\delta \cos T \quad (2-9)$$

$$\sin\theta \sin\beta = \cos\delta \sin T \quad (2-10)$$

and from amb

$$\cos\delta = \cos l / \cos l' \quad (2-11)$$

$$\sin\delta = \sin l \sin I \quad (2-12)$$

$$\tan l' = \tan l \cos I \quad (2-13)$$

Now  $T = x - l'$  and from (2-11), (12) and (13):

$$\cos\delta \cos T = \cos x \cos l + \sin x \sin l \cos I \quad (2-14)$$

$$\cos\theta \sin T = \sin x \cos l - \cos x \sin l \cos I \quad (2-15)$$

Substituting (14) and (15) in (8), (9) and (10) we obtain finally:

$$\cos\theta = \sin\lambda \sin l \sin I + \cos\lambda (\cos x \cos l + \sin x \sin l \cos I) \quad (2-16)$$

$$\sin\theta \cos\beta = -\cos\lambda \sin l \sin I + \sin\lambda (\cos x \cos l + \sin x \sin l \cos I) \quad (2-17)$$

$$\sin\theta \sin\beta = \sin x \cos l - \cos x \sin l \cos I \quad (2-18)$$

These are the three expressions needed to determine the three components of the tidal acceleration from equations (6) and (7) and from Longman's formulas for  $x$ ,  $l$  and  $I$ .

A computer program (ROBIN) based on these equations was written to determine the vertical tidal acceleration and the horizontal tidal acceleration along any specified azimuth. This direct method yielded more accurate results at less computing cost than the harmonic method and was used to check the latter method and to provide test data for the



data analysis program JANET. The program is documented in the appendix.

## 2-2 The Love Numbers and the Gravimetric and Diminishing Factors.

An ocean completely covering the Earth would everywhere define an equipotential surface. The tide-producing potential would displace such a universal sea radially a distance  $V/g$  where  $V$  is the tidal potential. This is called the height of the equilibrium tide. It is a useful concept in ocean tide theory although tidal heights actually experienced in the ocean are generally much altered from the equilibrium value because of the dynamic effects of friction and inertia. The equilibrium height is of greater use in connection with Earth tides where dynamic effects are negligible. Love<sup>gi</sup> (1911) has shown that both the surface displacement and the newly created potential due to the displacement are proportional to the equilibrium tidal height. He has introduced the constants  $h$  and  $k$  to describe the proportionality and it is these numbers that have become known as the Love Numbers.

The Love Numbers have been evaluated theoretically on the basis of different Earth models by many early workers (see Jeffereys<sup>reys</sup> Sec 7.05, The Earth) and more recently by Takeuchi (1950), Alterman Jarosch and Pekeris (1959) and Alsop and Kuo (1964). Experimentally the Love Numbers have been determined from measurements of various physical phenomena; those of interest here are tidal variations in

gravity and tidal deflections of the vertical with respect to the local crust. It is convenient to relate these phenomena to corresponding phenomena which would be observed on a perfectly rigid Earth. Thus the tidal variation in gravity can be expressed as:

$$G = [1 + h - (3k/2)] G'$$
$$= \delta G'$$

where  $G'$  is the rigid-Earth tidal gravity. The tidal tilt can be written:

$$T = [1 + k - h] T'$$
$$= D T'$$

where  $T'$  is the rigid-Earth tilt. The factors  $\delta$  and  $D$  defined in this way are called gravimetric and diminishing factors respectively. Typical observed values for  $\delta$  and  $D$  fall within the ranges of 1.135 to 1.230 and 0.550 to 0.850 respectively.

Alsop and Kuo (1964) have calculated values for the Love Numbers for a wide range of spherically-symmetric Earth models. They find that differences in the structure of the crust and upper mantle or the presence of a solid inner core have little influence on the Love Numbers. The presence of a universal ocean of thickness 5 km however is found to have a very large effect. This is shown in their Table 3 which is reproduced here as Table (2-1). The Bullen B modified model is the Jefferies-Bullen B with an oceanic crust. The Bullen-B Oceanic is the Bullen-B modified with the top 5 kms of the 10 km oceanic crust replaced with water. This can

(TIDAL PERIOD = 12 hr.)  
(INNER CORE  $\mu = 4.0 \times 10^{11}$  cgs)

JEFFREYS-BULLEN II

BULLEN B MODIFIED

BULLEN B OCEANIC

AVERAGE CORE $\mu (\times 10^{11})$	OUTER CORE $\mu (\times 10^{11})$	JEFFREYS-BULLEN II				BULLEN B MODIFIED				BULLEN B OCEANIC										
		$h$	$l$	$k$	$1 + h - 3/2 k$	$D$	$1 + k - h$	$1 + k - l$	$L$	$h$	$l$	$k$	$1 + k - h$	$D$	$1 + k - l$	$L$				
1.9	0.0367	.617	.088	.304	1.161	.687	1.216	1.216	.630	.088	.310	1.165	.680	1.222	.641	.088	.285	1.214	.644	1.197
2.0	0.142	.613	.088	.302	1.160	.689	1.214	1.214	.623	.089	.307	1.162	.684	1.218	.636	.088	.283	1.212	.647	1.195
2.1	0.247	.609	.088	.300	1.159	.691	1.212	1.212	.620	.089	.305	1.162	.685	1.216	.633	.088	.281	1.212	.648	1.193
2.2	0.351	.604	.088	.297	1.158	.693	1.209	1.209	.615	.089	.303	1.160	.688	1.214	.629	.088	.279	1.210	.650	1.191
2.3	0.456	.600	.088	.295	1.157	.695	1.207	1.207	.610	.089	.301	1.158	.691	1.212	.625	.088	.277	1.210	.652	1.189
2.4	0.561	.597	.088	.294	1.156	.697	1.206	1.206	.607	.089	.299	1.158	.692	1.210	.621	.088	.275	1.208	.654	1.187
2.5	0.666	.593	.088	.292	1.155	.699	1.204	1.204	.603	.089	.297	1.158	.694	1.208	.617	.088	.273	1.208	.656	1.185
2.75	0.928	.584	.088	.287	1.154	.703	1.199	1.199	.593	.089	.292	1.155	.699	1.203	.609	.088	.269	1.206	.660	1.181
3.00	1.19	.575	.088	.283	1.150	.708	1.195	1.195	.584	.089	.288	1.152	.704	1.199	.599	.088	.264	1.203	.665	1.176
3.25	1.45	.567	.088	.279	1.148	.712	1.191	1.191	.576	.089	.284	1.150	.708	1.195	.591	.088	.260	1.201	.669	1.172
3.50	1.71	.559	.088	.275	1.146	.716	1.187	1.187	.567	.089	.279	1.148	.712	1.190	.583	.088	.256	1.199	.673	1.168
3.75	1.98	.552	.088	.271	1.145	.719	1.183	1.183	.559	.089	.276	1.145	.717	1.187	.575	.088	.252	1.197	.677	1.164
4.00	2.24	.545	.088	.268	1.143	.723	1.180	1.180	.552	.089	.272	1.144	.720	1.183	.568	.088	.248	1.196	.680	1.160
4.25	2.50	.538	.089	.265	1.140	.727	1.176	1.176	.545	.090	.268	1.143	.723	1.178	.561	.088	.245	1.194	.684	1.157
4.50	2.76	.531	.089	.261	1.139	.730	1.172	1.172	.538	.090	.265	1.140	.727	1.175	.554	.088	.241	1.192	.687	1.153
4.75	3.03	.525	.089	.258	1.138	.733	1.169	1.169	.531	.090	.262	1.138	.731	1.172	.547	.088	.238	1.190	.691	1.150
5.00	3.29	.518	.089	.255	1.137	.737	1.165	1.165	.525	.090	.259	1.136	.734	1.169	.541	.088	.235	1.188	.694	1.147
6.0	4.34	.496	.089	.244	1.130	.748	1.155	1.155	.501	.090	.247	1.130	.746	1.157	.518	.088	.223	1.184	.705	1.145
7.0	5.39	.476	.089	.234	1.125	.758	1.145	1.145	.481	.090	.237	1.126	.756	1.147	.498	.088	.213	1.178	.715	1.135
8.0	6.44	.458	.089	.226	1.119	.768	1.137	1.137	.463	.090	.226	1.121	.765	1.138	.480	.088	.204	1.171	.724	1.116
9.0	7.48	.443	.089	.216	1.116	.775	1.129	1.129	.446	.090	.220	1.116	.774	1.130	.464	.088	.196	1.170	.732	1.108
10.0	8.53	.428	.089	.211	1.112	.783	1.122	1.122	.432	.090	.213	1.112	.781	1.123	.450	.088	.189	1.166	.739	1.101

TABLE (2-1) The Love Numbers (Alsop and Kuo)

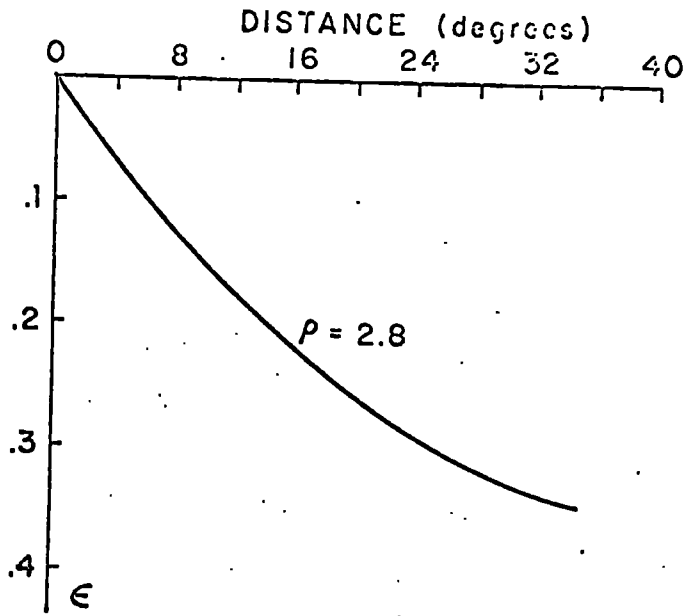


FIGURE (3-1) The function  $\epsilon$  near the load.

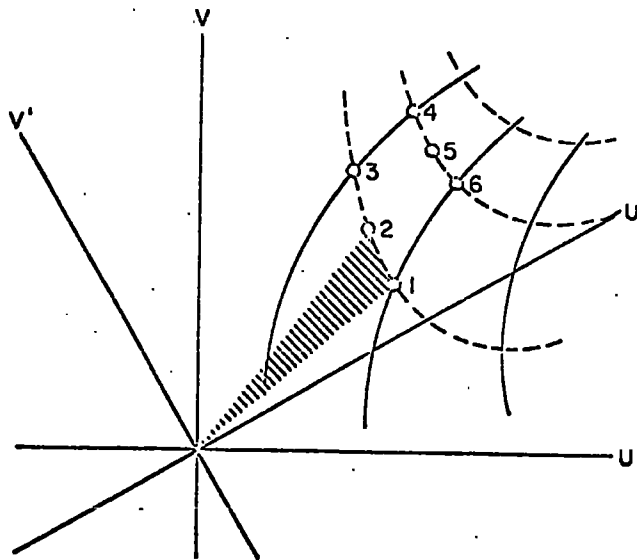


FIGURE (3-3) Construction for determining the attraction of n-sided polygon.

only be a rough approximation to reality but the result indicates that Love Numbers observed near oceans should be significantly larger than continental values.

CHAPTER 3

THE OCEAN-TIDE EFFECT\*

3-1 Introduction

An essential first step in the interpretation of measurements of the earth tide by tiltmeter or gravimeter is to estimate the effect of the ocean tide. This indirect effect is due to the gravitational attraction of the water and of the land masses which have elastically yielded to the weight of the water, as well as to the elastic displacement and possible tilting of the measuring site due to the loading of the surface. The ocean tide is not known generally and estimates of it for mid-ocean areas in particular are poor since they are inferred from coastal measurements made perhaps many hundreds of miles distant. In spite of these difficulties estimates of the indirect effect may be sufficient to correct observations of the bodily tide made at continental sites for the effects of the ocean tide. In the case of coastal sites where the indirect effect is large an estimate of its value may be useful in determining, through an iterative process incorporating the earth-tide observations, the elastic properties of the regional crust and upper mantle.

In what follows I describe the development of the various techniques which I have used to estimate the indirect effect throughout Britain and northwestern Europe and throughout the world generally. I describe first a method of determining the regional effects of the ocean tide

\* The ocean-tide effect referred to is that due to the  $M_2$  constituent

assuming an infinite, half-space earth. The particular method described differs from earlier ones in the manner in which the ocean tide is described and its attraction computed. It is a computer-oriented (rather than site oriented) method and permits working directly from cotidal-corange charts. This method is then applied to the case of a 2-shell Earth and the effects of ocean tides throughout the world are considered. The attraction computations for the global case are immediately usable in equations presented by Longman (1962, 1963) for determining the response of a Gutenberg-model Earth to surface forces. The series appearing in Longman's solutions are not convergent in the form presented by Longman for distances less than about 30 degrees but an extrapolation procedure permits solutions for distances down to a few degrees. The Longman results are tested by comparison with the results for the 2-shell Earth and by comparison with recent results determined by Beaumont (1971) using a finite-element method. The Beaumont results for surface displacement and tilt are adopted throughout the distance 0-80° where the Longman extrapolated results are likely to be in error. In this way a method of calculating the indirect effect from the computed attraction of the ocean tide has been determined which is valid over the globe.

### 3-2 The Effect On An Infinite Half-Space Earth.

In general the ocean tide throughout the world and the deformation of the earth due to the presence of the ocean

tide must be known before its influence on earth-tide measurements can be determined for a particular site. In the particular case of earth-tide tilt measurements however the influence of the ocean tide falls off rapidly enough with increasing distance to justify assuming, as a first approximation, a plane earth and considering only those waters within 20 or 30 degrees of the site. We will show later that the effect of sphericity and other real-Earth characteristics is to cause surface tilt to diminish even more quickly with increasing distance.

Assume that the earth can be represented by an homogeneous medium in the region  $z \geq 0$ . The normal deformation of the surface by the distributed normal load  $p(x,y)$  acting at the point  $x,y$  in the  $X, Y$  plane is given by: (Sokolnikoff, 1956)

$$w = [ (\lambda+2\mu) / (4\pi\mu(\lambda+\mu)) ] \iint [ p(x,y) / r \, dx \, dy ]$$

(3-1)

where  $r^2 = (X-x)^2 + (Y-y)^2$  and  $\mu$  and  $\lambda$  are the Lamé constants. It can be expressed too in terms of the gravitational potential of the load, which is:

$$E = \iint [ Gs(x,y) / r \, dx \, dy ]$$

(3-2)

when there is a surface mass density which can be expressed by:

$$p(x,y) = s(x,y) g \tag{3-3}$$

where  $g$  is the acceleration due to gravity. Equation 3-1 then becomes:



$$w = (\lambda+2\mu) gE/[4\pi\mu(\lambda+\mu)G] \quad (3-4)$$

where  $G$  is the gravitational constant. Adopting the terminology used by Melchior (1965, p192) we define the tilt due to the gravitational attraction of the load by:

$$A = \delta E/g\delta r \quad (3-5)$$

The tilt of the surface then is:

$$\begin{aligned} \delta w/\delta r &= (\lambda+2\mu) g^2 A/[4\pi\mu(\lambda+\mu)G] \\ &= \beta A \end{aligned} \quad (3-6)$$

The horizontal attraction due to the displaced masses of the medium is written in the form  $-\epsilon A$  where  $\epsilon$  is a function to be determined. The sum of the indirect effects on tilt then is:

$$I = (1 + \beta - \epsilon) A \quad (3-7)$$

An estimate of the horizontal attraction  $\epsilon A$  was obtained using the global deformation given by the solution of Slichter and Caputo (1960) for a homogeneous shell of rigidity  $\mu=1.2 \times 10^{12}$  (dynes/cm<sup>2</sup>) enclosing a fluid core. For the purpose of computing the horizontal attraction the deformation was represented by a global sheet of mass surface density  $2.8h$  where  $h$  is the deformation and 2.8 is the volume density assumed for the displaced masses. Thus all the displacement was assumed to take place on the surface. The function  $\epsilon$  then was determined for a range of distances from the loading mass by dividing the horizontal attraction by the horizontal attraction of the loading mass. The resulting function is reproduced in Figure (3-1). The function  $\epsilon$  is the same as the function  $T2/T3$  introduced

later and shown for further models in Fig.3-5.

Equation (3-7) demonstrates the three principal effects of the ocean tide on the measurement of tilt and expresses these effects in terms of the gravitational attraction of the tide. A fourth effect is the elastic uplift of ground caused by the gravitational attraction of the water masses. This effect is significant in the case of gravity measurements at great distances from the load but the associated tilting is negligible. Later we will compare the results obtained here assuming an infinite-plane earth with the results obtained using more realistic models.

#### 3-2-1. The Attraction Of The Ocean Tide.

We will introduce now a method of determining the potential of the M2 component of the ocean tide, from which the attraction<sup>m</sup> A can be found for use in Eqn. (3-7). Consider first the cotidal-corange chart shown in Fig. (3-2). This chart describes the behaviour of the M2 component of the ocean tide in the waters surrounding the British Isles. It is essentially British Admiralty Chart 5058 (1937) supplemented by material from the recent German North Atlantic Chart (W.Hansen, Institute fur Meereskunde der Universitat Hamburg, 1969). The contours are drawn through points of equal amplitude (solid lines) and phase (dotted lines). The range (double amplitude) is given in feet and the phase is in degrees lagging the lunar transit of Greenwich. The classical method of determining the gravitational attraction due to this distribution of mass is

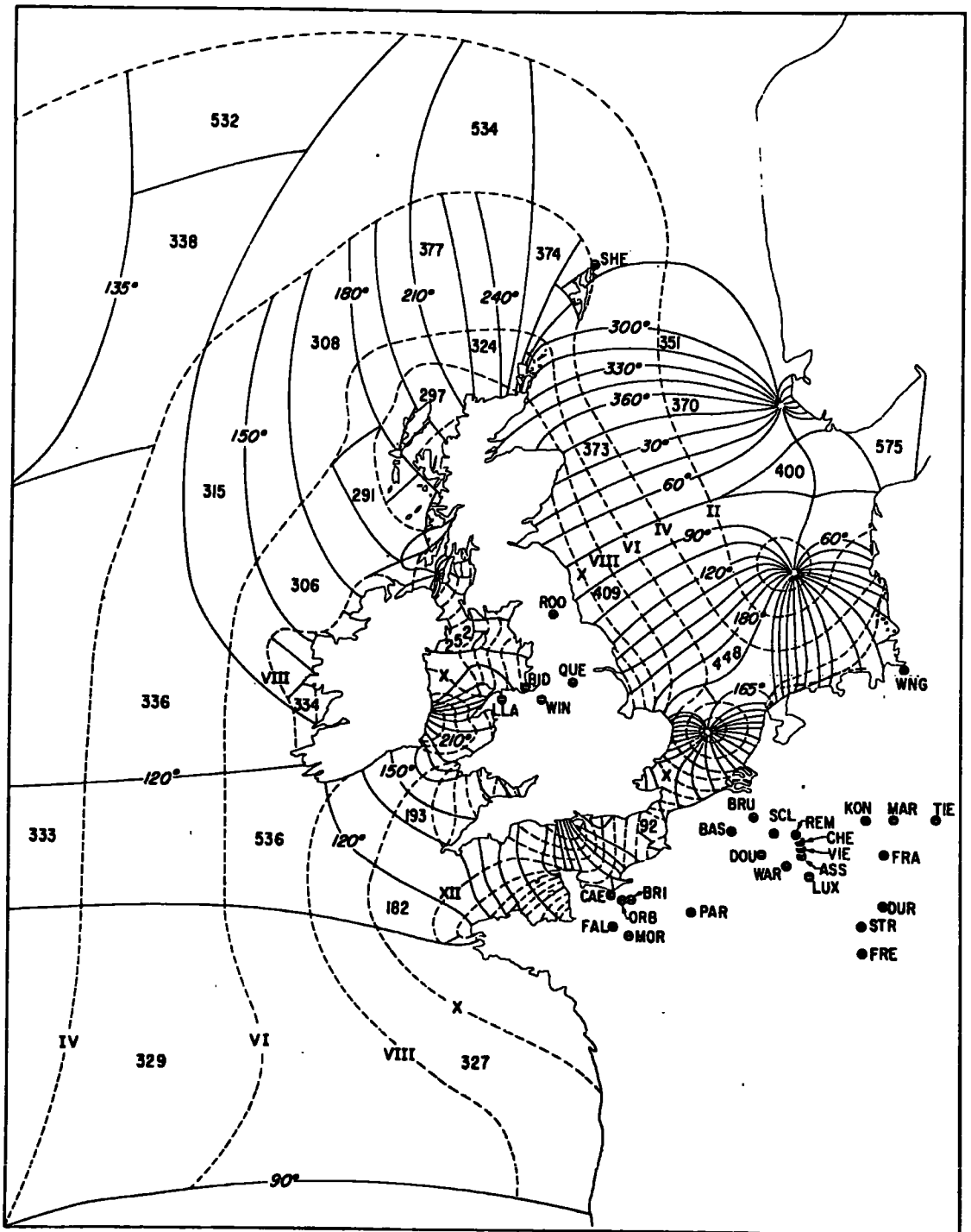


FIGURE (3-2) Ocean-tide contours near Britain (Region 0). Earth-tide measuring sites are identified by the first 3 figures in the name.

that using Hayford zones of constant amplitude and phase centered on the site where the attraction is to be determined. There are two objections to this method: It is difficult to fit the Hayford zones to the contour pattern and thus a large number of zones is required for an acceptable representation. The second objection is that a new system of Hayford zones must be set up for each site. An alternative method of representing the contour pattern is by a series of spherical harmonics. This harmonic method has been used by Pertsev (1966) in considering the effect of a world-wide distribution of ocean tides. Zones of equal amplitude and phase in this case are spherical trapezoids of equal area bounded by parallels and meridians. The zones of course are independent of site location but like the Hayford zones they are difficult to fit to the tidal contours and in addition they cannot be adjusted in size to fit requirements. This method then is practical only for first approximation global effects and not for determining the effects of regional tides. Since the principal aim of this investigation is to explain the spatial variations in earth-tide measurements the effect of regional tides is important and must be estimated for a dense distribution of sites. Consequently neither of the methods described was applicable.

It will be noticed that the corange and cotidal lines defining the tides tend to intersect orthogonally to form rectangles of approximately uniform amplitude and phase. In

fact it can be shown (Defant, 1961, p356) that in the absence of friction these lines would be everywhere perpendicular. To take advantage of this feature a general method of determining the attraction of such rectangles was developed but was subsequently abandoned in favour of a method suggested by Bott which was usable with polygons. This method is derived from one used by Bott (1963) for determining the magnetic field due to finite 3-dimensional bodies. We will use the method again later in three dimensions (program GLOBL) but it is best described in the simple 2-dimensional form required here.

Consider a n-sided polygon formed by the intersection of cotidal and corange lines drawn in the x,y plane (Fig. 3-3). The behaviour of the water within the polygon can be described by a single set of harmonic constants (contrast this with the case when the shape of the polygon is arbitrarily assigned). Number the polygon points clockwise from  $j=1$  to  $j=n$  and assume a right-handed coordinate frame  $u,v$  centered on the site  $o$ , where the potential is to be determined. Rotate the  $u,v$  axes to new positions  $u', v'$  so that the positive  $v'$  axis is in the same direction as the side  $j+1$  of the polygon. Denoting the coordinates of the  $j$ -th point with respect to the two positions of the axes by  $u(j), v(j)$  and  $u'(j), v'(j)$  the potential of the lamina  $j, 0, j+1$  then is:

$$\Delta E_j = C u(j) \log(M) \quad (3-8)$$

where:

$$M = [v'(j+1) + (v(j+1)^2 + u'(j)^2)^{1/2}] / [v'(j) + (v(j)^2 + u'(j)^2)^{1/2}]$$

and:

$$v'(j+1) = [u(j+1)(u(j+1)-u(j)) - v(j+1)(v(j+1)-v(j))] / L$$

$$v'(j) = [u(j)(u(j+1)-u(j)) + v(j)(v(j+1)-u(j))] / L$$

$$u'(j) = [u(j)(v(j+1)-v(j)) - v(j)(u(j+1)-u(j))] / L$$

$$u'(j+1) = u'(j)$$

L is the distance from point j to point j+1, and C is a constant incorporating the amplitude and phase factors, the density of water, and the gravitational constant. The potential of the entire polygon then is the algebraic sum of the potentials found for the n laminae:

$$E = \sum \Delta E_j \quad (3-9)$$

### 3-2-2 Program PRESS

A computer program (PRESS) has been written to compute the surface deformation on the basis of the foregoing assumptions. The region of W. Europe, particularly Britain, has been treated in detail using the cotidal-corange chart described earlier (Fig. 3-2). The ocean tide considered is that for the region east of longitude 25° west, south of latitude 62° north, and north of latitude 42° north. The cotidal charts were digitized using an electronic line follower to input the points defining each polygon. About 500 polygons were used initially; their general arrangement is indicated in Fig. (3-2). The number of every 25th polygon is shown. The amplitude and phase of the ocean tide throughout each polygon are given in Appendix VII. For this

tidal data, and for assigned values of rigidity and compressibility, program PRESS determines: 1. The amplitude and phase of the normal displacement of the surface. 2. The amplitude and the azimuth of tilt for 30 degree intervals of phase. The latter provides data for drawing ellipses describing the behaviour of the tilt vector (horizontal force vector/g) as a function of time. A copy of program PRESS is reproduced in Appendix III.

### 3-2-3 Discussion And Results.

It was originally intended to contour the amplitude and phase of the surface deformation in the same way as that of the ocean tide. The phase is fairly constant over the entire region however, lagging the transit of the moon at Greenwich by 120 to 140 degrees, and the corange lines alone are sufficient to represent the deformation. A map showing corange lines for the deformation due to loading by the ocean tide has been determined by PRESS and is presented in Fig. (3-4). The data from which this map was drawn was determined on the basis of an infinite half space with  $\mu = 1.0 \times 10^{12}$  dynes/cm<sup>2</sup> and Poisson's ratio equal to 0.5.

Results for 24 earth-tide observing sites are presented in Table 3-1. The location of each of these sites is shown in Fig. (3-2). These results represent a preliminary estimate of the ocean-tide effect in this important region where 90 percent of the world total of earth-tide observations have been made. Striking variations in the results of observations throughout this region have been reported and

SITE	LONG	LAT	A <sub>s</sub>	A <sub>w</sub>	I <sub>s</sub>	I <sub>w</sub>	U
LLA	-3.80	53.18	14.79(141°)	2.50(-166)	51.49(142°)	8.08(-157)	2.35(144°)
BID	-3.07	53.40	15.96(139°)	13.98(-56°)	56.36(140°)	54.08(-56°)	1.92(140°)
WIN	-2.50	53.20	5.15(150°)	2.48(-56°)	16.33(154°)	11.58(-52°)	2.55(140°)
ROO	-2.21	54.78	2.28(-109)	4.29(-74°)	9.47(-98°)	17.41(-69°)	2.46(130°)
CAE	-0.22	49.11	7.82(103°)	4.78(176°)	23.44(99°)	24.25(160°)	2.85(146°)
FAL	-0.12	48.53	4.06(098°)	4.75(153°)	9.10(085°)	19.61(151°)	3.06(140°)
ORD	0.24	49.10	6.29(109°)	4.89(170°)	18.67(106°)	17.58(172°)	2.60(144°)
MOR	0.33	48.32	3.17(101°)	5.05(143°)	6.70(088°)	15.35(148°)	2.87(139°)
BRI	0.43	49.12	5.97(113°)	4.62(172°)	17.76(112°)	15.85(176°)	2.51(143°)
VIL	2.19	49.07	2.20(124°)	2.39(149°)	5.86(127°)	5.50(163°)	2.06(138°)
PAR	2.33	48.83	1.86(120°)	2.69(144°)	4.66(122°)	6.21(155°)	2.09(137°)
BRU	4.35	50.80	0.40(141°)	0.94(106°)	0.68(-172)	1.36(57°)	1.57(136°)
DUR	4.63	50.10	0.64(125°)	1.35(131°)	1.31(134°)	2.05(136°)	1.59(137°)
SLA	5.02	50.50	0.47(117°)	1.30(128°)	0.72(121°)	2.01(127°)	1.52(137°)
WAR	5.38	49.83	0.50(115°)	1.52(133°)	0.93(118°)	2.74(139°)	1.52(136°)
REM	5.70	50.48	0.44(105°)	1.42(131°)	0.74(95°)	2.54(134°)	1.45(137°)
VIE	5.90	50.27	0.43(101°)	1.44(132°)	0.98(089°)	2.61(135°)	1.44(137°)
LUX	6.13	49.62	0.41(112°)	1.55(133°)	0.77(112°)	2.93(137°)	1.44(136°)
STR	7.77	48.58	0.23(096°)	1.46(133°)	0.44(091°)	2.78(138°)	1.28(135°)
FRI	7.87	48.00	0.18(082°)	1.50(132°)	0.36(074°)	2.87(137°)	1.28(135°)
NEU	7.93	50.78	0.40(104°)	1.36(137°)	0.83(097°)	2.69(144°)	1.20(137°)
DUR	8.48	49.00	0.21(099°)	1.37(134°)	0.40(094°)	2.59(139°)	1.20(136°)
MAR	8.80	50.80	0.35(110°)	1.25(138°)	0.73(108°)	2.41(146°)	1.11(137°)
TIE	10.17	50.72	0.28(116°)	1.09(137°)	0.57(118°)	1.99(145°)	0.99(137°)

TABLE (3-1) Elastic deformation of Western Europe due to ocean-tide loading. A is attraction tilt in msec and degrees lag relative to transit of the Moon at Greenwich. I is attraction plus elastic tilt; U is depression in cms; the subscripts s and w denote the directions south and west respectively. (Boussinesq solution with  $\mu = 10^{12}$  cgs)



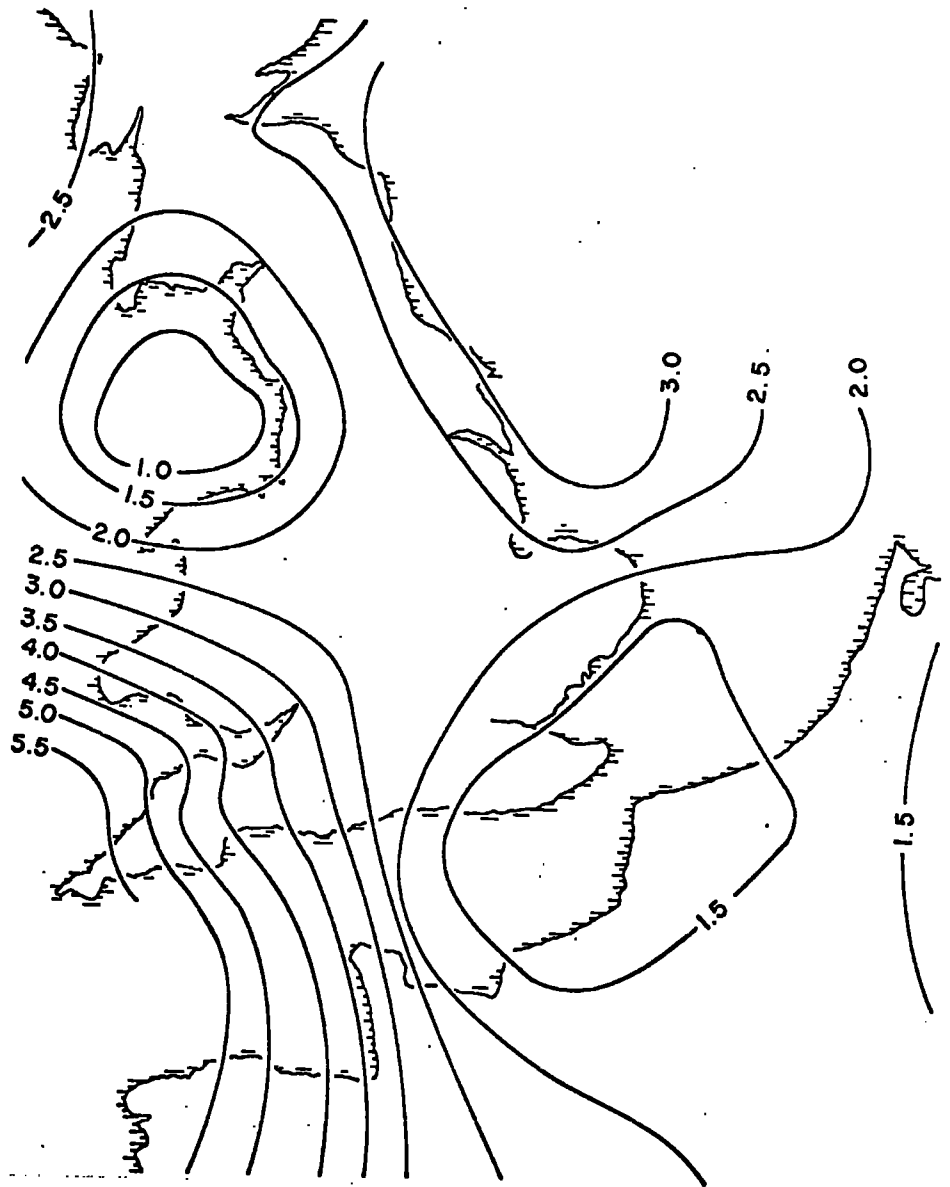


FIGURE (3-4) Elastic depression in cms due to ocean-tide loading (Boussinesq solution for plane).  
 For the case:  $\mu = 1.0 \times 10^{12}$ ,  $\lambda = \infty$

an early objective of this research was to determine whether such variations could possibly be due to ocean-tide effect. Program PRESS provides an economical means of rapidly evaluating the spatial variations in ocean-tide effect. Its use demonstrated that some of the observations must be affected by some anomalous local condition since they could not be explained on the basis of any reasonable ocean-tide loading effect. Most of the observations however reflected the predicted ocean-tide loading and this encouraged the use of a better model and more complete ocean-tide data. This is pursued in the sections which follow and the present PRESS results will not be discussed further.

### 3-3. The Effect On A 2-Shell Earth.

Slichter and Caputo (1960) and Caputo (1961) have considered the deformation of a layered earth by an axially symmetric surface mass distribution. I have used their method of solution for the non gravitating, homogeneous shell, fluid core case (Slichter and Caputo, 1960) to determine the radial deformation when the load is a single circular cap approximating a point mass (half angle of one degree). Using this result I have determined the tilting effect and the perturbation of gravity with an approximate correction for gravitation effects. The computation was implemented by program CAPS, which is documented in Appendix IV, and the results are presented in Tables 3-4 and 3-5 expressed in a convenient non-dimensional form introduced by Longman (1963). Longman's variables are  $u/(am'/m)$  and

Table 3-2a Influence values for surface displacements (Taylor):  
 point load  $\rho = I_{\rho}P/2\pi hE$   
 Vertical displacement  $\rho_z$

$r/h \backslash \nu$	0	0.2	0.4	0.5
0.05	37.580	35.921	31.052	27.351
0.1	17.586	16.728	14.260	13.360
0.2	7.624	7.162	5.897	4.914
0.3	4.327	4.016	3.154	2.480
0.4	2.720	2.478	1.827	1.320
0.5	1.792	1.599	1.092	0.699
0.6	1.212	1.048	0.635	0.290
0.7	0.823	0.690	0.352	0.051
0.8	0.560	0.450	0.168	-0.079
0.9	0.373	0.286	0.053	-0.160
1.0	0.250	0.182	-0.011	-0.183
1.25	0.080	0.031	-0.085	-0.194
1.5	0.013	-0.002	-0.077	-0.156
1.75	-0.007	-0.007	-0.048	-0.123
2.0	-0.012	-0.011	-0.039	-0.083
2.5	-0.004	-0.017	-0.025	-0.036
3.0	-0.003	0.001	-0.008	-0.025
3.5	-0.003	0.000	-0.004	-0.018
4.0	-0.001	0.000	-0.003	-0.012
6.0	-0.000	-0.000	-0.001	-0.002
8.0	-0.000	-0.000	-0.000	-0.000
10.0	-0.000	-0.000	-0.000	-0.000

Table 3-2b Influence values for surface displacements (Taylor):  
 point load  $\rho = I_{\rho}P/2\pi hE$   
 Radial displacement  $\rho_r$

$r/h \backslash \nu$	0	0.2	0.4	0.5
0.05	19.959	14.362	5.559	-0.041
0.1	9.948	7.124	2.723	-0.078
0.2	4.896	3.455	1.250	-0.156
0.3	3.183	2.184	0.716	-0.225
0.4	2.308	1.523	0.426	-0.288
0.5	1.773	1.064	0.232	-0.326
0.6	1.277	0.824	0.102	-0.376
0.7	1.000	0.620	0.008	-0.405
0.8	0.789	0.465	-0.063	-0.420
0.9	0.627	0.349	-0.011	-0.421
1.0	0.499	0.259	-0.141	-0.417
1.25	0.292	0.150	-0.175	-0.380
1.5	0.167	0.048	-0.163	-0.315
1.75	0.097	0.012	-0.134	-0.250
2.0	0.060	0.002	-0.109	-0.195
2.5	0.027	0.003	-0.070	-0.118
3.0	0.010	-0.002	-0.038	-0.072
3.5	0.003	-0.008	-0.022	-0.046
4.0	0.002	-0.000	-0.014	-0.029
6.0	0.000	-0.000	-0.002	-0.002
8.0	0.000	-0.000	-0.000	-0.001
10.0	0.000	-0.000	-0.000	-0.000

Table 3-3

*Properties of the Gutenberg Earth Model*

$a-r$ km	$\rho$ g/cm <sup>3</sup>	$C_p$ km/s	$C_s$ km/s	$\mu$ 10 <sup>11</sup> dyn/cm <sup>2</sup>	$\lambda$ 10 <sup>11</sup> dyn/cm <sup>2</sup>	$g$ cm/s <sup>2</sup>
0	2.74	6.14	3.55	3.45	3.42	982
19	3.00	6.58	3.80	4.33	4.32	983
38	3.32	8.20	4.65	7.18	7.97	984
50	3.34	8.17	4.62	7.13	8.04	985
60	3.35	8.14	4.57	7.00	8.20	985
70	3.36	8.10	4.51	6.83	8.38	986
80	3.37	8.07	4.46	6.70	8.54	986
90	3.38	8.02	4.41	6.57	8.59	986
100	3.39	7.93	4.37	6.47	8.37	986
125	3.41	7.85	4.35	6.45	8.11	987
150	3.43	7.89	4.36	6.52	8.31	988
175	3.46	7.98	4.38	6.64	8.76	989
200	3.48	8.10	4.42	6.80	9.23	989
225	3.50	8.21	4.46	6.96	9.67	990
250	3.53	8.38	4.54	7.28	10.24	991
300	3.58	8.62	4.68	7.84	10.92	992
350	3.62	8.87	4.85	8.52	11.45	993
400	3.69	9.15	5.04	9.37	12.15	995
450	3.82	9.45	5.21	10.37	13.38	996
500	4.01	9.88	5.45	11.91	15.32	997
600	4.21	10.30	5.76	13.97	16.73	998
700	4.40	10.71	6.03	16.00	18.47	998
800	4.56	11.10	6.23	17.70	20.79	997
900	4.63	11.35	6.32	18.49	22.66	995
1000	4.74	11.60	6.42	19.54	24.71	993
1200	4.85	11.93	6.55	20.81	27.41	990
1400	4.96	12.17	6.69	22.20	29.06	986

DST	U1	U3	U4	G1	G2	G4	G4/G3	T1	T2	T3
1	-63.23	3.45	-59.87	-120.11	46.56	-102.19	3.57	3040.662	-32.28	3282.76
2	-24.71	2.81	-21.99	-44.13	17.54	-40.91	2.86	1300.031	-19.06	820.66
3	-16.84	2.43	-14.50	-29.08	11.71	-26.92	2.82	344.749	-12.91	364.71
4	-12.03	2.16	-9.96	-19.99	8.17	-18.98	2.65	199.547	-9.21	205.13
5	-9.39	1.95	-7.53	-15.11	6.25	-14.59	2.55	110.902	-7.59	131.27
6	-7.78	1.78	-6.09	-12.22	5.10	-11.90	2.49	78.156	-6.10	91.15
7	-6.35	1.63	-4.80	-9.64	4.07	-9.66	2.36	55.217	-5.27	66.95
8	-5.58	1.50	-4.17	-8.36	3.55	-8.39	2.34	40.239	-4.56	51.25
9	-4.70	1.39	-3.40	-6.82	2.93	-7.08	2.22	32.999	-4.00	40.49
10	-4.22	1.29	-3.01	-6.05	2.61	-6.31	2.20	24.033	-3.63	32.79
11	-3.67	1.20	-2.56	-5.14	2.23	-5.51	2.11	21.626	-3.21	27.09
12	-3.29	1.12	-2.26	-4.53	1.98	-4.94	2.07	16.001	-2.99	22.76
13	-2.96	1.04	-2.00	-4.02	1.76	-4.46	2.02	14.858	-2.69	19.38
14	-2.62	0.97	-1.74	-3.49	1.54	-4.00	1.95	11.631	-2.53	16.71
15	-2.41	0.91	-1.60	-3.20	1.41	-3.70	1.93	10.478	-2.32	14.55
16	-2.13	0.84	-1.37	-2.76	1.23	-3.33	1.85	9.015	-2.17	12.78
17	-1.98	0.79	-1.28	-2.57	1.14	-3.12	1.85	7.574	-2.04	11.32
18	-1.75	0.73	-1.11	-2.23	1.00	-2.83	1.77	7.233	-1.90	10.09
19	-1.62	0.68	-1.03	-2.07	0.92	-2.66	1.76	5.684	-1.82	9.05
20	-1.46	0.63	-0.91	-1.83	0.82	-2.45	1.70	5.850	-1.69	8.16
21	-1.33	0.59	-0.83	-1.66	0.74	-2.29	1.67	4.509	-1.63	7.40
22	-1.21	0.55	-0.75	-1.51	0.67	-2.15	1.64	4.684	-1.52	6.74
23	-1.08	0.50	-0.66	-1.33	0.59	-1.99	1.59	3.798	-1.47	6.16
24	-1.00	0.47	-0.62	-1.25	0.55	-1.90	1.58	3.697	-1.39	5.66
25	-0.87	0.43	-0.53	-1.07	0.47	-1.75	1.51	3.341	-1.34	5.21
26	-0.81	0.39	-0.51	-1.01	0.44	-1.68	1.51	2.912	-1.28	4.81
27	-0.70	0.36	-0.43	-0.87	0.38	-1.56	1.45	2.978	-1.22	4.46
28	-0.64	0.33	-0.40	-0.81	0.35	-1.49	1.44	2.349	-1.19	4.14
29	-0.56	0.30	-0.35	-0.70	0.30	-1.40	1.40	2.616	-1.12	3.86
30	-0.49	0.27	-0.31	-0.62	0.26	-1.32	1.37	1.888	-1.10	3.60

TABLE (3-4) DATA FOR HOMOGENEOUS-SHELL EARTH (MU2= 1.86E+12)

DST	U1	U3	U4	G1	G2	G4	G4/G3	T1	T2	T3
35	-0.21	0.14	-0.16	-0.32	0.11	-1.03	1.24	1.551	-0.91	2.64
40	0.02	0.03	-0.04	-0.07	-0.01	-0.81	1.11	1.246	-0.76	2.01
45	0.20	-0.05	0.06	0.12	-0.10	-0.63	0.97	0.914	-0.63	1.58
50	0.33	-0.12	0.12	0.25	-0.17	-0.51	0.86	0.598	-0.53	1.27
55	0.42	-0.17	0.16	0.33	-0.21	-0.42	0.78	0.405	-0.42	1.04
60	0.48	-0.20	0.19	0.39	-0.25	-0.35	0.71	0.314	-0.32	0.87
65	0.53	-0.22	0.22	0.44	-0.27	-0.30	0.64	0.208	-0.22	0.73
70	0.56	-0.24	0.23	0.46	-0.29	-0.26	0.60	0.046	-0.13	0.62
75	0.55	-0.24	0.23	0.46	-0.29	-0.24	0.59	-0.098	-0.04	0.54
80	0.53	-0.23	0.21	0.43	-0.28	-0.24	0.62	-0.167	0.05	0.46
85	0.50	-0.22	0.20	0.40	-0.27	-0.24	0.65	-0.206	0.13	0.40
90	0.46	-0.20	0.18	0.36	-0.25	-0.25	0.70	-0.283	0.20	0.35
95	0.41	-0.17	0.15	0.30	-0.23	-0.27	0.79	-0.383	0.27	0.31
100	0.34	-0.14	0.11	0.22	-0.19	-0.30	0.91	-0.440	0.32	0.27
105	0.26	-0.10	0.07	.14	-0.16	-0.32	1.05	-0.443	0.37	0.24
110	0.19	-0.07	0.03	0.07	-0.12	-0.36	1.18	-0.450	0.40	0.21
115	0.11	-0.03	-0.01	-0.01	-0.09	-0.40	1.34	-0.494	0.41	0.19
120	0.02	0.01	-0.05	-0.11	-0.04	-0.44	1.52	-0.530	0.41	0.17
125	-0.06	0.05	-0.10	-0.20	-0.00	-0.48	1.71	-0.512	0.40	0.15
130	-0.15	0.09	-0.14	-0.28	0.04	-0.52	1.90	-0.464	0.37	0.13
135	-0.22	0.13	-0.18	-0.36	0.07	-0.56	2.06	-0.446	0.33	0.11
140	-0.30	0.17	-0.22	-0.44	0.11	-0.60	2.24	-0.455	0.27	0.10
145	-0.37	0.20	-0.26	-0.52	0.15	-0.64	2.43	-0.429	0.20	0.08
150	-0.44	0.23	-0.29	-0.59	0.18	-0.67	2.59	-0.348	0.12	0.07
155	-0.49	0.26	-0.32	-0.64	0.20	-0.70	2.71	-0.270	0.04	0.06
160	-0.54	0.29	-0.34	-0.68	0.22	-0.72	2.82	-0.247	-0.06	0.04
165	-0.58	0.30	-0.36	-0.73	0.24	-0.74	2.92	-0.238	-0.16	0.03
170	-0.61	0.32	-0.38	-0.77	0.26	-0.76	3.02	-0.159	-0.26	0.02
175	-0.63	0.32	-0.39	-0.78	0.27	-0.77	3.36	-0.027	-0.35	0.01

TABLE (3-5) DATA FOR HOMOGENEOUS-SHELL EARTH (MI2= 1.86D+12)

$\gamma/(gm'/m)$  rather than the radial displacement  $u$  and the perturbation of gravity  $\gamma$ , where  $m'$  is the mass of the load,  $m$  is the mass of the earth and  $a$  is the radius of the earth. In addition to these variables I have used the variable  $\phi/(m'/m)$  to represent tilt where  $\phi$  is the actual tilt in milliseconds of arc. The letters  $U$ ,  $G$  and  $T$  refer to non-dimensional displacement, gravity change and tilt respectively. In the description that follows, the symbols  $P(n)$  and  $Q(n)$  refer to the Legendre polynomials of degree  $n$  in  $\omega$  and  $\theta$  respectively where  $\omega$  is the half angle of the cap load and  $\theta$  is a variable denoting the angular distance to the load axis.

### 3-3-1. Program CAPS.

The solution obtained by Slichter and Caputo (1960) is solved in program CAPS for the case of a single cap load. The cap load is defined by the surface density:

$$\begin{aligned} f(\theta) &= T/g \quad 0 < \theta \leq \omega \\ &= 0 \quad \text{otherwise} \end{aligned} \quad (3-10)$$

where  $T$  is the assigned surface pressure and  $g$  is the acceleration due to gravity. This can be represented by the infinite series:

$$\begin{aligned} f(\theta) = \sum_n &= \sum T [P(n-1) - P(n+1)] Q(n) / 2g \\ &+ T(1 - \cos\omega) / 2g \end{aligned} \quad (3-11)$$

It will be shown later that the term  $n=1$  of this series requires special treatment. Slichter and Caputo (1960) avoid using this term by assuming instead of a single cap load two

identical anti-podal caps. In our implementation of their method we assume a single cap load but omit the term  $n=1$  from the computation. We calculate the effect of this term separately by a method described in Appendix IX and add it to the results determined for the other terms. The non-dimensional displacement due to this term is denoted by  $U_5$  in program CAPS. It is shown in the appendix to be, for a solid homogeneous earth:

$$U_5 = -(3g^2/(3\gamma+2)) (\cos\theta/8G\pi\mu) \quad (3-12)$$

where  $\gamma = \lambda/\mu$ . (The displacement for a homogeneous shell was determined also by this technique but was found to differ only slightly from the homogeneous earth case).

The elastic equilibrium considered by Slichter and Caputo is that of a spherical shell with the applied stress independent of longitude and the elastic parameters  $\lambda$  and  $\mu$  constant. A solution in the form:

$$u = \sum R(r,n) Q(n) \quad (3-13)$$

is assumed, where  $R(r,n)$  is determined by their Eqns. (21) and (22) in terms of the elastic parameters of the shell and the boundary conditions. The conditions appropriate to a fluid core are assumed on the inner boundary. On the outer boundary a surface-load function  $S(n,\omega)$  is assumed which, for the single-cap load considered here, becomes:

$$\begin{aligned} S(n,\omega) &= -rT(P(n-1) - P(n+1)) \frac{a^{(n)}}{r^n} / 2g \quad (n>0) \\ &= -rT(1 - \cos\omega) / 2g \quad (n=0) \end{aligned}$$

After determining  $R(r,n)$  the radial displacement  $U_1$  is determined using Eqn. (3-13), assuming  $\omega=1$  degree and summing



to  $n=200$ . There is in addition to this yielding due to the surface force an uplift due to the body force exerted by the load. Love (1927, Section 174) gives for this uplift on an homogeneous earth:

$$\delta U_n = V_n \rho n [ n ( (n+2) \lambda + (n+1) \mu ) a^2 - (n-1) ( (n+1) \lambda + n \mu ) r^2 ]$$
$$/ [ 2 (n-1) \mu ( (2n^2+4n+3) \lambda + 2 (n^2+n+1) \lambda ) ] \quad (3-14)$$

where  $\rho$  is the density of the homogeneous earth and  $V_n$  is the gravitational potential due to the loading mass. At a point on the surface  $V_n$  is given by:

$$V_n = (\Delta n) 4\pi G a / (2n+1) \quad (3-15)$$

where  $a$  is the radius of the Earth. This uplift has been computed by CAPS for a mean density of 4.47 and is tabulated as  $U_3$  in the Tables. The total radial displacement is taken as the algebraic sum of yielding and uplift and is shown as  $U_4$  in the tables. This includes too a small constant term  $U_c$  due to the displacement when  $n=0$  and the term  $U_5$  described above.

There are three tilting effects to consider. The principal one  $T_1$  is due to the radial displacement of the surface. This is the surface tilt and is found by differentiating the expression for the total radial displacement with respect to  $a\theta$ . The next largest tilting effect is called  $T_3$  and is due to the horizontal component of the gravitational attraction of the load; that referred to as  $A$  in Egn. (3-7). This has the effect of deflecting the vertical which, with the pendulum-type tiltmeters used here, is indistinguishable from a tilt of the surface. In the

non-dimensional form it has the simple form:

$$T3 = [\text{Cos}(\theta/2)]/[4 \text{Sin}^2(\theta/2)] \quad (3-16)$$

Finally there is a negative attraction due to the masses of the earth which have been displaced; the attraction denoted by  $-\epsilon A$  in Eqn. (3-7) and which will be called  $T2$  here. Nishimura (1950) assumed as a first approximation for this attraction the constant ratio  $-.5A$ . We obtain an expression for this factor by differentiating the gravitational potential of the radial displacement, Eqn. (3-19) below. The result expressed as  $T2/T3$  has been computed as a function of distance assuming a density for the displaced masses of 2.8 and is shown in Fig. (3-5) for two values of rigidity. Also shown in this figure is the ratio  $T2/T3$  determined by the Longman method discussed in Section (3-6) below.

There are also three parts in the perturbation of gravity. The principal part is called  $G1$  and is due to simple radial displacement in the Earth's exterior gravitational field. The part due to the vertical component of the gravitational attraction of the load is:

$$G3 = -1/4 \text{Sin}(\theta/2) \quad (3-17)$$

$G2$  is the vertical attraction due to the displaced masses. To estimate it we proceed as follows: We assume the Earth is incompressible and that the displacement of the surface is given by  $U4$ , determined above, which can be represented as a series of spherical harmonics in the form:

$$U4 = \sum u P(\text{Cos}\theta) \quad (3-18)$$

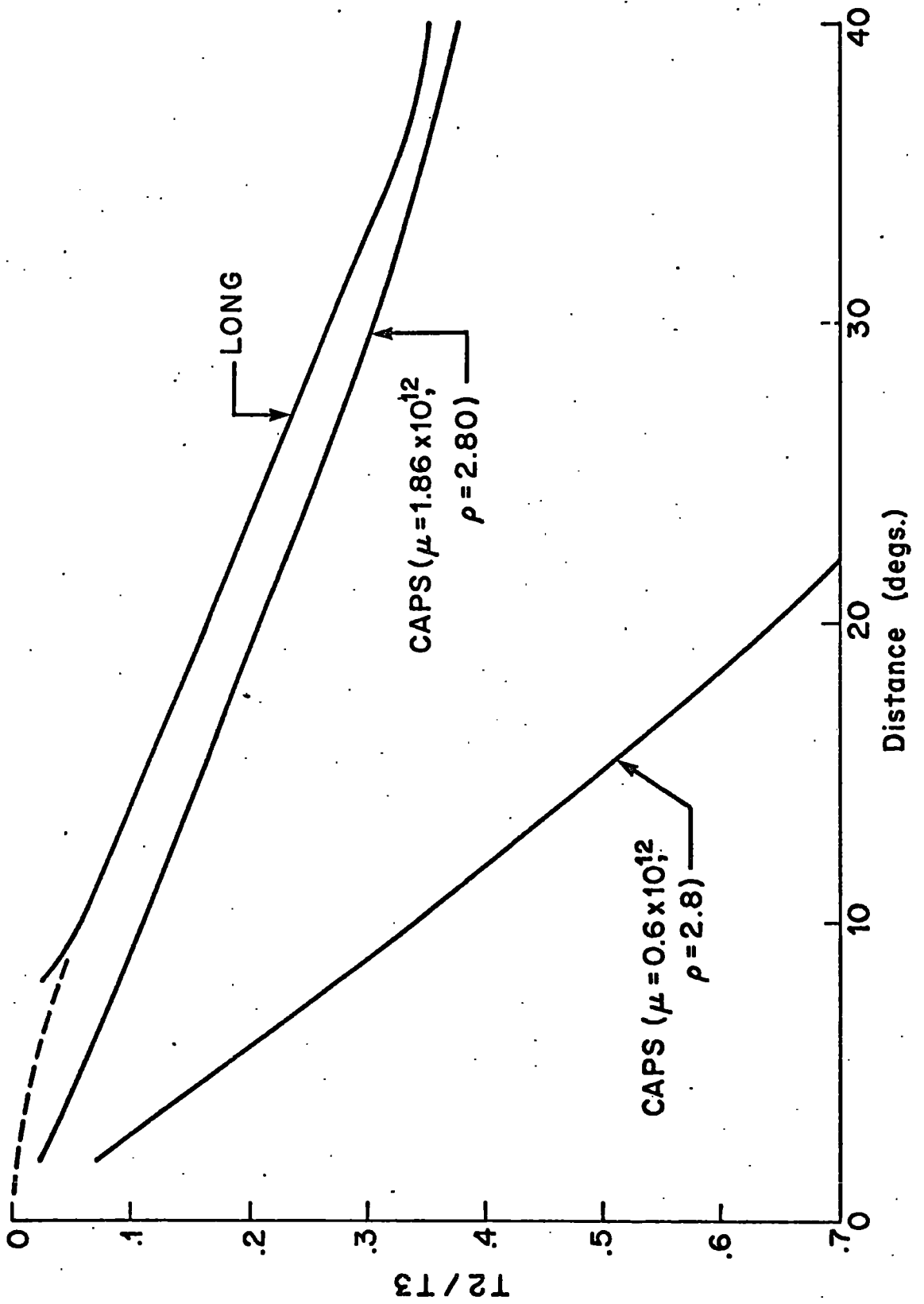


FIGURE (3-5) The function  $T_2/T_3$  for three models.

The gravitational potential due to this redistribution of mass is approximately:

$$V = \Sigma (4\pi G a) (a/r) (\rho u P_n(\cos\theta)) \quad (3-19)$$

This is the exterior potential of a sphere coated with the mass density  $s = \rho u$  where  $\rho$  is the density assumed for the displaced masses. The vertical component of attraction at the surface then is:

$$G2 = \Sigma (n+1) (4\pi G \rho u P_n(\cos\theta)) / (2n+1) \quad (3-20)$$

In this estimate we assume for the density the mean crustal value of 2.8. Note that the term  $n=0$  is not included in Eqn. (3-20) since it would not be present on an incompressible Earth.

The total gravity perturbation  $G4$  is the sum of  $G1$ ,  $G2$  and  $G3$ .

### 3-3-2 Discussion.

The displacement determined by program CAPS may be compared to that determined by Eqn. (3-1) for the infinite half space. As the distance is made small the radial displacement  $U1$  should approach and merge with the displacement determined by Eqn. (3-1). This result is demonstrated in Fig. (3-6) where displacement has been plotted for the two cases for a coefficient of rigidity of  $0.6 \times 10^{12}$  dynes/cm<sup>2</sup>. The displacement is less for the spherical model and less still when the uplift due to body forces ( $U3$ ) is added to  $U1$ .

The attraction tilt  $T3$  is of course identical in the

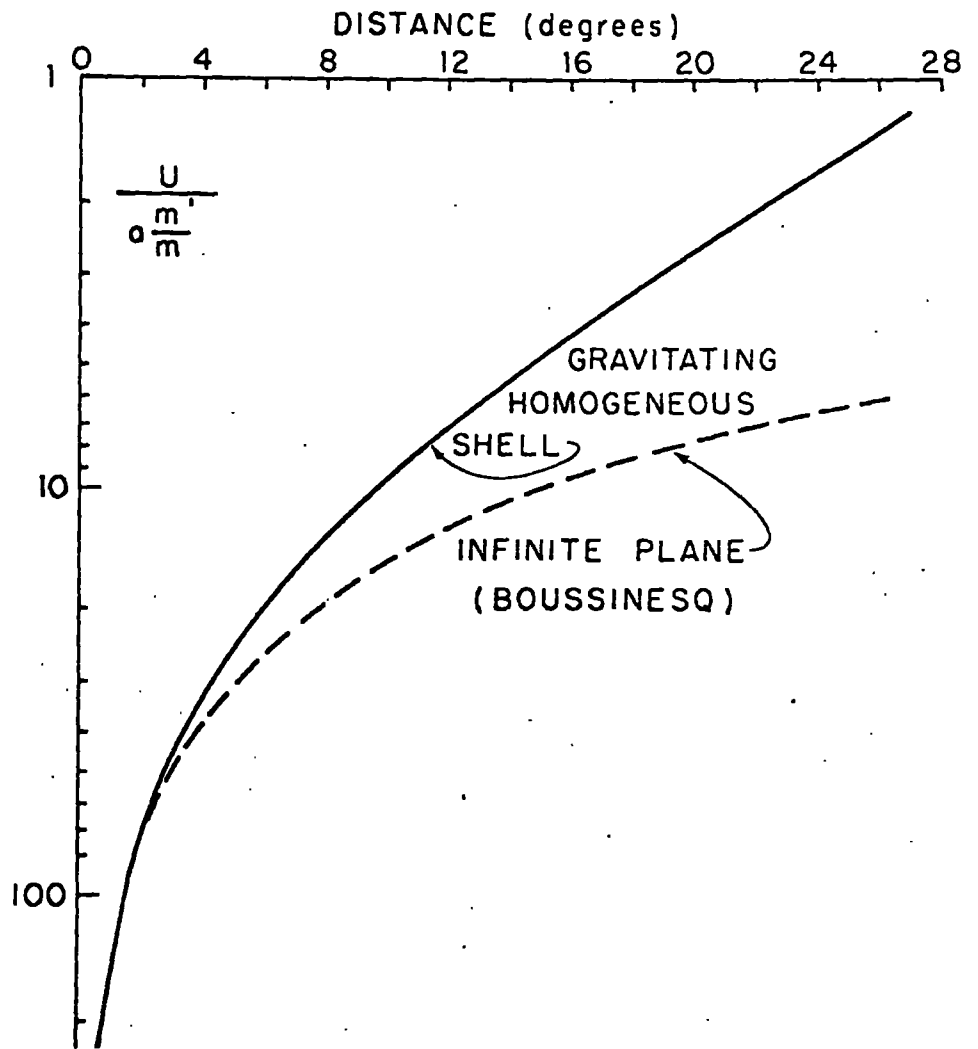


FIGURE (3-6) Comparison of elastic depression on Boussinesq and CAPS models.

two cases. The tilt  $T_2$  is too small to be significant at distances where the plane-Earth model is applicable.

### 3-4 The Effect On A Gutenberg-Model Earth.

#### 3-4-1 Program LONG.

Longman (1962, 1963) has derived the equations of equilibrium for an Earth model under the stress of a surface load when the three elastic parameters  $\lambda$ ,  $\mu$  and  $\rho$  are arbitrary functions of the depth. He has solved these equations for the case where the elastic parameters take on the values specified for the Gutenberg-model Earth (Alterman et al, 1961). Program LONG is an implementation based on these solutions but including additions and modifications which will be described later.

For the vertical displacement of the surface, the horizontal attraction (tilt) of the loading mass and of the displaced masses, and the change in the gravity field at the deformed surface Longman obtains the solutions:

$$U_n = H^n P_n(\cos \theta) \quad (3-21)$$

$$T_n = (1+K^n) P_n'(\cos \theta) \quad (3-22)$$

$$G_n = K^n [n+2H^n - (n+1) \frac{U_n}{U_n}] P_n(\cos \theta) \quad (3-23)$$

where  $P_n(\cos \theta)$  is the Legendre polynomial,  $P_n'(\cos \theta)$  is its derivative with respect to  $\theta$ ;  $U_n$ ,  $G_n$  and  $T_n$  are the non-dimensional forms introduced earlier for the displacement, tilt and gravity perturbation respectively.  $H^n$  and  $K^n$  are the load-deformation coefficients (Munk and Macdonald, 1960) which Longman determines for  $n$  up to 40 from the equations of equilibrium.

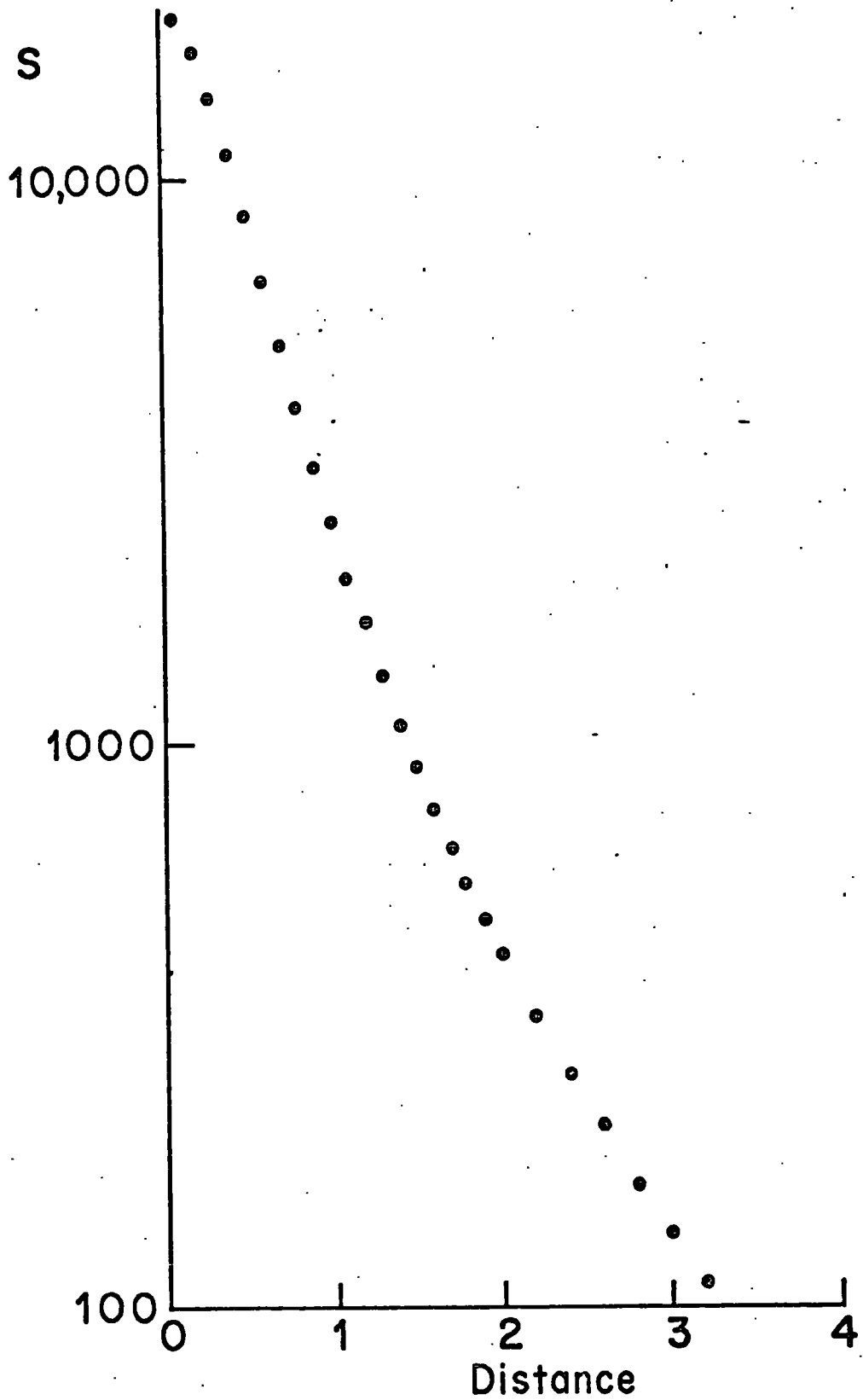


FIGURE (3-7) The surface-load function for  $p = 0.99$   
 (from Eqn. 3-24).

The numerically simple form of the equations is a consequence of the definition of the load deformation coefficients and the choice of a particularly convenient point-mass surface load equal to the mass of the Earth. The solution may be considered as a Green's function from which the response due to arbitrary surface loads can be obtained by convolution. The surface load assumed has the Legendre expansion:

$$S = (g/4\pi G) \lim_{p \rightarrow 1} \sum (2n+1) P_n(\cos\theta) \quad (3-24)$$

and the interior potential:

$$V_n = g a (r/a)^n \quad (3-25)$$

For the point-mass load assumed summations of the terms represented by Eqns. (3-21, 23, 24) diverge but the Poisson series obtained by multiplying each term by  $p^n$  does converge to the right value for  $p < 1$ . This has the effect however of broadening the representation of the load so that the assumed point mass may be distributed over several degrees. The expansion representing the load, Eqn. (3-24), is shown for  $p=0.99$  in Fig. (3-7). Longman finds for summation to  $n=40$  (the maximum for which he has determined  $n$ ) that  $p=0.85$  is the maximum value which can be used. Even for this value of  $p$  the effect of terms with  $n > 40$  becomes large when  $\theta$  is less than about  $30^\circ$  and consequently results within this limit are not correct. To permit  $p$  to approach as close as possible to 1.0 and computations to be made as close as possible to the load Longman suggests summing the series for very large values of  $n$ ; using the asymptotic behaviour of



$H'_n$  and  $K'_n$  as  $n$  tends to infinity to determine  $H'_n$  and  $K'_n$ . This is the procedure we have followed here to determine the displacement and gravity perturbation. Fig. (3-8) is a plot on a semi-logarithmic scale of the values given by Longman for  $H'_n$  and  $K'_n$ . The asymptotes for each of the coefficients are given by:

$$H'_n = -0.86 \log n + 0.58 \quad (3-26)$$

$$K'_n = 0.025 \log n - 0.127 \quad (3-27)$$

Using this procedure, summing to  $n=1000$  and putting  $p=0.99$ , produces reasonable looking results to within one degree of the load while for greater distances it reproduces closely the results obtained by Longman.

Longman omits the term  $n=1$  in the summation for total displacement and gravity perturbation because he considers the load-deformation coefficients for this term to imply displacement of the earth as a whole. This appears to be incorrect; it is shown in Appendix IX that mass loading represented by this term results in an equilibrating system of body and surface forces and significant elastic deformation. The term is neglected too by others: Munk and MacDonald (1960, p 31) find, that the opposing effects of yield due to surface force and uplift due to body force cancel for this term with the net result that the term is equivalent to a rigid body displacement of the earth with no effect on surface gravity. This result is true for the incompressible case treated by them but it is not generally true (see Eqn. (3-12)). An erroneous interpretation of the

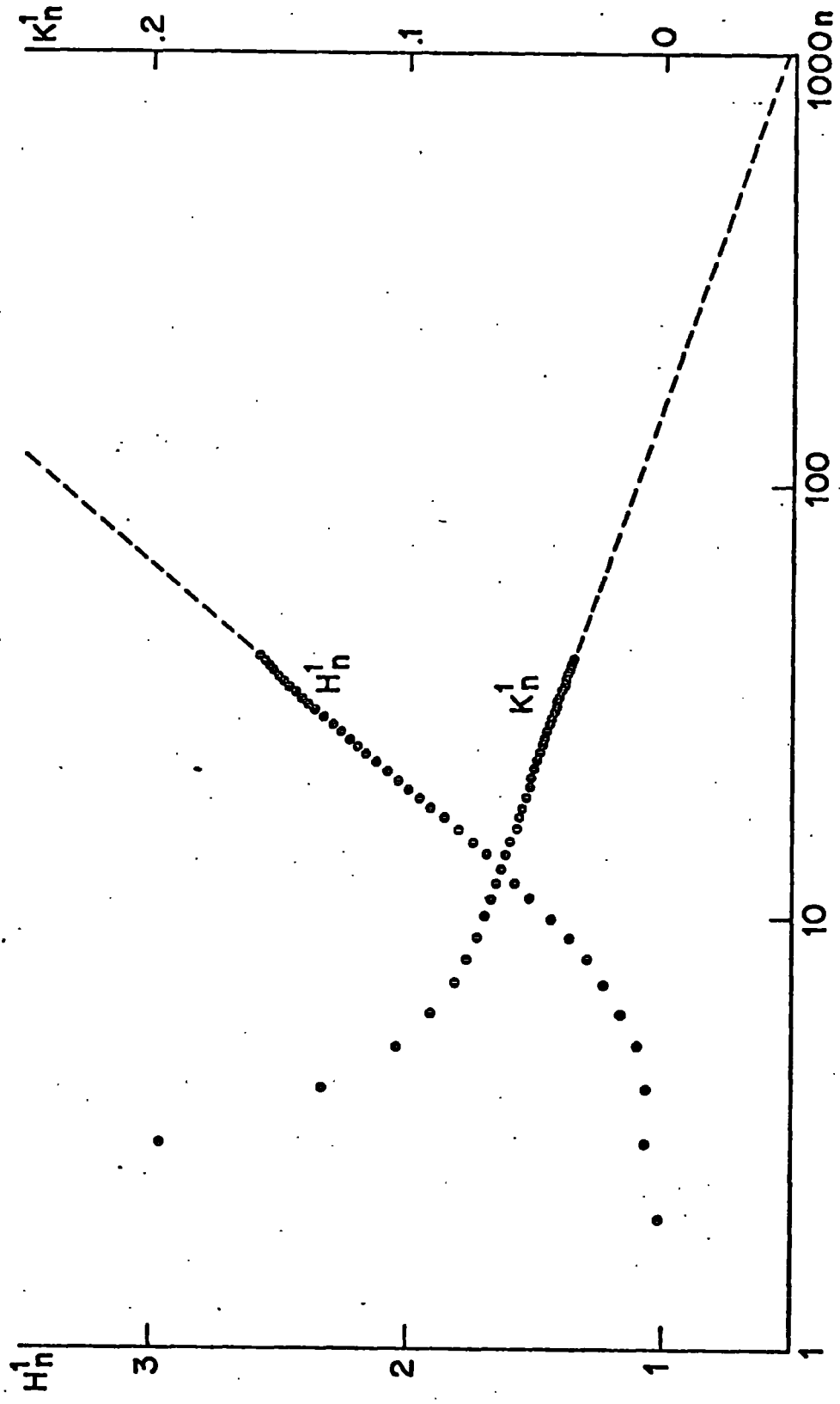


FIGURE (3-8) The load-deformation coefficients  $H_1^n$  and  $K_1^n$  showing the extrapolation used for  $n > 40$ .

effect of the  $n=1$  term might be made also from Jefferies' discussion of The Straining of a Sphere (1962, Appendix B) in which he deals separately with the effects of surface and body forces. The term  $n=1$  in the series representation of either of these forces taken separately does imply displacement of the earth as a whole because static equilibrium is impossible. This is reflected in the appearance of the factor  $n=1$  in the denominator of the expressions derived by Jeff<sup>reys</sup>~~reys~~.

The effect of omitting the  $n=1$  term in the series representation of the cap load is to distribute a loading mass over the entire hemisphere opposite the cap (and a negative mass over the hemisphere on the same side as the cap).

The effect of the term  $n=1$  on surface displacement is calculated in Appendix IX and added to the results determined below using Longman's method for the terms  $n \neq 1$ . The effect of the same term on surface gravity is calculated according to the method described in Section 3-3-1 and added to the Longman result. The tilt effect due to this term is negligible because of its large wavelength and relatively small amplitude.

To obtain the total Green's function for tilt the elastic tilt at the surface must be added to the solution given by Eqn. (3-22) which includes only the tilt due to attraction effects. This is done in program LONG by locally fitting the tabulated results for displacement to a

third-order polynomial and differentiating this approximating function.

### 3-5 Discussion.

The principal results obtained using programs CAPS and LONG are presented in Tables 3-4,7. Consider first the non-dimensional displacement determined for the distance range from 30 degrees to 180 degrees. The LONG results for this range and the CAPS results for rigidities of  $1.2 \times 10^{12}$  and  $1.86 \times 10^{12}$  and the same range are plotted in Fig. (3-9). This demonstrates that the displacement of a Gutenberg-model Earth due to surface loading by a point mass is approximately the same as that of an Earth consisting of a single homogeneous shell enclosing a fluid core; at least for loading at distances greater than 30 degrees. This corresponds fairly well with the figure of  $1.7 \times 10^{12}$  found for the 'mean' rigidity of the Earth's mantle to a depth of 2900 kilometers when Bullen's density law is assumed. (Melchior, p324, 1965).

The total gravity perturbation for the same three cases is shown in Fig. (3-10). The agreement between the LONG and CAPS results is not as good here. There is a systematic difference which is apparently due to the assumption made in the CAPS implementation that the displaced masses are simply redistributed on the surface.

### 3-6 Effects Within 30° Of The Load.

The results for the distance range 0-60° are shown in greater detail in Figs. (3-11,12). The total displacement U4

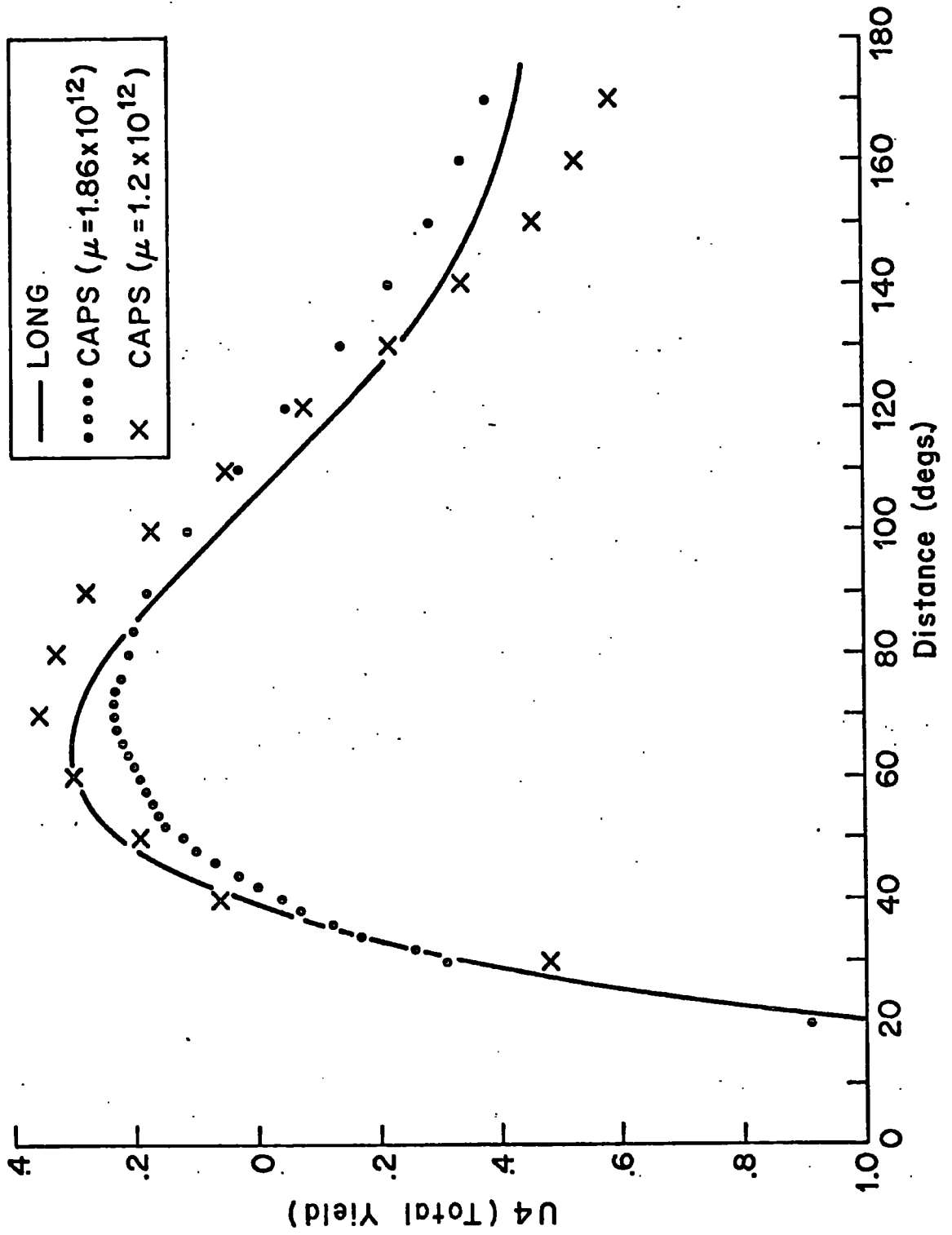


FIGURE (3-9) Comparison of elastic depression for 3 models.

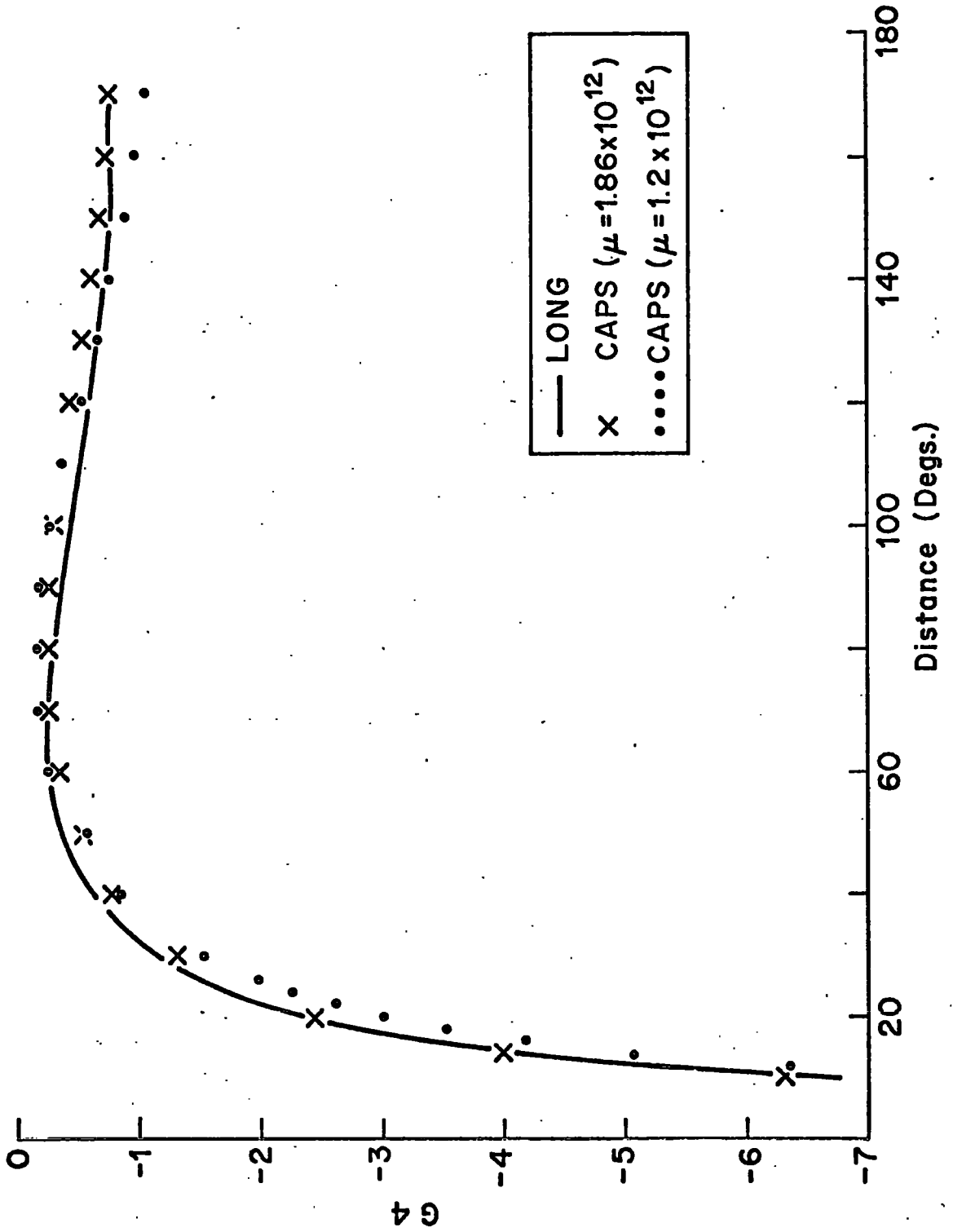


FIGURE (3-10) Comparison of gravity perturbation for 3 models.

DIST	W4	T1	T2	T3	T4	T4/T3	G4	G4/G3
1.0	-105.752	-5970.47	39.317	3282.765	-9213.92	2.807	-177.818	6.207
2.0	-41.945	-1926.74	28.577	-820.660	-2718.82	3.313	-72.421	5.056
3.0	-22.679	-604.42	18.530	-364.714	-950.60	2.606	-42.426	4.442
4.0	-14.132	-325.56	12.133	-205.134	-518.56	2.528	-27.303	3.812
5.0	-9.814	-183.48	8.853	-131.271	-305.90	2.330	-19.811	3.457
6.0	-7.193	-115.23	6.734	-91.147	-199.65	2.190	-14.664	3.070
7.0	-5.590	-74.89	5.422	-66.954	-136.42	2.037	-11.714	2.860
8.0	-4.469	-52.64	4.466	-51.252	-99.43	1.940	-9.416	2.627
9.0	-3.704	-37.26	3.803	-40.487	-73.95	1.826	-7.966	2.500
10.0	-3.134	-28.05	3.265	-32.786	-57.58	1.756	-6.787	2.366
11.0	-2.709	-21.17	2.862	-27.089	-45.40	1.676	-5.935	2.275
12.0	-2.381	-16.90	2.527	-22.755	-37.13	1.632	-5.242	2.192
13.0	-2.111	-13.78	2.275	-19.383	-30.89	1.594	-4.653	2.107
14.0	-1.893	-11.76	2.078	-16.707	-26.39	1.580	-4.187	2.041
15.0	-1.697	-10.37	1.931	-14.548	-22.99	1.580	-3.746	1.956
16.0	-1.530	-9.23	1.816	-12.782	-20.20	1.580	-3.410	1.899
17.0	-1.373	-8.38	1.719	-11.317	-17.98	1.589	-3.083	1.823
18.0	-1.238	-7.39	1.633	-10.090	-15.85	1.571	-2.835	1.774
19.0	-1.115	-6.58	1.545	-9.052	-14.09	1.557	-2.597	1.714
20.0	-1.008	-5.69	1.465	-8.165	-12.39	1.517	-2.404	1.670
21.0	-0.915	-5.04	1.386	-7.402	-11.05	1.493	-2.224	1.621
22.0	-0.831	-4.48	1.320	-6.740	-9.90	1.469	-2.061	1.573
23.0	-0.757	-4.16	1.263	-6.163	-9.06	1.469	-1.918	1.529
24.0	-0.686	-3.96	1.218	-5.657	-8.40	1.485	-1.774	1.476
25.0	-0.619	-3.83	1.180	-5.210	-7.86	1.509	-1.656	1.434
26.0	-0.552	-3.73	1.145	-4.814	-7.40	1.537	-1.534	1.380
27.0	-0.489	-3.51	1.109	-4.461	-6.86	1.538	-1.434	1.339
28.0	-0.429	-3.27	1.070	-4.145	-6.35	1.532	-1.331	1.288
29.0	-0.375	-2.93	1.034	-3.861	-5.76	1.492	-1.244	1.246
30.0	-0.327	-2.64	0.989	-3.605	-5.26	1.458	-1.160	1.201

TABLE (3-6) Data for Gutenberg-model Earth

DIST	U4	T1	T2	T3	T4	T4/T3	G4	G4/G3
35.0	-0.130	-2.27	0.871	-2.637	-4.03	1.530	-0.848	1.021
40.0	0.031	-1.50	0.728	-2.008	-2.78	1.383	-0.623	0.853
45.0	0.141	-1.06	0.606	-1.577	-2.04	1.290	-0.469	0.718
50.0	0.220	-0.74	0.494	-1.269	-1.51	1.194	-0.363	0.613
55.0	0.271	-0.40	0.386	-1.040	-1.06	1.017	-0.297	0.549
60.0	0.294	-0.18	0.292	-0.866	-0.76	0.873	-0.260	0.520
65.0	0.303	0.02	0.203	-0.730	-0.51	0.700	-0.252	0.541
70.0	0.291	0.21	0.121	-0.622	-0.29	0.469	-0.255	0.585
75.0	0.269	0.32	0.045	-0.535	-0.17	0.321	-0.278	0.677
80.0	0.226	0.42	-0.015	-0.464	-0.06	0.134	-0.290	0.745
85.0	0.197	0.49	-0.064	-0.404	0.02	-0.058	-0.331	0.895
90.0	0.151	0.54	-0.109	-0.354	0.07	-0.208	-0.365	1.033
95.0	0.104	0.57	-0.148	-0.311	0.11	-0.364	-0.405	1.195
100.0	0.052	0.59	-0.174	-0.274	0.14	-0.506	-0.436	1.336
105.0	0.002	0.56	-0.189	-0.242	0.13	-0.552	-0.477	1.515
110.0	-0.047	0.58	-0.202	-0.214	0.16	-0.762	-0.514	1.683
115.0	-0.098	0.57	-0.211	-0.189	0.17	-0.913	-0.556	1.876
120.0	-0.146	0.53	-0.211	-0.167	0.15	-0.888	-0.587	2.033
125.0	-0.190	0.50	-0.205	-0.147	0.15	-0.999	-0.624	2.213
130.0	-0.232	0.45	-0.2#1	-0.129	0.12	-0.967	-0.657	2.381
135.0	-0.270	0.43	-0.193	-0.112	0.12	-1.079	-0.681	2.517
140.0	-0.307	0.41	-0.178	-0.097	0.14	-1.424	-0.704	2.646
145.0	-0.341	0.34	-0.158	-0.083	0.10	-1.172	-0.733	2.795
150.0	-0.366	0.29	-0.139	-0.069	0.08	-1.175	-0.751	2.900
155.0	-0.391	0.24	-0.120	-0.057	0.06	-1.070	-0.771	3.011
160.0	-0.408	0.20	-0.097	-0.045	0.06	-1.268	-0.776	3.058
165.0	-0.426	0.16	-0.073	-0.033	0.05	-1.506	-0.797	3.161
170.0	-0.435	0.07	-0.052	-0.022	0.00	-0.014	-0.798	3.179
175.0	-0.444	0.19	-0.020	-0.311	0.16	-14.217	-0.813	3.249

TABLE (3-7) Data for Gutenberg-model Earth



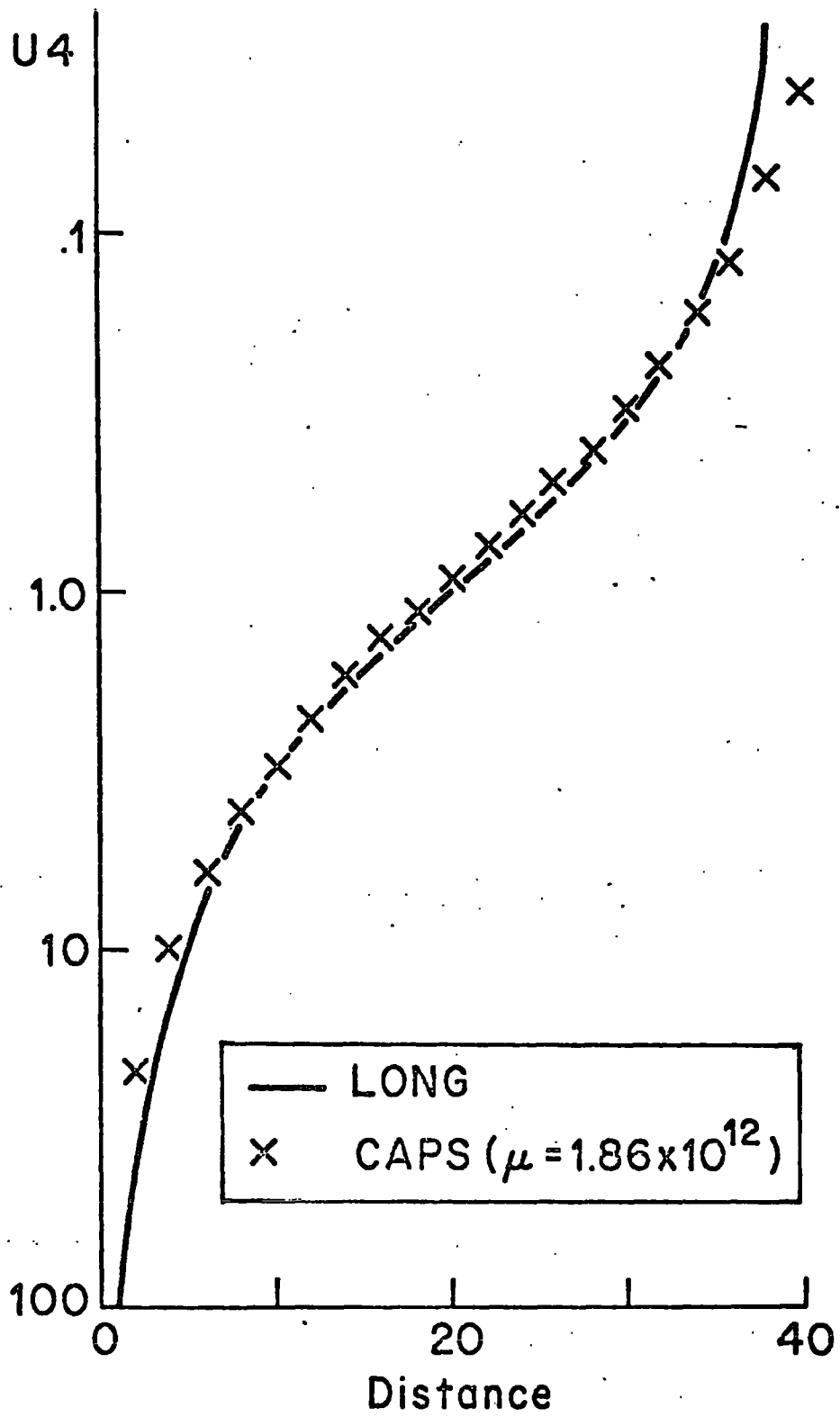


FIGURE (3-11) Elastic depression near the load- results for CAPS and LONG.

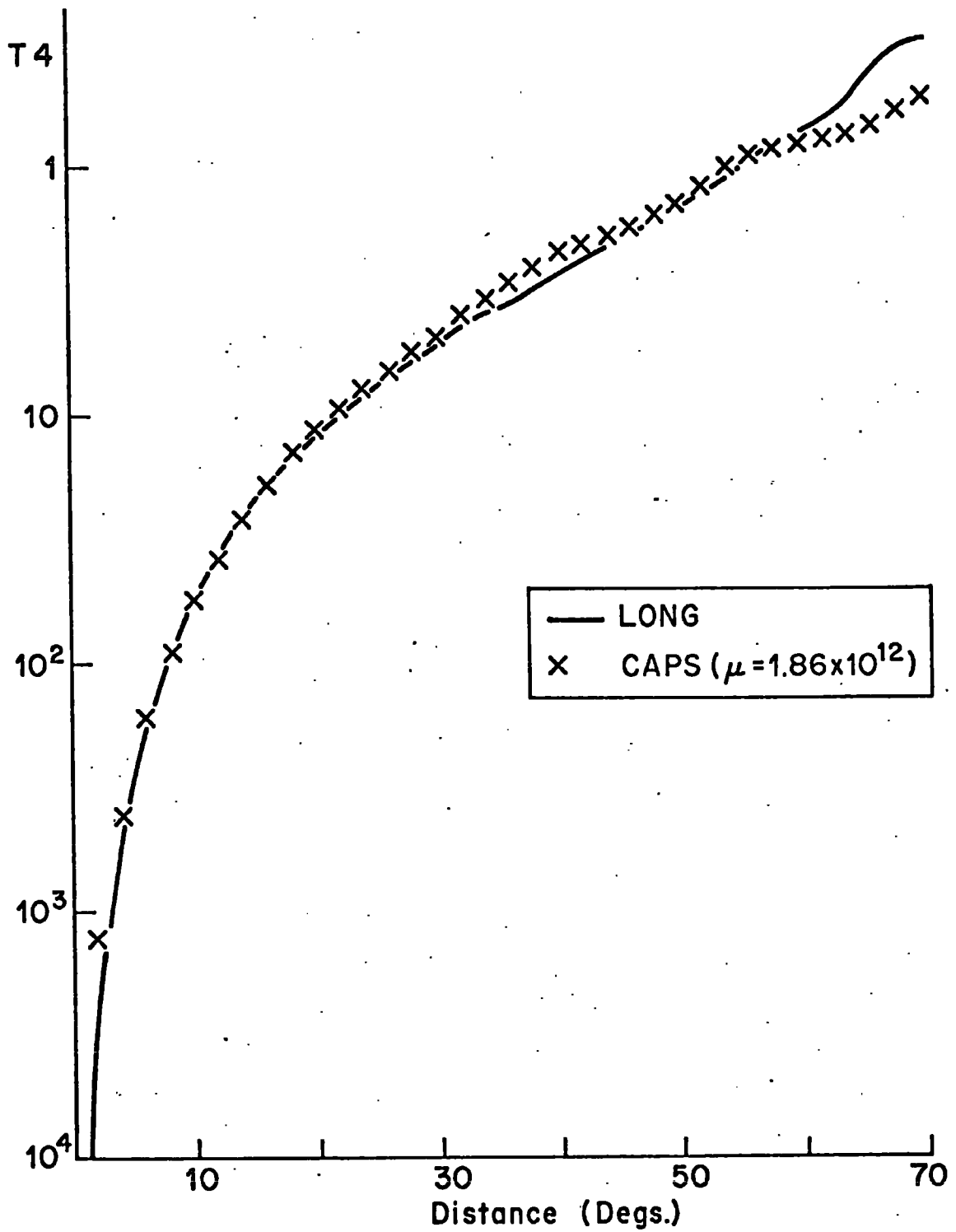


FIGURE (3-12) Comparison of total tilts near the load-results for CAPS and LONG.

and the total tilt  $T_4$  vary rapidly in this range and are reproduced here on a logarithmic scale. The agreement between LONG and CAPS results is very close down to within a few degrees of the load. We have previously seen that the elastic yield and tilt determined by CAPS agrees with that determined on the basis of the Boussinesq solution very close to the load. This result indicates that the LONG result too is valid in this range. We will look at this data in more detail later but before we do it is useful to consider the Burmister problem.

### 3-6-1 The Burmister Problem.

Burmister (1956) has treated the case of a point mass loading the surface of an elastic layer of thickness  $h$ , underlain by a rigid half space. We have reproduced in Table 3-2 numerical\* results presented by Poulos (1967) for the displacement of the first surface assuming several different values for Poisson's ratio. The 'influence factor' used in the tables is defined by the equation:

$$I = \rho^2 r h E / P \quad (3-28)$$

where  $I$  is the influence factor,  $\rho$  is the vertical displacement of the upper surface,  $h$  is the thickness of the upper layer,  $E$  is Young's Modulus and  $P$  is the force exerted by the point load at  $r=0$ .

It can be seen that the displacement falls to zero for  $r/h > 1.5$  (Table 3-2). Similar results are found for the stress exerted on the surface of the underlying layer (Poulos Table 1, 1967); the stress is zero for radii greater

than 1.5 h. The present problem is to calculate the surface deformation due to point-mass loading of a shallow layer of low mean rigidity underlain by a non-rigid half space. We want to determine the distance beyond which the effect of the first layer is negligible. If we assume that the underlying layer does not yield, then Burmister's results indicate that this distance is 1.5 h. The actual yielding of the underlying layer can be calculated using the solution given in the previous section for the infinite half space, assuming for the load a mass distribution determined by the stress distribution given by the Burmister result. We can approximate this load by a square surface mass of side 2 h. It can be shown that the horizontal attraction of this mass distribution beyond a distance of 3 h is approximately the same as a point distribution of equal mass. Thus, this is the distance beyond which the effect of layers to a depth of h is negligible.

In Table 3-3 I have reproduced part of the table of physical properties presented by Alterman et al (1961) for the Gutenberg Earth Model. It will be seen that the rigidity of layers deeper than 38 kilometers is uniformly near  $0.7 \times 10^{12}$  throughout the first 300 kilometers. From the Burmister results the influence of layers less than 38 kilometers in depth is negligible at distances greater than 114 kilometers, or approximately one degree. Thus the minimum effective rigidity for distances from the load greater than one degree would be expected to be about  $0.7 \times 10^{12}$ .

### 3-6-2 Comparison With Other Results.

We have seen that the results determined by program LONG become increasingly uncertain as the distance to the load is decreased. The extrapolation method described in Section 3-4-1 produces well-behaved results to within one degree of the load but it remains to be shown that these extrapolated results are accurate. In Fig. (3-13) I have reproduced the ratio  $T_4/T_3$  from both the LONG and CAPS results for the distance range 0-28°. The same ratio has been determined for the infinite half-space Earth, computed from the Boussinesq solution assuming the elastic constants shown in the figure. The LONG results appear reasonable; a straight line extrapolation from the LONG data intersects the zero-distance axis near 3.5 which, as pointed out in the last section, is the largest value expected for distances greater than 1 degree. The CAPS results are determined on the basis of a homogeneous shell of rigidity  $1.86 \times 10^{12}$  (dynes/cm<sup>2</sup>) which is much too hard to be representative of that part of the mantle concerned when the site is within a few degrees of the load. As expected therefore the CAPS ratios appear too small.

Until recently the only additional evidence on the response of the Earth to surface loads in the distance range 0-10 was the empirical determinations of Nishimura (1950) and the theoretical results of Takeuchi (1950) who considered the problem of surface loading on a semi-infinite elastic body with elastic constants which were a particular

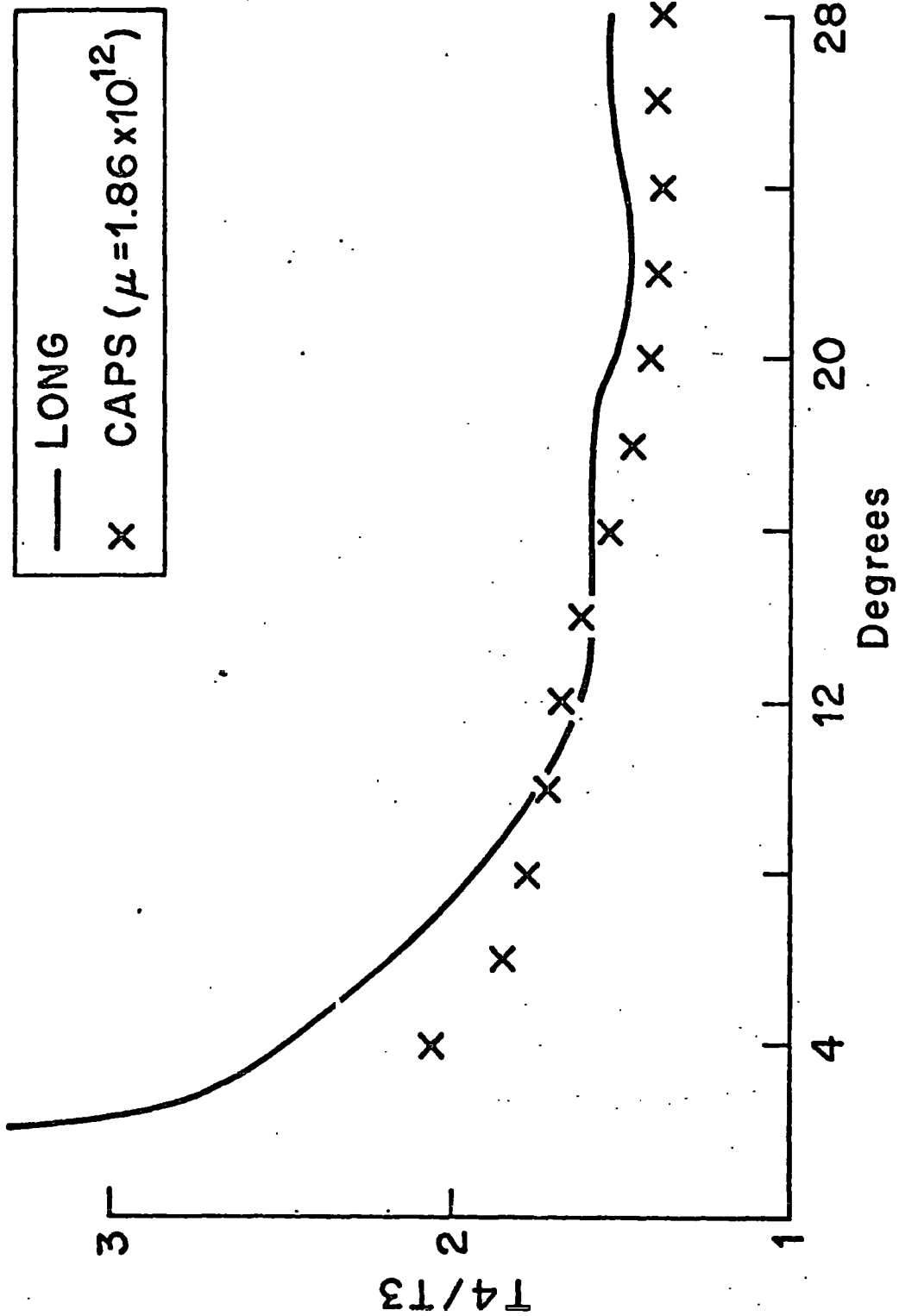


FIGURE (3-13) Comparison of tilt ratios near the load-results for CAPS and LONG. (The ratio T4/T3 is used in the analysis as a Green's function for determining tilt).

exponential function of depth. Recently however the finite-element method (Zienkiewicz, 1967) has been applied with great success to the general problem and preliminary results have been obtained by Beaumont (1971) for the surface displacement near a load on a Gutenberg earth. Beaumont's results are shown in Fig. (3-14) together with results determined by CAPS and LONG. From the displacement we have computed the tilt ratio  $T_4/T_3$  and this is shown in Fig. (3-15) together with tilt ratios determined by Nishimura and by Takeuchi. The tilt ratios shown previously for LONG are reproduced here also. The gravity perturbation ratio  $G_4/G_1$  is shown for the  $0-30^\circ$  region of the LONG result in Fig. (3-16).

It can be seen that the LONG and Beaumont results for displacement agree fairly well throughout the range  $10-14^\circ$  shown in Fig. (3-14). The Beaumont results would be expected to fall below (show a smaller displacement than) those of LONG where the effect of uplift, which is not considered by Beaumont, becomes important. This uplift is not determined separately in the LONG implementation since the load deformation coefficient contains both the uplift effect and the elastic yield. It is determined separately in program CAPS although subject to the assumption that the Earth is homogeneous and of mean rigidity 4.47 (see Eqn. 3-14). This is tabulated as U3 in the tables. The displacements shown for Beaumont's results in Fig. (3-14) should be decreased for the uplift effect which is approximated by U3. The

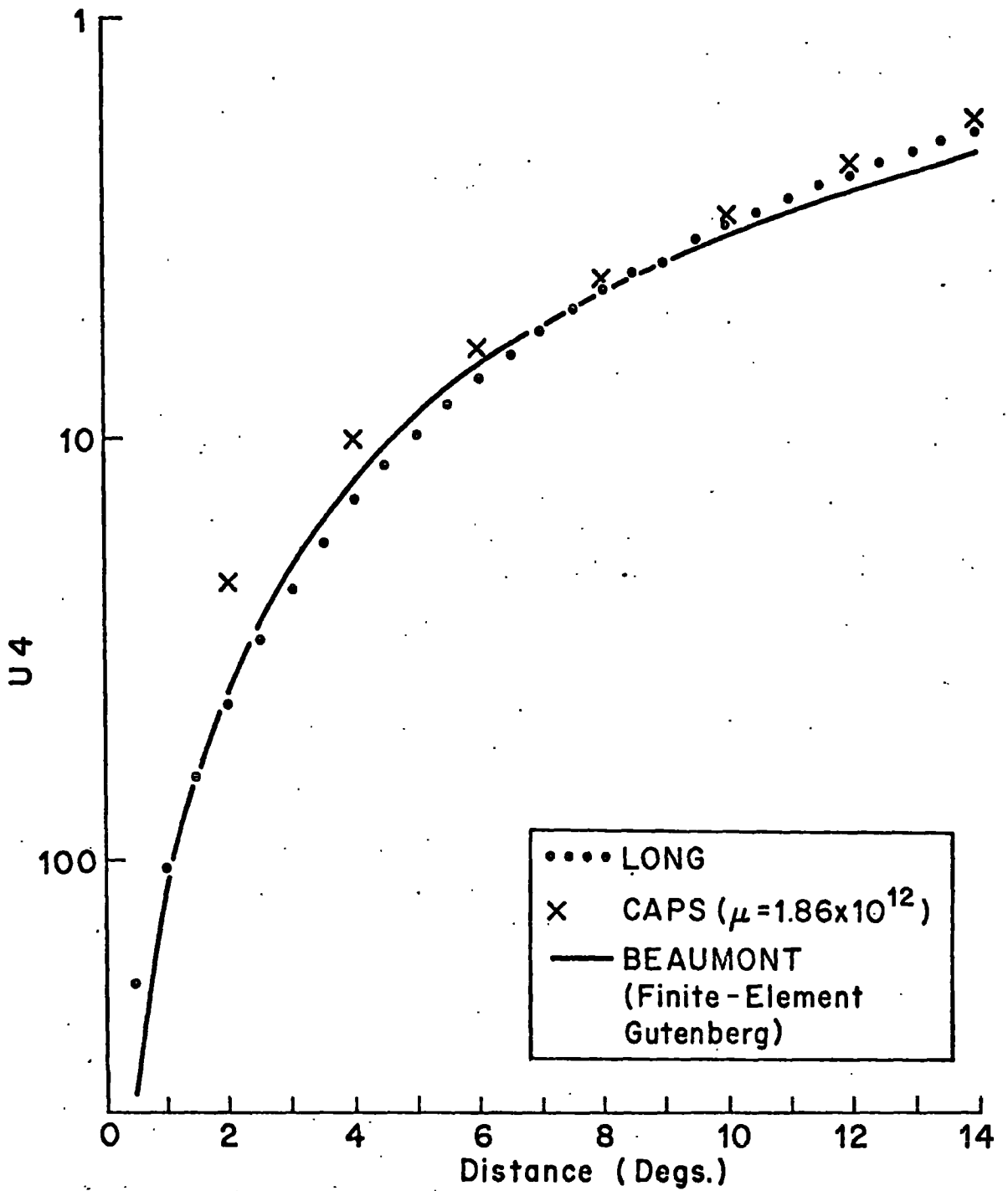


FIGURE (3-14) Depression near the load- results for CAPS, LONG and Beaumont.



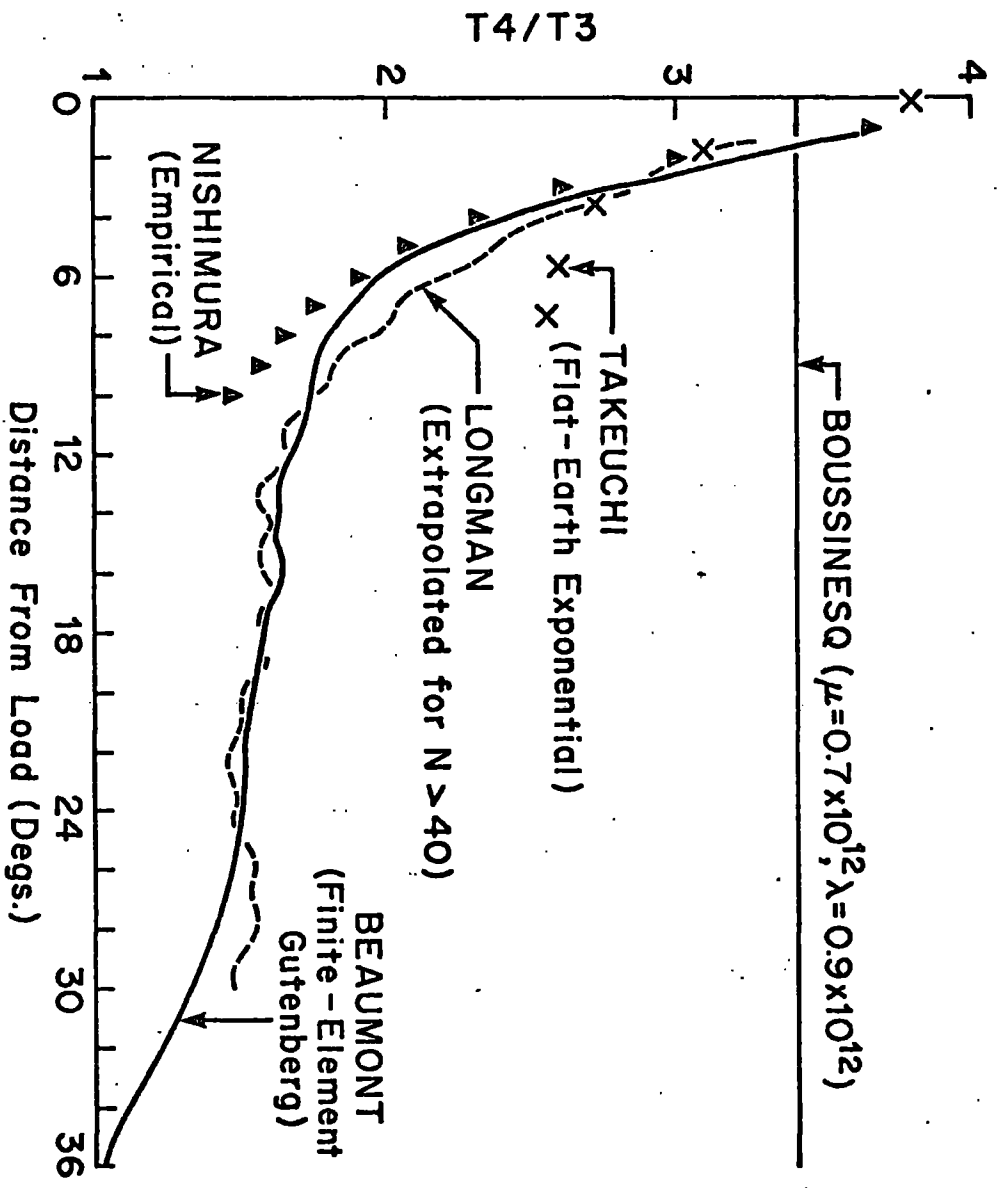


FIGURE (3-15) Tilt ratio(Green's function) near the load-comparison of several results.

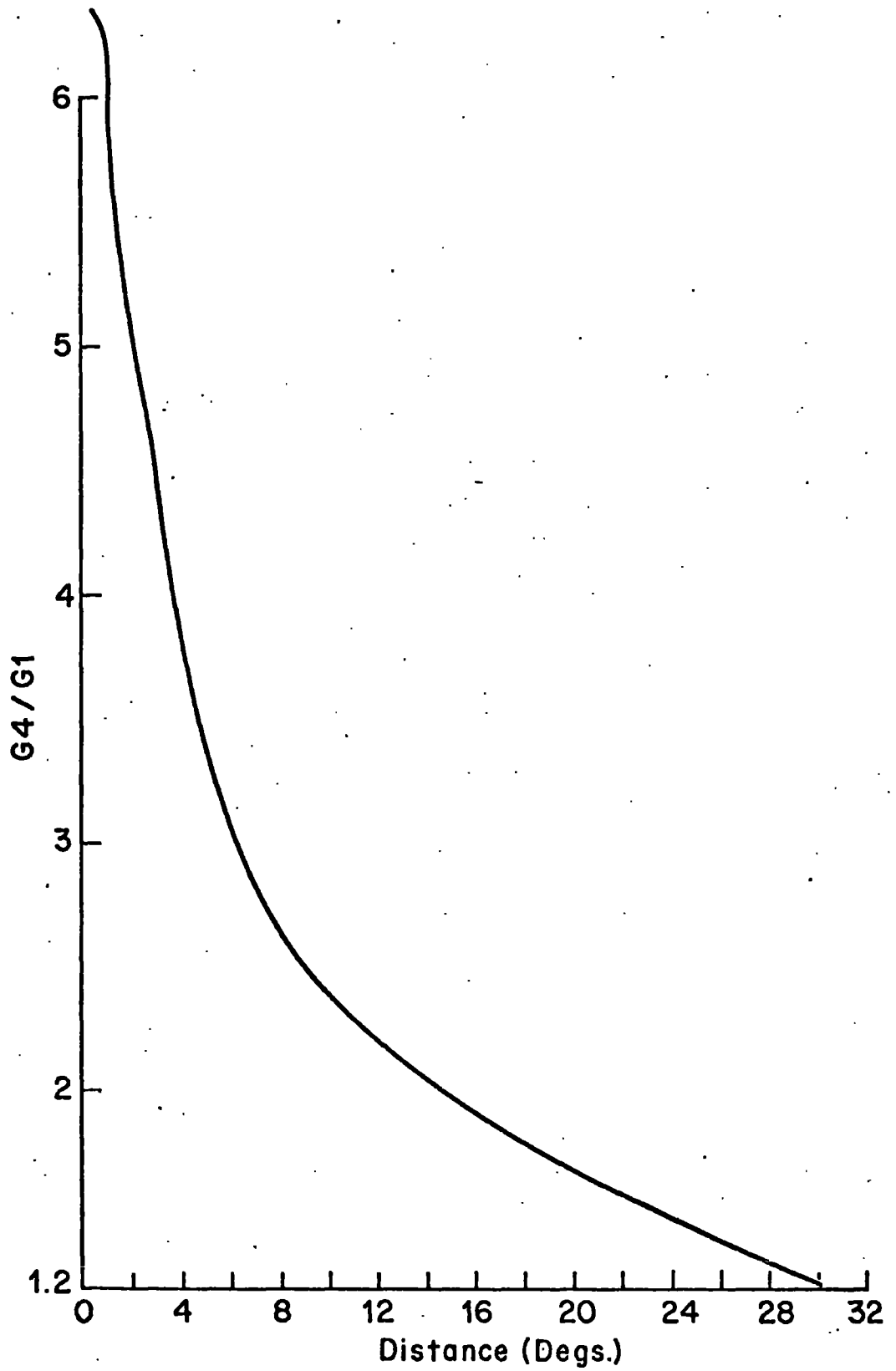


FIGURE (3-16) Gravity perturbation ratio (Green's function) near the load.(extrapolated LONG result).

displacements determined by Beaumont then appear too small with respect to the LONG results for distances greater than about  $7^\circ$ . In this particular Beaumont model however the Earth is assumed to be held fixed at the the distance  $\theta=90^\circ$ . This may explain the result here. The effect should be negligible closer to the load than  $7^\circ$ . The CAPS result shows the effect of a rigidity which is increasingly too large as the distance is decreased.

Tilt factors are compared in Fig.(3-15) for five results. The Beaumont and LONG results again agree quite well although, as previously mentioned, this may be fortuitous because gravitational uplift has been neglected by Beaumont. A valid comparison of the various results can be made best in the region between  $1^\circ$  and  $5^\circ$ ; that is, beyond that distance where the effect of the crust is shown by Beaumont's method. In the range  $1^\circ-4^\circ$  the Takeuchi and LONG results are virtually identical. This is convincing evidence for the validity of the LONG result since the Takeuchi function was determined theoretically on the basis of a flat Earth and a distribution of elastic constants which approximates that of Gutenberg's model to a depth of 1200 kilometers but omits the crust. The LONG implementation too would be expected to leave out the effect of the crust because the load deformation coefficients for large  $n$  were obtained by simple extrapolation from mantle-effective values. The flat-Earth assumption and the use of fictitious elastic constants for depths greater than 1200 kilometers

are the reasons for the failure of the Takeuchi function beyond about  $4^\circ$ . The Beaumont function, which includes the effect of a crust, does not disagree with Takeuchi and LONG results in this range. The result determined by Nishimura is of interest. This function was determined experimentally by Nishimura as that which best fitted more than two years of differential tilt measurements carried out in Japan. This differential method of treating a series of tilt measurements made throughout a small region does not seem to have been repeated by others. The basis for the method is that the difference between the tilt measured at two or more neighboring sites is relatively free of distant ocean-tide loading effects. Nishimura assumed that  $T_2/T_3$  was a constant equal to 0.5 and obtained the best fit to  $T_4/T_3$  to be:

$$T_4/T_3 = 0.5 + (12.6/[r+3]) \quad (3-30)$$

where  $r$  is the distance to the load in degrees. We have seen that the function  $T_2/T_3$  is in fact very different from 0.5, especially near the load, but this does not alter the validity of Nishimura's result for  $T_4/T_3$ .

Finally, in Fig. (3-16) the behaviour of the gravity perturbation ( $G_4/G_1$ ) is shown. I know of no previous results with which this could be compared, especially with regard to the region within  $10^\circ$  of the load.

CHAPTER 4

PREDICTION OF THE OCEAN-TIDE EFFECT

4-1 Introduction

In the previous chapter I described a method of determining the gravitational attraction of the ocean tide on a horizontal plane. I then used the Boussinesq solution for the elastic displacement of a plane due to a point-mass surface load to determine the displacements due to the load of the ocean tide. The Boussinesq solution in this way is used as a Green's Function and the displacement is determined by convolution with the gravitational attraction over the surface. Later in the same chapter the loading effects of a point mass located on a spherical, Gutenberg-model Earth are derived and these too may be considered as Green's Functions determining the effects of an arbitrary distribution of loading masses on the spherical Earth. Values determined for these Green's Functions are summarized in Table (4-1). The tilt-ratio function varies rapidly when the distance is less than  $1^\circ$ , reflecting the influence of the crust, and in this region the function has been determined at 5 km intervals and is shown in Figure (4-1). This latter data has not previously been presented; it was obtained from Beaumont's solution for a finite-element Gutenberg Earth using a 10 km mesh interval and a load of radius of 10 km. This is not quite the same Beaumont solution discussed in the previous chapter; a smaller mesh interval and load radius were assumed for a

(000-037)	(038-074)	(075-112)	(113-150)	(151-180)
632	144	35	-74	-118
334	143	31	-77	-118
305	142	28	-79	-118
287	141	25	-81	-118
255	139	21	-82	-119
237	137	18	-84	-120
219	136	15	-86	-121
204	134	11	-87	-121
195	132	8	-89	-122
181	130	5	-91	-124
177	127	1	-92	-126
165	125	-5	-92	-129
165	123	-6	-93	-131
158	121	-8	-94	-134
158	117	-13	-96	-135
157	115	-16	-96	-139
158	111	-18	-98	-143
159	107	-22	-99	-146
156	104	-25	-100	-149
156	100	-28	-101	-153
150	97	-32	-102	-155
150	93	-35	-103	-157
146	90	-37	-104	-159
147	87	-40	-106	-161
147	84	-43	-108	-163
151	81	-45	-109	-166
154	78	-48	-110	-167
154	75	-50	-111	-170
155	70	-52	-113	-173
149	66	-57	-113	-176
148	61	-58	-115	-179
151	57	-61	-116	-179
150	52	-64	-117	
150	49	-66	-118	
149	45	-68	-119	
148	41	-70	-119	
146	38	-73	-118	

TABLE (4-1b) Values of the Green's function for tilt.  
(Value x100 for each degree 0-180°)  
(Determined by LONG)

(000-036)	(037-074)	(075-112)	(113-150)	(151-180)
630	91	64	172	286
620	87	67	175	288
505	84	68	178	290
444	82	70	182	293
381	79	71	185	295
345	76	72	189	297
307	73	74	193	298
286	71	76	196	300
263	69	79	200	301
250	67	82	203	302
237	64	84	207	304
227	62	86	210	305
220	60	90	214	306
211	59	94	218	308
204	57	96	221	311
195	56	99	225	313
189	55	102	228	314
183	54	105	232	316
177	53	109	235	316
171	52	112	238	317
167	52	115	241	317
162	51	119	244	318
157	51	121	247	318
152	50	125	249	320
137	51	127	252	320
143	51	130	255	321
138	52	133	257	323
134	52	137	260	325
130	53	140	263	326
125	54	144	265	327
120	54	148	268	327
109	55	151	271	328
105	56	155	274	329
103	57	159	276	
100	59	162	279	
97	61	166	281	
93	62	169	284	

TABLE (4-1a) Values of the Green's function for gravity.  
(Value x100 for each degree 0-180°)  
(Determined by LONG)

0-100 kms	105-200 kms
625	339
620	338
610	336
594	336
578	335
558	335
533	334
506	334
476	334
445	333
416	333
393	332
375	330
361	331
350	330
344	330
340	330
340	328
340	327
340	326
339	

TABLE (4-1c) Values of the Green's function for tilt at 5 km intervals in the range 0-200 kms. (Values given are x100) (Beaumont preliminary solution for a Gutenberg model earth. (Beaumont, 1971)).

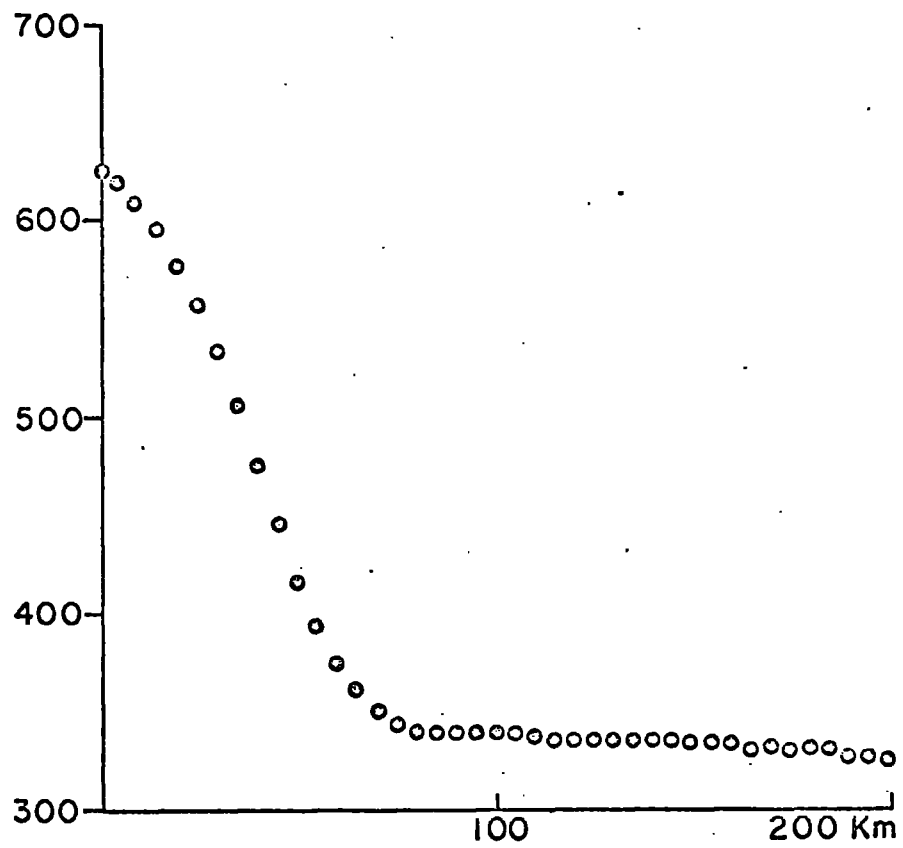


FIGURE (4-1) The Green's Function for Tilt. (Beaumont's preliminary solution for a Gutenberg earth)



better behaved solution in the critical region 0 to 200 km.

In this chapter I describe the method I have used to compute the gravitational attraction of the world-wide distribution of ocean tides and then, through the use of the Green's Functions, the calculation of the various loading effects.

#### 4-2 The Ocean-Tide Data.

Ocean-tide data is normally published in the form of contours representing lines of equal amplitude and phase. This representation can be conveniently digitized as a network of surface polygons containing regions of approximately constant amplitude and phase. This is the procedure I have followed here in digitizing world-wide data directly from published tidal maps. Each polygon was digitized and recorded according to the following format: Number of the polygon (3 figures), amplitude of the tide in centimetres (3 figures), phase lag of the tide in degrees relative to transit of the Moon at Greenwich (3 figures), the region of the Earth (1 figure), and the latitude and the longitude of each of the polygon points taken in clockwise order when viewed from above (up to 7 points at 10 figures per point). Each polygon can therefore be fully described on one 80 column card. The polygons used are listed in Appendix VIII. A discussion of the original ocean-tide data used together with figures showing the location of most of the polygons is presented below.

The polygons of region 0 were described and illustrated

(Fig.3-2) in the last chapter. This region is that affecting the many Earth-tide stations in Western Europe and for this reason it has been digitized in fine detail. Some small-scale polygons near Bidston (BID) are shown in Figure <sup>7-6</sup> (~~4-5~~). These are polygon numbers 1 through 12 and were drawn using data due to Lennon (1961). The tide assumed for the northern part of region 0 is of doubtful validity.

The main part of the North Atlantic is called region 1. The polygon map is reproduced in Figure (4-2). The original data from which the polygons were drawn is due to Hansen (1969) and is reproduced in Figure (4-3). The polygon map for region 3, the South Atlantic, is reproduced in Figure (4-4); the original data is due to Hansen (1969). Regions 3 and 4 are the North and South Pacific Ocean and are shown in Figure (4-5). \* The original data is due to Bogdanov (1961). Some polygons in region 3 near the west coast of North America were subsequently removed when this coastal region was included within region 6 which is described below.

Region 5 is taken as that water east of the southern tip of Africa, west of the east coast of Australia and south of Indonesia. The only ocean-tide data found for this region is that of Uneo (1964). Uneo solved the hydrodynamic equations for this region by finite difference methods using 5 meshes and neglecting bottom friction. The resulting data is not suitable for determining regional loading effects but should be adequate for determining global effects. The polygons for this region are simple 5° meshes and are not

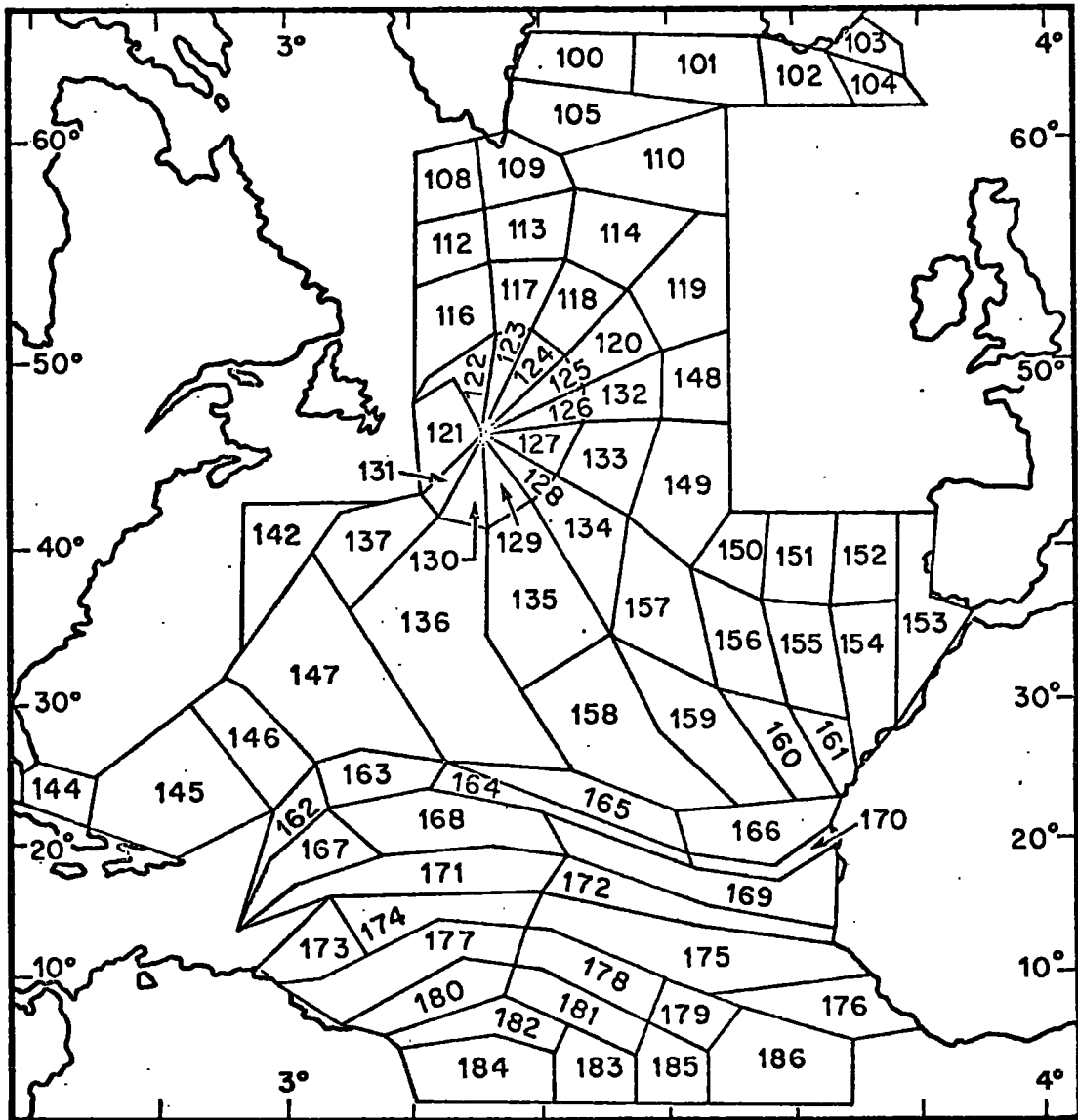


FIGURE (4-2) Ocean-tide polygons for the North Atlantic. (Region 1)

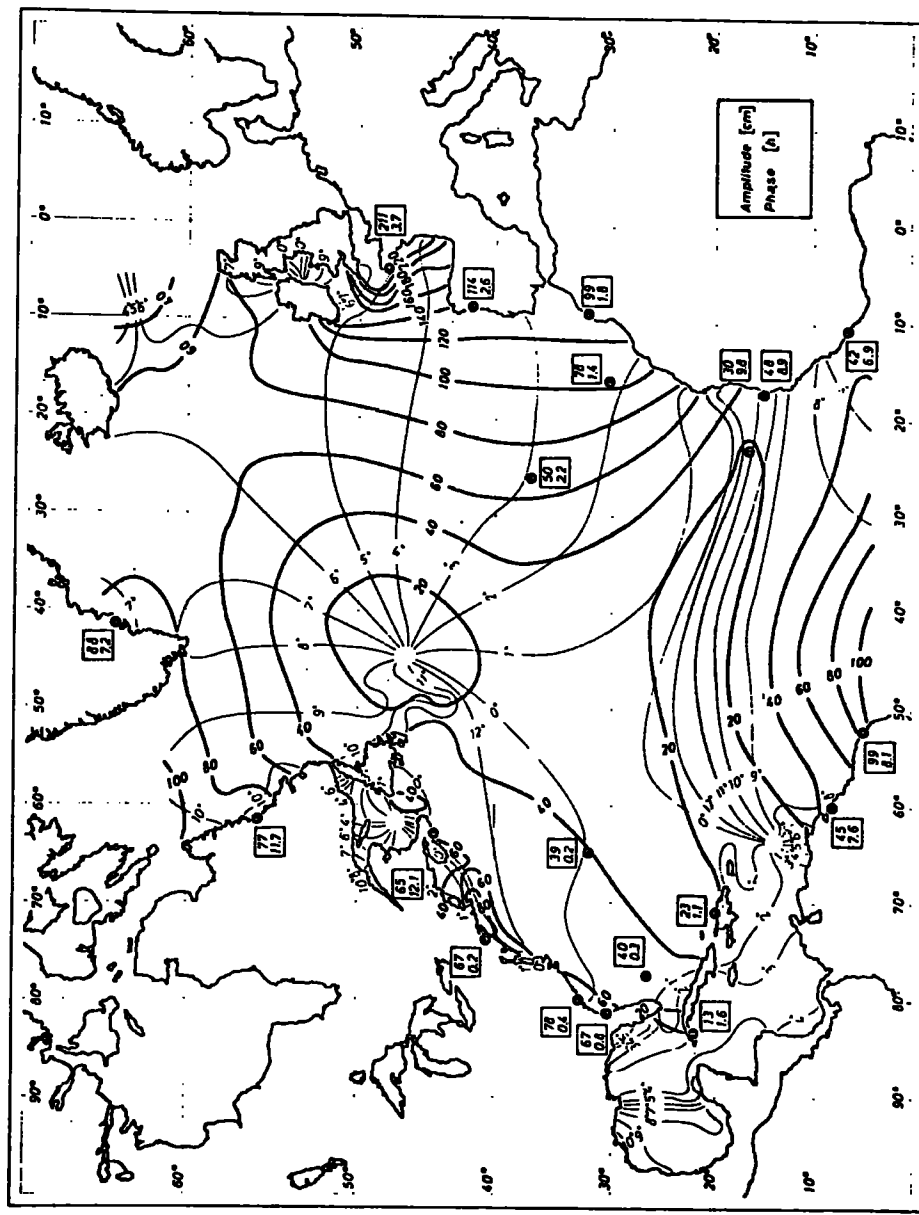
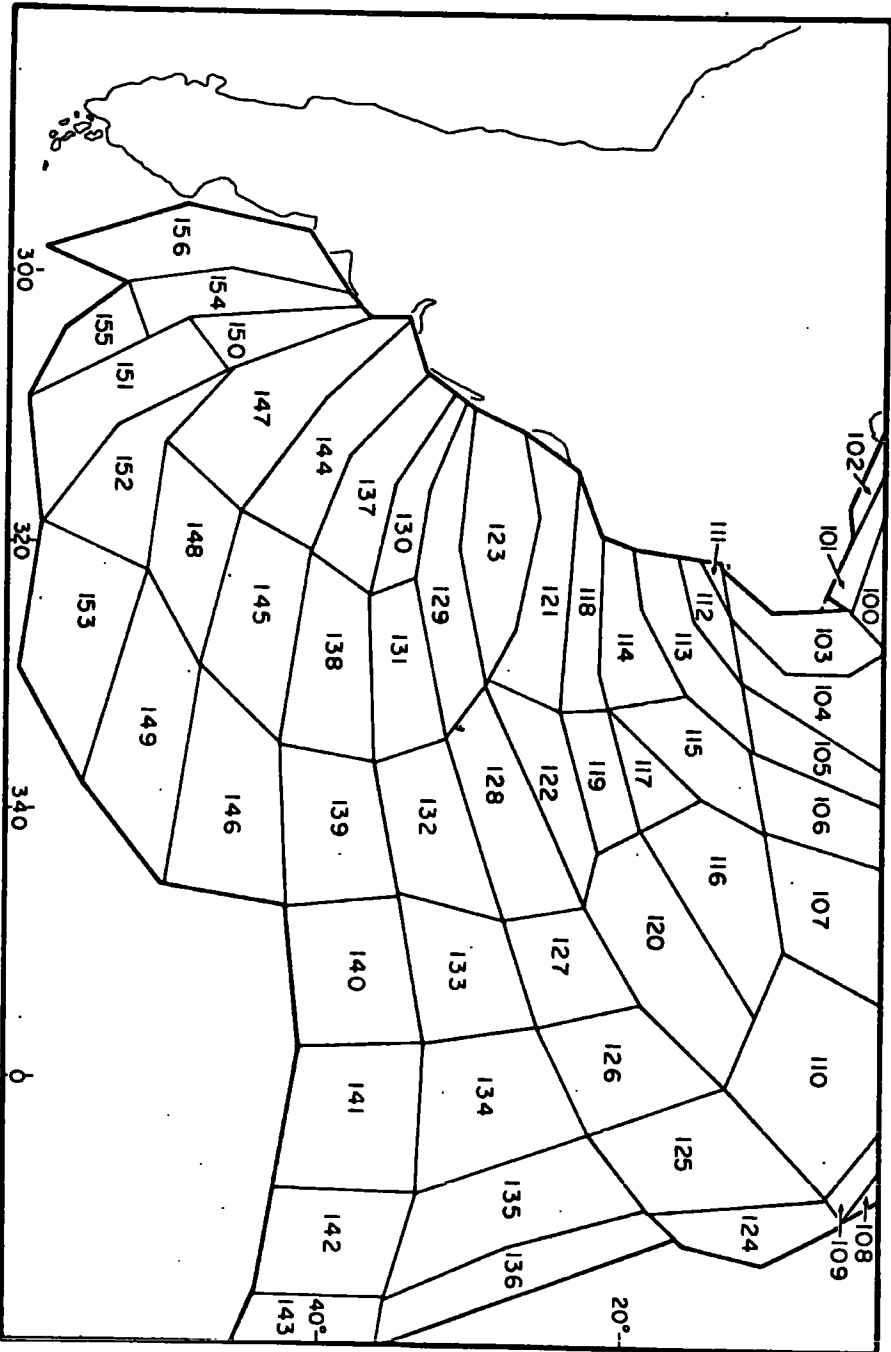


FIGURE (4-3) The ocean tide of the North Atlantic. (Hansen 1969)

FIGURE (4-4) Ocean-tide polygons for the South Atlantic. (Region 2)



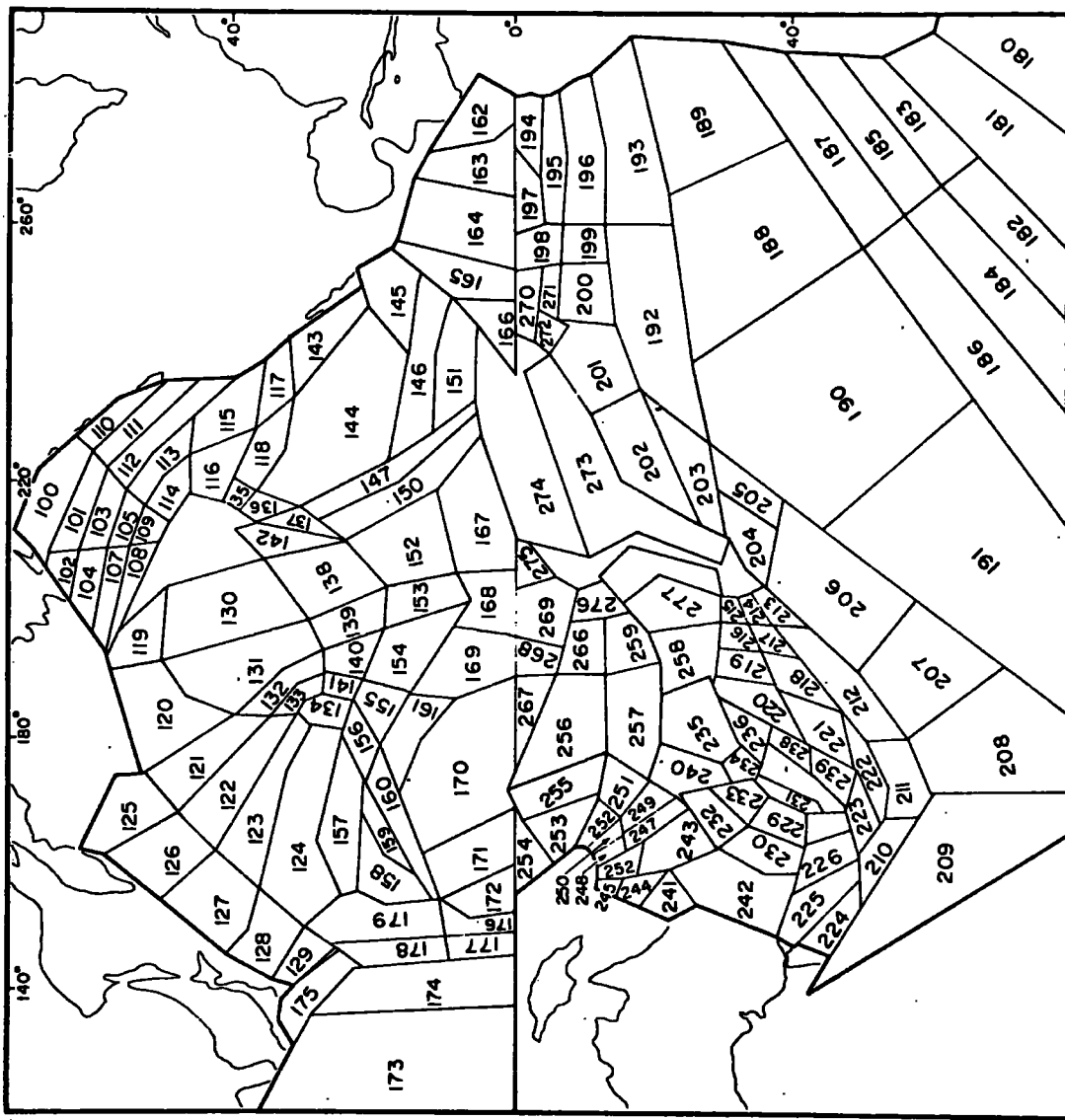


FIGURE (4-5) Ocean-tide polygons for the Pacific. (Regions 3, 4)

illustrated.

Region 6 includes much fine detail about the North American continent. Figures (4-6,7,8) illustrate the polygons assumed for the waters of off-shore eastern Canada, Hudson Bay and Straits, and Davis Strait respectively. The original data for these results is due to Dohler (1964). Figures (4-9,10) show the part of region 6 bordering the east coast of the United States and the Gulf of Mexico. Original data is that of Hansen (1969) with near-shore detail due to Emery (1970).

There are many tidal charts for the Pacific Ocean. Munk et al (1970) have summarized the most recent ones in charts which I have reproduced in Figures (4-11,12). The tidal distribution which we have assumed previously for the Pacific Ocean\* is that of Bogdanov (1962). It is not shown but it is very like that of Bogdanov et al (1964), shown in Figure (4-12), with the amphidromic point situated near 42 north latitude. The tidal data shown by Munk et al in Figure (4-12) is the first determination made on the basis of deep-sea tide measurements. The evidence for the existence of the amphidromic point shown by them appears strong and consequently I have removed the polygons determined previously for this area and replaced them with new polygons designed to fit Munk's results. The resulting polygon map is incorporated in region 6 and is illustrated in Figure (4-13).

Region 7 includes the Mediterranean, Adriatic and Red

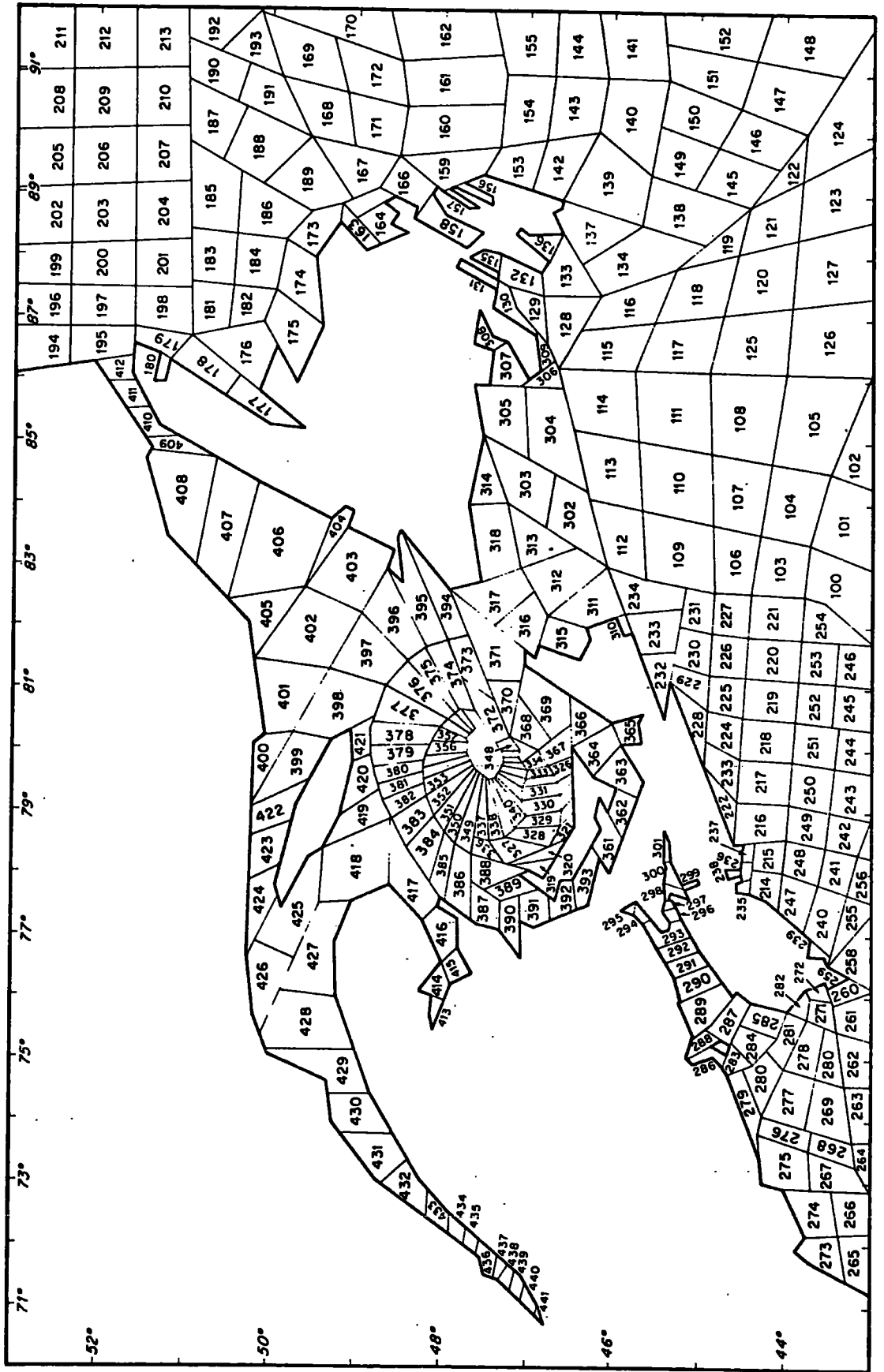


FIGURE (4-6) Ocean-tide polygons for Eastern Canada. (Part of Region 6)



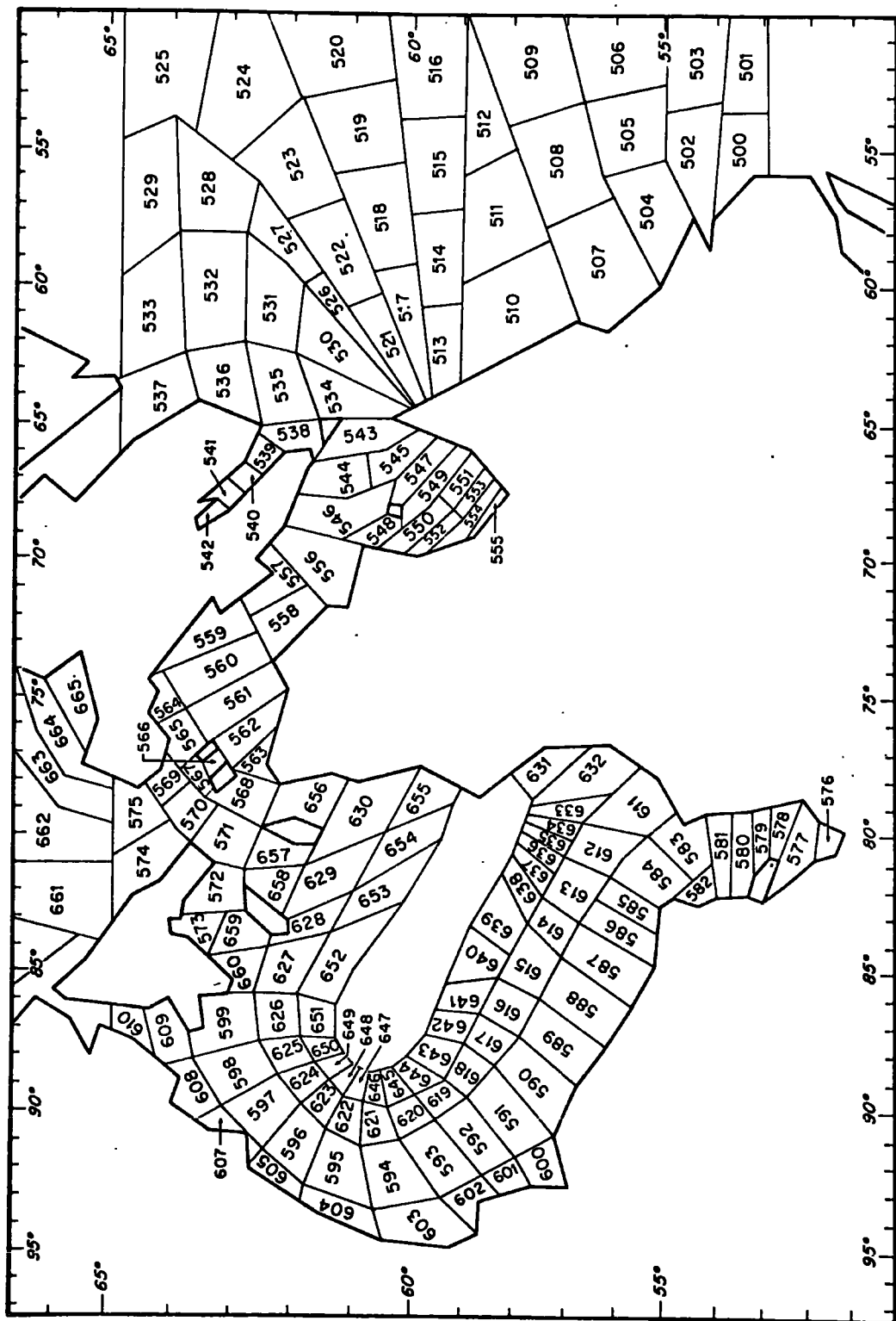


FIGURE (4-7) Ocean-tide polygons for Hudson Bay and Straits. (Part of Region 6)

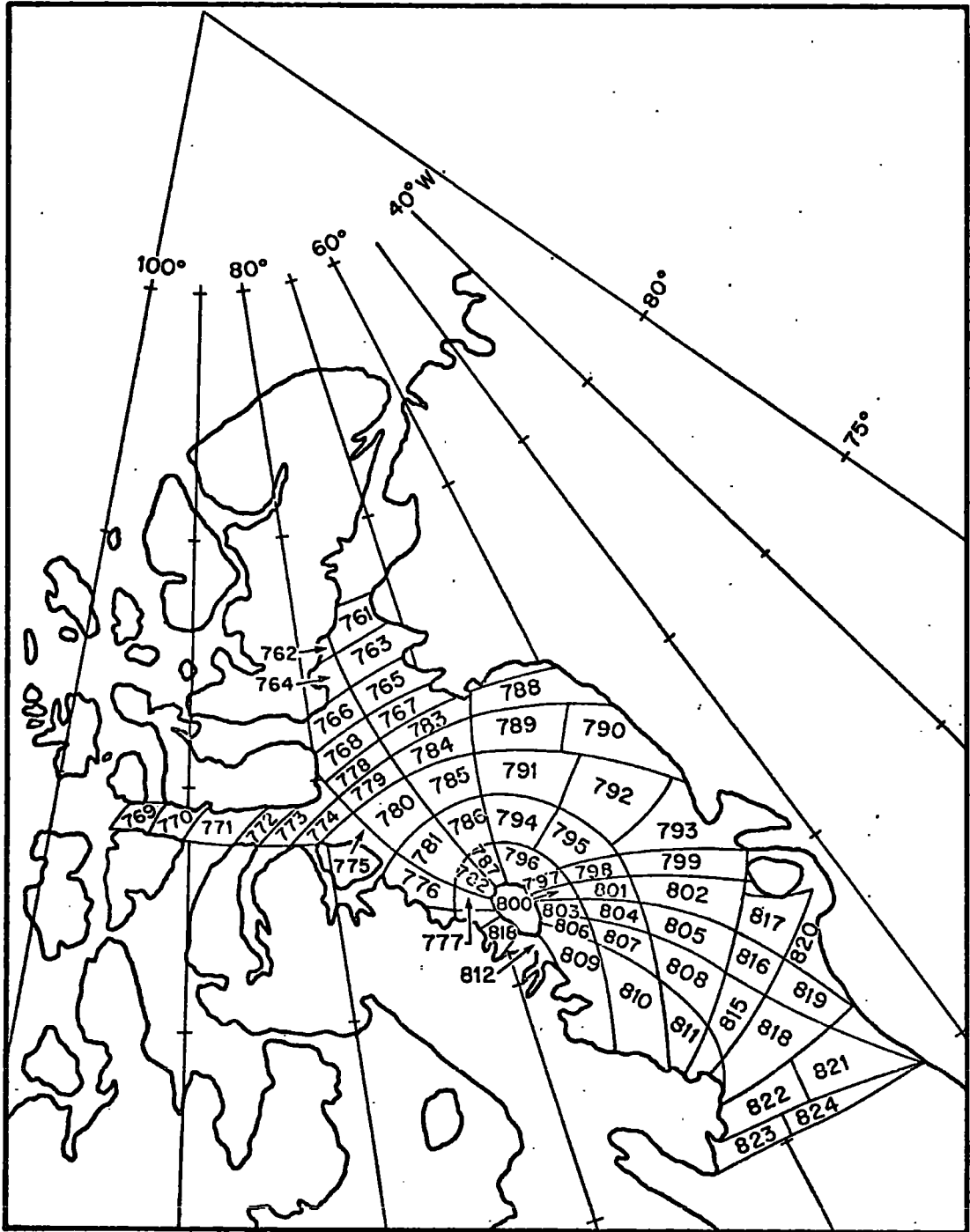


FIGURE ( 4-8) Ocean-tide polygons for Davis Strait.

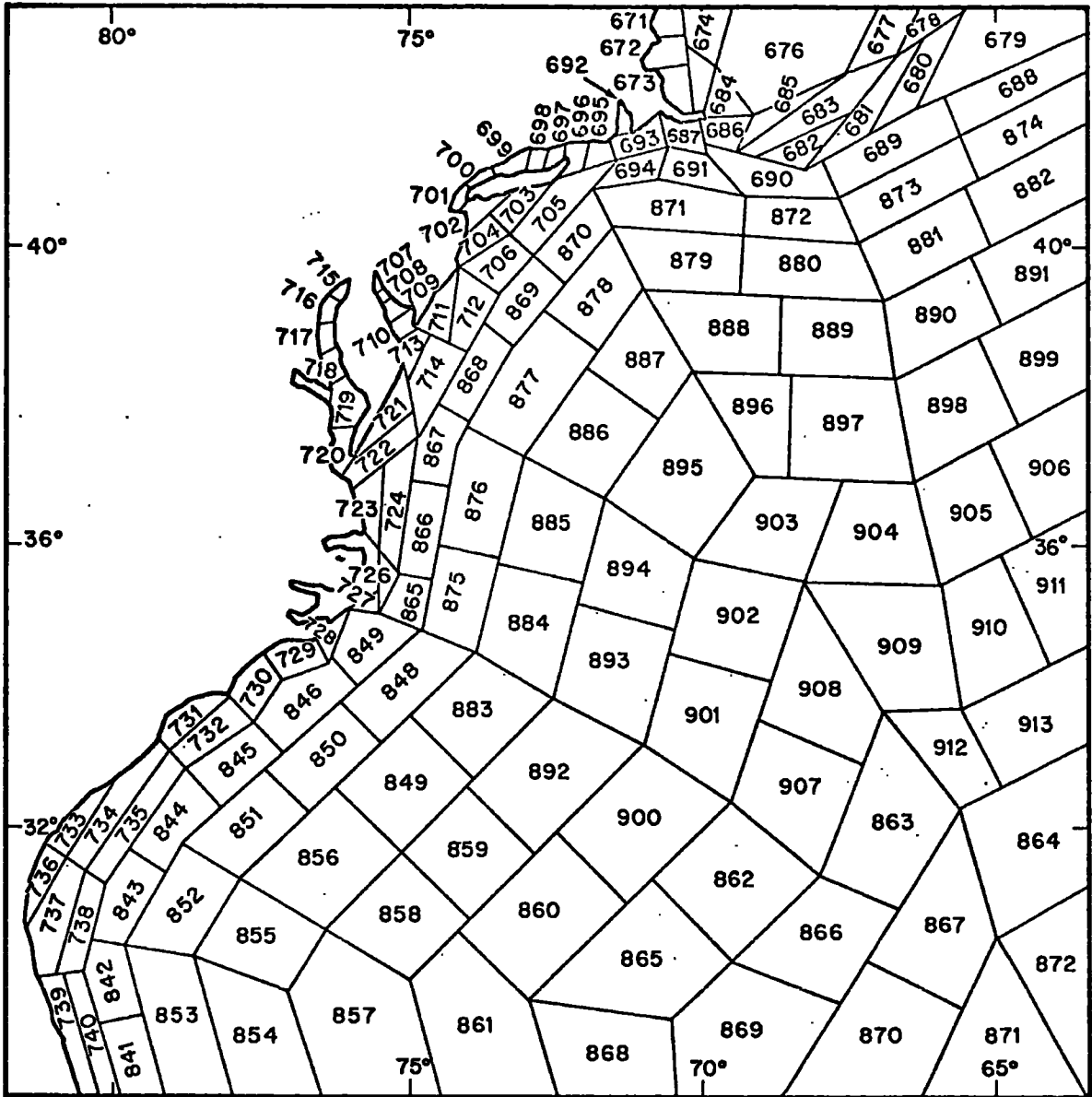


FIGURE (4-9) Ocean-tide polygons for U.S. East Coast.

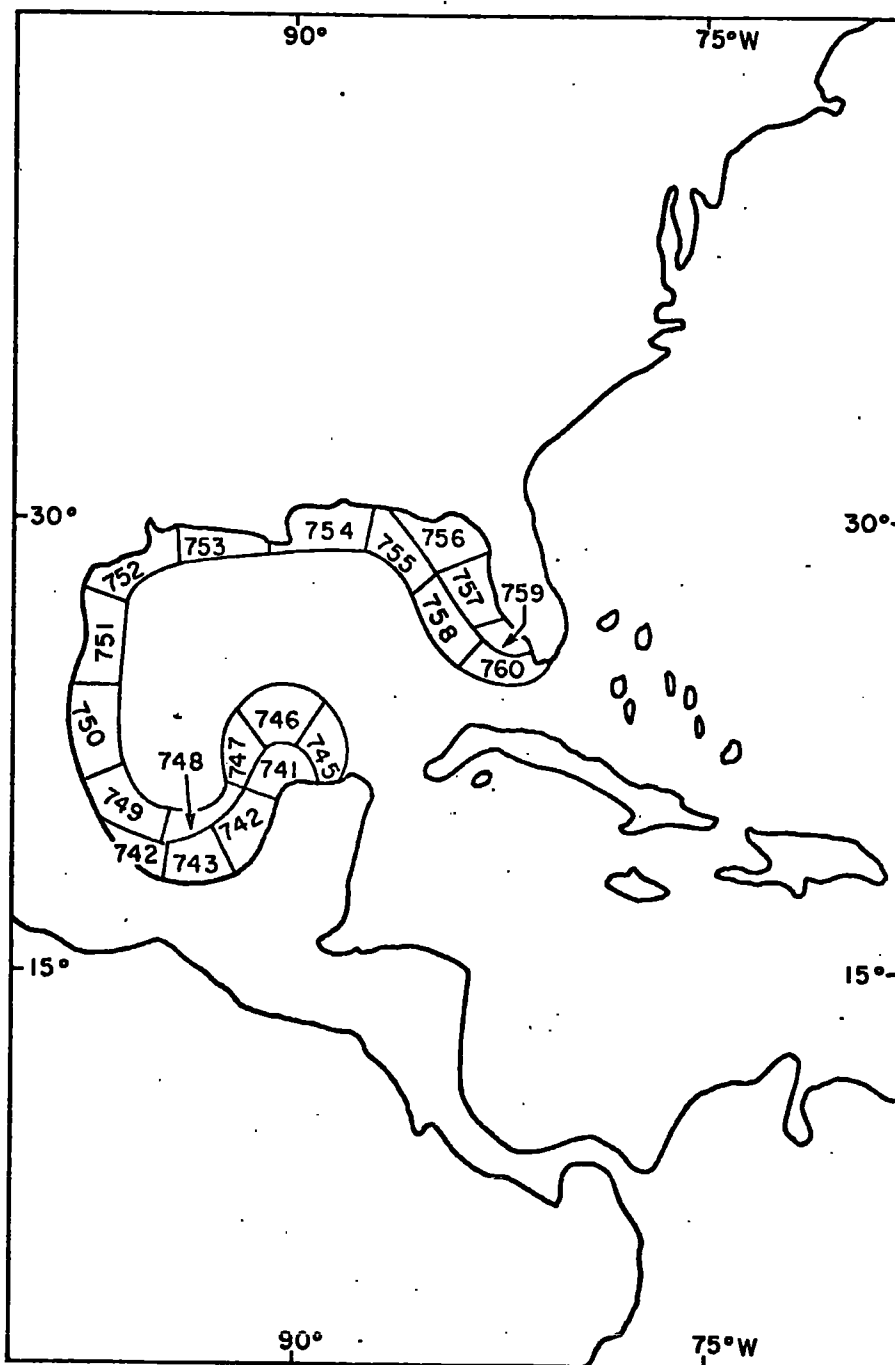


FIGURE (4-10) Ocean-tide polygons for Gulf of Mexico.  
 (Part of region 6.)

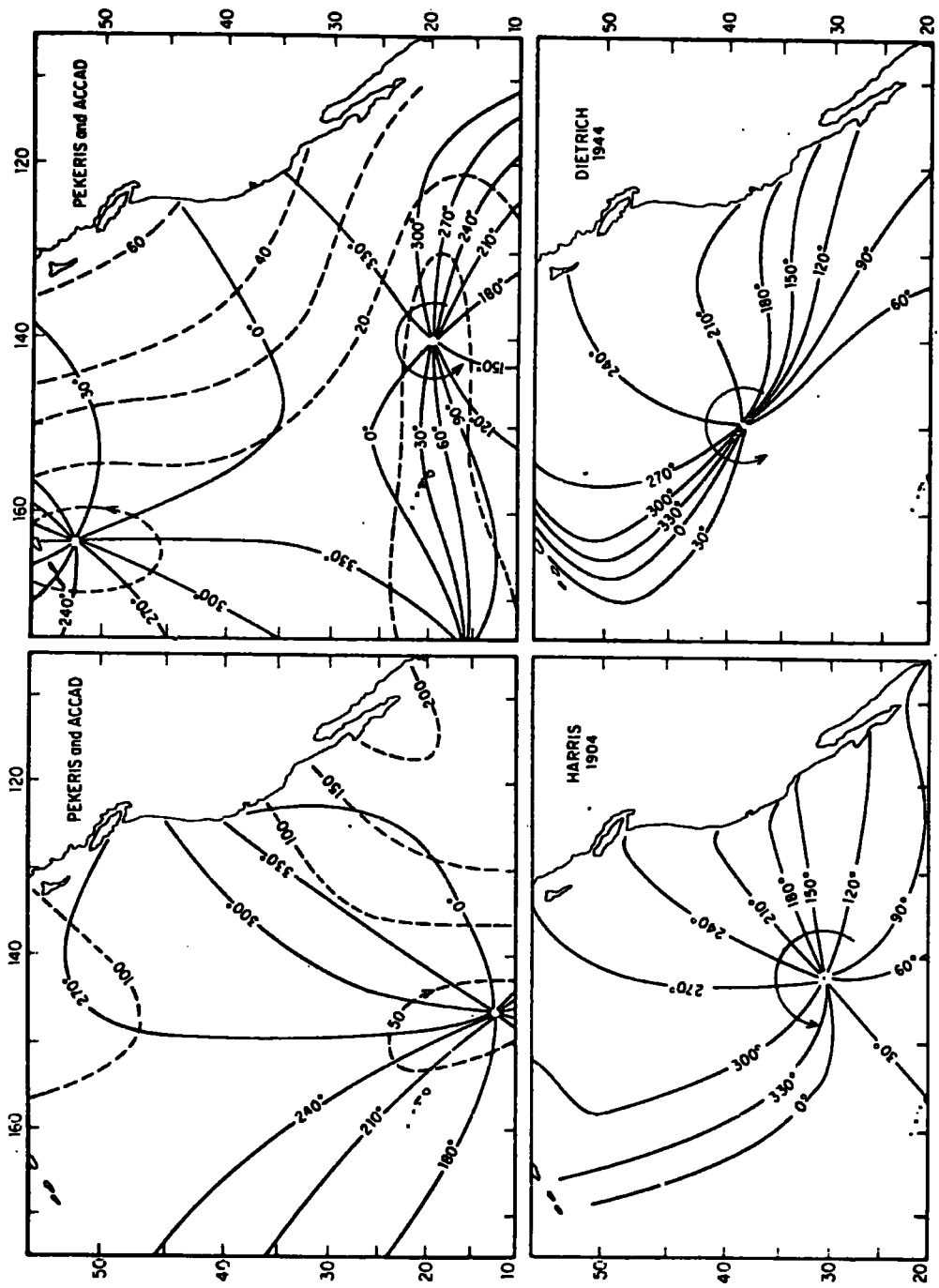


FIGURE (4-11) Tidal charts for the Pacific. (Summarized by Munk et al 1970)

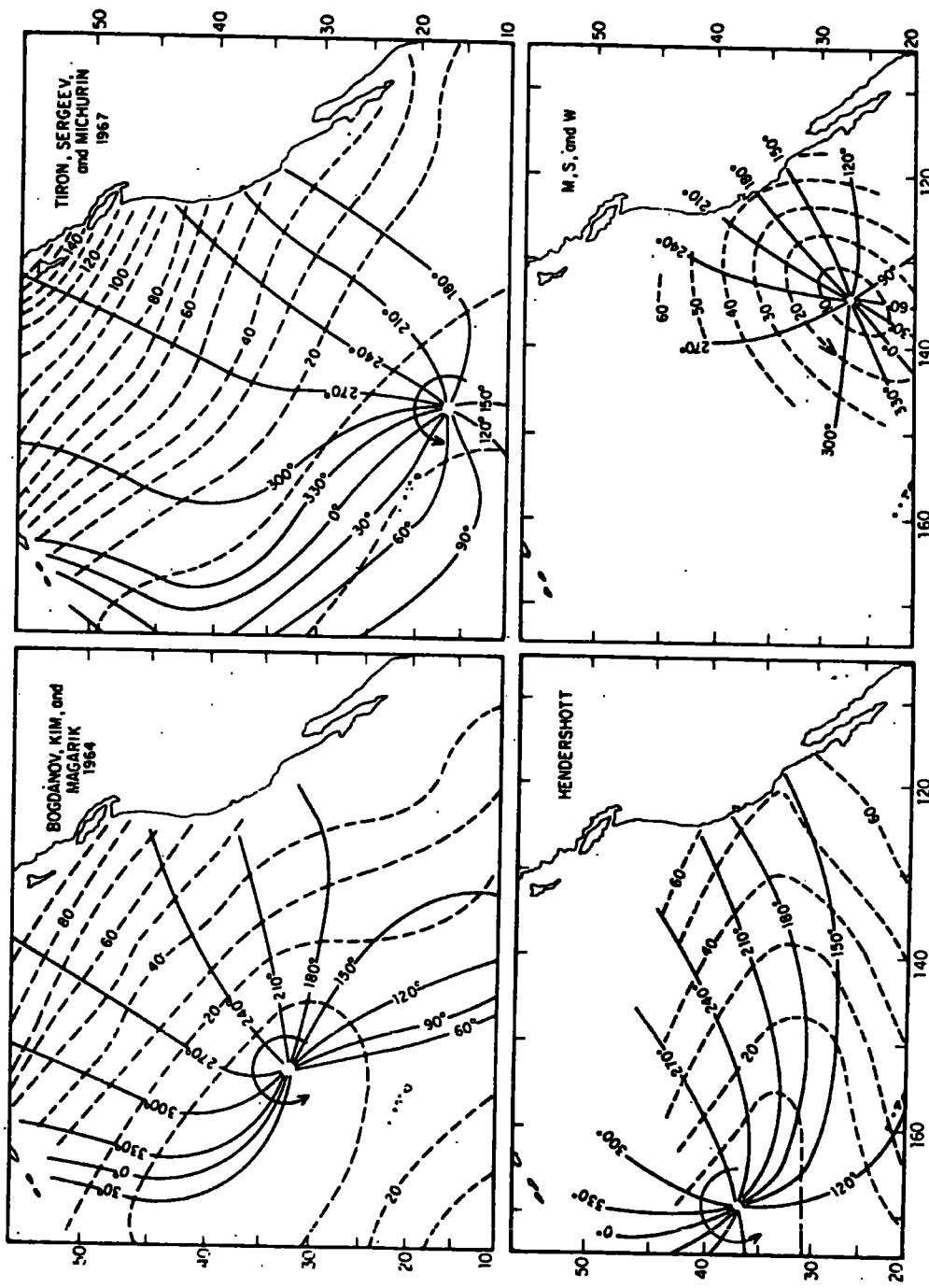


FIGURE (4-12) Tidal charts for the Pacific. (Summarized by Munk et al 1970)

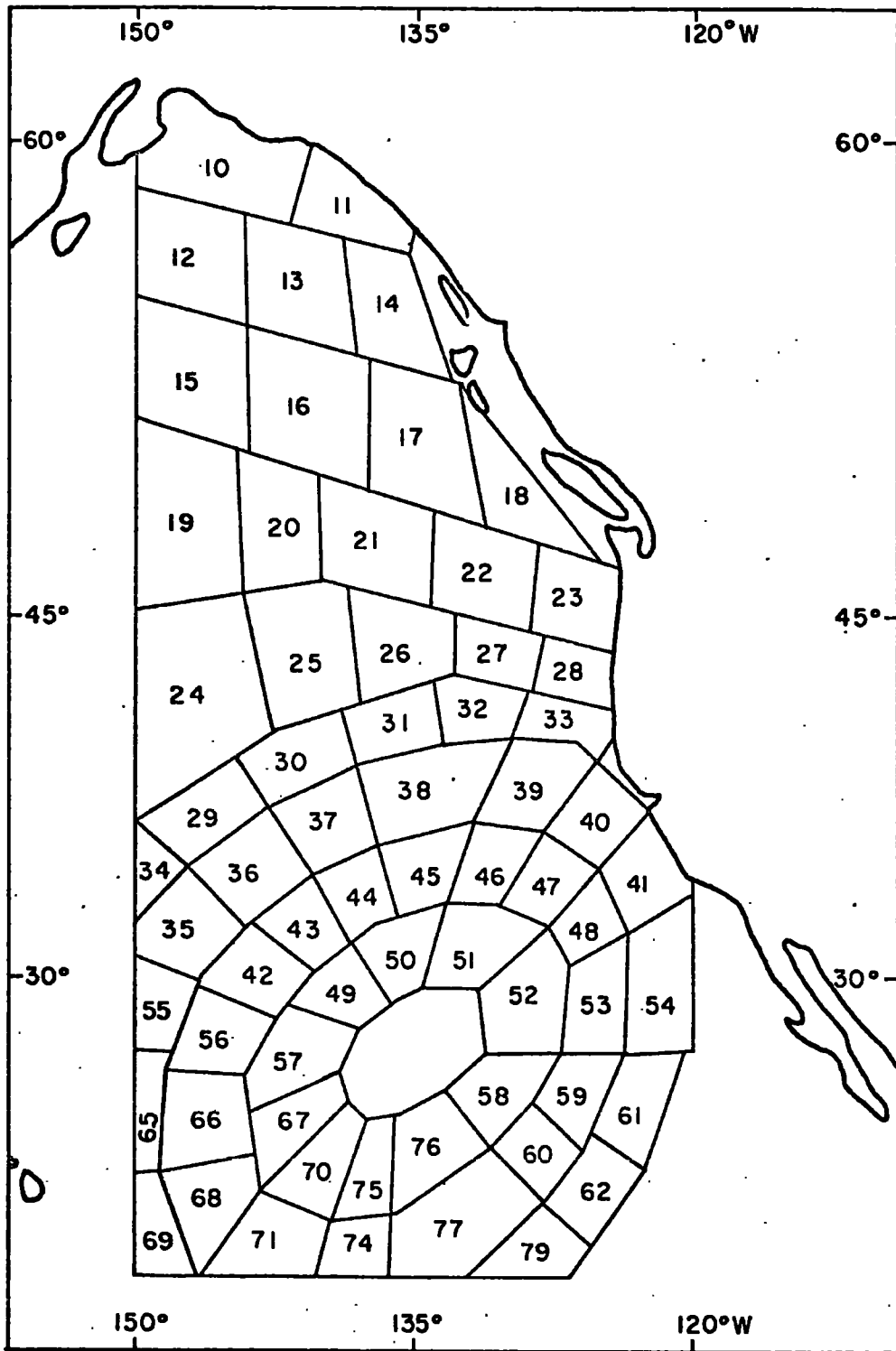


FIGURE (4-13) Ocean-tide polygons for the Pacific to fit M,S and W results of Fig. (4-12)

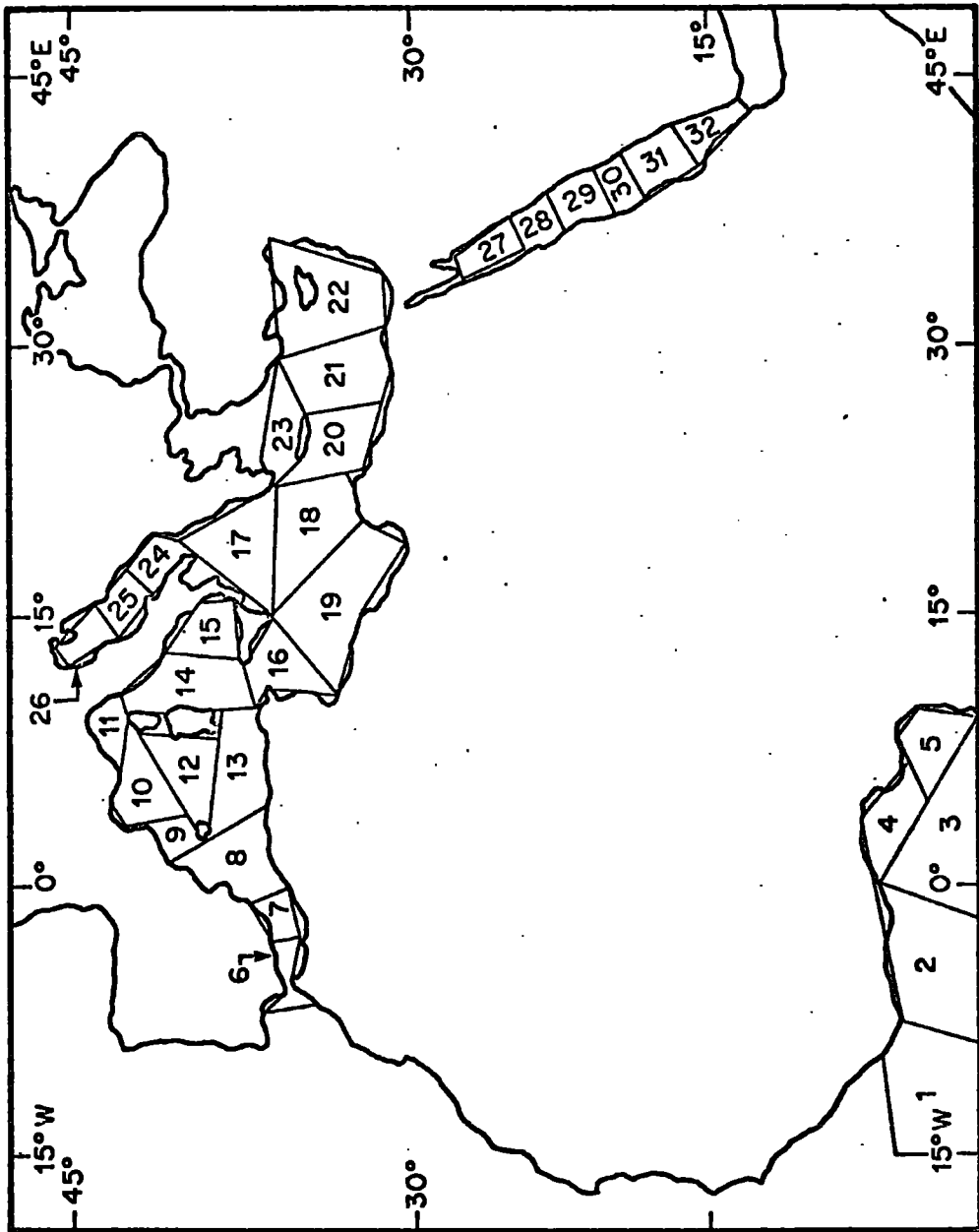


FIGURE (4-14) Ocean-tide polygons for the Mediterranean area. (Region 7)



Seas. The original data was drawn from Defant (1961). The polygons are shown in Fig. (4-14).

Region 9 is an alternative interpretation of that part of region 6 in the Pacific Ocean just discussed. The polygon map for this region is based on Dietrich's (1944) data shown in Figure (4-11) with amplitude contours taken from Kuo (1970). This will be referred to again in a later chapter. Region 8 has not been assigned.

This completes the description of the ocean-tide data used in the analysis to be discussed later. The most significant lack of data is that for the Arctic Ocean.

#### 4-3 Program GLOBL

This program accepts as a specification the latitude and longitude of the site where the loading effects are to be calculated. An ocean-tide polygon is then read in from a tape and the following computations performed:

1. A crude estimate of the attraction of the polygon is made by assuming it's area to be equal to the product of the first and second sides and taking the distance from the site as that to the first polygon point. If the resulting attraction is less than a certain limit, assignable as the specification: PULLSIZE, the polygon is omitted and another polygon is read from the input tape.

2. If the polygon is accepted then the direction of the radius vector drawn from the center of the earth to the center of the line joining the first point of the polygon to the third point is determined. This is an attempt to

approximate the center of the polygon as economically as possible. In the case of a rectangular-like polygon it is a good approximation. It is a poor approximation for a 3-sided polygon but there are very few such polygons and they will be avoided completely in future. This vector defines the  $w$  axis which remains fixed for all computations on this polygon.

3. A  $u,v$  plane is determined next passing through the site and perpendicular to the  $w$  axis. This now is the problem discussed in detail by Bott (1963) and I have implemented his results. The  $u,v$  axes are rotated for each lamina so that it is necessary to resolve the components of attraction of each lamina along  $x,y,z$  axes which remain fixed in the Earth. The net attraction due to the polygon is then determined and resolved along vertical, east and north axes through the site. Before storing these components of attractions for accumulation they are multiplied by the appropriate Green's Function (for gravity or tilt effects). A new Green's Function may be read in as input data by specifying on the header card: `NEWTON=2`. The default is to `NEWTON=0` which causes the Green's Function listed in the source program to be used. If `NEWTON=1` is specified the Green's Function for tilt is put equal to the constant 1.0. This is necessary when the height effect at a site is to be determined. The tilts computed then are due only to the Newtonian attraction and the height effect is the difference between the tilts found for `HEIGHT=0` and `HEIGHT` equal to the

actual site height.

A single line of output is listed for each polygon. This line includes the 3 loading effects (gravity in microgals, north and east tilt in millisees) due to the polygon and the accumulated effect due to all the polygons considered to that point.

4. When the final polygon has been processed the direct attraction of the Moon is calculated and resolved along the vertical and horizontal directions to determine the direct gravity and tilt effects. The accumulated gravity and tilt effects due to the polygons is then divided by these direct attraction effects and the resulting ratio is listed together with the phase difference. Finally, the gravity and tilt which would be expected on an 'average' Earth without oceans is estimated by multiplying the direct attraction effects by the gravimetric factor 1.16 and the diminishing factor 0.700. The calculated loading effect of the polygons is then added to this result to yield an estimate of the Earth-tide gravity and tilt which should actually be observed on such an Earth at the site. It is this final result which is later compared to Earth-tide observations made throughout the world.

#### 4-3-1 Refinement For Computing Local Effects.

When the distance to the polygon becomes comparable to its dimensions some defects which previously could be neglected become important. The normal to each polygon is determined by the radius vector to the center of the

polygon; if this point is assumed to lie in the plane of the polygon then the edges of the polygon will project out above the surface of the Earth. If the polygon is located near the site this projection may cause a large anomalous gravity effect. To minimize this type of error the polygon is adjusted along the w axis to pass through the first point of the polygon. The polygon therefore falls below the surface of the Earth near the center but the edges, nearer a potential site, are represented more realistically.

We have assumed that the Green's Functions vary sufficiently slowly with distance from the site that they can be evaluated at the closest degree distance and taken outside the attraction integral. Where the distance is less than one degree however the tilt Green's Function varies rapidly, as can be seen in Figure (4-1). In this region therefore it is necessary to proceed in a different way. The integrals concerned are: (See Bott, 1963)

$$DFU = \iint u K[R] (u^2 + v^2 + w^2)^{-3/2} du dv$$

$$DFV = \iint v K[R] (u^2 + v^2 + w^2)^{-3/2} du dv$$

where DFU and DFV are the u and v components of tilt due to the attraction of a single lamina of a polygon. K[R] is the Green's function for tilt evaluated at the distance R. The constant K[R] is taken outside the integral sign and applied as a final step to the tilts resolved along the north and east directions.

We can take into account the first order variation of the Green's Function over each lamina by writing: (Square

brackets are used here to mean 'function of')

$$K[r] = K[R] + \beta(r-R)$$

where  $\beta$  is the first derivative of  $K$  with respect to the distance  $r$  evaluated at  $R$ . Since we restrict this integral to distances of the order of one degree,  $w$  can be neglected and we can write:

$$\begin{aligned} DFU &= \iint K[r] u (u^2+v^2+w^2)^{3/2} du dv \\ &= (K[R]-\beta R) \iint u (u^2+v^2+w^2)^{3/2} du dv \\ &\quad + \iint \beta u (u^2+v^2)^{1/2} du dv \end{aligned}$$

with a similar expression for  $DFV$ . The second integral introduced here is an elementary form. This method of solution is implemented by the program when the distance is less than 200 km and the specification 'DETAIL' has been set equal to 1. Both the Green's Function for tilt and its derivatives have been set within the program to values at 5 km intervals from 0 to 200 kms.

CHAPTER 5

THE MEASUREMENTS

5-1 The Horizontal Pendulums.

In this device the pendulum is supported by wires or fibers so as to swing freely in a horizontal plane, much like a gate on it's hinges. Like a gate too, it is very sensitive to tilting of the hinge axis in a direction away from the plane defined by the pendulum and the hinge. It is this sensitivity, which can be increased to the point of instability by setting the hinge axis closer to the vertical, which makes the horizontal pendulum a useful device for the measurement of tidal tilts. The horizontal pendulums used both at Rookhope and at Holland Mills are of Verbaandert-Melchior (1958) design and are constructed entirely of fused quartz so as to be as friction free and dimensionally stable as possible. They are mounted on right-angled shaped aluminium bases supported on 3 legs, two of which are adjustable for independently controlling the sensitivity and the azimuth of the pendulum. The fixed leg is located directly under the near-vertical hinge axis of the pendulum. The sensitivity is increased by increasing the height of the period leg which is located in the plane of the pendulum and hinge beneath the pendulum bob. The pendulum is caused to rotate about the hinge axis by changing the height of the third leg which supports the third corner of the right-angled base; this is called the azimuth or drift leg.

Melchior (1965, p65) shows that the sensitivity of the pendulum to tilting depends upon the angle of the hinge axis to the vertical and that this determines too the period of natural oscillations of the pendulum. The sensitivity in fact varies as the inverse square of the natural period and thus is determined when both the period and proportionality constant are known. The proportionality  $K$  is measured when the pendulum is constructed by means of an independent method of tilt measurement. This second method has been devised by Verbaandert (1959) and utilizes a stainless-steel disk containing a small cavity which communicates with a reservoir of mercury by means of a connecting tube. The thick upper surface of the disk is caused to deflect slightly by raising or lowering the height of the mercury reservoir. The deflection is approximately linear and can be measured precisely using metrology techniques which Verbaandert describes. To determine the value of  $K$  the horizontal pendulum is tilted a precise amount by placing this disk under the drift leg of the pendulum and changing the height of the mercury reservoir.

Both the Holland Mills and Rookhope sites are equipped with disks permanently installed under the drift legs. The sensitivity of the pendulums can therefore be measured either from a period measurement or directly from the response to known deflections of the disk.

Motion of the pendulum is measured in the classic way by the deflection of a beam of light which is reflected from

a mirror mounted on the pendulum near its axis of rotation. The sensitivity of the pendulum to tilts is given for an optical lever length of 5 m by:

$$S = K/T^2 \quad (5-1)$$

where K is the proportionality constant and T is the period of free oscillations of the pendulum. The sensitivity S is expressed as the pendulum tilt in arc seconds required to produce a deflection of the reflected image of 1.0 mm. The pendulums are normally operated with natural periods in the range 70-85 seconds which yield, for a typical value for K of 6.000, a sensitivity of .0012 to .0008 arc seconds per mm.

The dynamic response of the pendulums it was found could be approximated with sufficient accuracy by the second-order differential equation describing a simple oscillator with linear damping. The static sensitivity of the pendulum expressed as the rotation of the pendulum in arc seconds per arc second tilt of the pendulum base is a useful term to isolate in this equation. It is related to the period of the pendulum and the proportionality constant K by:

$$s = 20.6 T^2/K \quad (5-2)$$

The pendulum equation then can be written:

$$(p^2 + p2\delta\omega' + \omega'^2)\theta = s\omega'^2d \quad (5-3)$$

where p is the differentiating operator of Laplace transformation notation,  $\omega'$  is the angular velocity of natural oscillations of the pendulum,  $\theta$  and d represent



rotation of the pendulum and tilt of the pendulum base respectively.  $\delta$  is the damping coefficient expressed as the fraction of critical damping and is typically near 0.01. The response of the pendulum to periodic tilting of the base with amplitude  $d$  and angular velocity  $\omega$  is:

$$\theta = s d \sin \omega t / [(1 - \omega^2 \omega'^2)^2 + (2\delta \omega / \omega')^2]^{1/2} \quad (5-4)$$

For frequencies not too close to the natural frequency of the pendulum the damping term is negligible and this equation can be written:

$$\theta = s d \omega'^2 / (\omega'^2 - \omega^2) \quad (5-5)$$

#### 5-2 Recording the Pendulum Measurements

The tilts detected by the pendulums are recorded by a two-channel light-spot follower (Sefram). The pens of this recorder are mounted on trolleys which are servo-driven to follow the light spot reflected from the pendulums. In order to use this device it was necessary to replace the optical system supplied with the pendulums with a collimated light source which placed an adequately bright slit image on the photcell for an absolute minimum of source power. A standard automobile bulb rated at 12 watts but used at half power gave several months of continuous operation. In addition to the analog record, made directly on metallic paper by pens mounted on the trolleys, an electrical signal was obtained from two linear potentiometers which were driven by the trolleys. These signals were used to detect when a light spot was approaching the limit of travel of a trolley. This condition caused a low-speed motor coupled to the drift

screw of the appropriate pendulum to be energized briefly to bring the pendulum back into the operating region. This action was more difficult to achieve than expected. It was necessary to contact and turn the drift screw without at the same time jarring the pendulum; a pure rotational motion was required at the coupling. The desired behaviour was finally achieved with a flexible fork and bar coupling suggested by J. Geuer (Dominion Observatory Drafting Office). The fork and bar contact only during driving and when the desired rotation has been achieved the motor is reversed to back the fork off slightly from the bar.

When the original spot follower recorder used at Rookhope was lost in a mine flood in December 1968 it was replaced by a new all-transistor model. This cooler running instrument was found to require supplementary heating to avoid deterioration of the metallic chart paper by moisture. The new recorder too was found to sometimes lose servo lock after the power had been interrupted briefly, a common occurrence in a working mine. This is a difficult fault to recognize because brief power failures are not obvious on the chart record. The trouble was overcome by introducing relays which delayed the restoration of power to the spot follower until the light sources had reached full brilliance.

### 5-3 Preparation of the Rookhope Site.

Rookhope is located in County Durham approximately mid-way between the east and west coasts. Geographical

coordinates are  $54^{\circ} 47'$  North,  $2^{\circ} 6.3'$  West and height above sea level is 350 m. The site used was in an operating fluorspar mine owned by the Weardale Lead Co., Ltd. A plan of part of the mine showing the pendulum site is reproduced in Figure (5-1).

An operating mine was selected as a site as a last resort after many non-operating properties had been investigated and found unsuitable because of flooding, poor rock conditions, remoteness or other reasons. The concern about an operating mine was that the movement of ore trains, the frequent dynamite blasts and the operation of pumps would produce an intolerable level of noise in the tiltmeter measurements. The advantages of an operating mine however, particularly for short-term measurements, proved irresistible and so it was decided to attempt to make tilt measurements in the Rookhope mine.

The site made available to us was a large room used originally as a chamber from which exploratory drilling could be made. It was located at the end of a 200m long cross-cut. This level was 17 fathoms (31 m) beneath the surface and near the base of the Great Limestone. The floor here was dry and sound under approximately 30 cm of rubble so it was decided to install the tiltmeters directly on the floor rather than in a large niche cut in the wall which is the normal practise. Niche cutting had proven expensive and time consuming at Holland Mills and it was desirable to find an alternative technique. The installation required for each

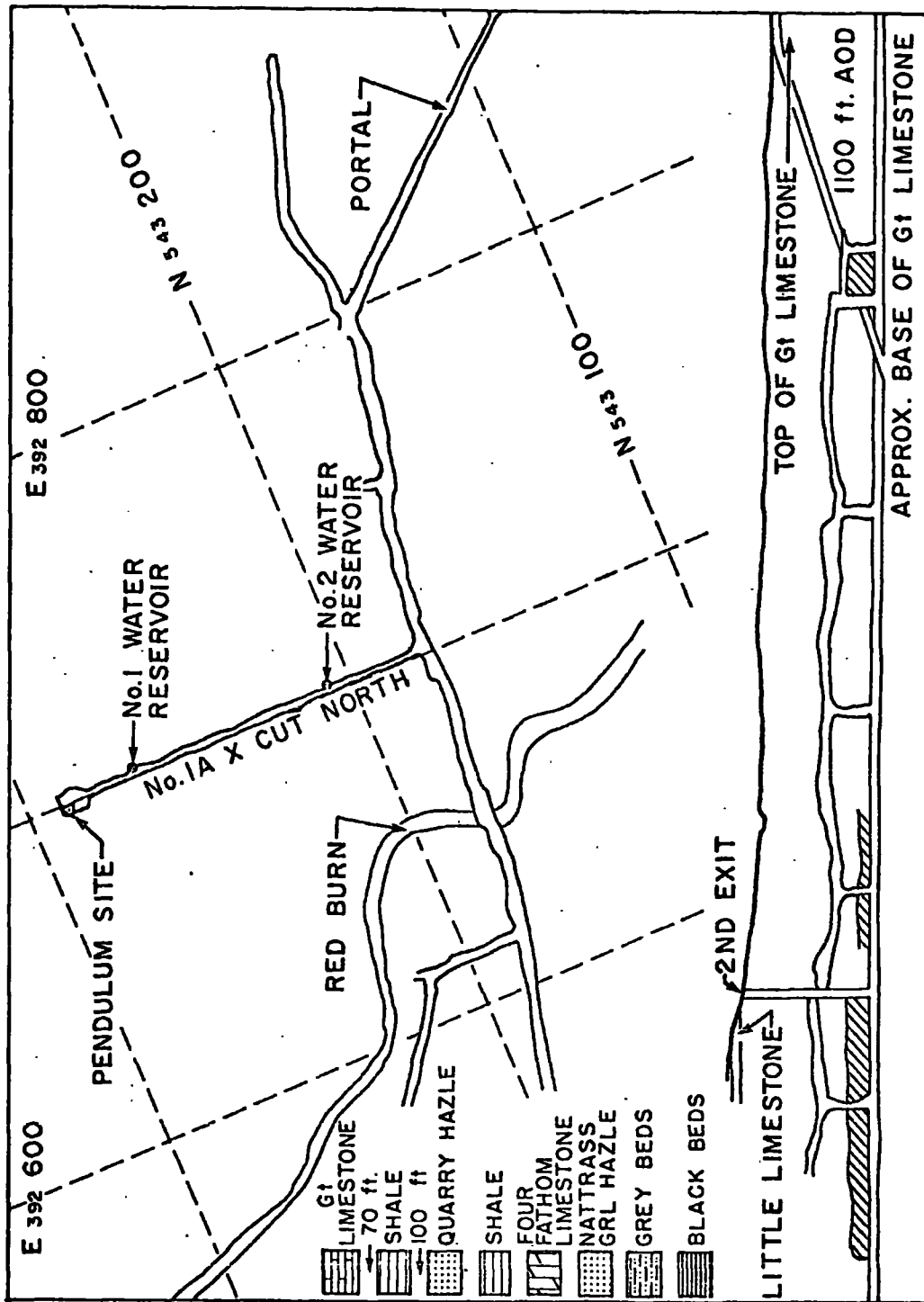


FIGURE (5-1) Plan of the Rookhope mine showing the pendulum and water-tube sites.

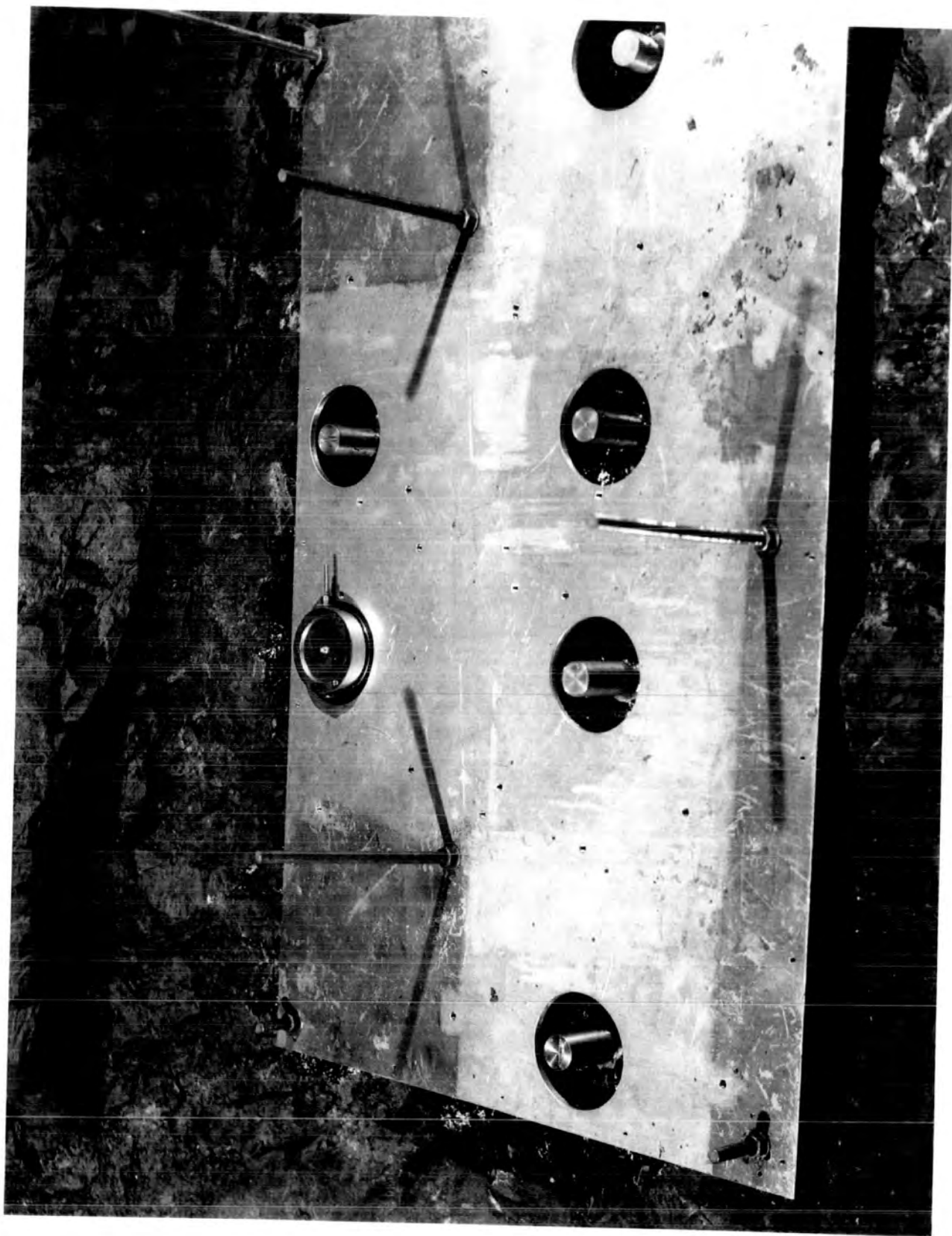


PLATE (5-1) Preparation of the Rookhope Site- The leveled base plate from which the holes for the support pins were drilled.

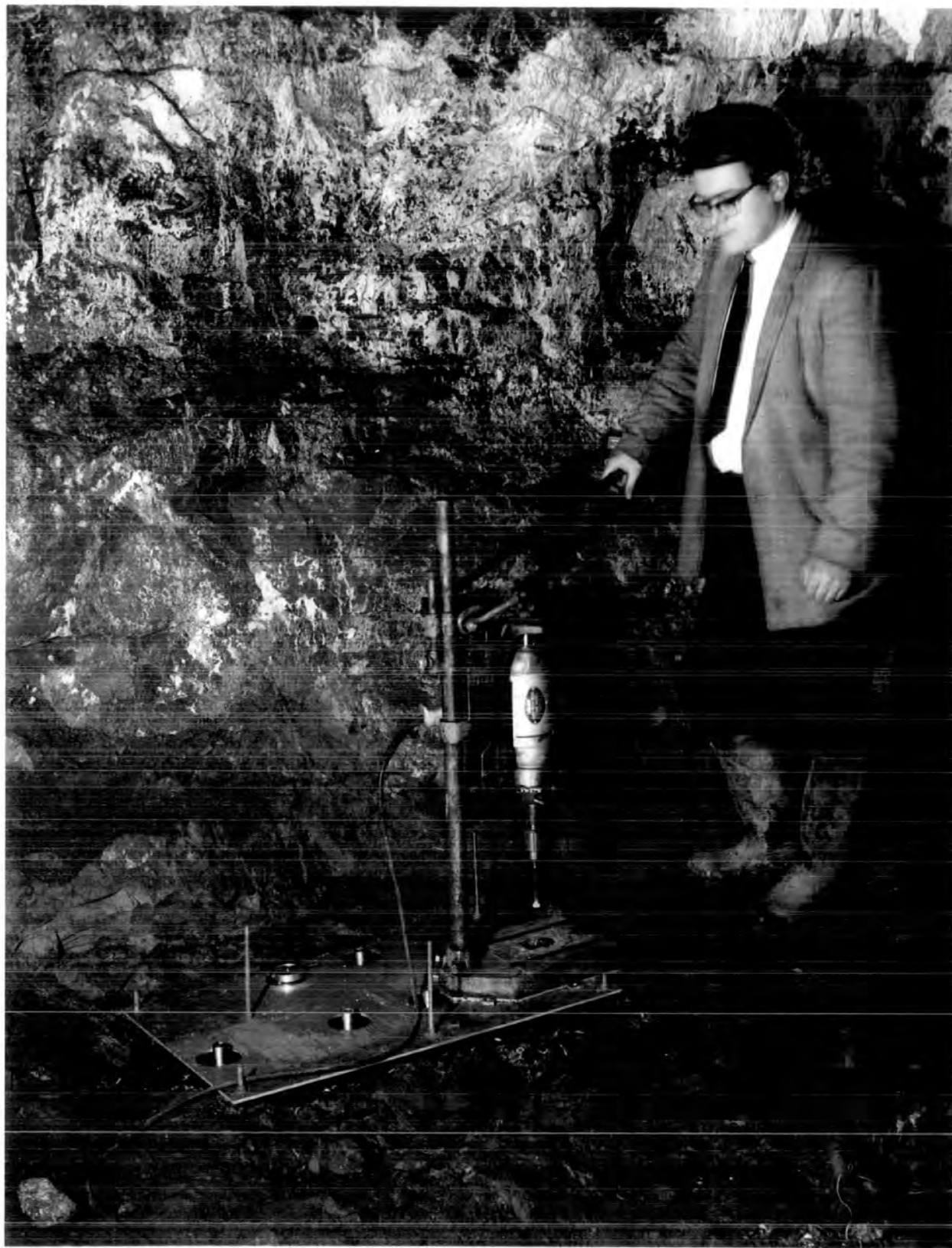


PLATE (5-2) Preparation of the Rookhope Site- Drilling the holes for the support pins. (Some of the support pins are shown in place.)

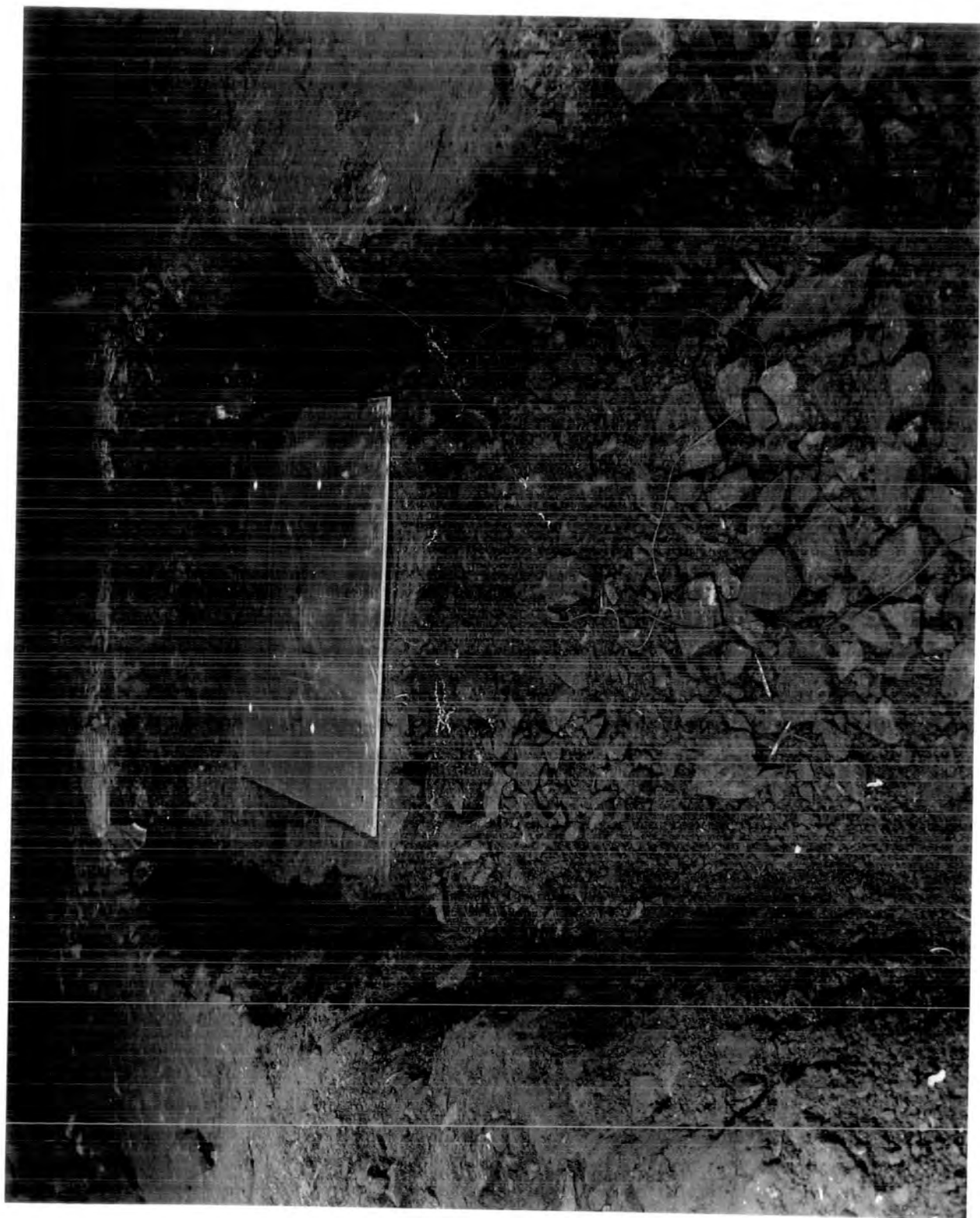


PLATE (5-3) Preparation of the Rookhope Site- The base plate for the Spot Follower installed on solid rock.



PLATE (5-4) Preparation of the Rookhope Site- The completed moisture-sealed pendulum case. The drift-compensating motors are mounted on the front of the case. The calibrating device is on top of the case.





PLATE (5-5) The Sefram 2-channel spot follower and the light sources

pendulum consisted of installing securely in the rock three stainless-steel pins on which the three legs of the pendulum would rest. Plates (5-1) and (5-2) illustrate how this was done. Long steel studs were first set in the floor by means of expansion plugs (Rawlplug). An aluminum plate was predrilled to mark the locations of the six holes to be drilled in the rock. This plate was mounted on the steel studs and washers and nuts on the studs were adjusted until the plate was supported precisely horizontal and as close to the floor as possible. (The floor had previously been cleaned to sound rock and leveled by chipping). A drill press was then clamped on the level plate and holes for the leg support pins were drilled to the required depth, about 15 cms. This technique ensured that the pins were all at the correct height and the upper surfaces level. Important too was the perfect roundness of the holes which was the result of clamping the drill press firmly to the plate during drilling. This was desirable in order to maintain a uniform clearance of about 0.25 mm around the pins for the adhesive, which was applied next. The adhesive is a two-component polyester resin of the type used for bonding strain-gauges to rock surfaces at low temperatures. This is generally considered to have better creep characteristics than an epoxy adhesive, particularly in moist areas.

The spot follower site was prepared next. This is shown in Plate (5-3); it consists simply of an aluminium base plate pre-drilled to accept the four feet of the spot



follower. It is secured to the floor at the proper horizontal level, distance and direction relative to the pendulum. This is a convenient stage at which to connect by surveying the pendulum azimuth to some known azimuth line in the mine. To do this it is generally assumed that the center of the fixed leg and the center of the period leg define the azimuth of the pendulum. A template was made which fitted the position constraints (the classic hole, slot and plane) on the surfaces of the three pins and at the same time provided marking pins on which a transit could be sighted. In this way azimuths of north  $29^{\circ}$  west and east  $29^{\circ}$  north were determined for the two pendulums.

The completed installation is shown in Plates (5-4) and (5-5). A large aluminum case is fitted to the base plate and sealed against moisture. Fiber glass and epoxy has been used to seal the holes where the pins enter the box. This glass cloth is thin enough not to transmit to the pendulum any motion of the box. The two motors which operate the drift screws can be seen mounted on the front of the box at the lower right. Mounted on top of the box is a clock-controlled mechanism for varying the height of the mercury reservoir which can be seen connected to the pendulums by long tubes. This calibrating device is energized once a week. Plate (5-5) shows the spot follower and its plastic cover which is essential for moisture protection. On either side of the spot follower a light source can be seen mounted on a vertical post. A slit of the proper dimensions is formed by

a mask fastened to the light source and an image of this slit is focused on the photocell by a 5 m focal length lens after reflection at the pendulum mirror. The 5 m lenses were mounted on the small plastic covers which can be seen enclosing each pendulum. It is worth noting here that these plastic covers, which are supplied by the manufacturer, should be modified by having a panel cut in the front so the pendulum can be accessed without having to move the cover over the top of the pendulum.

#### 5-4 Operation of the Rookhope Site.

##### 5-4-1 Initial Setting Up

The setting up procedure for the horizontal pendulums is described by Melchior in his book and in detailed instructions accompanying each Verbaandert-Melchior pendulum. The sensitivity is increased in small steps until a natural period of about 75 seconds is obtained. After each step change in sensitivity a trimming adjustment of the drift screw is required to keep the pendulum in its operating range. When the proper period range is reached the sensitivity is decreased, without changing the drift screw adjustment, to give a period of about 10 seconds. The position of the reflected slit image at this time is taken to represent zero tilt of the pendulum base; that is, the pendulum is assumed to lie parallel to the line joining the period screw and the fixed screw. This is the reference direction mentioned in the last section. The sensitivity is restored to the 75 second region for normal operation.

The difficulties in this technique are due mainly to the almost total lack of damping in the pendulum motion. At high periods a disturbance is introduced each time the period or drift screws is adjusted, however carefully, and this causes large oscillations of the pendulum which take several minutes to damp out. Moreover these adjustments must be carried out with the observer's weight immediately next to the pendulum so that even when stable operation is achieved it may be upset when the observer moves away. With patience, successful operation is eventually attained but the difficulties are a serious hindrance to the application of the tiltmeter. Some consideration was given to the possibility of achieving critical damping of the pendulum by causing the mercury reservoir to move up and down as part of a servo loop with controlling signals derived from the potentiometers of the spot follower. Analysis shows that this could be implemented by moving the reservoir at speeds less than 7.0 mm/sec and through a vertical range equal to three times the amplitude of expected tilt steps measured at the recorder. This was demonstrated by controlling the reservoir height manually but lack of time prevented construction of an operating system.

#### 5-4-2 Summary

The first tilt observations were made at the Rookhope site in April 1968. Many interruptions were experienced during the first few months due to failures of the spot follower or due to prolonged power interruptions. The site

could be visited only once or twice per week so that failures of any kind caused a data loss of a few days. Many of these early records are being salvaged now by identifying power interruptions and correcting timing errors. Continuously good records began to appear in August and continued until mid-December when a major rock fall closed the mine for several weeks. The pumps were without power after the rock fall and the tilt recording equipment was soon submerged under six feet of water. The spot follower was a total loss, mainly because of the corrosive effects of the water. The pendulums although unclamped throughout the the flood were found undamaged but very dirty. They were later scrubbed clean and the 40-micron suspension fibers broken off and replaced with new ones. A replacement spot follower was borrowed from the Dominion Observatory and the site reoccupied in February 1969. Regular recording began in May and continued until the project ended in December 1969.

In spite of the fact that the Rookhope site is a working mine the tilt records were generally quieter than the Holland Mills records. This is believed to be due to the difference in topography. The Holland Mills site is located in an abandoned asbestos mine in the midst of rough, irregular local topography. This topography is likely reflected in a complex distribution of underground water courses which cause anom<sup>a</sup>alous tilting effects during rain storms and possibly during seasonal changes as well. The

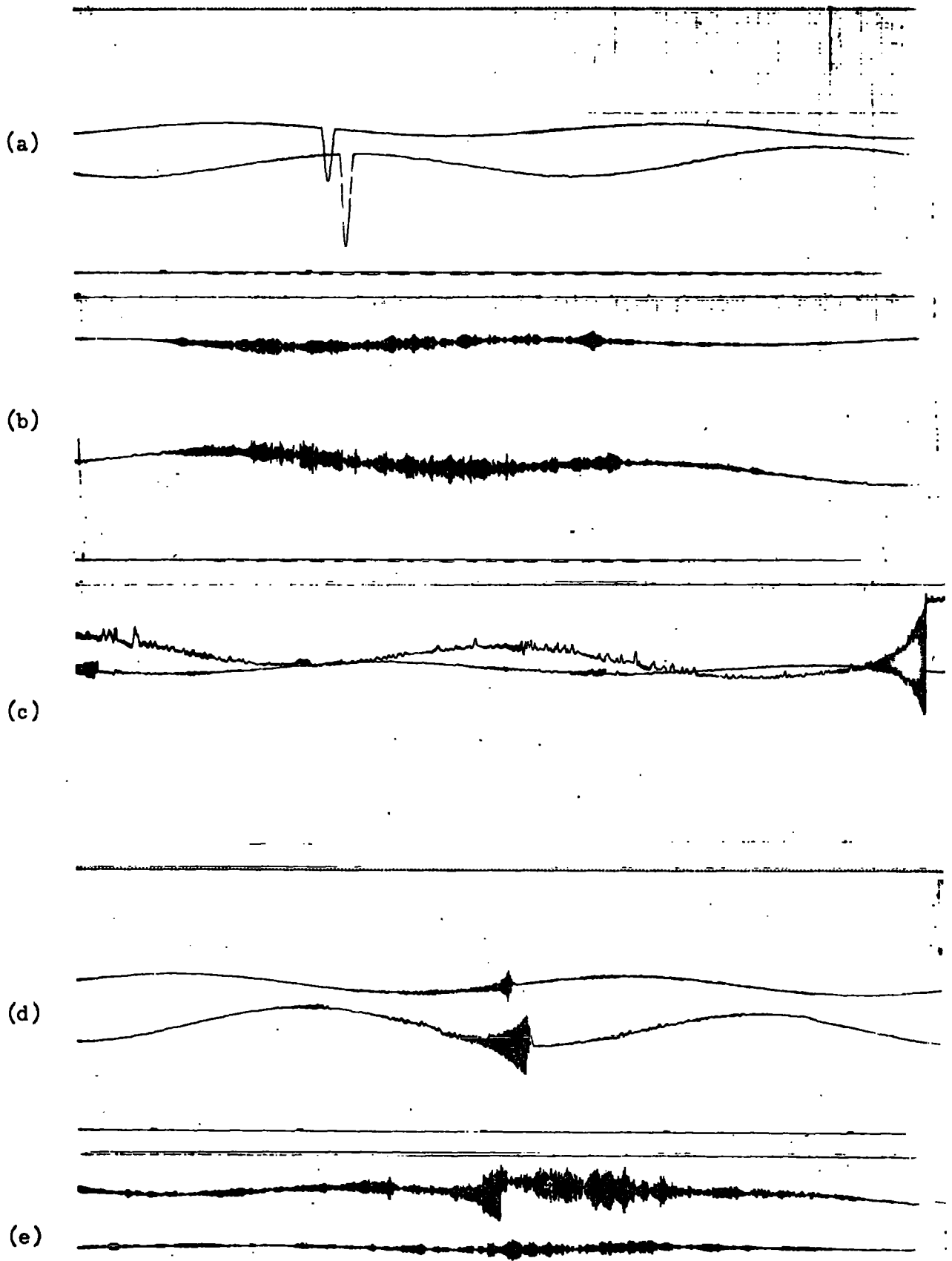


PLATE (5-6) Representative Records Of Tilt From The Holland Mills Site.  
(Horizontal scale:1.3cm/hr. Vertical scale:1.0cm/.05 arc secs.)

topography too results in a greater wind exposure than that at Rookhope.

Reproduced in Plate (5-6) are several records from the Holland Mills site which illustrate the behaviour of the horizontal pendulums. Frame (a) shows a typically 'quiet' record and a calibrating signal. This calibration was produced by a single rotation of the lever arm carrying the mercury reservoir. Normally several rotations are made so that the effect of noise can be averaged out. Frames (b) and (c) are typical records made during high winds and during heavy rains respectively. The low frequency noise in Frame (c) is principally on the east-west record; it is unsymmetrical with respect to the tidal curve and usually begins and ends with the rain. This same pendulum in the spring shows frequent permanent 'tares' in the same direction as this noise. An automatic scale shift appears at the right of Frame (c). The disturbance shown in Frame (d) resembles a seismic event but was not detected at the Ottawa seismological station. Frame (e) illustrates a particularly noisy record and a 'tare' of the type that seems to be observed by all horizontal pendulums occasionally.

Wind effects at Rookhope are much less noticeable than at Holland Mills, presumably because the smooth rolling topography near Rookhope presents little wind exposure. Low frequency noise of the type shown in Frame (c) is sometimes experienced at Rookhope but it does not seem to be related to rainfall.



Long term tilting measured at the Rookhope site was generally smaller than at Holland Mills. The direction of tilt measured at both sites was the same throughout the year and remained the same after the suspension fiber of a pendulum was changed. This indicates that the long term tilts measured were real although they are probably too large to represent tilting of more than a very local area about the pendulums. At Rookhope the tilting during the summer of 1968 was towards the direction west  $49^{\circ}$  south at the rate of 4.5 milliseecs/day. The following summer, after the rock fall in December 1968 and repairs to the tiltmeters, the direction was west  $29^{\circ}$  south at the rate of 8.0 milliseecs/day. These directions tend to be toward rather than away from the working area of the mine where approximately 500 tons of rock was being removed each week.

The effects of blasting and the movements of ore trains at Rookhope were of no importance in the measurement of tidal tilt at diurnal and semi-diurnal frequencies. The closest traffic and the closest blasting were located 1000 m and 7000 m respectively from the pendulums. The temperature in the pendulum room, which was not sealed off from the rest of the mine, remained at  $10.35^{\circ}\text{C} \pm 0.03^{\circ}$  throughout 1968. Throughout 1969, using a different thermometer, the temperature was  $10.27^{\circ}\text{C} \pm 0.03^{\circ}$ .

CHAPTER 6

DATA ANALYSIS

We will be concerned here with the problem of determining the amplitude and phase of the constituent waves in earth tide gravimeter and tiltmeter records.

6-1 Editing The Data.

The chart records were digitized using a line-follower device recording directly on magnetic tape. The output of this preliminary phase is put on cards. The chart values were scaled to a maximum value of 999 so that a single card carries 24 hourly values of 3 figures in addition to necessary identifying information. It will be shown later that the error associated with this level of resolution is negligible in comparison with the errors due to other causes. The data cards were next edited for isolated errors or level changes, missing data was estimated by interpolation where possible, the non-tidal noise level was estimated and finally, calibration constants were applied and corrected cards punched out. These editing functions were accomplished with the aid of program BETTY which will now be described.

Errors or level changes in the data are detected in a smoothness test (Cartwright, 1966) which compares each hourly data with a value found for that hour by interpolation according to the formula:

$$X'(n) = .75[X(n+1) + X(n-1)] - .30[X(n+2) + X(n-2)] \\ + .05[X(n+3) + X(n-3)] \quad (1)$$

The difference  $(X_n - X'_n)$  is zero for any 5-th order

polynomial. An isolated error produces a recognizable symmetrical sequence of differences and a general shift in level produces an anti-symmetrical sequence. The original data is corrected for isolated errors revealed by this test and level changes are subtracted from all subsequent data by adding to the program input assignment cards of the form  $FST(J,M)=C$ , where  $J$  is the day and  $M$  is the hour of the level change of magnitude  $C$ . A second running of the program will reveal whether the corrections have been applied correctly. Short sections of missing data, not exceeding a day in length, may sometimes be estimated at this stage. Equation 1 is used again for this interpolation with consecutive terms separated by 1, 2 and 3 days rather than 1, 2 and 3 hours. It can be shown that an interpolation made with this linear combination is not affected by the presence of periods of 12 hours or 24 hours. (Melchior, 1965, p71).

After the data has been proof-read and corrected in this way the computer is caused to apply calibration constants, estimate noise level and output data cards usable by the analysis program JANET, which will be described later. Daily calibrations are determined by interpolation between whatever calibration constants are entered as input. Noise is estimated by applying to the data for each day, a linear combination which discriminates against tidal periodicities. This is described by:

$$Y(t) = \sum W_i y(t-i)$$

where  $y(t)$  is the hourly data,  $W_i$  is a term of the linear

combination and  $Y(t)$  is the result of the linear combination and represents in this case the effect of noise only. If the noise in the original data is random with an rms value of  $\epsilon$  then:

$$Y^2(t) = \epsilon^2 \sum W_i^2$$

In the case of the Lecolazet (1959) filter used here:  $\sum W_i^2 = 1872$ . If there are  $n$  days of data then:

$$\epsilon^2 = [Y^2(t) + Y^2(t+24) \dots Y^2(t+n24)] / n \sum W_i^2$$

A typical value for tiltmeter records is given by Melchior as  $\epsilon=0.3$  mm. We can compare this to the error due to quantization when the resolution of a 250mm record is 0.001. The scale unit then is 0.25mm and the standard deviation of the quantization error is (Bendat, 1966),  $0.29 \times .25 = 0.075$  mm. This is negligible in comparison to the noise present in the record due to other causes. Program BETTY is described in more detail in the documentation presented in the appendix.

#### 6-2 The Fourier Method.

It was shown earlier that the potential of the tide-producing force can be written as a series of terms involving six fundamental frequencies. The six frequencies are not commensurable and as a result the tidal potential is not periodic in the sense that the function  $X(t)$  is periodic when for any integer  $n$ :  $X(t) = X(t + nT)$  where  $T$  is some finite time. On the other hand the tidal potential is perfectly predictable and its spectrum consists of a finite number of discrete lines. It is therefore fundamentally

different from non-periodic phenomena in general which is usually transitory and is represented in the frequency domain by a continuum of energies. The term 'almost-periodic' has been used (Bendat, 1966) to describe the predictable non-periodic function. The distinction is important because it is on these considerations that an optimum means of analysis is determined. If the function to be analysed is periodic then it can be precisely represented by a Fourier series. The series will contain all possible constituent waves; the complete orthonormal set of functions for the specified interval. The coefficients of the series are found term by term by multiplying both the series and the given function by a Fourier function and integrating throughout the interval. This turns out to be a simple operation because of the orthogonality of the Fourier functions. If the function to be analysed is not periodic it may be assumed to have a period equal to infinity and a Fourier representation as before. In this case however the Fourier coefficients must be determined by integration over an infinite interval. Since the given function will generally not be known for all times it must be replaced by a truncated function equal to the given function throughout the period in which it is defined and vanishing beyond this interval. We can in this way find the Fourier representation of the truncated function. This may or may not be a good representation of the real function. Truncation can be considered as multiplication of the given function by

another function of time. In the frequency domain this is represented by convolution of the two corresponding frequency functions which, in this case, results in a 'smearing' of the line spectra of the given function. Adjacent lines will tend to widen and merge. When the given spectrum is mainly a band limited continuum with very little line content truncation effects are not so serious. The Fourier transform and the power spectral density function, which are both developed from the Fourier representation described here, are useful in cases where the chief aim is to establish the frequency content of the given function. Here the situation is different; we are concerned with determining the amplitude and phase of a limited number of waves of known frequency. If there are  $p$  frequencies present we know that the function can be represented by the series:

$$y(t) = B_1 e^{j\omega_1 t} + B_1^* e^{-j\omega_1 t} + \dots + B_p e^{j\omega_p t} + B_p^* e^{-j\omega_p t}$$

The conjugate coefficients  $B_j$  and  $B_j^*$  must be determined by comparison with the given function. If there is any noise at all in the given function the determination can not be precise and some criterion of 'goodness of fit' must be assumed. It can be shown that if the interfering noise is normally distributed then the most probable value for the coefficient is obtained by minimizing the squares of the residuals (Murray, 1965). In this way we are led to the least-squares method of approximating almost periodic functions in terms of the known constituent waves.

### 6-3 The Least Square Method

There is a connection between the Fourier series method and the method of least squares. It can be shown that the Fourier coefficients give the best least-squares fit when a function is expanded in terms of an orthonormal set of functions. This is a special case of least-squares approximation; the orthogonality of the functions has the effect of 'decoupling' the normal equations reducing each to an equation in one unknown.

In general the functions of the least-squares approximation will not be an orthogonal set and consequently they will be, at least to some extent, linearly dependent. The solutions to the normal equations will become less and less well defined as this interdependence grows until finally when the determinant vanishes a solution becomes impossible. Since there will be a greater degree of interdependence between the waves of neighboring frequency than between waves having widely different frequency the question arises whether a 'smearing' effect similar to that encountered with the Fourier transform will be met with too in a least-squares approximation to a non-periodic function. This question has been dealt with by Munk and Hasselmann (1964), who compare the results obtained by the least-squares method with that obtained using the Fourier transform in the case of a data spectrum containing two neighboring lines plus a broad-band noise. A truncation effect is found with both methods but the 'smearing effect' of the Fourier method is found to

depend on the record length while smearing in the least-squares approximation is shown to depend on record length only through the accompanying noise and will be absent if there is no noise. Mumk and Hasselmann demonstrate that resolution significantly better ('super resolution') than the inverse of the record length is therefore possible in a least-squares approximation; this is a compelling argument for the choice of the least-squares method for the analysis of almost-periodic functions. Important too is the convenience of the least-squares method in being able to use data in the form of arbitrary-time samples of the given function. Gaps in earth-tide records are common, particularly in tiltmeter records, because of the difficult operating conditions met with in underground sites. The least-squares method is the only feasible method of data analysis when the record gaps are too large to be filled in by interpolation and the length of any continuous section is too short for a Fourier analysis. Beyond this, it may be more economical and just as reliable in many cases to obtain separation of neighboring constituents by a series of short recording intervals separated by long gaps than by a single long recording.

For these reasons I chose to use a least-squares method for analysing the earth-tide data. This analysis is implemented by program JANET.

#### 6-3-1 Program JANET

This program is based on a least-squares method



described by Venedikov (1966). In principal a least-squares method could be made to work for data observed at arbitrary times but the presence of drift would greatly complicate such a general method. To avoid considering drift, Venedikov's method requires a basic set of 48 continuous hours of data, although many such sets can be used in the analysis and they may be arbitrarily spaced in time. Each 48 hour set is filtered digitally to obtain two quadrature related numbers proportional to the diurnal wave amplitude in the data and two numbers proportional to the semidiurnal wave amplitude. The same four filters are applied to data determined theoretically for the site assuming a rigid earth. In this way four independent condition equations are determined by each 48 hour set. If there are a great number of such sets we could assume correction factors for the amplitude of each of the theoretical constituents and determine the most probable value for the factors on the basis of the least-squared residual of the condition equations. The resulting normal equations however would be ill defined unless the data span was very long relative to the reciprocal of the frequency difference between adjacent constituents. The customary remedy for this difficulty, and the one followed by Venedikov, is to assume that the amplitude factors (complex) are the same for all the constituents contained within certain narrow frequency bands. For data spans of less than six months Venedikov assumes 6 such bands enclosing 52 diurnal constituents and 5

bands enclosing 27 semidiurnal constituents, for a total of 22 unknowns. This assumption is valid for describing the effect of the tide-producing forces in the solid earth. It may not be valid for describing the behaviour of the ocean tide however and in areas where the ocean tide has a significant effect on measurements of the earth tide the assumption must be examined critically. Frequently the amplitude of the ocean tide is small for all but the main constituent within a frequency band (Murray, 1964) so that any error in assuming a constant factor must be small. In addition, Munk and Cartwright (1967) find that the function describing the response of the ocean to the tide-producing forces (their 'admittance' function) is smooth and can be considered constant throughout frequency bands of width  $1/6$  cycles per day. This is much wider than the frequency band assumed by Venedikov.

#### 6-4 Results

##### 6-4-1 Rookhope Results

The results of the analysis of horizontal pendulum measurements made at this site during periods in 1968 and 1969 are presented in Table 6-2. Results for hydrostatic tiltmeter measurements made at the same site are shown in Table 6-4.

##### 6-4-2 Ottawa Results

Results are presented in Table 6-1 for the analysis of horizontal pendulum tiltmeter measurements made at Holland Mills, Quebec. This site is located approximately 50 km from

Ottawa. In Table 6-3 results are shown for gravimeter measurements made at Ottawa.

ORB73-090		HOLLAND MILLS 1967		ORB74-180		HOLLAND MILLS 1967		238-275	
WAVE	RATIO	ERROR	PHASE	WAVE	RATIO	ERROR	PHASE	WAVE	ERROR
2N2	0.933	0.019	1.366	2N2	1.306	0.015	-22.75C	2N2	0.015
N2	0.915	0.005	1.085	N2	0.734	0.005	4.764	N2	0.005
M2	0.900	0.005	-0.423	M2	0.790	0.004	6.866	M2	0.004
L2	1.464	0.025	-17.672	L2	1.492	0.029	-51.263	L2	0.029
S2	0.831	0.002	-2.850	S2	0.832	0.001	1.325	S2	0.001
Q1	0.789	0.080	27.500	Q1	9.535	2.153	-67.674	Q1	2.153
O1	0.612	0.051	-7.555	O1	13.335	2.694	-30.873	O1	2.694
M1	1.366	0.161	-30.525	M1	8.596	2.075	134.543	M1	2.075
K1	0.792	0.053	-18.503	K1	11.319	2.627	-19.561	K1	2.627
J1	0.475	0.243	86.828	J1	14.910	6.785	-115.227	J1	6.785
001	0.848	0.171	-10.540	001	17.402	4.645	5.613	001	4.645

ORB73-090		HOLLAND MILLS 1968		ORB74-180		HOLLAND MILLS 1968		272-340	
WAVE	RATIO	ERROR	PHASE	WAVE	RATIO	ERROR	PHASE	WAVE	ERROR
2N2	0.157	0.012	27.667	2N2	0.401	0.010	-49.07C	2N2	0.010
N2	0.907	0.003	4.817	N2	0.639	0.005	-4.42C	N2	0.005
M2	0.889	0.005	-0.786	M2	0.760	0.003	6.19C	M2	0.003
L2	0.524	0.023	-42.412	L2	0.466	0.017	39.127	L2	0.017
S2	0.811	0.003	-1.842	S2	0.861	0.002	2.020	S2	0.002
Q1	0.537	0.071	-38.679	Q1	5.518	1.888	-94.545	Q1	1.888
O1	0.640	0.036	-13.922	O1	14.334	0.928	8.672	O1	0.928
M1	1.096	0.194	-32.314	M1	1.737	2.500	56.605	M1	2.500
K1	0.720	0.054	-14.462	K1	10.954	2.988	6.362	K1	2.988
J1	1.480	0.259	-17.731	J1	5.594	5.963	13.068	J1	5.963
001	0.448	0.701	-95.073	001	40.232	11.324	17.074	001	11.324

TABLE (6-1) Diminishing factors and phase lag (E.C.S) for 1967 east and south tilts (top) and 1968 east and south tilts (bottom). Multiply RATIO by 0.9 to obtain diminishing factor.

COMB188-270			ROOKHOPE			238-285			1968			COMB137-180			ROOKHOPE			238-285			1968		
WAVE	RATIO	ERROR	PHASE	ERROR	PHASE	ERROR	WAVE	RATIO	ERROR	PHASE	ERROR	WAVE	RATIO	ERROR	PHASE	ERROR	WAVE	RATIO	ERROR	PHASE	ERROR		
2N2	21.462	0.539	22.228	0.539	22.228	0.025	2N2	14.110	0.332	-65.684	0.024	2N2	14.110	0.332	-65.684	0.024	N2	1.510	0.140	29.417	0.093		
N2	1.436	0.220	134.510	0.153	134.510	0.065	M2	1.310	0.065	40.085	0.049	M2	1.310	0.065	40.085	0.049	L2	3.446	0.362	-128.563	0.105		
M2	1.489	0.097	143.235	0.086	143.235	0.086	S2	1.638	0.040	13.700	0.025	S2	1.638	0.040	13.700	0.025	Q1	3.609	1.157	76.303	0.321		
L2	6.094	0.527	-38.019	0.143	89.613	0.143	Q1	3.609	1.157	76.303	0.321	Q1	3.609	1.157	76.303	0.321	O1	0.678	0.701	87.760	1.034		
S2	1.591	0.227	89.613	0.329	-171.174	0.329	O1	0.678	0.856	-41.536	0.856	O1	0.678	0.701	87.760	1.034	M1	10.652	3.326	-51.589	0.313		
Q1	3.118	1.027	-171.174	0.856	-41.536	0.856	M1	10.652	0.254	16.357	0.254	M1	10.652	3.326	-51.589	0.313	K1	1.062	0.847	-37.430	0.758		
O1	0.505	0.432	-41.536	0.254	16.357	0.254	K1	1.062	0.489	-14.053	0.489	K1	1.062	0.847	-37.430	0.758	J1	4.732	2.916	-28.724	0.616		
M1	5.504	1.398	16.357	0.489	-14.053	0.489	J1	4.732	0.304	21.232	0.304	J1	4.732	2.916	-28.724	0.616	001	7.425	0.873	-172.274	0.118		
K1	1.446	0.707	-14.053	0.304	21.232	0.304	001	7.425	0.678	-69.644	0.678	001	7.425	0.873	-172.274	0.118							
J1	6.577	2.003	21.232	0.678	-69.644	0.678																	
001	6.217	4.216	-69.644	0.678	-69.644	0.678																	

COMB188-270			ROOKHOPE			163-217			1969			COMB197-180			ROOKHOPE			163-217			1969		
WAVE	RATIO	ERROR	PHASE	ERROR	PHASE	ERROR	WAVE	RATIO	ERROR	PHASE	ERROR	WAVE	RATIO	ERROR	PHASE	ERROR	WAVE	RATIO	ERROR	PHASE	ERROR		
2N2	2.754	0.059	-67.686	0.021	-67.686	0.021	2N2	1.259	0.063	178.758	0.050	2N2	1.259	0.063	178.758	0.050	N2	1.759	0.045	51.694	0.025		
N2	2.564	0.061	161.067	0.024	161.067	0.024	N2	1.759	0.045	51.694	0.025	M2	1.317	0.019	33.719	0.014	M2	1.317	0.019	33.719	0.014		
M2	1.676	0.023	140.982	0.014	140.982	0.014	L2	2.593	0.025	-3.510	0.007	L2	2.593	0.025	-3.510	0.007	L2	2.593	0.025	-3.510	0.007		
L2	5.584	0.152	87.394	0.027	87.394	0.027	S2	1.346	0.011	6.274	0.006	S2	1.346	0.011	6.274	0.006	S2	1.346	0.011	6.274	0.006		
S2	1.841	0.105	84.913	0.057	84.913	0.057	Q1	0.258	0.363	99.444	1.409	Q1	0.258	0.363	99.444	1.409	Q1	0.258	0.363	99.444	1.409		
Q1	0.292	0.208	3.270	0.713	3.270	0.713	O1	0.836	0.100	22.947	0.120	O1	0.836	0.100	22.947	0.120	O1	0.836	0.100	22.947	0.120		
O1	0.422	0.040	16.717	0.094	16.717	0.094	M1	4.760	0.928	-27.548	0.195	M1	4.760	0.928	-27.548	0.195	M1	4.760	0.928	-27.548	0.195		
M1	1.191	0.406	20.388	0.341	20.388	0.341	K1	0.973	0.083	-13.081	0.085	K1	0.973	0.083	-13.081	0.085	K1	0.973	0.083	-13.081	0.085		
K1	1.000	0.051	-16.342	0.051	-16.342	0.051	J1	1.069	0.966	171.775	0.903	J1	1.069	0.966	171.775	0.903	J1	1.069	0.966	171.775	0.903		
J1	0.479	0.406	-124.441	0.848	-124.441	0.848	001	1.098	1.795	-68.889	1.635	001	1.098	1.795	-68.889	1.635	001	1.098	1.795	-68.889	1.635		
001	2.788	0.943	112.003	0.238	112.003	0.238																	

TABLE (6-2) Diminishing factors and phase lag (E.C.S) for 1968 west and south tilts (top) and 1969 west and south tilts (bottom) at Rookhope. RATIO equals diminishing factor.

LR12 GRAVIMETER, OTTAWA

DAY 047 TO 093 1969

WAVE	RATIO	ERROR	PHASE	ERROR
2N2	1.810	0.025	27.078	0.014
N2	1.090	0.011	3.755	0.010
M2	1.196	0.004	-1.457	0.003
L2	1.843	0.022	-2.990	0.012
S2	1.199	0.001	-2.321	0.001
Q1	1.071	0.073	-3.144	0.068
O1	1.173	0.029	-0.503	0.025
M1	1.134	0.100	-6.870	0.088
K1	1.168	0.025	0.169	0.021
J1	1.171	0.091	11.228	0.078
001	1.638	0.012	-1.101	0.007

TABLE (6-3) Gravimetric factor and phase lag (E.C.S) for 1969 at Ottawa. RATIO equals gravimetric factor.

HY001-180 ROOKHOPE 206-259 1969

WAVE	RATIO	ERROR	PHASE	ERROR
2N2	0.420	0.033	103.541	0.079
N2	0.532	0.017	60.453	0.033
M2	0.800	0.014	57.409	0.017
L2	1.037	0.084	71.013	0.081
S2	0.943	0.027	23.555	0.029
Q1	0.522	0.176	-139.852	0.338
O1	0.596	0.049	30.329	0.083
M1	3.680	0.341	-75.334	0.093
K1	0.775	0.113	-12.077	0.146
J1	0.955	0.270	148.400	0.283
CO1	2.067	1.348	-103.916	0.652

TABLE (6-4) Diminishing factor and phase lag (E.C.S) for 1969 at Rookhope determined by the hydrostatic tiltmeter. Multiply RATIO by 1.04 to obtain diminishing factor.

CHAPTER 7

SPATIAL VARIATIONS OF THE EARTH TIDE

7-1 Introduction

It is necessary to state clearly the definitions adopted for the discussion which follows. Tidal-gravity amplitudes are measured in microgals and referred to either in this form or in the non-dimensional form called  $\delta$  obtained by normalizing to the theoretical rigid-Earth tidal gravity amplitude at the site. This latter amplitude is given by:

$$V = 74.711 \text{ Cos}^2\lambda_c \quad (\text{microgals}) \quad (7-1)$$

where  $\lambda_c$  is the geocentric latitude found from the geographical latitude  $\lambda$  by:

$$\lambda_c = \lambda - (\text{Sin}2\lambda/5.1826) \quad (7-2)$$

Tidal-tilt amplitudes are measured in milliseconds of arc and referred to either in this form or in the non-dimensional form called  $D$  obtained by normalizing to the theoretical rigid-Earth tidal tilt amplitudes at the site. These latter amplitudes, for the directions north and east respectively, are given by:

$$N = 7.8706 \text{ Sin}2\lambda_c [1 - (\text{Sin}^2\lambda_c/297)] [1 + (2\text{Cos}^2\lambda_c/297)] \quad (7-3)$$

$$E = 15.741 \text{ Cos}\lambda_c [1 - (\text{Sin}^2\lambda_c/297)] \quad (7-4)$$

These three tidal components are considered positive when directed away from the center of the Earth, toward the north and toward the east respectively. When expressed in the dimensioned form the phase is a lag with respect to the phase of the equilibrium constituent at Greenwich (E.C.G.).



Thus the phases of the rigid-Earth components are given by:

$$gV = -2\theta \quad (7-5)$$

$$gN = -2\theta - 180 \quad (7-6)$$

$$gE = -2\theta - 90 \quad (7-7)$$

where  $\theta$  is the longitude, in degrees east of Greenwich, of the site. When the amplitude is expressed in the non-dimensional form it is more appropriate to use the phase relative to the phase of the rigid-Earth component at the site. This latter phase is the same as the phase of the equilibrium constituent through the site (E.C.S). The phase used in the non-dimensional case is given by the symbol  $k$  and is called phase lag re. E.C.S.

Reference is made to the 'global gravimetric factor' and to the 'global diminishing factor'. These are nominal values for  $\delta$  and  $D$  intended to approximate the factors which would be experienced on the Earth if there was no ocean loading effect. Seismological evidence and model studies indicate that these factors are approximately 1.16 and 0.700 respectively.

The gravimeter site at Bidston is located on a hill overlooking tidal waters at a distance of only 2 or 3 kms. It is necessary here to calculate the direct attraction effect due to this height. Provision is made in program GLOBL to make this computation: The Green's Function for gravity is put equal to 1.0 for all distances and two computations are made, one with the height set equal to zero

and the other using the actual height; the difference between the two results is the desired attraction effect due to height alone.

## 7-2 Gravity and Tilt Observations in Britain.

### 7-2-1 Bidston

The gravity perturbation due to ocean loading is estimated by program GLOEL to be:

$$G = 1.978 \text{ } (-78^\circ) \quad (7-8)$$

This is calculated on the basis of zero height at the site. The attraction effect alone, assuming zero height is:

$$\Delta G_a (h=0) = .875 \text{ } (-53.4^\circ) \quad (7-9)$$

The attraction effect for the true height of 5425 cms is:

$$\Delta G_a (h=5425) = .574 \text{ } (154.5^\circ) \quad (7-10)$$

The net perturbation due to height effect alone is the difference between these two attraction terms:

$$\Delta G_h = 1.408 \text{ } (137.5^\circ) \quad (7-11)$$

Adding this to the perturbation found assuming zero height yields the net perturbation due to all effects of the ocean tide; denoting this as  $\Delta G_t$  we have:

$$\Delta G_t = \Delta G + \Delta G_h = 1.163 \text{ } (-122.2^\circ) \quad (7-12)$$

The M2 constituent of the gravity tide observed, assuming a gravimetric factor of 1.16, then should be:

$$G_o = 1.16 G_t + \Delta G_t \quad (7-13)$$

where  $G_t$  is the gravity tide which would be observed on an oceanless and rigid Earth.

This predicted result is compared with the IGY earth-tide gravity observations made in 1958 by Harrison et

Site	Observed	Calculated	Ocean-tide Contribution	Theoretical Rigid Earth
Bidston	30.94 (4.4°)	30.37 (4.4°)	1.16 (-122°)	26.79 (6.1°)
Winsford	32.84 (2.2°)	32.74 (1.4°)	3.84 (-67°)	27.03 (5.0°)
Llanrwst	-	25.2 (21.3°)	6.42 (119°)	26.83 (7.6°)
Rookhope	-	28.63 (-3.6°)	4.00 (-89°)	24.65 (4.4°)

TABLE (7-1) Comparison of observed and calculated gravity tide.  
(Amplitudes in  $\mu\text{gals}$ , phase lag re E.C.G.)

0	N.E. Atlantic Ocean	0.795 (-70°)
1	N. Atlantic (remainder)	1.06 (-75°)
2	S. Atlantic	.26 (-116°)
3	N. Pacific	.23 (- 4°)
4	S. Pacific	.67 (-125°)
5	Indian Ocean	.53 (54°)
6	N. American coastal areas	.31 (117°)
7	Mediterranean area	.07 (-106°)
8	Arctic Ocean	
	Total Effect.....	1.163(-122°)

TABLE (7-2) Bidston - Contribution to gravity tide by global zones (microgals).

Poly. Nr.	Amplitude (phase)	Cal. tilt effect North	Cal. tilt effect East	Cal. grav. effect	Height effect
1	274 (315 <sup>0</sup> )	27.936	17.077	1.021	1.090
2	183 (325 <sup>0</sup> )	5.518	5.910	.056	.030
3	107 (350 <sup>0</sup> )	1.255	.209	.009	.004
4	320 (330 <sup>0</sup> )	5.001	16.857	.196	.181
5	198 (345 <sup>0</sup> )	2.339	5.029	.033	.023
6	76 (020 <sup>0</sup> )	.317	.450	.004	.001
7	274 (316 <sup>0</sup> )	.756	9.515	.065	.031
8	290 (315 <sup>0</sup> )	20.666	13.100	.184	.086
9	274 (315 <sup>0</sup> )	3.503	.803	.042	.007
10	290 (310 <sup>0</sup> )	3.350	3.278	.058	.009
11	290 (310 <sup>0</sup> )	.784	5.340	.075	.010
12	60 (318 <sup>0</sup> )	.011	.607	---	---

TABLE (7-3) Bidston - Calculated effects due to local polygons

Site	Observed			Calculated			Ocean-tide contr.			Theoretical		
	North	East		North	East		North	East		North	East	
Bidston	70.80(317)	54.03(137)		73.80(314)	47.72(129)		77.16(-43)	53.45(125)		7.55(186)	9.43(-83)	
Winsford	-	-		11.74(314)	5.71(167)		15.60(-31)	9.98(128)		7.56(185)	9.46(-85)	
Llanrwst	-	-		54.13(311)	9.11(325)		57.15(-45)	6.77( 12)		7.55(188)	9.43(-82)	
Rookhope <sup>1968</sup>	9.38(136)	13.05(131)		8.59(118)	9.39(120)		8.01( 82)	15.36(110)		7.43(184)	9.12(-86)	
Rookhope <sup>1969</sup>	9.38(139)	14.69(133)		"	"		"	"		"	"	
Rookhope(1)	-	-		9.38(136)	13.05(131)		7.05(103)	18.55(119)		"	"	
Rookhope(2)	-	-		9.90(113)	11.50(120)		9:58( 82)	17.46(111)		"	"	
Rawdon	26.40(136)	27.40(-48)		18.00(151)	20.77(-31)		20.52(148)	19.33(-53)		3.87(-52)	11.15( 37)	

TABLE (7-4) Comparison of observed and calculated tidal tilts (amplitude in msec, phase lag E.C.G)

al (1963) in Table (7-1).

It is useful to consider the gravity perturbation contributed by each of the global zones to make up the total given in Table (7-1). These are shown in Table (7-2). The 12 polygons shown in Figure (7-6), which are local to the Bidston site, have a large influence on the gravity tide measured at the site. Data for these polygons are summarized in Table (7-3). Since the ocean-tide effect is small and due principally to local loading in the distance range where the Green's function for gravity has been extrapolated this result can not be used to infer any particular crustal structure.

Tilt measurements have been made at the Bidston site for many years. Lennon and Vanicek (1969) have recently summarized the results of tilt measurements made since 1952 using several different instrument types and methods of installation. These results cover a wide range of values and there seems to be no grounds for deciding which values are the more likely. A simple average of all the numbers referred to in their Table 2 yields the 'observed' results reproduced in Table (7-4) (Bidston) below. The 'calculated' values were determined by program GLOBL. It can be seen in Table (7-3) that the tilt effect due to local polygons is relatively enormous; polygon number 1 alone contributes 36 percent of the total north effect. This illustrates the importance of precisely representing the ocean tide when the site is very close. If the reliability of the tilt

observations warranted greater prediction accuracy these local polygons could be subdivided and the variation of the tide over the surface could be estimated more accurately. Improved accuracy could be obtained too by referring to the geographical coordinates of both the site and the polygons to the nearest .001 degrees rather than to .01 degrees as used here. For this distance range all these steps would be required before the predicted results could be compared to the observations with a view to appraising the suitability of the Green's Function used for tilt. In this particular case the measurements appear to be influenced by other effects and these refinements are not warranted.

#### 7-2-2 Winsford

Calculated effects are presented for this site for both the gravity tide and the tilt tide although only the IGY gravity observations of Harrison et al (1963) are available for this site. (A short series of tilt measurements made by Tomaschek in 1953 at this site is chiefly of historical interest.) The close agreement between calculated and observed results demonstrates the probable validity of the extrapolated values assumed for the Green's Function.

#### 7-2-3 Llanrwst

Gravity and tilt calculations are presented in Tables (7-1) and (7-4) for this new site established by G. W. Lennon in 1968. Observations at this site have not yet been published. The gravity result will be particularly interesting when it becomes available because the calculated

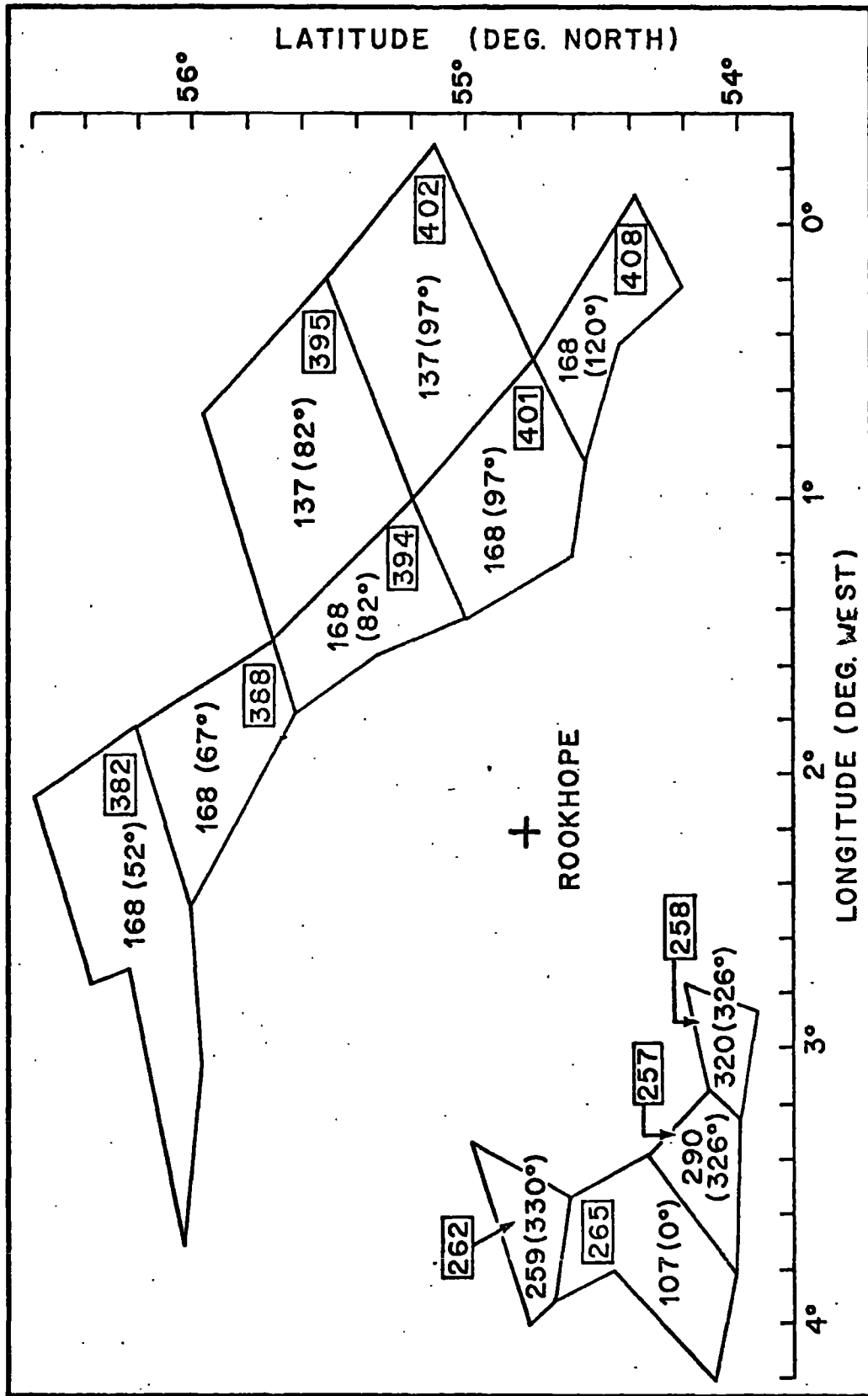


FIGURE (7-1) Ocean-tide polygons near Rookhope, England. Each polygon is numbered (blocks) and assigned an amplitude (in cms) and phase (lag relative to moon's transit of Greenwich). (Data from Admiralty Chart No. 5038).



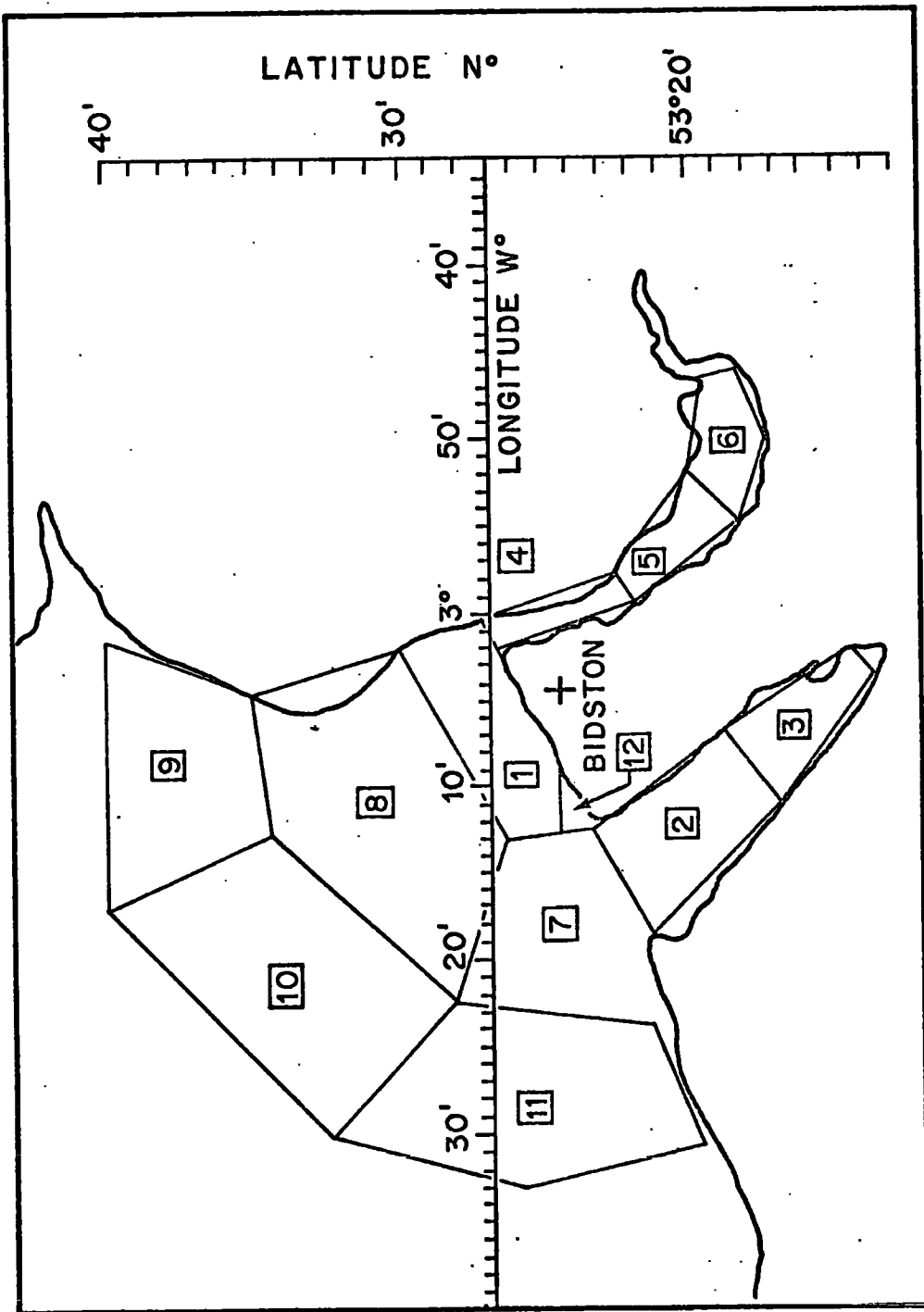


FIGURE (7-6) Ocean-tide Polygons near Bidston, England.

ocean-tide contribution is so large. Accurate observations of the gravity tide should lead to an experimental determination of the local Green's function accurate to within a few percent.

#### 7-2-4 Rookhope

This site is ideally situated for investigating the elastic properties of the upper mantle by means of tilt measurements. Figure (7-1) shows the location of the nearest ocean-tide polygons; the site is approximately 60 kms from the nearest coast. According to Beaumont's results (1971-unpublished) the Green's Function for tilt is the same for a wide range of Earth models for distances greater than about 200 kms. In the distance range of 50-150 kms however the Green's Function for tilt is sensitive to upper mantle and deep crustal structure but not at all sensitive to the superficial layers near the surface.

Results for data obtained in the years 1968 and 1969 are presented in Table (7-4). Precisely the same north-south tilt was obtained in both years while the east-west tilt measured during the second year was about 12 percent higher than for the first. The net calculated tilt shown is the sum of the ocean-tide contribution computed by program GLOBL and the theoretical rigid-Earth tilt diminished by the factor 0.7, which is the global diminishing factor accepted throughout this thesis. There is relatively poor agreement between the calculated and observed results; particularly in the east-west direction. Working backwards from the observed

and theoretical values the ocean-tide contribution required for agreement of calculated and observed results can be found; this is shown in the line marked 1. Although the required east-west ocean effect is substantially larger than that determined by GLOBL the required north-south ocean effect is smaller. This rules out any suggestion that a simple increase of several percent in the Green's Function for distances from 50 kms to 100 kms is required. To illustrate the unsatisfactory effect the ocean-tide contribution has been recomputed for an increase in the Green's function for distances from 50 kms to 100 kms of 10 percent. (Line 2). As the Green's Function is increased to correct the east-west calculation the phase of the north-south calculation becomes increasingly in error. At least for a laterally homogeneous mantle the Green's Function assumed is probably nearly correct.

The next step in the treatment of this data should be to more precisely delineate the local tides shown in Figure (7-1); showing the large amplitudes near shore. If this better definition does not lead to better agreement between calculated and observed tilts then tilt measurements at another site in the same area should be made to confirm the peculiar features noted here. In particular if the large east-west tilt is confirmed it would constitute evidence for lateral inhomogeneities in the mantle or for possible non-elastic effects such as block-tilting. (Tom<sup>a</sup>schek 1953).

Site	Observed		Calculated (D = .7)		Calculated (D = .6)		Ocean-tide effect	
	North	East	North	East	North	East	North	East
Warmifontaine (1)	4.75(188)	9.65(-81)	4.67(181)	8.36(-86)	3.93(182)	7.80(-85)	.97(-58)	2.50(-51)
Warmifontaine (2)	5.01(185)	10.19(-84)	"	"	"	"	"	"
Dourbes (1)	3.32(181)	8.40(255)	4.17(186)	8.56(-86)	3.45(189)	7.60(-85)	1.54(-47)	2.26(-50)
Dourbes (2)	3.36(179)	8.04(256)	"	"	"	"	"	"
Sclaigneaux (1)	7.29(181)	8.70(252)	4.78(179)	8.42(-91)	4.04(180)	7.46(-90)	.80(-61)	1.92(-64)
Sclaigneaux (3)		7.86(250)	"	"	"	"	"	"
Remouchamps	2.86(180)	8.05(-85)	5.05(178)	8.58(-89)	4.30(179)	7.63(-88)	.72(-81)	2.32(-55)
Sclaigneaux (2)	6.19(179)	8.19(252)						
<b>M e a n s</b>	4.68	8.63	4.63	8.46				

TABLE (7-5) Comparison of observed and calculated tidal tilts. (Amplitude in  $\mu$ gals, phase re E.C.G)

### 7-2-5 A Suggested Site

As can be seen from Fig. (3-4) the ocean-tide loading effect in the south-west part of England should be exceptionally high. For a site located at latitude  $50.50^{\circ}\text{N}$ , longitude  $356.00^{\circ}\text{E}$ , the effects on gravity ( $\mu\text{gals}$ ) and tilt (msecs) are computed by program GLOBL to be 10.332 ( $-44^{\circ}$ ) and 37.893 ( $-35^{\circ}$ ) north, 28.523 ( $-64^{\circ}$ ) east. The corresponding gravimetric and diminishing factors are 1.400 ( $-12^{\circ}$ ), 4.590 ( $130^{\circ}$ ) north, 3.618 ( $14^{\circ}$ ) east. These values are large and at the same time the particular site is more than 20 kms from the nearest coast so that there are no very local loads and thus no influence from superficial surface structure. For this reason this region is suggested as a site for measurement of the gravity tide for the purpose of determining empirically the near-load Green's function.

### 7-3 Belgium Tilt Measurements

Observed and calculated tilts are presented below (Table 7-5) for 4 sites in Belgium where anomalous results have been observed which Melchior has suggested may be due to upper mantle heterogeneities. For each series of measurements at each site I have listed the north and east components of tilt observed. For each site I have calculated and listed the ocean-tide effect, the net tilt which should be observed assuming this ocean-tide effect and a diminishing factor of 0.7, and the net tilt assuming a diminishing factor of 0.6. The small values observed for the north-south tilts at Dourbes and Remouchamps have been noted

by Melchior (1967) and similar results have been obtained at the neighboring sites of Chevron and Vielsalm. The very large north-south tilt observed at Sclaigneaux is at least as anomalous as these small values but has attracted less attention.

The difference between calculated and observed north-south results is between -2.19 and +3.01 milliseconds for the seven observations listed. This is about equal to the amplitude of the vector representing the tilt due to loading and attraction by the ocean tide. The corresponding differences for the east-west results are -.56 and +1.83.

This pattern of variations can not be explained by crustal or mantle inhomogeneities. All the sites are located more than 100 kms from the nearest coast thus the surface loading effects of the ocean tide will be determined mainly by the elastic properties of the mantle rather than the crust. Inhomogeneities at this depth could not account for the small-scale regional variations evidenced by the results. The spatial change in the direct attraction of the water masses is similarly restricted; this can be seen from the Boussinesq solution for an elastic half-space which relates the attraction to the surface deformation. Thus the variation observed can not be the result of local differences in the response of the Earth to the ocean-tide surface force.

The body tide of the Earth is a function of even deeper layers (Takeuchi, 1950) and therefore, although the

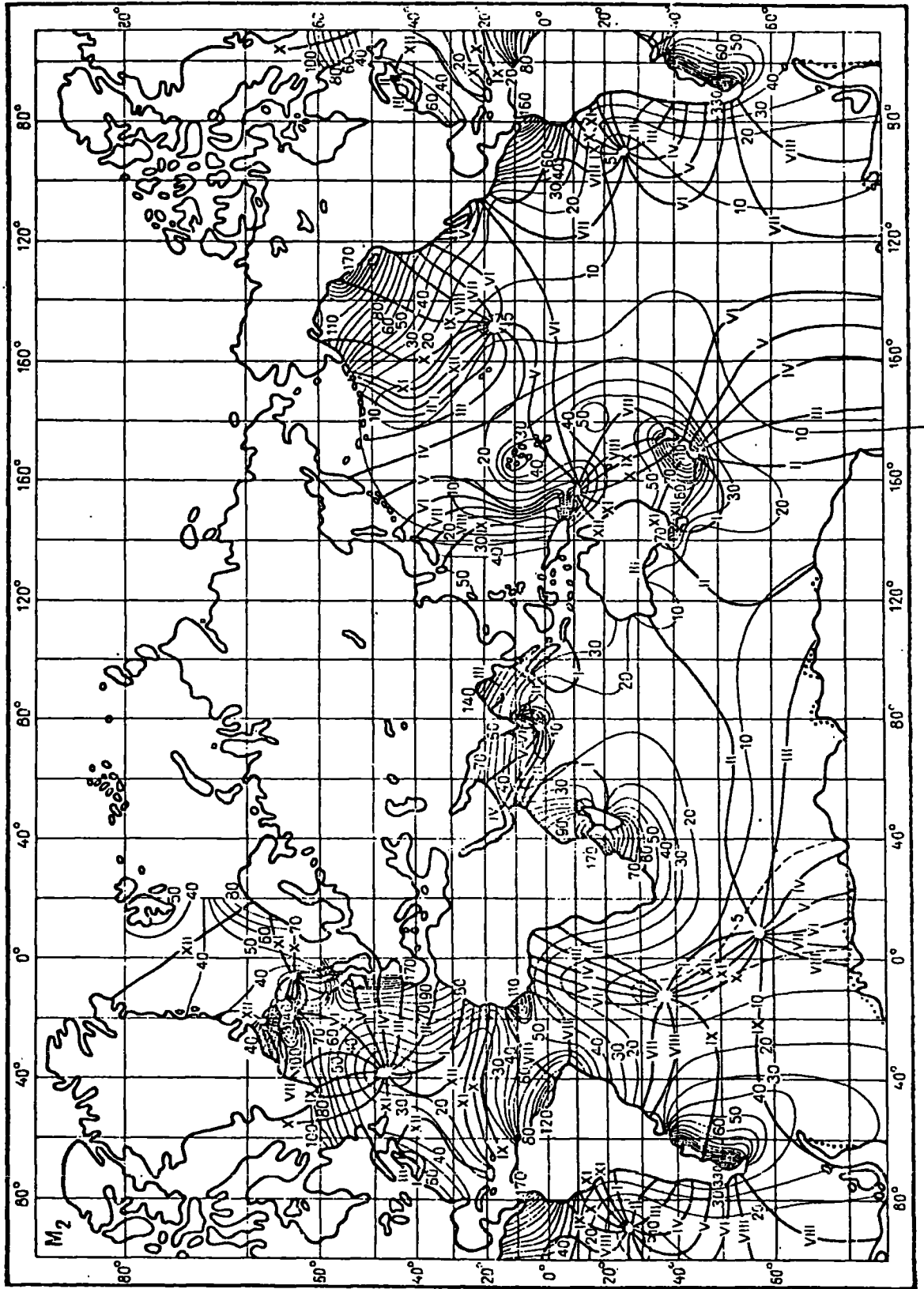


FIGURE (7-2) Coamplitude-Cophase chart of the global ocean tide. (Tiron et al 1967).

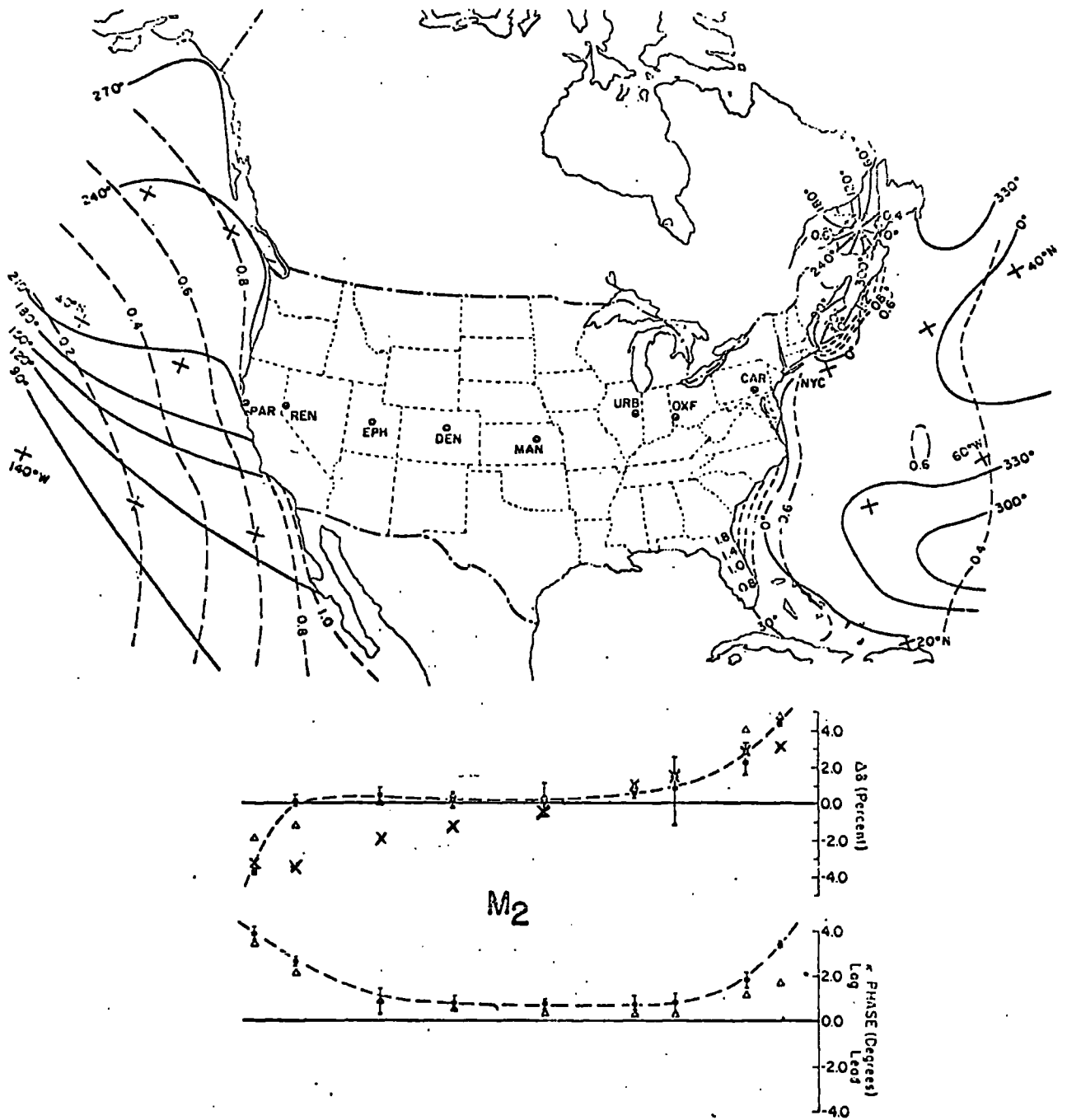


FIGURE (7-3) Trans-U.S.A earth-tide profile (Kuo et al. 1969). Observed values (solid dots), calculated (triangles) by Kuo et al based on ocean-tide data shown, calculated (crosses) by GLOBL based on ocean-tide data described in text.



diminishing factor assumed may be in error by several percent, it must have the same value throughout regions having dimensions in the order of hundreds of kilometers. I have listed in Table (7-5) calculated results for each of the sites assuming a diminishing factor of 0.600 to illustrate the effect of this factor. Clearly the results can not be explained as spatial variations in the body tide.

The most likely reason for spatial variations of the diminishing factor on the scale noted here is the presence of large underground water courses. A water-saturated zone confined by impermeable walls, except for a few cracks through which water may be forced when the zone is compressed, has the ability to integrate the earth-tide body force throughout the entire zone and to concentrate certain of its effects over a small area. This is demonstrated by the tidal variation in the level of wells. It is easy to imagine a situation where the tiltmeter is installed directly on a rock which caps a water-saturated zone and which is caused to tilt by tidal variations of the hydrostatic pressure in the zone.

Finally, it is interesting to observe the good agreement between the arithmetic means of the observed and the calculated results.

#### 7-3-1 The Influence of Hydrology

Confined and unconfined aquifers in general are discussed by Brown (1968) and are illustrated in his Figure

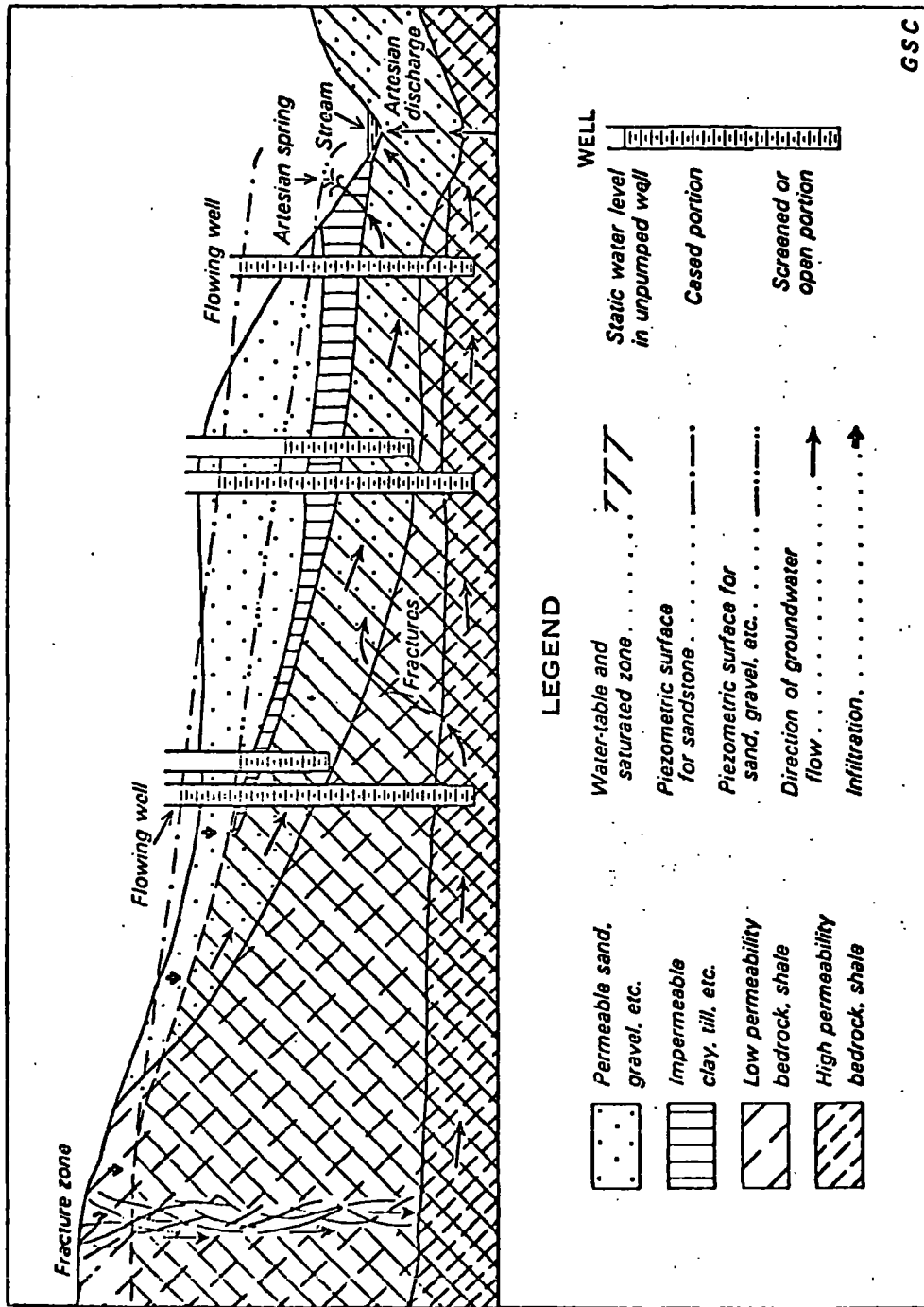


FIGURE (7-4) Confined and unconfined aquifers. (Geology and Economic Minerals of Canada, 1968).

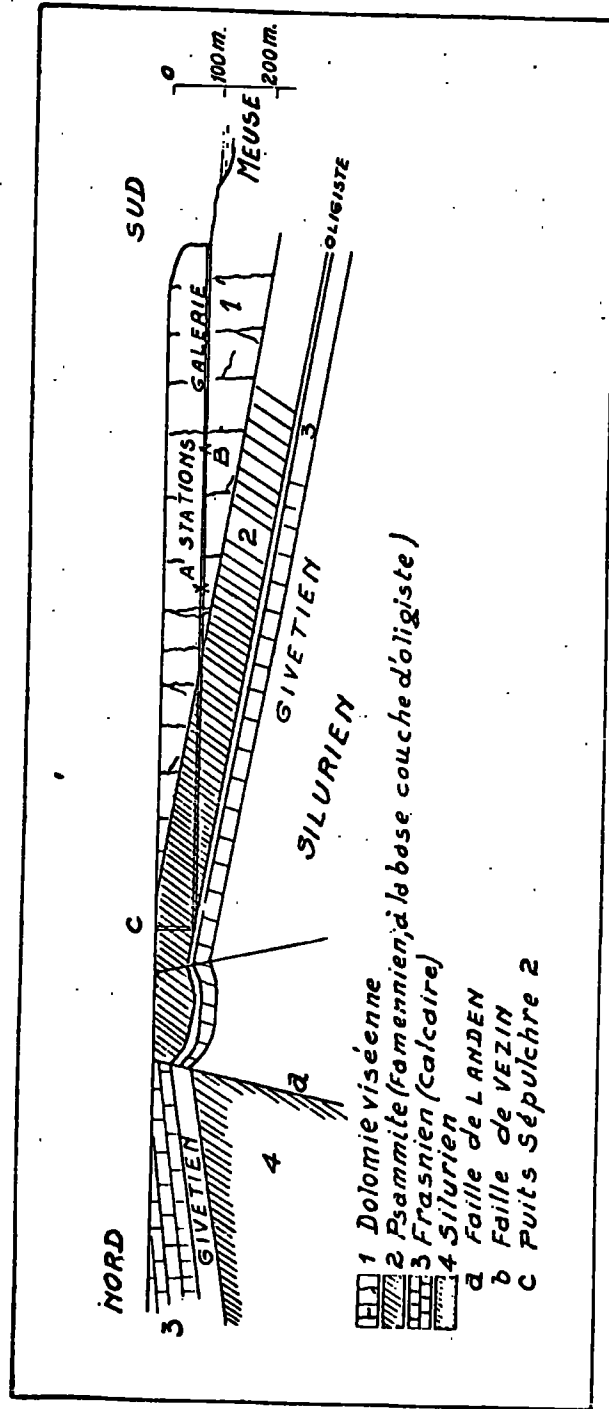


FIGURE (7-5) Geological section through the Sclaigieux site. (Melchior and Brouët, 1964).

XIII-4 which is reproduced here in Fig. (7-4). Referring to this figure it can be seen that volume changes due to the strain of the earth tide will cause changes in the hydrostatic pressure in both the confined and unconfined aquifers. The pressure acting on the under surface of the impermeable layer will therefore vary periodically and the layer may be displaced as a consequence; perhaps differentially to cause the upper surface to tilt. In the practical case the hydrogeology is not generally known but a useful criterion for the possible influence of groundwater on earth-tide measurements may be the drift or long-term behaviour of the recorded tilt. If the measurements are influenced by groundwater then this behaviour should reflect the seasonal fluctuations due to groundwater recharge and discharge.

The site at Sclaigneaux is known to be affected by flooding of the near-by river Meuse. Melchior and Brouet (1964) have found that the observed tilt due to this flooding is about an order of magnitude greater than that due to loading of an infinite plane of rigidity equal to  $10^{11}$  cgs units. They find too that the tilt-load relation is not linear nor is it completely reversible. A cross-section through the mine adit leading to the Sclaigneaux sites is reproduced in Figure (7-5) (Melchior and Brouet, 1964). Layer 2 is a sandstone much more porous than the dolomite of layer 1. The situation is similar to that illustrated in Fig. (7-4) and it is conceivable that the hydrostatic

SITE	$\delta_o$	( $\kappa$ )	LONG(E)	LAT(N)	$\Delta\delta$	$\kappa$	$\delta_{corr}$	$\kappa$
Uccle	1.180	(-1.3)	4.21	50.48	.107	(-54)	1.118	(3)
Luxembourg	1.198	(-1.1)	6.08	49.37	.098	(-52)	1.138	(3)
Karlsruhe	1.211	(-1.0)	8.25	49.01	* .080	(-48)	1.158	(2)
Hannover	1.179	(-1.5)	9.43	50.23	* .080	(-48)	1.125	(1.5)
Kiesflbach	1.192	( 4.9)	10.07	50.51	* .080	(-48)	1.146	(8.0)
Bad Salzungen	1.131	( 0.0)	10.14	50.48	* .080	(-48)	1.079	(3.0)
Potsdam	1.209	( 0.5)	13.04	52.23	.073	(-42)	1.156	(3.0)
Freiberg	1.127	(-0.3)	13.14	50.55	* .073	(-42)	1.074	(2.0)
Berggieshubel	1.273	( 3.6)	13.57	50.52	* .073	(-42)	1.223	(6.0)
Dourbes	1.308	( 0.0)	4.36	50.06	.106	(-53)	1.247	(4.0)
Strasbourg	1.202	(-1.0)	7.46	48.35	* .09	(-52)	1.147	(2.5)
Frankfurt	1.180	(-1.0)	8.31	50.05	* .08	(-48)	1.127	(2.0)
Bonn 1	1.202	( 0.0)	7.5	50.44	* .09	(-52)	1.144	(3.0)
Bonn 2	1.209	(-1.0)	7.5	50.44	* .09	(-52)	1.150	(2.0)
Paris	1.195		2.33	48.83	.123	(-55)	1.129	(5.0)
Vedrin	1.197		4.85	50.50	* .106	(-53)	1.136	(4.0)
M E A N S	1.200				.087		1.142	

TABLE (7-6) Comparison of observed and corrected gravity tide in western Europe. (Gravimeter factor  $\delta$ , phase lags  $\kappa$ ).

SITE	OCEAN-TIDE GRAVITY EFFECT	CALCULATED GRAV. FACTOR
New York	2.039 (-179)	1.201 (-1)
Carlisle	1.280 ( 163)	1.190 ( 0)
Oxford	0.823 ( 133)	1.175 (-1)
Urbana	0.739 ( 119)	1.169 (-1)
Manhattan	0.719 ( 90)	1.156 (-1)
Denver	0.776 ( 80)	1.148 (-1)
Ephraim	0.927 ( 73)	1.141 (-1)
Reno	1.556 ( 61)	1.124 ( 0)
Pt. Arena	2.772 ( 43)	1.103 ( 1)

TABLE (7-7) Calculated gravimetric factors and ocean-tide effect ( $\mu\text{gals}$ ) for Trans-U.S.A profile.

(Phase of ocean-tide effect is lag re E.C.G, phase of gravimetric factor is lag re E.C.S)

pressure on layer 1 is caused to vary with the earth tide. The effect of this pressure may be particularly complex because of the fractured state of the rock. There is thus sufficient reason to suspect the anomalous north-south results determined at this site.

The hydrogeological conditions at the other sites have not been discussed. Melchior has however singled out the Warmifontaine site as being particularly stable; both from the standpoint of long-term drift and of constancy in sensitivity. The observations from this station show the best agreement with the calculated results in Table (7-5).

#### 7-4 Gravity Measurements in Western Europe.

The results of Earth-tide gravity measurements made in recent years at seventeen sites in Western Europe are listed in Table (7-6) together with calculated ocean-tide effects. The column headed  $\Delta\delta$  is the perturbation of the gravimeter factor determined by program GLOBL. Values of  $\Delta\delta$  marked by an asterisk were determined for neighboring sites and thus may be slightly in error.  $\delta_{corr}$  is the net corrected gravimetric factor found by subtracting  $\Delta\delta$  from the observed factor  $\delta_o$ .

It can be seen that the observed values are generally larger than the value of  $1.16 \pm .005$  suggested by Alsop and Kuo (1964) as the most probable value of  $\delta$  for the Earth as a whole. The calculated perturbation leads the phase of the equilibrium constituent at the sites by approximately  $50^\circ$  and has an average amplitude of .087. When these calculated

perturbations are subtracted from the observed gravimeter factors the result is generally too small relative to the probable global value. Taken individually the gravity measurements may reflect various unknown effects which have no geophysical significance. Taken as a group however this large number of measurements would be expected to yield a significant result and the low value of 1.142 for the average corrected gravimetric factor suggests a systematic error. Several possible reasons for a systematic error in the computation of the ocean-tide effect were considered and the most likely is the neglect of the ocean tide in the Norwegian and Greenland Seas. These waters were omitted because reliable tidal charts were thought not be available at the time the ocean-tide data was compiled for program GLOBL. The tidal charts of Tiron et al (1967) have become available since and these do include part of the area in question. Tiron's chart for the global M2 tide is reproduced in Figure 7-2. It will be seen that the tide in the Greenland Sea-Norwegian Sea area has a nearly uniform phase lag of 11 to 12 hours and a mean amplitude of 45 cms. This phase is in near opposition to the perturbing effect already noted and therefore will tend to yield larger values for the corrected gravimetric factors  $\delta_{corr}$ . A rough estimate of the maximum effect on the perturbing vector  $\Delta\delta$  is 0.10 (.29  $\mu$ gals) which, if applied uniformly to all the results, would raise the average gravimetric factor to 1.152. This result still seems low but definite conclusions must await a

detailed treatment.

#### 7-5 North American Measurements

##### 7-5-1 Gravity Along A Trans-U.S.A Profile

Kuo et al (1969,70) have conducted a tidal-gravity survey across the United States as a basis for investigating the spatial variations of tidal gravity. A total of nine sites were occupied, each for a minimum duration of six months with at least six sites in simultaneous operation at one time. Relative calibrations among the gravimeters was determined to within 1 percent throughout the measurements.

Their Figure 7, which is reproduced here as Figure (7-3), shows the location of the sites, the ocean-tide contours assumed, and the gravimetric factors which they observed (solid dots) and which they calculated (triangles) on the basis of a Boussinesq solution of the half-space loading problem. As a first approximation they neglected the effect of ocean tides beyond the area shown in the figure. Rather than extrapolate the Green's Function determined by Longman (1961) they chose to determine first the displacement by the Boussinesq solution and then to compute the gravitational effect of the displaced masses numerically.

The close agreement between their observed and calculated results (better than 1 percent except for one site) was taken by Kuo et al as confirmation of an earlier theoretical result (Kuo and Ewing, 1966) that the effects of



ZONE		OCEAN-TIDE EFFECT	ACCUMULATING OCEAN-TIDE EFFECT	PERCENT OF RIGID-EARTH TIDE
N.E. Atlantic	0	.077 (- 57)	.077 (- 57)	.1
N. Atlantic	1	.013 (-179)	.071 (- 66)	.0
S. Atlantic	2	.738 (-102)	.797 (- 99)	1.6
N. Pacific	3	.113 ( 26)	.704 (- 86)	- .3
S. Pacific	4	.363 (-134)	.983 (-102)	.8
Indian	5	.817 ( 75)	.170 (- 90)	-1.8
N. American Coast	6	1.796 ( 65)	1.643 ( 63)	-4.2
Mediterranean	7	.103 (- 85)	1.556 ( 61)	.2
T O T A L				-3.6

TABLE (7-8) The calculated ocean-tide effect on tidal gravity measured at Reno, Nevada. (Ocean-tide effect in  $\mu$ gals and degrees lag re E.C.G)

ZONE		OCEAN-TIDE EFFECT	ACCUMULATING OCEAN-TIDE EFFECT	PERCENT OF RIGID-EARTH TIDE
N.E. Atlantic	0	.142 (- 55)	.142 (- 55)	-.3
N. Atlantic	1	.590 (-169)	.549 (-155)	1.1
S. Atlantic	2	.455 (-112)	.938 (-136)	.0
N. Pacific	3	.464 ( 50)	.479 (-142)	- .3
S. Pacific	4	.321 (-129)	.796 (-137)	.2
Indian	5	.828 ( 70)	.383 ( 142)	2.1
N. American Coast	6	.949 ( 168)	1.303 ( 161)	2.2
Mediterranean	7	.051 (- 81)	1,280 ( 163)	- .1
T O T A L				+2.9

TABLE (7-9) The calculated ocean-tide effect on tidal gravity measured at Carlisle. (Ocean-tide effect in  $\mu$ gals and degrees lag re. E.C.G).

crustal and upper mantle structure on tidal gravity must be small. In view of the results presented earlier in this chapter this close agreement must be considered fortuitous. In the case of Bidston for example the perturbation due to loading by the tide of the South Pacific Ocean represents 2.5 percent of the rigid-Earth value and that due to the Indian Ocean represents 2.0 percent. A flat Earth approximation for determining the ocean-tide effect on tidal gravity is clearly not generally acceptable.

We have presented in Table (7-7) results calculated by program GLOBL for the ocean-tide effect on tidal gravity at each of the trans-U.S.A sites. These results have been plotted too in Figure (7-3) where they can be compared with the results of Kuo et al. We have assumed that their  $\Delta\delta=0$  is with reference to the global-probable value of  $\delta$ , 1.16. Their observed results for the western half of the profile now appear anom<sup>a</sup>olous. This is an interesting result but is unlikely in view of the theoretical results of Kuo and Ewing (1966) and must be examined critically. In Tables (7-8) and (7-9) I have listed results calculated by program GLOBL for Reno and Carlisle; representative of western and eastern sites respectively. These tables show the influence of the various global zones on the ocean-tide effect and are presented here to demonstrate that low gravimetric factors calculated for the west and high factors calculated for the east are not due to distanc<sup>t</sup>e ocean tides which were not considered by Kuo et al. Approximately the same result is

obtained when only the ocean tides bordering North America are considered. In this particular case the effects of distant ocean tides tend to cancel and therefore consideration of the ocean tides on the limited scale adopted by Kuo should produce fairly accurate results.

Comparison of the calculated results determined by program GLOBL with the calculated results of Kuo et al for ocean tides within a distance of  $30^\circ$  is subject to the criticism that the Green's Function used by GLOBL has been determined by extrapolation. To avoid this objection I will demonstrate in another way that  $\Delta\delta$  for the western sites is probably substantially negative rather than near zero as assumed by Kuo et al. The gravity tide at Reno (measured positive outward from the Earth) due to body forces lags the equilibrium constituent at Greenwich by approximately  $240^\circ$ . High water occurring off the western coast at the same time will depress the site and cause a gravity effect opposing the body tide effect. In general, the loading effects of the regional ocean tides can be expressed as follows:

$$\Delta\delta > 0 \quad \text{if} \quad -30^\circ < g < 150^\circ \quad (7-7)$$

$$\Delta\delta < 0 \quad \text{if} \quad 150^\circ < g < 330^\circ \quad (7-8)$$

where  $g$  is the phase lag of the regional ocean tide on Greenwich (E.C.G). The calculated results of Kuo et al mean that the loading effect of the ocean tide north of the  $150^\circ$  contour shown in Figure (7-3) is nearly cancelled by the effect of the ocean tide south of this contour. The position of the  $150^\circ$  cotidal line is therefore crucial in determining

SITE	GRAVIMETRIC FACTOR		CALCULATED OCEAN-TIDE EFFECT	PERCENTAGE OF RIGID-EARTH TIDE
	OBSERVED	CALCULATED		
Ottawa	1.196 (+1.0)	1.190 (+1.0)	1.133 (172)	3.2 (21.0)

TABLE (7-10) Comparison of observed and calculated tidal gravity at Ottawa. (Ocean-tide effect in  $\mu$ gals and degrees lag re E.C.G)

ZONE		OCEAN-TIDE EFFECT	ACCUMULATING OCEAN-TIDE EFFECT	PERCENTAGE OF RIGID-EARTH TIDE
N.E. Atlantic	0	.189 (- 53)	.189 (- 53)	.5
N. Atlantic	1	.463 (-165)	.429 (-141)	1.2
S. Atlantic	2	.465 (-144)	.870 (-127)	1.2
N. Pacific	3	.353 ( 50)	.518 (-125)	1.0
S. Pacific	4	.393 (-125)	.911 (-125)	1.1
Indian	5	.805 ( 70)	.244 ( 178)	2.2
N. American Coasts	6	.908 ( 166)	1.148 ( 169)	2.4
Mediterranean etc.	7	.062 (- 85)	1.133 ( 172)	.2
			T O T A L	3.1

TABLE (7-11) The calculated ocean-tide effect on tidal gravity measured at Ottawa. (Ocean-tide effect is in  $\mu$ gals and degrees re E.C.G)

whether or not the western observations are anomalous. The particular tidal chart used by Kuo et al is one of several that have been postulated. Munk et al (1971) have recently gathered together the various charts available and have discussed them with respect to a new chart which they have derived based on off-shore tidal measurements. I have reproduced their summary of the tidal charts in Figures (4-10) and (4-11). The chart used by Kuo et al is based on that of Dietrich (1944). Amongst all the charts, it will be seen that the Dietrich chart contains the highest proportion of tidal water having a phase less than  $150^\circ$ ; favouring a near-zero value for  $\Delta\delta$ . The most recent charts would all yield more negative results for  $\Delta\delta$ .

It is reasonable to conclude that the values of tidal gravity observed by Kuo et al along the western half of the trans-U.S.A profile are significantly larger than expected on the basis of a spherically-symmetric model of the Earth and the 'best' presently available ocean-tide data. The most likely reason for this result is large-scale errors in the ocean tide data, particularly throughout the central part of the N. Pacific Ocean.

#### 7-5-2 Gravity Measurements At Ottawa

Observed and calculated tidal-gravity results are presented in Table (7-10). The contribution of the various zones is shown in Table (7-11).

#### 7-5-3 Tilt Measurements

Results are presented here for Williams Bay, Wisconsin

SITE	OBSERVED		CALCULATED D=.7		CALCULATED D=.66	
	NORTH	EAST	NORTH	EAST	NORTH	EAST
Holland Mills (1967)	.711(-7)	.811( 0)	.664(-6)	.849(-3)	.624(-6)	.809(-3)
Holland Mills (1968)	.684(-6)	.800(+1)	"	"	"	"
Williams Bay	.676(-1)	.691(-6)	.720(+3)	.729(-4)	.680(+3)	.689(-4)

TABLE (7-12) Comparison of observed and calculated tidal tilts. (Diminishing factors with phase lags re. E.C.G)

(Yerkes Observatory), Holland Hills, Quebec (near Ottawa) and Rawdon Nova Scotia.

The observations referred to at Williams Bay are the classic Earth-tilt measurements of Michelson and Gale made in 1917 (Michelson and Gale, 1919). This was a water-tube type measurement using pipes 502 feet long and 6 inches in diameter buried 6 feet underground. This type of device in general offers several advantages over short-based instruments of the horizontal pendulum type: It is not sensitive to yielding at supporting feet, or to local tilting of rocks; the sensitive direction is clearly defined and the sensitivity can be readily determined in terms of fundamental units; it is inherently zero-stable and can be used to measure secular as well as periodic tilts. Because of these reasons the measurements of Michelson and Gale, which extended over a year, must be treated with a good deal of respect in spite of their antiquity. These results are shown in Table (7-12) together with results from the Holland Mills pendulum site and ocean-tide effects calculated for both sites. (Michelson and Gale seem to have misinterpreted their phase results. In their conclusion they refer to both the observed phases as lags with respect to the tide-producing forces. However, from the description given of their analysis method and from their illustrations it seems clear that the observed phases lead the theoretical phase. Phases shown in Table (7-12) therefore are shown leading). The lack of agreement between the 1967 and the

1968 Holland Mills north-south results indicates that neither is reliable. The east-west results on the other hand are quite consistent. The first calculated results shown were determined on the basis of a global diminishing factor of 0.700. This is simply the round number closest to the factor commonly observed. The second calculated results assume a factor of 0.66 and are much closer to the results observed. This is precisely the number found by Kelvin (1890) from observations of the fortnightly tide in the Indian Ocean; the observations on which he based his now famous remark that the Earth was more rigid than steel. The number 0.66 was determined too by Schweydar (1907) using the same technique but with more frequent observations. The present result shows that the measurements of Michelson and Gale (1919) at a semi-diurnal frequency yield the same number when the measurements are corrected for the surface loading effect of the ocean tide. The number 0.66 is confirmed too by the calibrated pendulum measurements made at Holland Mills.

Rawdon is located in Nova Scotia near the large loading tides of the Bay of Fundy. Lambert (1970) has measured the two components of tilt there using Verbaandert-Melchior pendulums. His observed results are listed in Table (7-4) together with the calculated results assuming a global diminishing factor of 0.7 and an ocean tide effect computed by program GLOBL. Both calculated results are small in comparison with the results observed. The Green's Function



SITE	$\delta\sigma$ (k)	$\Delta\delta$ (k)	$\delta\sigma$ (k)	Ocean-tide			LONG °E	LONG °N
				Effect	Effect	Effect		
Bamako I	1.227 (-1.0)	.049 (- 58)	1.187 (-2)	3.380 (- 41)	351.99	12.39		
Bamako II	1.180 ( 3.0)	"	"	"	"	"	"	
New Delhi	1.153 (-2.0)	.008 ( 72)	1.163 ( 0)	0.496 (- 82)	77.18	28.43		
Bunia	1.185 ( 0)	.017 (- 19)	1.176 ( 0)	1.305 (- 78)	30.18	1.53		
Langchow	1.148 ( 3.5)	.015 ( 42)	1.171 ( 0)	0.715 (-167)	103.85	36.08		
Novosibirsk	1.158 ( 1.1)	.030 ( 55)	1.178 ( 1)	0.715 (-113)	83.05	55.04		
Tashkent	1.143 ( 4.3)	.015 ( 41)	1.171 ( 0)	0.590 (- 99)	69.30	41.53		
Talgar	1.166 ( 3.0)	.017 ( 59)	1.169 ( 1)	0.637 (- 96)	77.15	43.15		

TABLE (7-13) Comparison of observed and calculated gravimetric factors for sites in Africa, Asia and India (Ocean-tide effect in  $\mu\text{gals}$  and phase E.C.G)

used here was the same as that used to calculate the tilt at Bidston and Rookhope; the varying degrees of agreement obtained between observed and calculated results may reflect differences in crustal or (particularly in the case of Rookhope) upper mantle structure. Experimental work in this unique area is being continued by Beaumont with a view to determining an accurate finite-element model of the regional crust and mantle.

#### 7-6 Africa, Asia and Japan

Results for seven sites are shown in Table (7-13). The ocean-tide effect determined by GLOBL for the four mid-Asian sites appears to be in error. Except for Talgar the observed values are all very low although the ocean-tide effect is computed as being additive. This may be due to major errors in the assumed distribution of ocean tides in the Indian Ocean or to omitting the effects of the tide of the Arctic Ocean. Tiron et al (1967) have recently presented a new cotidal chart for the Indian Ocean which is likely much improved over the purely theoretically-derived chart of Uneo (1965) used in program GLOBL. This new chart is being fitted to the program now. The absence of tidal charts for the Arctic basin remains a difficulty.

The first tilt measurements in Africa were made recently by Blum (1969) at Ecker, Algeria (Long 5.08 °E. Lat 24.05°N). The diminishing factors observed for the M2 constituent are  $D=0.668$  for the east-west component and  $D=0.351$  for the north-south component. This site is located

approximately 2000 kms from the closest ocean and thus should be little influenced by ocean tides. When the correction computed by program GLOBL is applied to Blum's factor the result is:  $D=0.608$  (NS) and  $D=0.405$  (EW). The only apparent explanation available for the anomalously low east-west factor is a hydrological condition such as that suggested previously to explain the Belgium results.

The results of tilt measurements made at 27 sites in the Soviet Union have been summarized by Aksentieva et al (1969). Although the ocean-tide effect for all of these sites is small the range of values determined for the diminishing factor is from 0.476 to 0.955; there is one value of 0.252. The means however are 0.653 (+0.015) for the north-south direction and 0.683 (+0.007) for the east-west. This is further support for a global diminishing factor near 0.66.

## CHAPTER 8

### DEVELOPMENT OF A SENSITIVE HYDROSTATIC TILTMETER

#### 8-1 Introduction

The initial aim of the research described in this thesis was to experimentally observe tidal tilts at several points throughout Britain. The impracticability of this plan only became apparent as the difficulties of site preparation and the peculiarities of horizontal pendulum operation were realized. The basic difficulty is that the horizontal pendulum responds to the tilt of a base which is only 23 cms long. The great sensitivity required of the tiltmeter is obtained at the expense of stability of the zero or initial position of the pendulum and sensitivity to dimensional change. The short base line contributes too to the problem of placing the tiltmeter on the Earth's surface so that the tilt it experiences will represent the large-scale tilt due to the tide rather than spurious movements of the small rock or of the support pins on which the tiltmeter is placed. In practise these difficulties have the following consequences: The horizontal pendulum is difficult and expensive to set up; frequent and skilled attention is required to keep it in operation; site occupancy of one year is probably required for reliable (repeatable) results; the results obtained may not represent regional tilting but rather a spurious local effect; all pendulum tiltmeters exhibit a long-term drift and none are suitable for studying secular tilting.

Faced with these difficulties we abandoned plans to

measure tilt at more than one site and investigated alternative means of measuring tilt. Several modern tiltmeters of the short-base type were available but were rejected in favour of the classic water-tube tiltmeter used for the first time for measuring tidal tilts by Michelson and Gale in 1914 (see Section 7-7). Theoretically at least the hydrostatic tiltmeter is zero stable and its sensitivity is determined solely by the length of the base line. Some additional advantages over the horizontal pendulum are: The placement problem is no longer critical and installation is quick and cheap; the direction in which tilting is measured is precisely determined; a system sealed to prevent evaporation will operate for long periods of time without attention.

Extensive bibliographies on hydrostatic leveling are presented in Melchior's book (1965) and in Scheel (1956) who develops the theory and deals with the problem of eliminating errors due to temperature and pressure effects. Modern semi-portable hydrostatic tiltmeters are described by Eaton (1950), Bonchkovskiy and Skur'yat (1961), and by Eto (1966). None of these tiltmeters however provide a sensitivity near that of the horizontal pendulum, which is typically 1.0 mm of chart displacement per 1.0 millisecond of tilt. Melchior (1965, p91) quotes an rms error of 0.3 mm in reading the horizontal pendulum tiltmeter chart so that the rms error in reading the gross tilt (the sum of all harmonic constituents) is 0.3 milliseconds. To measure the

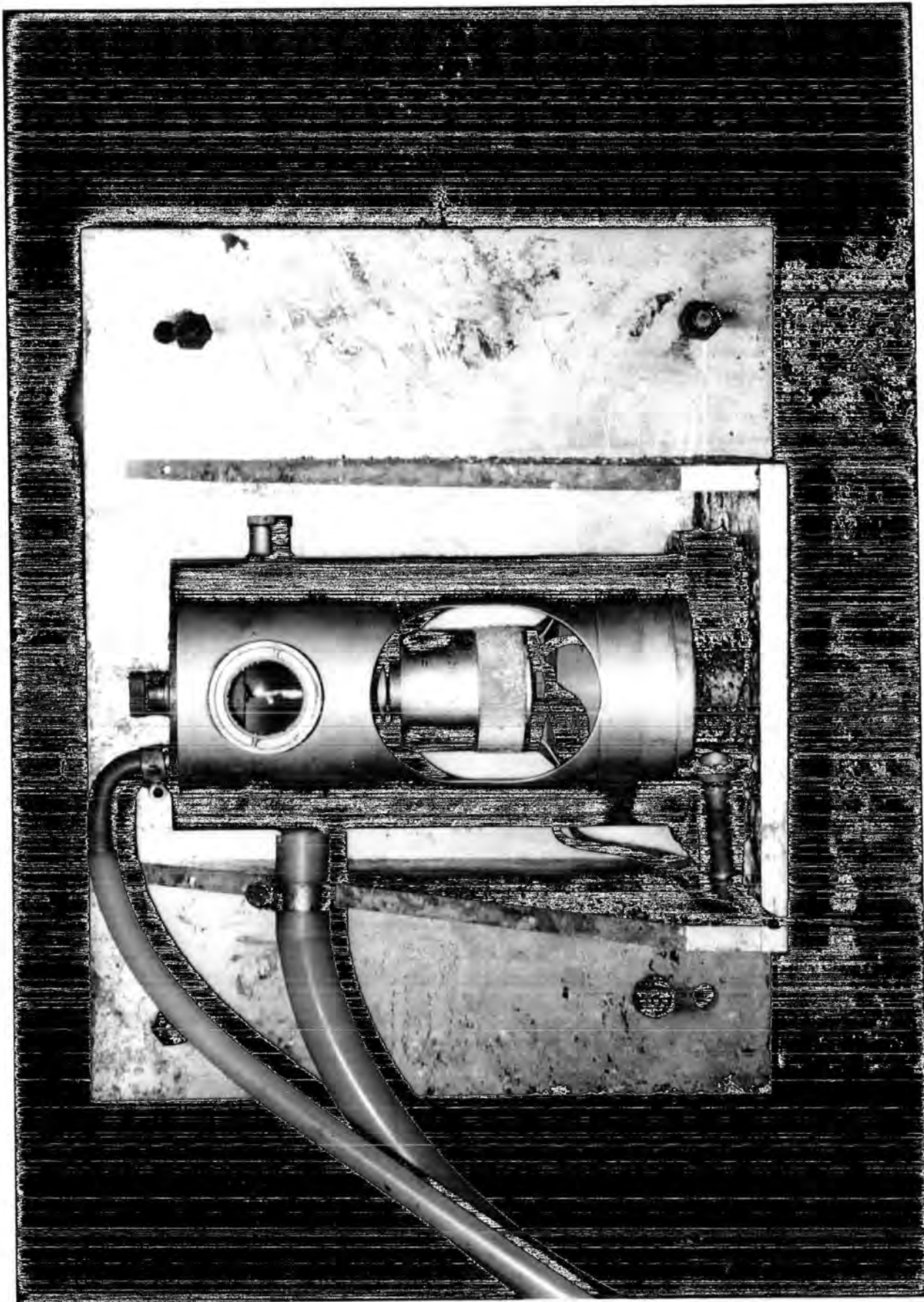


PLATE 8-1) The measuring pot of the water-tube tiltmeter mounted on a shelf bolted to the rock face.

tilt of a hydrostatic tiltmeter with a 100-meter base length to the same accuracy the water level at each end must be measured to an accuracy of  $\pm 0.065\mu$  ( $\pm 2.6$  microinches). This is just within the capability of modern displacement measuring transducers of the differential transformer type. In particular a transducing system manufactured by the Boulton-Paul Aircraft Company of England measures the displacement of the armature of a differential transformer to an accuracy (at constant temperature) of 1 percent throughout a range of 250 microinches. The remainder of this chapter will deal with the design and use of a sensitive hydrostatic tiltmeter incorporating these Boulton-Paul transducers.

#### 8-2 Description of the Apparatus.

The tiltmeter was designed originally as an exact copy of the visually-read tiltmeter described by Eaton (1959). This tiltmeter consists of two pots with connecting water and air tubes. The pots are approximately 10 cms in diameter and 20 cms in height. A manually-adjustable micrometer is fitted through the bottom of each pot through a rubber seal. This micrometer adjusts the height of a pointed-head spindle which, when viewed through a window in the wall of the pot, can be set to mark the level of the water. Variations in the water level can in this way be measured with an rms error of about  $1.5\mu$ .

To accept the Boulton-Paul transducers the upper end of the micrometer spindle was modified so that the transducer

could be inserted into it and sealed with epoxy. The transducer connecting leads were taken out through a hole drilled axially through the spindle and micrometer head. The transducer armature, which has the form of an iron rod of diameter 1.5 mm and length 1.5 cm, was fastened to a light plastic float so that when the float rested on the water surface the armature projected into the axial space of the transformer with approximately 0.2 mm clearance on all sides. Subsequent changes in the water level, within the linear range of the transducer, were then detected and outputted as proportional changes in voltage.

After laboratory tests and modifications, which will be described in the next section, the apparatus was installed in the long straight adit leading to the pendulum site. The pots were clamped to aluminum shelves secured to the rock wall with bolts and expansion nuts (Rawlplug) and located 60 m apart. The air and water lines were of diameter 0.93 and 1.27 cms respectively. The installation of one pot is shown in Plate (8-1).

### 8-3 Laboratory Tests and Modifications.

Laboratory tests of the water-tube tiltmeter began in October 1968 with the system filled with tap water. At first the output voltage was observed to drift off quickly in a series of steps or sudden 'tares'. Much of the drift was eliminated by rebuilding the rubber seal through which the micrometer entered the pot and by boiling the water to remove dissolved air. 'Tares' were still observed however



when the pots were tapped lightly. This was thought to be due to rubbing of the armature against the transducer body and a mechanical vibrator was constructed and fastened to the pot in an attempt to keep the armature in continuous motion. The vibrator completely removed the tares but when the sensitivity of the system was increased another trouble became apparent. On first sight this seemed to be a repetition on a smaller scale of the taring effect noticed previously. The behaviour however was different; repeated tapping of the tiltmeter pot would cause the output to tare repeatedly in the same direction. This is consistent with the hysteresis effect of capillary forces described by Landau and Lifshitz (1959). The contact angle of a liquid on a solid surface is in general different depending on whether the liquid is advancing over a dry surface or receding from a previously wetted one. Changes in the capillary forces acting on the float are balanced by the buoyancy forces and the depth of immersion required to balance the capillary force is:

$$h = 2\gamma\cos\theta/\rho gr \quad (8-1)$$

Here  $\gamma$  is the surface tension of the fluid,  $\theta$  is the angle between the surface contacted and the tangent to the fluid surface,  $\rho$  is the density of the fluid and  $r$  is the radius of the float. For the case here  $r=4.0$  cm,  $\rho =1.0$ ,  $\gamma=74.0$  and the immersion depth assuming perfect wetting ( $\theta=0^\circ$ ) is  $h=380\mu$ . Clearly, variations in contact angle in general and the hysteresis effect in particular represent serious

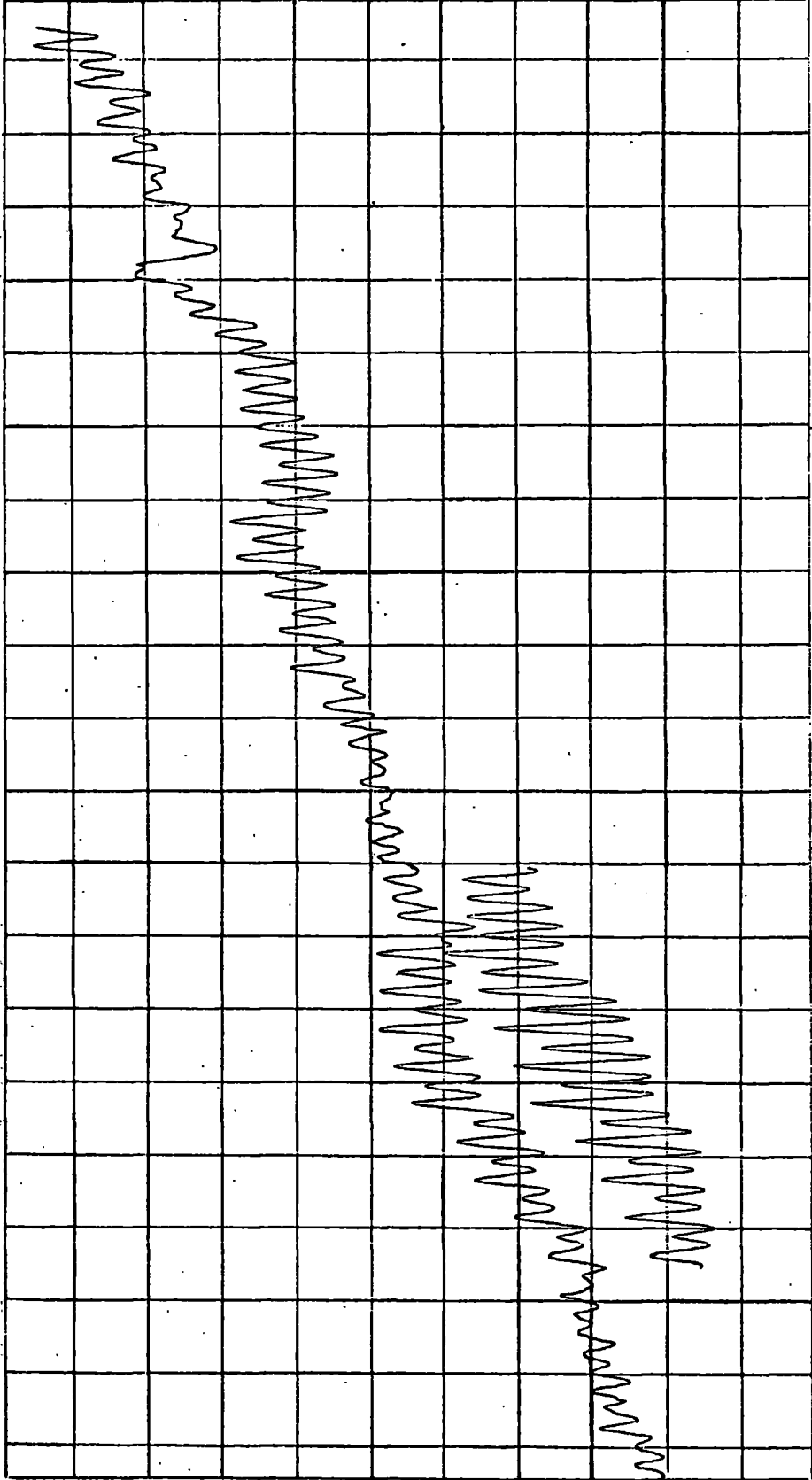


FIGURE (8-1) Records of tilt measured by the water-tube tiltmeter (upper trace) and by the horizontal pendulum (lower trace) at Rockhope, day 200 to day 240 1969. (Horizontal interval = 48 hours vertical interval = 0.100 arc seconds).

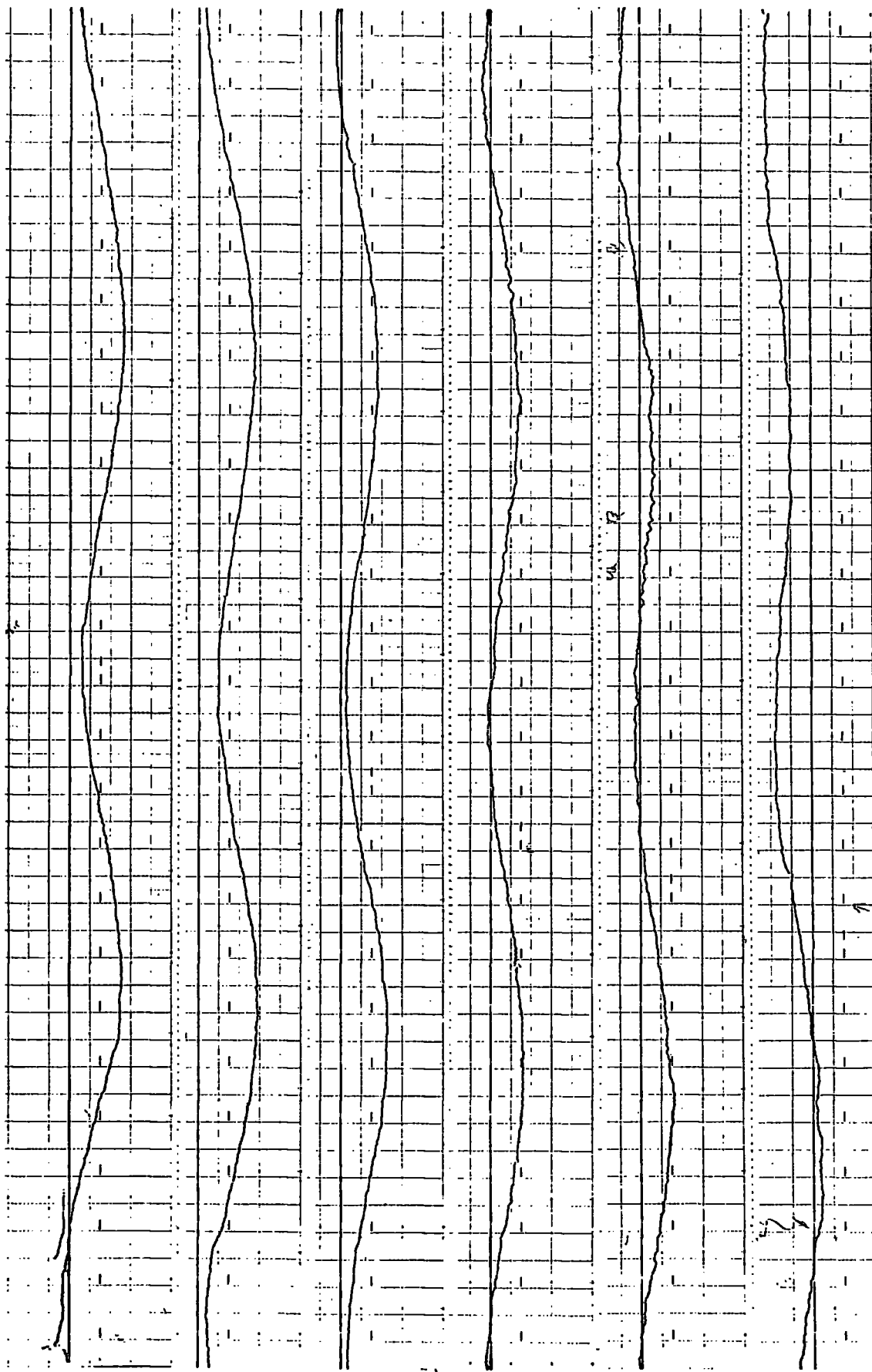


FIGURE (8-2) Water-tube tiltmeter record for the period 1200 GMT Aug 14, 1969 (top left) to 1700 GMT Aug 20, 1969 (bottom right) at Rockhope, England.  
(Timing marks at intervals of one hour with double marks at midnight. Major vertical div = 10 Msecs.)

problems since we are attempting to measure the water level to an accuracy of  $\pm 0.065\mu$ . Given the float radius all that can be done to lessen the effect of variable forces of capillary is to choose a fluid with a low ratio of surface tension to density and ensure that all surfaces are as clean and as smooth as possible and either completely wetted ( $\theta=0^\circ$ ) or completely unwetted ( $\theta=180^\circ$ ) by the fluid. In the present case the surface tension was lowered by about one third by adding a detergent to the water. An examination then of the contact line of water and float revealed that the contact was very irregular. Thorough degreasing of the float improved on this situation but irregularities were still present apparently due to surface roughness. Finally the surface of the float was coated with teflon and polished smooth. This changed the contact angle drastically, from near perfect wetting to non-wetting. More important however was the fact that the contact angle now appeared uniform about the circumference. With these modifications the tiltmeter still showed occasional 'stiction' effects but they were much smaller than previously.

Before installing the tiltmeter in the mine the vibrator system was replaced with a loud speaker introduced into the air line. A speaker of diameter 18 cm was driven by approximately 10 watts of power at a frequency of 50 hertz. The configuration of the vibrating system was arbitrary except that the materials were convenient and it had the desired the effect.

#### 8-4 Results

The water-tube tiltmeter was operated intermittently over the period April 1969 to March 1970. There were frequent breakdowns of the transducer electronics which had to be returned to the manufacturer twice for long periods. Unfortunately too, defects in the transducer electronics produced an effect which resembled the 'stiction' effect due to capillary forces. Consequently the latter effect could not be explored in a systematic way. Observations made during the period July 8, 1969 to September 16, 1969 were analysed by the methods described in Chapter 6 and the results are presented in Section 6-4-1. The tilt measured by the water-tube tiltmeter is anomalously low for all harmonic constituents. The manufacturer's calibration was used to determine the transducer sensitivity for this analysis. There was no convenient method of confirming this sensitivity on the assembled water-tube tiltmeter. In principle it would be sufficient to change the water capacity of the system by a precise amount, by dropping a ball bearing of known volume into one of the pots for example, but it was impossible to open the air seal of the system without introducing other effects. A method of calibrating which will avoid this difficulty is discussed in the next section.

In Figure (8-1) simultaneous tilt measurements by both the water-tube apparatus and the horizontal pendulums are shown for the period July 24, 1969 to August 6, 1969. The

drift behaviour of both tiltmeters is very nearly the same which suggests that it is real. The water-tube tiltmeter record is shown in more detail in Figure (8-2).

#### 8-5 Conclusions.

The results demonstrate the feasibility of building a sensitive water-tube tiltmeter to replace the horizontal pendulum. For a system using a float to define the level of the water some error due to varying capillary forces seems inevitable. These variations can be minimized by using a large diameter, massive float and ensuring that its surface is uniformly clean and smooth and is either completely wetted or not wetted by the fluid. The hysteresis effect discussed in Section 8-3 seems unavoidable but can be kept small enough to be unimportant in tidal studies. It may be a handicap though in measuring secular tilts or in measuring residual tilts due to seismic events.

The detergent-water solution used here was selected on the basis of immediate availability. Propyl alcohol (preferred name is 1-propanol) has been suggested as being more suitable because of its tendency to dissolve grease or other contaminants which might collect on the surface of the float.

The experiment demonstrated the need for a method for frequently measuring the sensitivity of the water-tube system without disturbing it in anyway. A means of doing this is suggested by the calibrating device of Verbaandert (1958) which was described in Chapter 5. A precise variation

in the water-carrying volume of the water-tube tiltmeter will induce an equally precise variation in water level in each of the pots. The precise variation in volume could be obtained by the elastic deformation of a Verbaandert-type device forming part of the system volume and caused to deform by the hydrostatic force exerted by a column of mercury. The height of the mercury column could be caused to vary periodically in the same way as in the Verbaandert method of pendulum calibration. The transducer outputs would be read out individually rather than as a difference and the sensitivity of each transducer determined.

The anomalously low sensitivity observed in the water-tube tiltmeter results is not the same for all constituents. This suggests that the tiltmeter is in some way distorting the harmonic constituents of the tide. The calibration apparatus described above is suitable for driving the system smoothly at any given frequency and therefore will be useful in determining both the frequency response of the system and the degree of non-linear distortion.

CHAPTER 9

CONCLUSIONS

A method of determining the effect of the ocean tide on measurements of the earth tide has been applied for the particular case of an 'extrapolated' Gutenberg-model earth. The results suggest values for the gravimetric and diminishing factors of 1.16 and 0.66 respectively although it is clear that the global ocean tides are not yet well enough known to correct accurately for their effects. The computed ocean-tide effects are consistent with observations throughout eastern North America but western observations of tidal gravity suggest a major error in the assumed ocean tide distribution in the North Pacific. Observations of tidal gravity throughout Asia, and to a lesser degree throughout Europe, lead to anomalously low gravimetric factors when corrected for the computed ocean-tide effect. The European measurements may be brought into line with theory when the ocean tide of the Norwegian-Greenland Seas, which has just recently become available, is considered. The anomalous Asian determinations may be due to the effect of unknown Arctic Ocean tides but are more likely due to systematic errors in the distribution assumed for the tide in the Indian Ocean.

In the above it can be seen that a gravimetric factor has been assumed and the tidal-gravity observations have then been used to appraise the accuracy of the ocean-tide data, rather than to determine the gravimetric factor. This



is the appropriate direction to take because seismological evidence limits allowable variations of the gravimetric factor to about 1 per cent which, in typical conditions, is less than the effect of assuming different but equally probable ocean-tide models. The case is different for tidal-tilt measurements because the effect of ocean tides at distances greater than about 50 degrees is negligible. This reduces the need for accurate ocean-tide data to a regional scale and a mid-continental site may require no ocean-tide correction at all. However, the large number of tidal-tilt measurements made throughout Europe and Asia during the past several years have produced a wide variety of results for the amplitude and phase of the diminishing factor. Many of the anomalous results have been shown to be reliable by parallel observations but the sites are too far inland for the discrepancies to be due to ocean-tide effects. The only apparent explanation for anomalous tilting at tidal frequencies is a differential surface displacement due to the effects of tidal strain in an underlying confined aquifer. The presence of such an aquifer effect is indicated when 'drift' tilting correlates with periods of precipitation or atmospheric pressure variations. This characteristic in the drift behaviour suggests a much-needed means of identifying inaccurate results and poor sites.

Aquifer effects may be lessened by using a tiltmeter having a longer base-line length; such as the water-tube tiltmeter described here. In any case, future emphasis on

water-tube instruments is suggested because of their inherent stability and ease of installation.

The determination of the effects on earth-tide measurements of very local ocean tides has been demonstrated and the basis has been established for using such local loads for investigating the mechanical properties of the crust and upper mantle.



APPENDIX I

Program JANET

00000100

JANET:PROCEDURE OPTIONS(MAIN):

```

1
JANET:PROCEDURE OPTIONS(MAIN):
/******
/*DESCRIPTION:
/*THIS PROGRAM FINDS BY THE METHOD OF LEAST-SQUARES THE COEFFICIENTS*00000100
/*OF THE EXPANSION OF A GIVEN TIME SERIES IN TERMS OF THE 52*00000003
/*PRINCIPAL DIURNAL CONSTITUENTS OF THE TIME PRODUCING POTENTIAL AND*00000007
/*THE 27 PRINCIPAL SEMI-DIURNAL CONSTITUENTS. THE GIVEN TIME SERIES*00000009
/*MAY BE OBSERVATIONS MADE BY EITHER GRAVIMETER (VORPH=1) OR TILTMETER*00000011
/*(VORH=2). IN THE LATTER CASE THE AZIMUTH (AZ) FOR POSITIVE DATA*00000013
/*MUST BE GIVEN. AZIMUTH IS MEASURED CLOCKWISE FROM NORTH. THE TIME*00000015
/*SERIES MUST BE ENTERED AS AN ARBITRARY NUMBER OF COMPLETE 2-DAY*00000019
/*SETS. EACH SET MUST CONTAIN 48 CONSECUTIVE HOURLY OBSERVATIONS AND*00000021
/*BE IDENTIFIED BY COLUMNS CONTAINING THE DAY OF THE YEAR AND THE*00000023
/*LEAST SIGNIFICANT DIGIT OF THE YEAR. THERE MAY BE ANY NUMBER OF*00000025
/*SETS (N) (SEE STORACE REQUIREMENTS), SEPARATED BY ANY NUMBER OF*00000027
/*DAYS, THE SINGLE PRECISO IS THAT IF THE DATA EXTENDS OVER MORE*00000029
/*ONE YEAR THEN THE DAY NUMBERS OF SETS IN THE FOLLOWING YEARS*00000031
/*BE INCREASED BY THE NUMBER OF DAYS IN THE PRECEDING YEARS.
/*INPUT REQUIRED:
/*TWO GROUPS OF FIXED DATA ARE ENTERED FIRST. THE FIRST GROUP*00000033
/*CONTAINS ON 48 CARDS THE WEIGHTING COEFFICIENTS FOR THE FOUR*00000037
/*VEFERIKOV FILTERS. THE SECOND GROUP CONTAINS ON 79 CARDS ALL*00000039
/*REQUIRED DATA PERTAINING TO THE INDIVIDUAL CONSTITUENTS, INCLUDING*00000043
/*THE AMPLITUDE RESPONSE OF THE VEFERIKOV FILTERS TO THE*00000045
/*CONSTITUENT. THE N,2-CARD SETS ARE: N=V ENTERED, PRECEDED BY 1*00000047
/*HEADER CARDS. THE FIRST HEADER CARD (CRD1) IS NOT USED IN THE*00000049
/*ANALYSIS BUT SIMPLY COPIED AS A TITLE LINE FOR THE OUTPUT LISTING.*00000051
/*THE SECOND HEADER CARD SHOULD CONTAIN A7, N, VORPH, YEAR, DAY1, LAT,*00000053
/*AND LONG. THE FIRST THREE OF THESE HAVE BEEN EXPLAINED; DAY1*00000055
/*YEAR ARE THE DAY AND THE YEAR OF THE FIRST DAY OF THE FIRST SET;*00000057
/*LAT AND LONG ARE THE LATITUDE AND THE LONGITUDE OF THE SITE IN*00000059
/*ARBITRARY NUMBER OF THESE 2-CARD DATA SETS WITH HEADER CARDS
/*MAY BE USED.
/******
ON ENDFILE(SYSIN) GO TO FIN;
DECLARE
V FIXED,
(CRAY, YEAR, AZ, DAY1, FIRST, SECOND,
VORH, LAT, LONG, SH, SP, MP, MN, PSI) FLOAT
INITIAL(0),
(HCR(79), HAZ(79), PHG(79), PHZ(79), O(79),
D(179), D2(79), D3(79), D4(79), D5(79),
D6(79), P1(79), HQ(79), CK(79), PHX(79))
FLOAT INITIAL(179, 10),
(CT1(48), ST1(48), CT2(48), ST2(48))
FLOAT(12), ITEST, DLM) FIXED,
(C12, 79), S12, 79), H(2, 79)) FLOAT,
R(12) FLOAT, (Y(11), Z(11)) FIXED,
ANGLE ENTRY FLOAT(12), FLOAT(12), FLOAT(12),
FLOAT(12), FLOAT(12)) RETURNS FLOAT(12)),
CTA(24) FLOAT, LI(48) FLOAT,
2
4

```

```

5      (1,J,JA,JB,JC,JD,JE,K,KAJ,KM,L,N,M,FIXED 9IN(31),
6      (DAY2,DAY3,DAY4),FIXED BIN(31),
7      CRD1 CHARACTER(80),T FLOUNT(12),
8      E(6) CHARACTER(3):
9      DO K=1 TO 48:
10     GET EDIT(J,CTI(J),STI(J),CT2(J),ST2(J),F(1)):END:
11     DO J= 1 TO 79:
12     GET EDIT(K,DI(K),O2(K),O3(K),O4(K),
13     O5(K),O6(K),PI(K),OIK),HO(K),CK(K),
14     C(1,K),S(1,K),C(2,K),S(2,K),F(4),X(1)),
15     F(1),F(3),F(11),F(16),F(2),X(4),
16     3 F(1C),F(13)): END:
17     J=J-1:
18     IF(J=K) THEN DO:
19     PUT EDIT('LAST CON. CARD IS NOT 79 ')
20     (A)SKIP:
21     GO TO FIN:END:
22     READ3:
23     GET DATA(GRAV,AZ,N,VDRH,YEAR,DAVI,
24     LAT,LONG,TEST,FIPST,SECOND):
25     AZ=AZ+19C+0:
26     ANGLE:PRQ(A,B,C,D,T)FLQAT(12):
27     DCL(A,B,C,D,T)FLCAT(12):
28     P=A+B*T+C*(T**2)+D*(T**3):
29     P=P-(FLCOR(P/360))*360:
30     RETURN(P):END ANGLE:
31     ORBIT:
32     T=(365*(YEAR-1900)+
33     FLDR((YEAR-1901)/4)+DAVI-.5)/36525:
34     SH=ANGLE(279.6967,360C0,7699+0,C,T):
35     SP=ANGLE(281.22C8,1.719C2,0C045,C,T):
36     MP=ANGLE(334.32566,4C69.C34,-01032,C,T):
37     MN=ANGLE(259.1833,-1934.142,00208,C,T):
38     MS=ANGLE(27C.4366,4E1267.8936,.002,C,T):
39     *MEAN LONG OF SUN.
40     *MEAN LONG. OF PERHELION.
41     *MEAN LONG OF LUNAR PERIGEE.
42     *ASCENDING NODE OF MOON.
43     *INVERTED FOR DODDSON'S NP.
44     *MEAN LONG OF MOON.
45     *MELCHIPP AMPLITUDE.
46     *FACTORS:
47     *MELCHIPP AMPLITUDE.
48     *FACTORS:
49     *MELCHIPP AMPLITUDE.
50     *FACTORS:
51     AMPFAC=CST1=1.73854:CST2=.36300:CST3=1.29904:EF=.0335:CST4=1.0E-04:
52     CST5=1.0E-C9:FFF=86689*98C*(1-EE*(SIND(LAT)**2))/GRAV:
53     LAT=(LAT+1.745E-C2)-EE*(SIND(2*LAT):LAT=LAT*57.29577:
54     R(1)=8.2275*(SIND(2*LAT)):
55     R(2)=8.9618867F+0*CCSD(LAT)*(1.0E+0-5.2F+0*(SIND(LAT)**2)):
56     R(3)=16.455*(CCSD(LAT)**2):
57     R(4)=2.5980R*(SIND(LAT))*(COSD(LAT)**2):
58     R(5)=P(1)*(CST4:R(2)=R(2)*CST4:R(3)=R(3)*CST4:R(4)=R(4)*CST4:
59     R(5)=-2*FFF*(CCSD(2*LAT)-EE*(SIND(2*LAT)**2))*COSD(AZ):
60     R(6)=-.72618*FFF*(SIND(LAT))*(15*(COSD(LAT)**2)-4)*COSD(AZ):

```

```

00001800
00001900
00002000
00002100
00002200
00002300
00002400
00002500
00002600
00002700
00002800
00002900
00003000
00003100
00003200
00003300
00003400
00003500
00003600
00003700
00003800
00003900
00004000
00004100
00004200
00004300
00004400
00004500
00004600
00004700
00004800
00004900
00005000
00005100
00005200
00005300
00005400
00005500
00005600
00005700
00005800
00005900
00006000
00006100
00006200
00006300
00006400
00006500
00006600
00006700
00006800
00006900

```

JANET:PROCEDURE OPTIONS(MAIN) :

```

52 R(7)=2*EFF*SIND(2*LAT)*(1+2*EE*(COSD(LAT)**2))*COSD(AZ):
53 R(8)=2*2.59808*EFF*COSD(LAT)*2-3*(COSD(LAT)**2))*COSD(AZ):
54 R(5)=R(5)*CST5;R(6)=R(6)*CST5;R(7)=R(7)*CST5;R(8)=R(8)*CST5;
55 R(9)=2*EFF*SIND(LAT)*SIND(AZ);
56 R(10)=4*72618*EFF*(1-5*(SIND(LAT)**2))*SIND(AZ);
57 R(11)=4*EFF*COSD(LAT)*SIND(AZ);
58 R(12)=2*2.59808*EFF*SIND(2*LAT)*SIND(AZ);R(13)=R(13)*CST5;
59 R(9)=R(9)*CST5;R(10)=R(10)*CST5;R(11)=R(11)*CST5;
60 /#NUMBER OF OBSERVATION EOVNS. */00006100
61 NBLCK=BEGIN;
62 DECLARE
63 (DAYKAJ),MI(2,KAJ),TI(N),VC(2,79,N);
64 RES(KAJ)IFLOAT;
65 READC4:DO K=1 TO N;
66 /*****
67 /#READ IN N, 2-DAY, 4 CARD SETS OF DATA. TFST*/00006700
68 /#AND IF THE 2 DAYS COMPOSING EACH SET ARE
69 /#CCNSEQUITIVE.
70 GET EDIT(DAY(K),LIT(J),DO J= 1 TO 12);X(4),F(3),X(1),12 F(6));
71 GET EDIT(DAY2 ,LIT(J),DO J=13 TO 24);X(4),F(3),X(1),12 F(6));
72 GET EDIT(DAY3 ,LIT(J),DO J=25 TO 36);X(4),F(3),X(1),12 F(6));
73 GET EDIT(DAY4 ,LIT(J),DO J=37 TO 48);X(4),F(3),X(1),12 F(6));
74 IF((DAY(K)-DAY2))-(DAY3-DAY4) (DAY2-DAY3-1));
75 THEN DO:PUT EDIT(CARD PHASING IS WRONG IN THIS RUN*(I)SKIP;
76 PUT EDIT(LOCK AT DAY ',DAY(K))(A,F(3))SKIP;
77 GO TO FIN:END;
78
79 /#APPLY VENEDIKOV'S FOUR DIGITAL FILTERS
80 MI(1,K )=SUM(CT1*LIT); /*TO EACH 2-DAY SET AND STORE THE RESULTING
81 MI(1,N+K)=SUM(ST1*LIT); /*4 VALUES DETERMINED FOR EACH SET.
82 MI(2,K )=SUM(CT2*LIT); /*
83 MI(2,N+K)=SUM(ST2*LIT); /*
84 END READC4;
85 /*****
86 /#CENTRAL HOUR OF FIRST SET */00006800
87 /#FROM 0000 Z ON DAY 1 IS 23.5.*/00006800
88 /#TIMSET DETERMINES CENTRAL */00006800
89 /#HOUR OF SUBSEQUENT SETS.NOTE*/00006800
90 /#THAT DAYS NEED NOT BE CONSECUTIVE EXCEPT WITHIN A SET. */00006800
91 /#DETERMINATION OF AMPLITUDE */00006800
92 /#OF TIDAL GRAVITY AND TILT. */00006800
93 /#BASED ON MELCHIOR TABLE BA */00006800
94
95 HAZ(J)=SQRT((HC(J)*R(JR))**2+(HD(J)*R(JC))**2);
96
97 H(1,-)=HGR(*);H(2,*)=HAZ(*);
98
99 PHASE=
100 PHG=D1*(SH-MS-LONG)+(D2-5)*MS+(D3-5)*SH /*PHASE. (PHG=GRAVITY PHASE) */00010000
101 +(D4-5)*SP+(D5-5)*MN+(D6-5)*SP+PI*9; /*(PHZ=TILT PHASE).
102 DO J=1 TO 79; DO I=1 TO N;
103 VO(1,J,I)=PHG(J)+CI(J)*TI(I);

```

```

104 V0(2,J,1)=PHZ(J)+0(J)*TI(1);END;END;
107 LIMITS:
108 Y(1)=1;Z(1)=1;Y(2)=12; Z(2)=21;Y(3)=22; /*HARMONIC CONSTITUENTS TO
112 Z(3)=29;Y(4)=30;Z(4)=40;Y(5)=41;Z(5)=45; /*REF INCLUDED IN GROUP K.THE
117 Y(6)=46;Z(6)=52;Y(7)=53;Z(7)=57;Y(8)=58; /*LIMITS ARE THOSE OF VENDOR*/00010600
122 Z(8)=61;Y(9)=62;Z(9)=66;Y(10)=67;Z(10)=
127 Y(11)=72;Z(11)=79;L=VORH;
130 PHX=PHG*(2-L)+PHZ*(L-1);
131 IF(TEST=1) THEN GO TO CONT1;
133 SPECL:DO K=C TO KAJ-1;
134 DAY(K+1)=DAY(1)+K;
135 DO J=0 TO 23;
136 CTA(J)=5L*(H(L,*)+CCSN(PHX*(*)
137 *Q(1)+(J*K*24)));END;
138 PUT EDIT(LST, DAY(K+1), '00', (CTA(I) DO
139 I=C TO 11))A,F(3),A,I2 F(6,0,1))SKIP;
140 PUT EDIT(LST, DAY(K+1), '12', (CTA(I) DO
141 I=12 TO 23))A,F(3),A,I2 F(6,0,1))SKIP;
142 END SPECL;
143 CONT1:
144 PUT PAGE;
145 PUT EDIT(CR01,DATE)(A,A)SKIP(4);
146 PUT EDIT(WAVE, 'BATIC', 'ERR0R', 'PHASE', 'ERR0R', 'ERR0R') /*PRINT COL HEADINGS*/ 0001240
147 (A,X(4),A,X(3),A,X(4),A,X(3),A)SKIP(3); /*FOR MAIN DATA OUTPUT.
148 L=VORH;
149 L=VORH;
150 IF(FIRST=1) THEN DO;SECOND=0;V=1;END;
151 IF(FIRST=7) THEN DO;SECOND=11;V=2;END;
152 JP=(SECOND+1-FIRST);
153 JC=JP*2;
154 JLOCK=BEGIN;
155 DECLARE
156 (GAPMA(JP),KAPPA(JP),ERRGA(JP),
157 ERRKA(JP))FLOAT,
158 (F(JC,JC),F1(JC,JC))FLOCAT,
159 (K(JC),*L(JC),X(JC))FLOCAT,
160 A(KAJ,JC)FLOCAT,RMS(JC)FLOCAT;
161 F,F1=0; K,M1,X=0; A=C;
162 DCL SOLVE ENTRY(=*)FLOCAT,(*,*)FLOCAT, /*FIXED BIN(31));
163 EQUSS:DO I=1 TO N;
164 DO K=FIRST TO SECOND;M=K-FIRST+1;
165 DO J=Y(K) TO Z(K);
166 A(I,*)=A(I,M)+C(V,J)*H(L,J)
167 COSD(V0(L,J,I));
168 A(I,JP+M)=A(I,JP+M)+C(V,J)*H(L,J)*
169 SIND(V0(L,J,I));
170 A(I,M)=A(I,M)-S(V,J)*H(L,J)*
171 SIND(V0(L,J,I));
172 A(N+1,JP+M)=A(N+1,JP+M)+S(V,J)*H(L,J)*
173 COSD(V0(L,J,I));
174 END EQUSS;
175 NORME:

```

```

00010230
00010300
00010400
00010500
00010600
00010700
00010800
00010900
00011000
00011100
00011200
00011300
00011400
00011500
00011600
00011700
00011800
00011900
00012000
00012100
00012200
00012300
00012400
00012500
00012600
00012650
00012700
00012800
00012900
00013000
00013100
00013200
00013300
00013400
00013500
00013600
00013700
00013800
00013850
00013900
00014000
00014100
00014200
00014300
00014400
00014500
00014600
00014700
00014800
00014900
00015000
00015100

```

```

/*Y(K) AND Z(K) DEFINE THE
/*HARMONIC CONSTITUENTS TO
/*REF INCLUDED IN GROUP K.THE
/*LIMITS ARE THOSE OF VENDOR*/00010600
/*DV (TABLE VI) FOR DATA SPAN*/00010700
/*DE SIX MONTHS OR LESS
00010800
00010900
00011000
/*FOR TESTING PURPOSES SPECL */00011100
/*LISTS THE TIDAL
/*GRAVITY/TILT FOR KAJ COUSE--*/00011200
/*CUTIVE DAYS BEGINNING AT
/*DAY1. FORMAT OF LISTING IS
/*THE SAME AS THAT OF DATA
/*INPUT.
00011300
00011400
00011500
00011600
00011700
00011800
00011900
00012000
00012100
/* PRINT TITLE CARD AT TOP */00012200
/* OF NEW PAGE.
00012300
/*PRINT COL HEADINGS*/ 0001240
/*FOR MAIN DATA OUTPUT.
00012500
/*JURNAL COMPONENTS PROCESSED*/00012600
00012650
/*WHEN FIRST=1, SEMIJURNAL
00012700
/*COMPONENTS WHEN FIRST=7.
00012800
/*NUMBER OF CONSTITUENT GROUPS*/00012900
/*TOTAL NR OF UNKNOWNNS.
00013000
00013100
00013200
00013300
00013400
00013500
00013600
00013700
00013800
00013850
00013900
00013900
00014000
00014100
00014200
00014300
00014400
00014500
00014600
00014700
00014800
00014900
00015000
00015100
/*THE NORMAL EQUATIONS ARE

```

```

176 DO I=1 TO JC:DO J=1 TO JC:DO K=1 TO KAJ:/*DEVELOPED HERE IN THE FORM */OAC15200
177 F(I,J)=F(I+J)+A(K,I)*A(K,J):
178 END NORMF:
179 /* F(JC,JC)*X(JC)=W(JC)
180 00015400
181 00015500
182 00015600
183 00015700
184 W(I)=W(I)+A(K,I)*W(V,K):
185 END NCPNM:
/******
/* SUBROUTINE SOLVE
/* SELVES THE M SIMULTANEOUS EQNS: AY=C
/******
00016300
00016400
00016500
00016600
00016700
00016800
00016900
00017000
00017100
/*F1 AND W1 WILL BE DESTROYED */OAC17200
/*BY SOLVE,SOLUTION IN X(JC). */OAC17300
/*RESID DETERMINES RESIDUALS */OAC17400
/*IN OBSERVATION EQUATIONS. */OAC17500
00017600
/*EVALUATE COMPUTES THE
/*REDUCED COFACTORS OF THE
/*DIAGONAL PART OF THE MATRIX */OAC17800
/*F(JC,JC),THE JC TERMS ARE
/*STOPPED IN RMS(JC) (SEE
/*HILDEBRAND CHAPTER 7).
00018200
00018300
00018400
00018500
00018600
00018700
00018800
/*RMS(JC) IS CHANGED HERE TO
/*THE ESTIMATED RMS ERROR IN
/*THE DETERMINATION OF X(JC).
00019100
/*VALUOT COMPUTES THE FACTORS
/*GAMMA AND KAPPA AND FINDS
/*THE CORRESPONDING RMS ERRORS*/OAC19300
00019700
00019800
/*DIURNAL WAVES.
/*SET LINE TITLES.
00020100
00020150
/*SENTIURNAL WAVES.
00020200

```



```

248 E(1)=1/2N2;E(2)=1/2 ;E(3)=1/2 ;
251 E(4)=1/2 ;E(5)=1/2 ;END;
254 GAMMA=GAMMA/10.C;ERRGA=ERRGA/10.0;
256 DO J=1 TO JP;
257 PUT EDIT(E(J),GAMMA(J),ERRGA(J),KAPPA(J),F(8,3),F(8,3),X(1),F(8,3),F(8,3))SKIP;
258 END LOOP;
261 GO TO READ03;
262 FIN:END JANET;

```

/\*SET LINE TITLES.

\*/00020300  
00020400

/\*DATA INPUT IS MSEC TIMES 10\*/00020500

/\*OR MICROGALS TIMES 10. \*/00020600

/\*PRINTS BUT JP LINES LISTING:\*/00020700

/\*ERRORS BUT JP LINES LISTING:\*/00020800

/\*AND PHASE WITH \*/00020900

/\*ESTIMATE OF RMS ERROR. \*/00021000

/\*LOCKS FOR ANOTHER INPUT. \*/00021100

/\*TERMINUS \*/00021400

APPENDIX II

Program ROBIN

```

MEYER NAME ROBIN
ROBIN:PROCEDURE OPTIONS(MAIN):
*****
BEARINGS GIVEN AT START OF EACH LINE ARE CORRECT MEASURED CLOCKWISE FROM NORTH. AZIMUTH IS THAT OF NOMINAL NORTH AT SITE MEASURED EASTWARD FROM NORTH.
*****
DECL SYSPNCH FILE STREAM OUTPUT:
DECLARE(GM(0:24),GS(0:24),HZS(0:24),HZW(0:24),HZSF(0:24),HZWF(0:24))
FLOAT(12):
GM,GS,HZS,HZK,HZSF,HZWF=0;
DECLARE ANGLE ENTRY(FLOAT(12),FLOAT(12),FLOAT(12),FLOAT(12),FLNAT(12))
FTURNS(FLOAT(12)):
DECL (TM,PAT)CHAR(9),PLACE CHAR(20);
DECLARE (MI,MN,MV,ME,ML,MP,MS,MZC,MZS,MO,SH,SL,SP,SZC,SZS,SD,SE,ER,RT,
RJ,RX,RXA,RM,OC,CY,T)FLOAT(12);
MI,MN,MV,ME,ML,MP,MS,MZC,MZS,MO,SH,SL,SP,SZC,SZS,SD,SE,FR,RT,RJ,RX,RXA,
SHARD,RY=0;
/*ASSIGN CONSTANTS*/
/*EARTHS EQUATORIAL RADIUS*/
/*EARTH'S CENTRIFUGAL ACCELERATION*/
/*RATIO OF MEAN MOTIONS, SUN TO MOON*/
/*INCLINATION OF EARTHS EQUATOR TO ECLIPTIC*/
/*INCLINATION OF MOONS ORBIT TO ECLIPTIC*/
/*NEWTONS GRAVITATIONAL CONSTANT*/
/*MASS OF MOON*/
/*MASS OF SUN*/
/*MEAN DISTANCE EARTH MOON*/
/*MEAN DISTANCE EARTH SUN*/
/*ASSIGN INPUT: IDENTIFICATION AS FOLLOWS:
HEIGHT OF SITE ABOVE SEA LEVEL
LONGITUDE OF SITE
LATITUDE OF SITE
FIRST RESULT REQUIRED:YEAR DAY OF YEAR
NUMBER OF DAYS TO DETERMINED
INCLINATION OF LUNAR ORBIT TO EQUATOR
LONGITUDE OF LUNAR ASCENDING NODE
LONGITUDE IN CELESTIAL EQUATOR OF ASC. INTERSECTION
LONGITUDE IN ORBIT OF ASC. INT. WITH CELESTIAL EQ.
*/IDENTIFICATION OF PROCESS VARIABLES:
MOON LONGITUDE IN ORBIT FROM A SCENDING INTERSECTION
MEAN LONGITUDE OF LUNAR PERIGEE
MEAN LONGITUDE IN ORBIT FROM REFERRED EQUINOX (ARRAY)
ZENITH ANGLE (ADD C FOR COSINE'S FOR SINE) (ARRAYS)
DISTANCE EARTH CENTER TO MOON CENTER
SUN :MEAN LONGITUDE
LONGITUDE IN ECLIPTIC FROM VERNAL EQUINOX
MEAN LONGITUDE OF PERIGEE
ZENITH ANGLE (ADD C FOR COSINE'S FOR SINE) (ARRAYS)
DISTANCE EARTH CENTER TO SUN CENTER
EARTH:CENTRIFUGAL ACCELERATION
DISTANCE SITE TO CENTER OF EARTH
REMAINDER: GUT WHICH CIVIL TIME MEASURED IN HOURS
NUMBER OF JULIAN CENTIPEDES SINCE 1200 OCT DEC31,1800
RIGHT ASCENSION OF MERIDIAN OF SITE FROM RA
RIGHT ASCENSION OF MERIDIAN FROM VERNAL EQUINOX
GUT HOUR
00000100
00000300
00000300
00000300
00000400
00000500
00000500
00000600
00000600
00000700
00000800
00000900
00001000
00001100
00001200
00001300
00001400
00001500
00001600
00001700
00001800
00001900
00002000
00002100
00002200
00002300
00002400
00002500
00002600
00002700
00002800
00002900
00003000
00003100
00003200
00003300
00003400
00003500
00003600
00003700
00003800
00003900
00004000
00004100
00004200
00004300
00004400
00004500
00004600
00004700
00004800
00004900
00005000
00005100
00005200
00005300
00005400
00005500
00005600
00005700
00005800
00005900
00006000

```

```

MEMBER NAME ROBIN
GCT DAY OF THE YEAR
GCT YEAR
CONSTANT FROM EQ 2
CONSTANT FROM EQ 3
DECLINATION MOON SINE
DECLINATION MOON COS
DECLINATION SUN SINE
DECLINATION SUN COS
HORIZONTAL ACC MOON SOUTH
" " SUN
" " MOON WEST
" " SUN
" " SUN
HOUR ANGLE MOON (WESTERLY)
HOUR ANGLE SUN (WESTERLY)
AZIMUTH MOON COS (CW FROM SOUTH)
AZIMUTH SUN COS (CW FROM SOUTH)
TOTAL SOUTH ACC
TOTAL WEST ACC
TOTAL HORIZ MOON FROM EQ 2
TOTAL HORIZ SUN FROM EQ 3
ANGLE:PROC(A,B,C,D,T)FLOAT(12):DCL(A,B,C,D,T,Y)FLCAT(12):
Y=A+B*T+C*(T**2)+D*(T**3):Y=Y-(FLOOR(Y/360))*360:
RETURN(Y):END ANGLE:
DCL(AH,AG,AL,AYA,ADA,ALPHA)FLOAT: DCL (JNRB)FIXED:
ON ENDFILE(SYSIN) GO TO FIN:
START:
GET DATA:
GAMMA=180+ALPHA: BETA=270+ALPHA:
TE=(365*(AYA-1900)+FLOOR((AYA-1901)/4)+ADA-.5)/36525:
AYA=AYA-1900:
JNRB=JNRB-1:
FR=(SORT(1/(1+.006738*(SIND(AL)*#2))))*CR+AH:
APP=1/(CC*(1-(CF**2))):
DAT=DATE:
GROUP:DO JNRB TO JNRB BY 7:
PUT EDIT(PLACE,PROBIN, DAT,LAT=AL, LONG=AG, AZIMUTH=ALPHA)
(PAGE,LIN(4),4(A),F(6.2),A,F(7.2),A,F(7.2)):
DATA:DO JC=JNR-6 TO JNR:JA=24#JC:JE=JA+23:
VP=ANGLE(334,3206,4.069,034,-.01032,-.00001,T):
SP=ANGLE(291,2208,1.71902,00045,.00003,T):
FE=ANGLE(.01675104,-.0000418,-.00000126,0,T):
MN=ANGLE(259,1833,-1934,142,00208,.000002,T):
MI=(COS(CL)*COSD(CI))-(SIND(CO)*SIND(CI)*COSD(MN)):
MI=ATAND(SORT(1-(MI**2)))/MI:
MV=SIND(CI)*SIND(MN)/SIND(MI):
MV=ATAND(MV/SORT(1-(MV**2))):
RSA=SIND(CO)*SIND(MN)/SIND(MI):
RSC=COSD(MN)*COSD(MV)+SIND(MN)*SIND(MV)*COSD(CO):
RSC=RSC+1:
ME=2*ATAND(AS,ASC):
ME=MN-ME:
MS=ANGLE(270,4366,491267,8906,+.002,.000002,T):
SH=ANGL(273,6967,36000,7589,.0003,0,T):
PUT DATA(VS,SH)SKIP:
PUT DATA(MB,SP,MN)SKIP:
DATB:DO J=JA TO JE:
SH=ANGLE(279,6967,36000,7589,.0003,0,T):
SL= +2+4+6+8+SIND(SH-SP):

```

```

PD 00005900
PY 00006000
XM 00006100
XS 00006200
ZMS 00006300
DWC 00006400
DSC 00006500
HMS 00006600
HSS 00006700
HAW 00006800
HSW 00006900
HN 00007000
HS 00007100
AVC 00007200
ASC 00007300
HTS 00007400
HTW 00007500
HMY 00007600
HST 00007700
*/00007800
00007900
00008000
00008100
00008200
00008300
00008400
00008500
00008600
00008700
00008800
00008900
00009000
00009100
00009200
00009300
00009400
00009500
00009600
00009700
00009800
00009900
00010000
00010100
00010200
00010300
00010400
00010500
00010600
00010700
00010800
00010900
00011000
00011100
00011200
00011300
00011400
00011500
00011600
00011700
00011800
00011900

```

```

/SEQ 26 */00009400
/SEQ 27 */00009500
/SEQ 20 */00010100
/SEQ 21 */00010300
/SEQ 19 */00011600
/SEQ 25 */00011900

```

```

MEMBER NAME: RDRIN
SL=57.29577*SL+SH;
SD=(1/CO)*(1/(CD*(1-(EE**2))))*(E*COSD(SH-SP));
SD=1/SD;
MS=ANGLE(270.4356,481267.9906,+.002,+.000002,T);
ML=+.2*CE*SIND(MS-MP)+1.25*(CE**2)*SIND(2*(MS-MP))+
3.75*CE*CE*SIND(MS-(2*SH)+MP)+1.375*(CE**2)*SIND(2*(MS-SH));
ML=57.29577*VL+WS-VE;
ND=(1/CO)*APR*CE*COSD(MS-MP)+APR*(CE**2)*COSD(2*(MS-MP))+1.875*APR*CE*
CE*COSD(MS-(2*SH)+MP)+APR*(CE**2)*COSD(2*(MS-SH));
ND=1/ND;
XM=3*CU*CM*ER/(MD**3);
XS=3*CU*CS*ER/(SD**3);
AHA=0;
RD=ADA+PI*CR((AHA+J)/24);
RH=AHA+J-24*(RD-ADA);
RX=15*(RH-12)-AG+SH-MV;
RZA=15*(RH-12)-AG+SH;
MZC=SIND(AL)*SIND(MI)*SIND(ML)+COSD(AL)*COSD(MI/2)**2)
*COSD(ML-RX)+(SIND(MI/2)**2)*COSD(ML+RX));
SZC=SIND(AL)*SIND(CO)*SIND(SL)**2)*COSD(CO/2)**2)
*COSD(SL-RXA)+(SIND(CO/2)**2)*COSD(SL+RXA));
JNE=J-JA;
GM(JN)=(CU*CM*ER/(MD**3))*(3*(M7C**2)-1);
GM(JN)=GM(JN)+(1.5)*(CU*CM*ER/(MD**2))/(MD**4))*(5*(M7C**3)-3*MZC);
GS(JN)=(CU*CS*ER/(SD**3))*(3*(SZC**2)-1);
GM(JN)=GM(JN)+GS(JN);
DMS=SIND(MI)*SIND(ML);DMC=SQRT(1-(DMS**2));
DSS=SIND(CO)*SIND(SL);DSC=SQRT(1-(DSS**2));
HRMC=(COSD(RX)*COSD(VL)+SIND(RX)*SIND(VL)*COSD(MI))/DMC;
HRSC=(SIND(RXA)*COSD(SL)-COSD(RX)*SIND(VL)*SIND(MI))/DMC;
HRSS=(SIND(RXA)*COSD(SL)+SIND(RXA)*SIND(SL)*COSD(CO))/DSC;
HMS=(XM*VZC)*(-(COSD(AL)*DMC)+(SIND(AL)*DMC*HRMC));
HMS=HMS+.5*XM*(ER/(MD**3))*(5*(M7C**2)-1)*(-(COSD(AL)*DMS)+(SIND(AL)
*DMC*HRMC));
HSS=(XS*S7C)*(-(COSD(AL)*DSS)+(SIND(AL)*DSC*HRSC));
HMW=(XM*VZC)*DMC*HRMS;
HMW=HMW+.5*XM*(ER/(MD**3))*(5*(M7C**2)-1)*DMC*HRMS;
HSW=(XS*S7C)*DSC*HRSS;
HTS=HMS+HSS;
HTW=HMW+HSW;
HMT=XM*M7C*SQRT(1-(M7C**2));
HST=XS*S7C*SQRT(1-(S7C**2));
HZS(JN)=(HMS+HSS)/(9.8204*4.8481E-7);
HZW(JN)=(HMW+HSW)/(9.8204*4.8481E-7);
T=T+(1/24)*(1/3,65250054);
END PATH;
GM=GM+(.05E-6)*SIGN(GM);
HZSE=HZS*COSD(ALPHA)+HZW*SIND(ALPHA);
HZWF=HZW*COSD(ALPHA)-HZS*SIND(ALPHA);
HZSE=HZSF;HZWF=ZWF;
HZS=HZS+(.05)*SIGN(HZS);
HZW=HZW+(.05)*SIGN(HZW);
PUT EDIT (.VERT,20,AYA,AL,AG,120),(GM(1)D0 I=0 TO 11)(A,F(3),
F(2),F(3),F(4),A,(12)F(5,0,7)SKIP(2);
PUT EDIT (.VERT,20,AYA,AL,AG,12),(GM(1) D0 I=12 TO 23)(A,F(3),
F(2),F(3),F(4),A,(12)F(5,0,7)SKIP(2);
PUT EDIT (.H,GAMA,RC,AYA,AL,AG,120),(HTS(1)D0 I=0 TO 11)(A,F(3),

```

```

00011700
00011800 */00011800
00011900
00012000
00012100 */00012100
00012200
00012300
00012400
00012500
00012600
00012700
00012800
00012900
00013000
00013100
00013200
00013300
00013400
00013500
00013600
00013700
00013800
00013900
00014000
00014100
00014200
00014300
00014400
00014500
00014600
00014700
00014800
00014900
00015000
00015100
00015200
00015300
00015400
00015500
00015600
00015700
00015800
00015900
00016000
00016100
00016200
00016300
00016400
00016500
00016600
00016700
00016800
00016900
00017000
00017100
00017200
00017300
00017400

```

```

/*EQ 30
/*EQ 23
/*EQ 28
/*EQ 8

```

```

MEMBER NAME ROBIN
F(2),F(3),F(4),A,(12)(X(1),F(4,0,1))SKIP;
PUT EDIT(H,GAWA,PD,AVA,AL,AG,12,(H7S(I)DO I=12 TO 23))(A,2 F(3),
F(2),F(3),F(4),A,(12)(X(1),F(4,0,1))SKIP;
PUT EDIT(H,BETA,PD,AVA,AL,AG,100,(H7W(I)DO I=0 TO 11))(A,2 F(3),
F(2),F(7),F(4),A,(12)(X(1),F(4,0,1))SKIP;
PUT EDIT(H,BETA,PD,AVA,AL,AG,12,(H7*(I)DO I=12 TO 23))(A,2 F(3),
F(2),F(3),F(4),A,(12)(X(1),F(4,0,1))SKIP;
IF (CARDS=1)THEN DO;
PUT FILE(SYSPNCH)EDIT(1,PD,00,(H7S(I)DO I= 0 TO 11))(A,F(5),A,12
F(5,0,1));
PUT FILE(SYSPNCH)EDIT(1,PD,12,(H7S(I)DO I=12 TO 23))(A,F(5),A,12
F(6,0,1));
END;ELSE IF (CARDS=2) THEN DO;
PUT FILE(SYSPNCH)EDIT(2,PD,00,(H7W(I)DO I= 0 TO 11))(A,F(5),A,12
F(6,0,1));
PUT FILE(SYSPNCH)EDIT(2,PD,12,(H7*(I)DO I=12 TO 23))(A,F(5),A,12
F(6,0,1));
END;ELSE IF (CARDS=3) THEN DO;
PUT FILE(SYSPNCH)EDIT(3,PD,00,(GM(I) DO I= 0 TO 11))(A,F(5),A,12
F(6,0,7));
PUT FILE(SYSPNCH)EDIT(3,PD,12,(GV(I) DO I=12 TO 23))(A,F(5),A,12
F(6,0,7));
END;
END DATA;
END GROUP;
GO TO START;
FIN:END ROBIN;
00017500
00017600
00017700
00017800
00017900
00018000
00018100
00018200
00018300
00018400
00018500
00018600
00018700
00018800
00018900
00019000
00019100
00019200
00019300
00019400
00019500
00019600
00019700
00019800
00019900
00020000
00020100

```

APPENDIX III

Program PRESS

PRESS:PROCEDURE OPTIONS(\*MAIN);

```

1  PRESS:PROCEDURE OPTICAS(*MAIN);
2  MUZ=0.6E12; /*THIS ASSIGAS RIGIDITY */
3  DCL MUZ FLOAT;
4  DECLARE(RFAC(9),GST(9),CEC(9),NABLA(9))FLOAT(12);
5  DCL NXR(5);
6  DCL (TIM,CAT)CHAR(9);
7  DCL (DOP(9),DOQ(9),XAG(9),RPO(5))FLOAT(12);
8  DECLARE (AMP(9),PMS(9))FLCAT(12);
9  DECLARE (DELX,DELY,UD,US,LU,VC,VS,VK,WC,WAS,WS,PCIC,PCTS,PCFW)FLCAT(12);
10 DCL(RK(53)),P(53),Y(53),Y(53),Y(53),Y(53),Y(53))FLOAT(12);
11 KA,MA,CN=:XK,YN=:;
12 DECLARE(XS(5),YS(5),Y(9),X(9),Y(9),XX(9),YY(9),XC(9),YC(9),PC(9),PS(9),PK(9),TSP(9),
13 TSC(9),TWP(9),TWC(9),RAS(5),RPS(9),RAK(9),RPA(9))FLCAT;
14 JUT=:;
15 CE=2.063%COI;
16 /* CONSTANT CE CONVERTS DIFFERENCES OF COMPUTED DISPLACEMENTS (IN CMS
17 X E5) AT SITES SEPARATED BY 1) KM TC TILTS (IN MSECS)
18 CD=(6.67E-8)*(37.46)/(2.*981.*U); CD=CD*1.7E13;
19 /* FACTOR 2 IN DEN CONVERTS INPLT RANGE TC AMPLITUDE */
20 CA=6.3735E+8;CH=1.7453E-9;CC=CA*CB;
21 RNC=:;
22 DO I=1 TO 520 WHILE(RNC/=535);/*LAST CARD MUST BE RUN 535 */
23 GET EDIT(RN(I),PAL(I),CN(I)),(YNI(I),J),XN(I),J)DO J=1 TO 9))F(3),F(2),F(3)
24 *18 F(4));RNC=RN(I);EAD;ILAST=I-1;
25 UN ENDFILE(SYSIN) GO TO FINAL;
26 ENICIN;
27 XS,YS,Y,X,YY,XX,PC,PM,PS,TSP,TSQ,TWP,TWO,RAS,RPS,RAW,RPW=:;
28 DOP,DOQ=:;
29 GET LIST((IBK(J)),XS(J),YS(J)) DO J=1 TO 9));
30 PUT PAGE;
31 DATE=:;
32 PUT SKIP(3);
33 STANF:DO I=1 TO ILAST;
34 RUN=RN(I);FH(I)=CN(I);Q=QN(I);Y(9)=YH(I,*);X(9)=XN(I,*);
35 CA,ZERODIVIDE BEGIN;
36 PUT EDIT(,ZERODIVIDE ERROR')(SKIP(2),A);
37 PUT DATA(RDQ,J,K,DELY,DELX,LO,WD,VC,UD,JS,WS,VK,VA,VA,KA)SKIP;
38 P0,PS,PW=:;
39 GO TO SHUT:END;
40 CC J=1 TO 9 WHILE(X(J)=JBY(J)=3);JMAX=J:END;
41 DO K=1 TO 5;
42 YY=(Y-YS(K))*CC;XX=(X-XS(K))*CC;CDSO(Y(I)/IG(I));
43 /* YY AND XX ARE IN KILOMETERS */
44 /* DST IS DISTANCE IN CMS FROM SITE K TO FIRST PT. OF POLYGN I.
45 *FAC WILL BE TAKEUCHI'S RATIO (THIS EQN 578) OR NISHIMURA'S FACTOR. CNE CF
46 THE FAC BEINGIN CARUS MUST BE OMITTED BY ASTERISK CARDS. DEG IS
47 ANGLE IN DEGREES FROM POLYGN I TC SITE K
48 DST(K)=SQRT((X(I)*2+Y(I)*2)*1.0E+05);
49 DEGR(K)=2*ATANC(DST(K),SQRT(4*(6.378E+8)*2)-DST(K)*2));

```

NOTE



```

64 /#BUSSINESSQ FORM WITH LAMBDA=1.44 X MLZ */
65 RFAC(K)=(19.81E2)**2)*1.44/(12.56*6.67E-8*MU2);
66 DO J=1 TO JMAX;
67 DELX=YY(J+1)-YY(J); DELX=XX(J+1)-XX(J);
68 LC=SQRT(DELX**2+DELX**2);
69 AC=(XX(J+1)+DELX+YY(J+1)+DELY)/LD;
70 VC=(XX(J)+DELX+YY(J)+DELY)/LD;
71 WJ=(XX(J)+YY(J+1)-XX(J+1)+YY(J))/LD;
72 IF (UD**2)K<1 THEN DO:PGTC=0;GO TO PA;END;
73 ARGD=LQG+SQRT((WJ**2)+(UD**2))/(VG+SQRT((VW**2)+(UD**2)));
74 IF ARGD<0 THEN DO:PLT EDIT('LOG ARG ZERL CR NEGATIVE');(SKIP(2)+A);
81 PUT DATA(RUN,J,K,DELY,DELX,LD,WJ,VO,UD,US,WS,VS,UM,VW,WW)SKIP;
82 PUT SKIP(3);I=ILAST;CC TC SHUT;END;
85 PGTB=-UU*LOG(ARGD);
87 PA:
88 DELX=10*DELX; DELY=10*DELY; /*THIS SETS DISTANCE OVER WHICH TILT IS
DETERMINED TO 10 KMS */
89 US=UD-(DELX/LD);VS=VU+(DELY/LD);WS=WJ+(DELY/LD);
92 IF (US**2)K<1 THEN DO:PUTS=J;GO TO PB;END;
93 ARGD=(WS+SQRT((KS**2)+(US**2)))/(VS+SQRT((VW**2)+(US**2)));
95 IF ARGD<0 THEN DO:PLT EDIT('LOG ARG ZERL CR NEGATIVE');(SKIP(2)+A);
101 PUT DATA(RUN,J,K,DELY,DELX,LD,WJ,VO,UD,US,WS,VS,UM,VW,WW)SKIP;
102 PUT SKIP(3);I=ILAST;CC TC SHUT;END;
106 PUTS=-US*LOG(ARGD);
107 PB:
108 UM=UC+(DELY/LD);VM=VU+(DELY/LD);WV=WJ+(DELY/LD);
110 IF (UM**2)K<1 THEN DO:PUTW=0;GC TC PO;END;
115 ARGD=(WV+SQRT((VW**2)+(UM**2)))/(VM+SQRT((VW**2)+(UM**2)));
116 IF ARGD<0 THEN DO:PLT EDIT('LOG ARG ZERL CR NEGATIVE');(SKIP(2)+A);
119 PUT DATA(RUN,J,K,DELY,DELX,LD,WJ,VO,UD,US,WS,VS,UM,VW,WW)SKIP;
121 PUT SKIP(3);I=ILAST;GO TO SHUT;END;
124 PCTW=-UW*LOG(ARGD);
125 PC:
126 FTHA=PU(K)+PCK(K)+PCTG;PS(K)=PS(K)+PCTS;PW(K)=PW(K)+PUTW;END;
/* TO THIS POINT PU,PS,PW HAVE DIMENSIONS OF KM.
RFAC=RFAC*(1-2.435*(DST/CA)+1.59*(DST**2/CA**2));
/*CORRECT TC RFAC DETERMINED BY POWER FROM CAPS DATA FOR
SPHERICAL, HOMOGENECUS SHELL.
MABLA=1.1*(DST/GA)-.71*(DST/CA)**2);
/* FACTOR DETERMINED AS ABOVE TO ACCOUNT FOR ATTRACTION OF
DISPLACED EARTH MASSES FROM BEGINNING 1.01 USES DENSITY 2.8 */
PO=H*CD*PO*RFAC;PS=H*CO*PS*RFAC;PW=H*CO*PW*RFAC;
/*PC(K),PS(K),PW(K) NOW ARE VERTICAL DISPLACEMENTS IN CMS E+5 POSITIVE
TOWARDS CENTER OF EARTH) AT THE K TH SITE (PO), 10 KM SOUTH OF K TH SITE
(PS) AND 10 KM WEST OF KTH SITE WITH COEFFICIENT INVOLVING ELASTIC
CONSTANTS REPLACED BY APPROPRIATE EXPRESSION IN RFAC */
/* TSP AND TWP ARE POSITIVE FOR TILTS TOWARDS THE SOUTH AND THE WEST RE
SPECIALLY
CCP=CCP+PC*COSEC(C); DUL=DUL+PD*SIND(Q);
RFAC=11*RFAC-MABLA/RFAC;
TSP=TSP-(PC-PS)*CC*CCSD(C)*RFAC;
TSO=TSO-(PC-PS)*CE*SIND(Q)*RFAC;
TWP=TWP-(PC-PA)*CC*CCSD(C)*RFAC;
TWO=TWO-(PC-PA)*CE*SIND(C)*RFAC;
/*TSP AND TSO ARE IN-PHASE AND QUADRATURE COMPONENTS OF SEUTHERLY TILT NOTE
WITH RESPECT TO TIDAL REFERENCE PHASE. THEY ARE TOTAL TILTS DUE TO
SUM OF BOTH DIRECT AND INDIRECT EFFECTS. UNITS ARE MSECS. */

```

PRESS:PROCEDURE OPTIONS(MAIN):

```

142 PC*PS*PK=0:
143 SNU:
144 END START:
145 FINIS=RAW=SCRT(TSP**2+TSQ**2):RPS=ATAND(TSQ,TSP):
146 RAW=SCRT(TDP**2+DPC**2):RPW=ATAND(TDP,TWP):
147 RAC=SCRT(DCP**2+DCQ**2):RPC=ATAND(DCQ,DCP):
148 /* THE 4 TILT TOWARDS SOUTH =KAS COS(AT-RPS),TOWARDS WEST=RAW CCS(AT-RPW).
    */
149 PUT SKIP:
150 PUT EDIT(KAS AND RPS ARE AMP AND PHASE WITH RESPECT TO LUNAR TRANSIT
151 OF GREENWICH OF SOUTHERLY TILT IN MSECS,KAW AND RPW SAME FOR WEST)(A):
152 PUT DATA(RAS,RPS,RAW,RPW)SKIP(1):
153 PUT SKIP(3):
154 PUT EDIT(RAD AND RPD ARE AMP AND PHASE WITH RESPECT TO LUNAR TRANSIT
155 OF GREENWICH OF DISPLACEMENT IN MICRONS ASSUMING LAMBDA =1.44 X MU2 AND
156 RIGIDITY EQUAL TO MU2)(A):
157 PUT DATA(KAU,RPW)SKIP(2):
158 PUT SKIP(3):
159 PUT EDIT(AMPLITUDE MAC AZIMUTH FROM SOUTH FOR 21=0 TO 330 DEGS FOLLOW
160 /* NOTE 1 HERE REFERS TO LUNAR TIME
    */
161 DC J=0 TO 330 BY 30:
162 AMP=SRIT((RAS**2)+(CCSD(J-RPS)**2)+(RAW**2)*(COSD(J-RPW)**2)):
163 PHS=ATAND((RAW*CCSD(J-RPW)),(RAS*CCSD(J-RPS))):
164 PUT EDIT(AMP)(SKIP(2),9 F(8,2)):
165 PUT EDIT(PHS)(SKIP(2),9 F(6,1)):END:
166 /*FOLLOWING COMPUTES PHASE 21 FOR MAX OR MIN AMPLITUDE SQUARED (ARGN) T,LUNAR
167 AZIMUTH COMPUTED THEN FOR THIS PHASE CW FROM SOUTH (ARGA)
168 AND FOR THIS PHASE + 90 DEGS (ARGB)
169 THE AMPLITUDE CORRESPONDING TO ARGA IS COMPUTED (ARGB)
170 AND ALSO THAT CORRESPONDING TO ARGB (ARGB)
171 DCL (ARGA(9),ARGB(9),ARGB(9),AMPA(9),AMPA(9))FLUAT:
172 ARGV=SWATAND((RAS**2)*SINC(2*RPW)+(RAW**2)*SINC(2*RPW)),
173 ((KAW**2)*CCSD(2*RPW)+(RAS*CCSD(ARCV-RPS))):
174 ARGA=JANE((RAW*CCSD(ARCV-RPW)),(RAS*CCSD(ARCV-RPS))):
175 ARGB=ATAND((KAW*CCSD(ARCV-RPW)),(RAS*CCSD(ARCV-RPS))):
176 ARCM=ARGV-90:
177 AMPA=RAW*CCSD(ARCN-RPS)*CCSC(ARCA)+RAW*CCSD(ARCB-RPW)*SINC(ARCA):
178 ARGN=ARCN+90:
179 AMPA=RAW*CCSD(ARCN-RPS)*CCSD(ARGB)+RAW*CCSD(ARCA-RPW)*SINC(ARGB):
180 PUT DATA(ARCN,ARCA,ARCB,ARGB,AMPA,AMPB)SKIP(3):
181 ARCA=ARCA+100: ARGB=ARGB+120: ARCN=ARCN+90: XS=XS-2000:
182 XS=XS/100: YS=YS/100:
183 PUT SKIP(2):
184 PUT EDIT(INDX LONG LAT RAC RPC AMPA AMPB ARGN RAS RA
185 W RPS RPW)(A):
186 DC J=1 TO 9:
187 PUT SKIP:
188 PUT EDIT(ABS(J),XS(J),YS(J),RAC(J),RPC(J),AMPA(J),AMPB(J),ARGN(J),RAS(J)
189 ),RAW(J),RPS(J),RPW(J))(F(3),F(8,2),F(7,2),F(6,2),F(7,1),F(6,2),
190 F(6,1),F(6,2),F(7,2),F(7,1),F(7,1)):END:
191 PUT EDIT('PRESS ,0AT,')(3 A)SKIP(2):
192 PUT EDIT('CHANGES JULY 10 POLYGONS ABOUT BORDERS ALTERED TO LIMIT THE
193 REGION TO THAT WITHIN LAT 42N,LAT 62N,AND LONG 25W.THE SHAPE OF THE SOU
194 THERN POLYGONS WAS ALTERED TO CONFORM WITH LATEST HANSEN CHART,AMP
    
```

PRESS:PROCEDURE OPTICNS(MAIN):

PAGE 5

AND PHASE CONSTANTS WERE CHANGED SLIGHTLY. ON AUG 25, 1969 PROGRAM  
WAS MODIFIED TO TAKE REAC AND NABLA COMPUTED NUMERICALLY FROM CAPUTO  
AND LINGMAN PAPERS\*)(A)SKIP(2);  
PUT EDIT('FOLLOWING POLYCCNS HAVE BEEN REMOVED FOR CKING')(A)SKIP;  
PUT EDIT('112,527,523,376,372,367')(P)SKIP;  
GO TO ORIGIN;  
FINAL;  
END PRESS;

189  
190  
191  
192

□<sub>c</sub>

APPENDIX IV

Program CAPS

```

MEMBER NAME      CAPS
(INUNDERFLOW):
CAPS:PROCEDURE  OPTIONS(MAIN):
/*****
/** COMPUTES RADIAL DISPLACEMENT, GRAVITY PERTURBATION AND TILT ON
/** HOMOGENEOUS SHELL OF ARBITRARY RIGIDITY AND THICKNESS ENCLDS-
/** ING A FLUID CORE WHEN SURFACE STRESS IS UNIFORM. PRESSURE OVER
/** A SINGLE AXIALLY-SYMMETRIC CAP OF ARBITRARY DIAMETER. (SOME
/** LESSER CONTRIBUTIONS ARE DETERMINED ON THE BASIS OF A HOMO-
/** GENEUS EARTH).
/**
/**
/*****
R2=6.371E+0F;
R1=0.545*R2;
TETA=1.0;
TETA=30.C;
TETA=INC=1.0;
MU2= 0.4E+12;
RHO=2.8;
RHO2=4.47;
DIM=200;
MEGA=1.0000;
ON ENDFILE(SYSIN) GO TO FIN;
PD=1.0E+6;
DECLARE
(R1,R2,MU2,LAMBDA2,LAMBDA1,PD,KST1,KST2)FLOAT,
DIM FIXED,
(K1,K2)FLOAT(12),
(G1,G2)FLOAT(12),
(C11,C12,C21,C22)FLOAT(12),
(A,D,S)FLOAT(12),
HZERO FLOAT(12),
(DGL1,DGL2,DGL3,DELT,DTL1,DTL3)FLOAT,
DLN FLOAT(12),
(A1,A2,A3,A4)FLOAT(12),
(UR,UL,X1,X2,X3)FLOAT,
(MEGA,TETA,TMN,TLN,TILT)FLOAT(12),
(ARGC) FLOAT BIN(53),ERROR EXTERNAL CHAR(1),
ANGNR BINARY FIXED,
(CST1,CST2) FLOAT;
DECLARE (J,N)FIXED BIN(31);
START:
GET DATA(MU2, RHO,RHO2,MEGA,TETA,TETA,INC);
ARGD=.01745*TETA=INC;
LAMBDA2=0.1273E+1*MU2;
LAMBDA1=3.0*MU2;
TOP=DIM;
LEN=((TETA-TETA)/TETA=INC)+1;
ANGN=LEN;
SCENT=9F;
DECLARE
SHAPE(LEN), (DZ1(LEN),DZ2(LEN),DZ3(LEN),DZ4(LEN))BIN FLOAT(53);
SHAPE=0;
DECLARE RIN(OIM) FLOAT(12);
DECLARE(CST3,CST4,CST5,CST6,CST7,CST8)FLOAT(12);
DECLARE
P(O:TOP)FLOAT(12);
Q(O:TOP)FLOAT(12);
00000001
0000200
0000300
0000400
0000500
0000600
0000700
0000800
0000900
0001000
0001100
0001200
0001300
0001400
0001500
0001600
0001700
0001800
0001900
0002000
0002100
0002200
0002300
0002400
0002500
0002600
0002700
0002800
0002900
0003000
0003100
0003200
0003300
0003400
0003500
0003600
0003700
0003800
0003900
0004000
0004100
0004200
0004300
0004400
0004500
0004600
0004700
0004800
0004900
0005000
0005100
0005200
0005300

```

```

MEMBER NAME      CAPS
CST2=CST2/2;
CST3=PO*4*0*3,14159*6,57*6,371/(980*616);
ACT:DO J=1 TO DIM-2 BY 1;
P(J+1)=(2*J+1)*COSD(MEGA)*P(J)-(J)*P(J-1))/(J+1);
P(J+2)=(2*J+3)*COSD(MEGA)*P(J+1)-(J+1)*P(J)/(J+2);
Q(J+1)=(2*J+1)*COSD(TETA)*Q(J)-(J)*Q(J-1)/(J+1);
Q(J+2)=(2*J+3)*COSD(TETA)*Q(J+1)-(J+1)*Q(J)/(J+2);
N=J+1; J=J+1;
S=CST1*(P(J-1)-P(J+1))*Q;
XLOAD=XLOAD+S*D(J);
VN=CST3*(P(J-1)-P(J+1))/(2*(2*J+1));
VM=CST3*(P(J-1)-P(J+1))/(2*(2*J+1));
CST4=J*(J+2)*LAMBDA2+(J+1)*MU2)*R2;
CST5=(J-1)*((J+1)*LAMBDA2+J*MU2)*R2;
CST6=(2*(J+2)+(4*J)+3)*LAMBDA2;
CST7=2*(J+2)+J+1)*MU2;
CST8=5.51*J*VN/(2*(J-1)*MU2);
CST9=5.51*J*VM/(2*(J-1)*MU2);
UC=UC+((CST4-CST5)*CST8/(CST6+CST7));
UR=UR+D(J)*R2*(J)*S;
DELTA=Q(J)*RN(J)*S+((CST4-CST5)*CST8/(CST6+CST7));
DELTA=RN(J)*S+((CST4-CST5)*CST8/(CST6+CST7));
DELTA=J*(J+1)*C(J+1)-Q(J-1)/(2*J+1)*SIND(TETA); /*P*(COS TETA)*/
TILT=S/TILT+(D*LV*DELTA/(R2)); /*TILT OF SURFACE*/
TILT=X*4*3,14*5,07*8*RHQ*DELTA*DELTA;
TILTM=TILTM+(TILT/(950*5*(2*J+1))); /*TILT DUE TO DISPLACED MASS*/
DGL2=DGL2+(3,086*DELTA);
DGL3=DGL3+((J+1)*4*3,14*DELTA*6,67E-8*RHQ/(2*J+1));
J=J-1;
END ACT;
TETA=(TETA-TETA)/TETAINC)+1;
UR1=-((3*R2*PO*(SIND(MEGA)**2)*COSD(TETA))/(H*MU2*(3*G2+2)));
UR=UR+UR1;
DGL2=DGL2+3,086*UR1;
DGL3=DGL3+(2)*4*3,14*UR1*6,67E-8*RHQ/(3));
SHAPE(TETA)=XLOAD+(CST1*PO*(1-COSD(MEGA)))/2;
DGL2=DGL2+3,086*CST2;
DGL2=DGL2*1,005*-6;
DEN=(PO/980*516)*(R2/6,0E+27)*2*3,14159*(R2**2)*(1-P(1));
/*U1 IS RADIAL DISPLACEMENT,
/*U2 IS CONSTNT TERM, U3 IS
/*DUE TO BODY FORCE OF LOAD,
U1=UR/DEN; U2=CST2/DEN;
U3=UC/DEN; U4=U1+U2+U3;
DGL1=-1/(4*SIND(TETA/2));
DGL2=DGL2*R2/(DEN*980*0);
DGL3=-DGL3/(DEN*980*616/R2);
DIL1=(U4-PR*U)/57,4/TETAINC; /*SERIES SOLN IS:DIL1=TILTS*R2/DEN*/
/*THIS FORM APPLIES TO DISTANCE TETA*/
/*MINUS TETA/2,
DIL3=(COSD(TETA/2)/(4*(SIND(TETA/2)**2))); /*TILT DUE TO ATTRACTION,
DIL4=(TILTM*R2/DEN; /*ATTRACTION OF DISPLACED MASS*/
DGL4=DGL1+DGL2+DGL3;
RATIO=DGL4/DGL1;
FGA=MEGA;TETA=TETA;
/*
PUT DIL1(,),TETA(,),U1(,),U3(,),U4(,),DGL2(,),DGL3(,),DGL4(,);
RATIO(,);

```

```

00010600
00010700
00010800
00010900
00011000
00011100
00011200
00011300
00011400
00011500
00011600
00011700
00011800
00011900
00012000
00012100
00012200
00012300
00012400
00012500
00012600
00012700
00012800
00012900
00013000
00013100
00013200
00013300
00013400
00013500
00013600
00013700
00013800
00013900
00014000
00014100
00014200
00014300
00014400
00014500
00014600
00014700
00014800
00014900
00015000
00015100
00015200
00015300
00015400
00015500
00015600
00015700
00015800
00015900
00016000
00016100
00016200

```



APPENDIX V

Program LONG



```

MEMBER NAME LONG
(NOUNDFLOW):
LONG:PROCEDURE *****
/* *****
/* TO SUM LONGMAN'S SERIES FOR VERTICAL DISPLACEMENT (EQU. 37)
/* AND FOR THE INCREASE IN THE VERTICAL COMPONENT OF GRAVITY (41)
/* *****
/* *****
DECLARE
DIM BINARY FIXED,
PP BINARY FLOAT(53);
DIM=1000;
RESU1=0;
BEGIN;
DECLARE POSV ENTRY(BINARY FLOAT(53),(*)BINARY FLOAT(53),BINARY FIXED,
CHARACTER(1),BINARY FLOAT(53));
DECLARE
(H( 41),K( 41),G(DIM),F(DIM),D(DIM))BINARY FLOAT(53),
(HH,KK)BINARY FLOAT(53),
PUR CHARACTER(1),
(ARG,ANG,P,RESU,RESS)BINARY FLOAT(53);
PUR='P';
H( 1)=0.134;H( 2)=0.000;H( 3)=1.007;H( 4)=1.059;H( 5)=1.059;
H( 6)=1.093;H( 7)=1.152;H( 8)=1.223;H( 9)=1.296;H(10)=1.369;
H(11)=1.439;H(12)=1.506;H(13)=1.572;H(14)=1.631;H(15)=1.691;
H(16)=1.747;H(17)=1.798;H(18)=1.852;H(19)=1.902;H(20)=1.949;
H(21)=1.994;H(22)=2.037;H(23)=2.076;H(24)=2.117;H(25)=2.156;
H(26)=2.194;H(27)=2.223;H(28)=2.257;H(29)=2.291;H(30)=2.322;
H(31)=2.351;H(32)=2.380;H(33)=2.408;H(34)=2.429;H(35)=2.455;
H(36)=2.470;H(37)=2.497;H(38)=2.521;H(39)=2.535;H(40)=2.552;
H(41)=2.581;
K( 1)=0.000;K( 2)=0.000;K( 3)=0.310;K( 4)=0.197;K( 5)=0.133;
K( 6)=0.104;K( 7)=0.050;K( 8)=0.042;K( 9)=0.075;K(10)=0.072;
K(11)=0.069;K(12)=0.066;K(13)=0.064;K(14)=0.062;K(15)=0.060;
K(16)=0.058;K(17)=0.056;K(18)=0.055;K(19)=0.054;K(20)=0.052;
K(21)=0.051;K(22)=0.050;K(23)=0.049;K(24)=0.048;K(25)=0.047;
K(26)=0.046;K(27)=0.045;K(28)=0.044;K(29)=0.043;K(30)=0.042;
K(31)=0.041;K(32)=0.040;K(33)=0.040;K(34)=0.039;K(35)=0.039;
K(36)=0.037;K(37)=0.037;K(38)=0.036;K(39)=0.035;K(40)=0.034;
K(41)=0.034;
ON ENDFILL(SYSIN) GO TO FIN;
START;
GET DATA(ANG1,ANG2, ANGINC);
PUT PAGE;
PUT EDIT( DISTANCE | TILT | DISPLACE | GRAVITY | RATIO | ) (A)SKIP;
PUT EDIT( ANGLE | TO ANGE | BY ANGINC | ) (A)SKIP;
ANGLE=00 ANGE=00 ANGINC=0;
ARG=COSD(ANG);
LIMIT=00 PE=99;
PP=1/P;
FORM:00 J=1 TO 41 ;
PP=PP*P;
C(J)=-H(J)*PP;
D(J)=(2*(J-1)+1)*PP;
E(J)=PP*(J-1-(2*(J)))+(J)*K(J);
END FORM;
EXIT:00 J=42 TO 014;
00000100
00000200
00000300
00000400
00000500
00000600
00000700
00000800
00000900
00001000
00001100
00001200
00001300
00001400
00001500
00001600
00001700
00001800
00001900
00002000
00002100
00002200
00002300
00002400
00002500
00002600
00002700
00002800
00002900
00003000
00003100
00003200
00003300
00003400
00003500
00003600
00003700
00003800
00003900
00004000
00004100
00004200
00004300
00004400
00004500
00004600
00004700
00004800
00004900
00005000
00005100
00005200
00005300
00005400
00005500
00005600
00005700
00005800
00005900

```

MEMBER NAME LUNG

```

HH=+.86*LOG(J-1)-.54;
KK=-.025*LOG(J-1)+.127;
PP=PP*P;
C(J)=-HH*PP;
D(J)=(2*(J-1)+1)*PP;
F(J)=PP*(J-1-(2*HH)+J*KK);
END EXTR;
THEORGE=-1/(4*SIND(ANG/2));
CALL POSV(ARG,C,DIR,DIR,PESU);
CALL POSV(ARG,I,DIR,DIR,REFSG);
TILT=(REFSU-RESU1)*57*4;
FATD=REFSG/THEORG;
PUT EDIT('T,ANG,|',RESU,|',REFSG,|',PATO,|');
(A,F(6,1),X(2),A,F(8,2),X(1),A,F(7,2),X(1),A,F(6,3),
X(1),A)SKIP;
RESU1=RESU;
END LIMIT;
END ANGLE;
PUT SKIP(4);
PUT EDIT('TABLE DATA FOR GUTENERG-MODEL EARTH ');(A)SKIP;
GO TO START;
POSV:
*****
/* EVALUATE N-TERM SEPIFS EXPANSION IN ORTHOGONAL POLYNOMIALS */
/*
/*
/* PROCEDURE (X,C,N,OPT,SJM);
DEclare
(LX,U,H0,H1,H2,FN) BINARY FLOAT(53),
(X,C(7),SUM)
BINARY FLOAT,
(N,I) BINARY FIXED,
OPT CHARACTER(1);
EN;
IF I >= 1
THEN DO;
LX =X;
IF OPT='L'
THEN LX =1-LX;
H2,H1=0;
IF OPT='T'
THEN DO;
H0 =FX*H1;
H =H0-H2+H0;
END;
CO;
IF OPT='H'
THEN N CO;
ELSE
H =FX*H1-FN*H2;
H =H+H;
FN;
ELSE CO;

```

```

MEMBER NAME LONG
H0 =H1; /*SAVE U(I+1)
HI =H1/HN; /*COMPUTE V(I+1)
H1 =H1-H; /*LAGUERRE POLYNOMIALS L(X)
IF OPT=1; /*H = 2*V(I+1)+(1-X)*U(I+1)
THEN H =H1+LX**H+HI; /*LEGENDRE POLYNOMIALS L(X)
ELSE H =LX*(H1+H0); /*H = X*(V(I+1)+U(I+1))
H =H-H2; /*FOR BOTH H = H-V(I+2)
END; /*DECREASE INTEGER FACTOR
FN =FN-1;
END;
H2 =H1; /*SAVE U(I+1) RESP, V(I+1)
HI =H+C(I); /*COMP. U(I) = H+C(I)
I =I-1; /*DECREASE COUNTER I
IF I > 0 /*END OF LOOP OVER I
THEN GO TO ITER;
IF OPT=1; /*MODIFY U(I) IN CHEBYSHEV CASE
THEN HI =H1-H0; /*RETURN VALUE OF SERIES
SUM =H1;
END;
END POSV:
FIN:
END LONG:
00011700
00011500
00011900
00012000
00012100
00012100
00012500
00012400
00012500
00012600
00012700
00012800
00012900
00013000
00013100
00013200
00013300
00013400
00013500
00013600
00013700
00013800

```

APPENDIX VI

Program GLOBL

```

GLDRL:PROCEDURE OPTIONS(MAIN):
DECLARE ORB FLOAT(12)INITIAL(0);
DECLARE Z(0:180) INITIAL
(630, 620, 505, 444, 381, 345, 307, 286, 263, 250, 237, 227, 220, 211, 200,1000
204,195,189,183, 177, 171, 167, 162, 157, 152, 137, 143, 138, 134, 130,00001100
125,120,109,105, 103, 100, 97, 93, 91, 87, 84, 82, 79, 76, 73,00001200
71,69, 67, 64, 52, 50, 59, 57, 56, 55, 54, 53, 52, 51,00001300
51,50, 51, 51, 52, 53, 54, 54, 55, 56, 57, 59, 61, 62,00001400
64,67, 68, 70, 71, 72, 74, 76, 79, 82, 84, 86, 90, 94, 96,00001500
99,102, 105, 109, 112, 115, 119, 121, 125, 127, 130, 133, 137, 140,144,00001600
148,151,155, 159, 162, 166, 169, 172, 175, 178, 182, 185, 189, 193,196,00001700
200,203,207, 210, 214, 218, 221, 225, 228, 232, 235, 238, 241, 244,247,00001800
249,252,255, 257, 260, 263, 265, 268, 271, 274, 276, 279, 281, 284,286,00001900
288,290,293, 295, 297, 298, 300, 301, 302, 304, 305, 306, 308, 311,313,00002000
314,316,318, 317, 318, 318, 320, 320, 320, 321, 323, 325, 326, 327,327,00002100
328,329);
DECLARE INCC BINARY FLOAT, IDEG BINARY FIXED;
DECLARE XAMP(41) BINARY FLOAT INITIAL(
930,740,605,530,462,425,382,350,323,299,279,263,251,242,236,231,229,
220,228,226,224,223,222,221,220,219,216,214,211,209,206,204,202,200,
198,196,195,193,192,191,190);
DECLARE ZH(0:180) INITIAL
(382, 334, 305, 287, 255, 237, 219, 204, 195, 181, 177, 165, 165,158,
158,157,158,159, 156, 156, 150, 150, 146, 147, 147, 151, 154, 153,155,
149,148,151,150, 150, 149, 148, 146, 144, 143, 142, 141, 139, 137,136,
134,132,130,127, 125, 123, 121, 117, 115, 111, 107, 104, 100, 97,93,
90,87, 84, 81, 78, 75, 70, 66, 61, 57, 52, 49, 45, 41,38,
35,31, 28, 25, 21, 18, 15, 11, 8, 5, 1, -5, -6, -8,-13,
-16,-18,-22,-25, -28, -32, -35, -37, -40, -43, -45, -48, -50, -52,-57,
-58,-61,-64,-66, -68, -70, -73, -74, -77, -79, -81, -82, -84, -86,-87,
-89,-91,-92,-92, -93, -94, -96, -98, -99, -100, -101, -102, -103, -104,00003100
-105,-108,-109, -110, -111, -113, -113, -113, -116, -116, -117, -118, -118, -118,00003200
-118,-118,-118, -118, -119, -120, -120, -121, -121, -122, -124, -126, -129, -131,00003300
-134,-135,-139,-143, -146, -149, -153, -155, -157, -159, -161, -163, -166, -167,00003400
-170,-173,-176,-179);
DECLARE XAMP(41) BINARY FLOAT INITIAL(
000,000,000,000,000,000,000,000,000,000,000,000,000,000,000,000,000,
000,000,000,000,000,000,000,000,000,000,000,000,000,000,000,
000,000,000,000,000,000,000,000,000,000,000,000,000,000,000,
000,000,000,000,000,000,000,000,000,000,000,000,000,000,000,
XAMP=XAMP/100; XAMP=XAMP*0.9)+1.0;
XAMP=(XAMP*0.9)+1.0;
DECLARE (CODE)FLOAT;
DECLARE (HH(0:100))FLOAT; HH=100;
DCL(FV,FN,FE,FVQ,FNQ,FEQ,XI,YT,H,O,LV,MV,NV,LN,MN,NV,LE,ME,NE,L3,M3,N3,
L6,L2,M2,N2,L1,M1,N1,XJ,ZJ,XJJ,YJJ,ZJJ,XS,YS,ZS,LL,UJ,VJ,WJ,UJJ,VJJ,00003700
,M6,WJ,J,AJ,PJ,RJ,FJ,CJ,DFU,DFV,DFW,DFX,DFY,DFZ,DRV,DRN,DRE,FVC,FNC,FEC,00004100
,N6,L7,M7,N7,AV,AN,AE,PV,PN,PE,AJJ,PJJ,RJJ,FJJ)FLOAT(12)INITIAL(0);
DECLARE (UNIT,DELX,DELY,LO,UO,WO,VO,ARGO)FLOAT(12)INITIAL(0);
DECLARE
LOGI FILE RECORD,
BUFF1 CHAR(80),
CRBE FILE PRINT;
ON ENDFILE(LOGI) GO TO FIN;
ON ENDFILE(SYSIN) GOTO FIN2;
DCL(YD(8),XD(8),X(8),Y(8));
CA=6,3783F+8; CH=1.7453E-9; CC=CA*CB;
/*THIS PROGRAM DETERMINES THE GRAVITATIONAL ATTRACTION IN MICROGALS AT

```

```

00000700
00000800
00000900
00001000
00001100
00001200
00001300
00001400
00001500
00001600
00001700
00001800
00001900
00002000
00002100
00002200
00002300
00002400
00002500
00002600
00002700
00002800
00002900
00003000
00003100
00003200
00003300
00003400
00003500
00003600
00003700
00003800
00003900
00004000
00004100
00004200
00004300
00004400
00004500
00004600
00004700
00004800
00004900
00005000
00005100
00005200
00005300
00005400
00005500
00005600

```

```

DECLARE XAMP(41) BINARY FLOAT INITIAL(
000,000,000,000,000,000,000,000,000,000,000,000,000,000,000,000,
000,000,000,000,000,000,000,000,000,000,000,000,000,000,000,
000,000,000,000,000,000,000,000,000,000,000,000,000,000,000,
000,000,000,000,000,000,000,000,000,000,000,000,000,000,000,
XAMP=XAMP/100; XAMP=XAMP*0.9)+1.0;
XAMP=(XAMP*0.9)+1.0;
DECLARE (CODE)FLOAT;
DECLARE (HH(0:100))FLOAT; HH=100;
DCL(FV,FN,FE,FVQ,FNQ,FEQ,XI,YT,H,O,LV,MV,NV,LN,MN,NV,LE,ME,NE,L3,M3,N3,
L6,L2,M2,N2,L1,M1,N1,XJ,ZJ,XJJ,YJJ,ZJJ,XS,YS,ZS,LL,UJ,VJ,WJ,UJJ,VJJ,00003700
,M6,WJ,J,AJ,PJ,RJ,FJ,CJ,DFU,DFV,DFW,DFX,DFY,DFZ,DRV,DRN,DRE,FVC,FNC,FEC,00004100
,N6,L7,M7,N7,AV,AN,AE,PV,PN,PE,AJJ,PJJ,RJJ,FJJ)FLOAT(12)INITIAL(0);
DECLARE (UNIT,DELX,DELY,LO,UO,WO,VO,ARGO)FLOAT(12)INITIAL(0);
DECLARE
LOGI FILE RECORD,
BUFF1 CHAR(80),
CRBE FILE PRINT;
ON ENDFILE(LOGI) GO TO FIN;
ON ENDFILE(SYSIN) GOTO FIN2;
DCL(YD(8),XD(8),X(8),Y(8));
CA=6,3783F+8; CH=1.7453E-9; CC=CA*CB;
/*THIS PROGRAM DETERMINES THE GRAVITATIONAL ATTRACTION IN MICROGALS AT

```

```

SITE XT(LONG EAST TIMES 100),YT (LAT NORTH TIMES 100) DUE TO TIDAL WA00005700
DEFINED BY SURFACE POLYGONS WITH ASSIGNED AMPLITUDE (H IN CMS) AND P00005300
(Q IN DEGS).THE POLYGONS MAY BE LOCATED ANYWHERE ON THE GLOBE BUT MJS00005900
DEFINED BY NOT MORE THAN 7 POINTS. BEFORE COMPUTATION EACH
POLYGON IS PROJECTED ONTO A PLANE WHOSE NORMAL IS THE VERTICAL
THROUGH THE FIRST POINT OF THE POLYGON. THE METHOD AND MANY OF THE
SYMBOLS USED ARE THOSE OF BOTT (GEO. PRCS. VOL XI,3,1963.)
/*SYMBOL LIST FOLLOWS
XT,YT POSITION OF SITE. X IS LONG (EAST DEGS*100),Y IS LAT00006400
XD(8),YD(8) POSITION OF POLYGON POINTS. ONLY 7 MAY BE ASSIGNED(A00006500
H AMPLITUDE OF TIDE(IN CMS).LATER MADE H*6.664E-R*E+6.00006700
Q PHASE ANGLE WITH RESPECT TO LUNAR TRANSIT OF GREENWI00006900
X,Y(R) POSITION OF POLYGON POINTS IN KMS FROM SITE (EAST AN00006900
L,M,N ALL OF THIS TYPE ARE DIRECTION COSINES WITH RESPECT 00007000
AXES DIRECTED TO LAT,LONG (0,0),(0,90),(90,0).
LV,MV,NV DIR. COS. OF VERTICAL THROUGH SITE.
LE,ME,NE DIR. COS. OF NORTH THROUGH SITE.
L7,M7,N7 EQUAL TO 3X5.
L6,M6,N6 WHERE 2 IS FIRST VECTOR 2.
L3,M3,N3,W DIR. COS. OF VERTICAL THROUGH PT. J OF POLYGON. (W A00007700
L2,M2,N2,V DIR. COS. OF VECTOR PT. J TO PT. J+1 OF POLYGON. (V A00007800
/*SEE ALSO PROGRAM NOTES CONCERNING THIS VECTOR)
L1,M1,N1,U DIR. COS. OF VECTOR ORTHOGONEL TO BOTH 2 ABOVE. (U A00008000
XJ,XJJ,XS X COORD OF PT. J,J+1 AND SITE. (CMS)
YJ,YJJ,YS Y COORD OF PT. J,J+1 AND SITE. (CMS)
ZJ,ZJJ,ZS Z COORD OF PT. J,J+1 AND SITE. (CMS)
LL DISTANCE PT. J TO PT. J+1. (CMS)
UJ,VJ,WJ DISTANCE SITE TO PT. J ALONG U,V AND W AXES.
UJJ,VJJ,WJJ DISTANCE SITE TO PT. J+1 ALONG U,V, AND W AXES.
AJ,PJ,RJ,FJ BOTT'S SYMBOLS ALPHA,RHO,R,F FOR PT. J. ADD J FOR J+00008700
CJ DETERMINES WHETHER LAMINA IS ADDED OR SUBTRACTED.SEE00008900
DFU,DFV,DFW FORCE COMPONENTS ALONG U,V,W AXES AT SITE.NON-ACCUMU00009100
DFX,DFY,DFZ FORCE COMPONENTS ALONG X,Y,Z AXES AT SITE.ACCUMULATI00009200
DRV,DBN,DBE FORCE COMPONENTS ALONG VERTICAL,NORTH,EAST AT SITE.
FVC,FNC,FEC ACCUMULATING IN-PHASE COMPONENT OF ABOVE.
FVO,FNO,FEO ACCUMULATING QUADRATURE COMPONENT OF ABOVE.
AV,AN,AE AMPLITUDE OF VERTICAL,NORTH AND EAST ATTRACTION.(MIC00009400
PV,PN,PE PHASE OF VERTICAL,NORTH AND EAST ATTRACTION.(DEG00009500
HH,V1,V2,V3,W1,W2,W3 ADDED TEMPORARILY
END OF SYMBOL LIST
/* READ SITE POSITION, CHANGE TO DEGREES. COMPUTE DIR. COSINES OF VERTI00009700
NORTHWARD, AND EASTWARD VECTORS THROUGH SITE. COMPUTE X,Y,Z COORDS 00009900
SITE (XS,YS,ZS). PRINT OUT ALL SITE DATA.
SKIPZONE=9;
PULLSIZE=.002;
ACT1:GET DATA; /*REQUIRES SITE COORDS:XT AND YT. ACCEPTS CHANGES IN*/*
/*Z,ZH,ZH, ZH, SKIPZONE OR PULLSIZE.
SZ0=ZH(0); 7H=ZH/100.0;
SG0=Z(0); S71=ZH(1); S72=ZH(2); SZ3=ZH(3);
OPEN FILE(LOGI) INPUT;
LV=COSD(YT)*COSD(XT);MV=COSD(YT)*SIND(XT);NV=SIND(YT);
LN=-SIND(YT)*COSD(XT);MN=-SIND(YT)*SIND(XT);NN=COSD(YT);
LE=MN*NV-MV*NN;ME=-LN*NV+LV*NN;NE=LN*MV-LV*NN;
XS=LV*CA; YS=MV*CA; ZS=NV*CA;
/* START READS DATA AND COMPUTES RESULTS FOR ONE POLYGON WITH STORAGE
CO011100

```

```

FOR CONTINUED ACCUMULATION WITHOUT LIMIT.      */
/*
PUT PAGE;
PUT EDIT('NBR AREA VERTICAL NORTH EAST')(A)SKIP(3);
PUT EDIT('CORRECTED GRAVITATIONAL ATTRACTION IN MICROGALS DUE TO')(A)
SKIP(2);
PUT EDIT('GLOBAL TIDAL WATERS')(A)SKIP;
PUT EDIT('AREAS ARE:(1)-N.ATLANTIC,(2)-S.ATLANTIC,(3)-N.PACIFIC,(4)-S.P
ACIFIC,(5)-INDIAN OCEAN,(6)-E AND NE CANADA DETAIL')(A)SKIP;
PUT EDIT('REGIONAL DETAIL WILL BE REQUIRED FOR COASTAL SITES')(A)SKIP;
PUT EDIT('NOTE 1. LAST PROGRAM CHANGE- FEB 2/1971')(A)SKIP;
PUT EDIT('SITE COORDINATES FOLLOW')(A)SKIP(2);
PUT EDIT('LAT=, Y, LONG=, XT)(A,F(6,2),X(2),A,F(6,2))SKIP;
PUT EDIT('Z(0)=, Z(1)=, Z(2)=, Z(3)=')(A,F(6,2),Z(1),Z(2),Z(3))
(4)(X(3),A,F(5,3))SKIP;
PUT EDIT('ZH(0)=, ZH(1)=, ZH(2)=, ZH(3)=')(A,F(6,2),ZH(1),ZH(2),ZH(3))
(4)(X(3),A,F(5,3))SKIP;
PUT EDIT('SKIPZONE=, SKIPZONE, PULLSIZE, PULLSIZE)
(X(3),A,F(2),X(3),A,F(9,4));
*/
PUT SKIP(2);
INCC=5; IDEG=41; DDFU,DDFV,DDFW=0;
CALL DET5(INCC,XAMP,XRAT,IDEG);
XRAT=XRAT*1.0E-5;
START;
ZH(0)=SZ0; ZH(1)=SZ1; ZH(2)=SZ2; ZH(3)=SZ3;
Z(0)=SG0; Z(1)=SG1; Z(2)=SZ2; Z(3)=SG3;
/*READ FILE(LOGI) INTO (BUFF1); */
GET EDIT(BUFF1)(A(80));
GET STRING(BUFF1) EDIT(RUN,H,O,CODE,(XD(J),YD(J) DO J=1 TO 7))
(3 F(3),F(1),14 F(5));
/*MULTIPLY TIDAL HALF RANGE BY GRAVITATIONAL CONSTANT(6.6E-8) AND
H=M*.06664;
/*DETERMINE GREAT CIRCLE DISTANCE TO FIRST POLYGON PT */
AA=90-(YD(1)/100);
BB=90-YI;
CC=XI-(XD(1)/100);
/* CSC IS COS C WHERE C IS ANGLE SUBTENDED AT CENTER OF EARTH BY
GREAT CIRCLE DISTANCE GCD. */
CSC=COSD(AA-BB)-SIND(AA)*SIND(BB)*(1-COSD(CC));
/* LL IS DISTANCE TO FIRST POLYGON PT IN PLANE OF POLYGON */
LL=CA#SQRT(1-CSC**2);
DST2=LL**2;
IF(DST2<4.0E+14) THEN DO;
IDST=(SQRT(DST2)*1.0E-5)+2.5)/5; IDST=IDST+1;
XP=XAMP*(IDST)-XRAT*(IDST)*SQRT(DST2);
XR=XRAT*(IDST); ZH(0),ZH(1),ZH(2),ZH(3),Z(0),Z(1),Z(2),Z(3)=I;
END;
ELSE DO; XP=1; XR=0; END;
PUT DATA(DST2,XP,XR);
SIDE1=SQRT((XD(1)-XD(2))**2+(YD(1)-YD(2))**2);
SIDE2=SQRT((XD(3)-XD(2))**2+(YD(3)-YD(2))**2);
AREA=SIDE1*SIDE2*1.0E10;
PULL=(AREA*H)/DST2; /*ATTRACTION IN MICROGALS */
00011200
00011300
00011400
00011500
00011600
00011700
00011900
00012000
00012100
00012200
00012300
00012400
00012410
00012420
00012430
00012440
00012450
00012460
00012500
00012500
00012700
00012800
00012900
00013000
00013100
00013200
00013300
00013700
00013800
00013900
00014000

```

```

IF(PULLKULLSIZE) THEN GO TO START;
XD(8)=0;YD(8)=0;
/* DETERMINE NUMBER OF POLYGON SIDES (JMAX) */
DO J=1 TO 7 WHILE(YD(J)-=0|XD(J)-=0);JMAX=J;END;
YD(JMAX+1)=YD(1);XD(JMAX+1)=XD(1);
YD=YD/100; XD=XD/100;
DFX+DFY+DFZ=0;
/* COMPUTE DIRECTION COSINES OF OUTWARD NORMAL TO POLYGON CALLED RUN AND
DESIGNATE BY L3,M3,N3. THIS NOW IS DIRECTION OF W AXIS */
J=1;
XJJ=CA*COSD(YD(J+1))*COSD(XD(J+1));XJ=CA*COSD(YD(J))*COSD(XD(J));
YJJ=CA*COSD(YD(J+1))*SIND(XD(J+1));YJ=CA*COSD(YD(J))*SIND(XD(J));
ZJJ=CA*SIND(YD(J+1)); ZJ=CA*SIND(YD(J));
L3=XJ/CA; M3=YJ/CA; N3=ZJ/CA; WJ=-WJ;
WJ=L3*(XJ-XS)+M3*(YJ-YS)+N3*(ZJ-ZS);
/* LAT AND LONG OF NORMAL AT SURFACE */
CLONG=ATAND(L3,M3);
CBASE=SQRT(L3**2+M3**2);
CLAT=ATAND(CBASE,N3);
/* STRAIGHT-LINE DISTANCE SITE TO NORMAL AT SURFACE */
DSTSC=SQRT(L3*CA-XS)**2+(M3*CA-YS)**2+(N3*CA-ZS)**2);
/* TEST OUTPUT */
PUT DATA(L3,M3,N3,CLONG)SKIP;
PUT DATA(CBASE,CLAT,DSTSC)SKIP;
/* LOOP COMPUTES THE ATTRACTION DUE TO EACH OF THE JMAX LAMINAS AND
ACCUMULATES THE X,Y AND Z COMPONENTS OF THIS ATTRACTION IN
DFX, DFY AND DFZ.
JLOOP:DO J= 1 TO JMAX;
XJJ=CA*COSD(YD(J+1))*COSD(XD(J+1));XJ=CA*COSD(YD(J))*COSD(XD(J));
YJJ=CA*COSD(YD(J+1))*SIND(XD(J+1));YJ=CA*COSD(YD(J))*SIND(XD(J));
ZJJ=CA*SIND(YD(J+1)); ZJ=CA*SIND(YD(J));
LJ=SQRT((XJJ-XJ)**2+(YJJ-YJ)**2+(ZJJ-ZJ)**2);
L2=(XJJ-XJ)/LJ; M2=(YJJ-YJ)/LJ; N2=(ZJJ-ZJ)/LJ;
/*THE COMPONENT OF VECTOR 2 IN THE PLANE PERPENDICULAR TO THE W AXIS
(VECTOR 3) IS NEXT DETERMINED AND CALLED VECTOR 7. VECTOR 7 IS THEN
MADE A UNIT VECTOR AND CALLED THE NEW VECTOR 2 WHICH THEN BECOMES THE
V AXIS. THIS EACH LAMINA OF THE POLYGON IS PROJECTED ON TO THE SAME
PLANE, PERPENDICULAR TO THE SINGLE W AXIS. THE W AXIS IS DETERMINED BY
THE EARTH'S RADIUS VECTOR THROUGH THE FIRST POINT OF THE POLYGON.
L6=(M2*N3-N2*M3); M6=-L2*N3-N2*L3; N6=(L2*M3-M2*L3);
L7=(M3*N6-M6*N3); M7=-L3*N6-L6*N3; N7=(L3*M6-M3*L6);
UNIT=L7*M7+M7*N7+N7; UNIT=SQRT(UNIT);
L2=L7/UNIT; M2=M7/UNIT; N2=N7/UNIT;
L1=(M2*N3-N2*M3);M1=(L3*N2-L2*N3);N1=(L2*M3-L3*M2);
UJ=L1*(XJ-XS)+M1*(YJ-YS)+N1*(ZJ-ZS);
VJ=L2*(XJ-XS)+M2*(YJ-YS)+N2*(ZJ-ZS);
WJ=L2*(XJJ-XS)+M2*(YJJ-YS)+N2*(ZJJ-ZS);
IF UJ>0 THEN CJ=1; IF UJ=0 THEN CJ=0; IF UJ<0 THEN DO:CJ=-1;UJ=-UJ;
L1=-L1;M1=-M1;N1=-N1;END;
AJ=VJ/UJ;AJJ=VJJ/UJJ;PJ=SQRT(UJ**2+VJ**2);PJJ=SQRT(UJJ**2+VJJ**2);
RJ=SQRT(1+AJ**2);RJJ=SQRT(1+AJJ**2);
FJ=SQRT(1+AJ**2);FJJ=SQRT(1+AJJ**2);
DFU=(AJJ*LOG((RJJ+PJJ)/ABS(WJ)))/ABS(WJ);FJJ)/FJJ)-.5*LOG(RJJ-VJJ)
-AJ*LOG((PJ+PJJ)/ABS(WJ))/FJJ+.5*LOG(RJ+VJ)-.5*LOG(RJ-VJ);
DFV=-1*LOG((RJJ+PJJ)/ABS(WJ))/FJJ+1*LOG((RJJ+PJJ)/ABS(WJ))/FJ;
DFW=-((WJ/ABS(WJ))*ATAN(AJJ*(RJJ-ABS(WJ)))+(RJJ*(AJJ**2)*ABS(WJ))
+(WJ/ABS(WJ))*ATAN(AJ *(RJJ -ABS(WJ)))+(RJJ *(AJ**2) *ABS(WJ)));

```

00014100  
00014200  
00014300  
00014400  
00014500  
00014600  
00014700  
00014800  
00014900  
00015000  
00015100  
00015200  
00015300  
00015400  
00015500

00015600  
00015700  
00015800  
00015900  
00016000  
00016100  
00016200  
00016300  
00016400  
00016500  
00016600  
00016700  
00016800  
00016900  
00017000  
00017100  
00017200  
00017300  
00017400  
00017500  
00017600  
00017700  
00017800  
00017900  
00018000  
00018100  
00018200  
00018300  
00018400  
00018500  
00018600  
00018700  
00018800  
00018900



```

PUT DATA(DFU,DFV)SKIP;
DO:
DDF=UJ*(ATAN(VJJ,UJ)-ATAN(VJ,UJ));
DDFV=UJ*(LOG(PJJ)-LOG(PJ));
DFU=(DFU*XP)+(DDFU*XR);
DFV=(DFV*XP)+(DDFV*XR);
END;
PUT DATA(DFW)SKIP;
PUT DATA(DDFU,DDFV,DFU,DFV)SKIP;
PUT DATA(UJ,VJ,VJJ,WJ)SKIP;
DFW=-DFW+DFU*(L1*DFU+L2*DFV+L3*DFW); /*ORIGINAL EQNS ASSUME NEG GRADIENTS */
DFV=DFV+CJ*(M1*DFU+M2*DFV+M3*DFW);
DFZ=DFZ+CJ*(N1*DFU+N2*DFV+N3*DFW);
END JLOOP;
/* RESOLVE THE X,Y,Z COMPONENTS OF ATTRACTION DUE TO THE ENTIRE POLYGON
ALONG VERTICAL NORTHWARD AND EASTWARD AXES THROUGH THE SITE AND ACCURATELY
SEPARATELY BOTH THE IN-PHASE COMPONENTS (FV,FN,FE) AND THE QUADRATURE
COMPONENTS (FVQ,FNQ,FEQ) FOR ALL POLYGONS */
DBV=DFX*LV+DFY*MV+DFZ*NV;
DRB=(4*CA*CA/(RJ*RJ))-1;
DRH=ABS(DRB)+.001;
KR=ABS(2*ATAND(1/SQRT(DRB)))+0.5; /*KR IS ANGULAR DISTANCE IN ROUNDED
DEGREES */
DBV=DBV*Z(KR);
FV=DBV*H*COSD(Q)*FV;FVQ=DBV*H*SIND(Q)+FVQ;
DBN=DFX*LN+DFY*MN+DFZ*NN; DBN=DBN*ZH(KR)/(.98*.4.848);
DBE=DFX*LE+DFY*ME+DFZ*NE; DBE=DBE*ZH(KR)/(.98*.4.848);
FE=DBE*H*COSD(Q)+FE;FEQ=DBE*H*SIND(Q)+FEQ;
/* OUTPUT NET AMPLITUDE AND PHASE AT SITE IN MICROGALS AND DEGREES */
AV=SQRT(FV**2+FVQ**2);IF AV=0 THEN PV=ATAND(FVQ,FV);
AN=SQRT(FN**2+FNQ**2);IF AN=0 THEN PN=ATAND(FNQ,FN);
AE=SQRT(FE**2+FEQ**2);IF AE=0 THEN PE=ATAND(FEQ,FE);
/*PV, PN, AND PE ARE PHASE LAGS OF UP,NORTH AND EAST EFFECTS
/*RELATIVE TO TRANSIT OF GREENWICH BY MOON.
DBV=DRV*H; DRN=DRN*H; DRE=DRE*H;
/*DRV, DBN, AND DRE ARE POSITIVE FOR UP, NORTH AND EAST.*/
/*DBV IN MICROGALS, DBN AND DRE IN MILLISECS.
PUT EDIT(RUN,CODE,AV,(PV,PN,AN),(PE,FE,AE),(FV,FE,FVQ,FNQ,FEQ,FEQ),F(4),F(4),F(4),F(4),F(4),F(4));
2 F(4,0,2))SKIP;
PUT DATA(DRV,DRN,DRE)SKIP;
/* GO TO START; */
FIN;
PUT FILE(CBRE) DATA(XT,YT,AV,PV,AN,PN,AE,PE)SKIP(3);
CLOSE FILE(LOG1);
TV=74.702*(COSD(YT)**2); /*EARTH TIDE GRAVITY */
TN=7.8630*(SIND(2*YT)); /*EARTH TIDE TILT NORTH */
TE=15.7261*(COSD(YT)); /*EARTH TIDE TILT EAST */
AV=AV/TV; AN=AN/TN; AE=AE/TE; /*AMP FACTOR ASSUMED
TV=1.16; /*TILT FACTOR ASSUMED
TN=0.700; /*TILT FACTOR ASSUMED
TE=0.700; /*THEORETICAL PHASE LAG, UP POSITIVE.
TVP=(-2*XT); /*THEORETICAL PHASE LAG, NORTH POSITIVE.
TNP=(-2*XT)-180; /*THEORETICAL PHASE LAG, EAST POSITIVE.
TEP=(-2*XT)-90;

```

00018900  
00019000  
00019100  
00019200  
00019300  
00019400  
00019500  
00019600  
00019700  
00019800  
00019900  
00020000  
00020100  
00020200  
00020300  
00020400  
00020500  
00020600  
00020700  
00020800  
00020900  
00021000  
00021100  
00021200  
00021300  
00021400  
00021500  
00021600  
00021700  
00021800  
00021900  
00022000  
00022100  
00022200  
00022300  
00022400  
00022500  
00022600  
00022700  
00022800  
00022900  
00023000  
00023100  
00023200  
00023300  
00023400  
00023500

:PROCEDURE OPTIONS(MAIN);

00000700

PAGE

7

```
QV=PV-TVP; IQV=(QV+180)/360; QV=QV-(IQV*360);
QN=PN-TNP; IQN=(QN+180)/360; QN=QN-(IQN*360);
RVX=TV*COSD(TVP); RYV=TV*SIND(TVP);
QE=PE-TEP; IQE=(QE+180)/360; QE=QE-(IQE*360);
RAVX=AV*COSD(PV); RAVY=AV*SIND(PV);
RVX=RAVX+RVY; RYV=RAVY+RVY;
PUT EDIT(RUN, CODE, AV, ('QV, '), AN, ('QN, '), AE, ('QE, '), DBV, DBN,
DBE, KR, Z(KR), ZH(KR))(F(3), F(2), 3(F(9,3), A, F(4), A), X(3), 3 F(7,4), F(4),
2 F(4,0,2))SKIP(3);
AV=SQRT(RVX**2+RYV**2);
PV=ATAND(RVY, RVX);
RNX=TN*COSD(TNP); RNY=TN*SIND(TNP);
RANX=AN*COSD(PN); RANY=AN*SIND(PN);
RNX=RANX+RNX; RNY=RANY+RNY;
AN=SQRT(RNX**2+RNY**2);
PN=ATAND(RNY, RNX);
RFX=TE*COSD(TEP); REY=TE*SIND(TEP);
RAEX=AE*COSD(PE); RAEY=AE*SIND(PE);
REX=RAEX+REY; REY=RAEY+REY;
AE=SQRT(REX**2+REY**2);
PE=ATAND(REY, REX);
PV=PV-TVP; IPV=(PV+180)/360; PV=PV-(IPV*360);
PN=PN-TNP; IPN=(PN+180)/360; PN=PN-(IPN*360);
PE=PE-TEP; IPE=(PE+180)/360; PE=PE-(IPE*360);
/*PV, PN AND DE NOW ARE PHASE LAGS OF CALCULATED RESULTANT DIMINISHING
(TILT) OR AMPLIFICATION (GRAVITY) FACTORS RELATIVE TO THAT WHICH
WOULD BE OBSERVED ON A YIELDING BUT OCEANLESS EARTH WHERE THESE
FACTORS ARE 0.7 AND 1.16 RESPECTIVELY.
PUT EDIT(RUN, CODE, AV, ('PV, '), AN, ('PN, '), AE, ('PE, '), DBV, DBN,
DBE, KR, Z(KR), ZH(KR))(F(3), F(2), 3(F(9,3), A, F(4), A), X(3), 3 F(7,4), F(4),
2 F(4,0,2))SKIP(3);
PUT FILE(CRHE) DATA(XI, YT, AV, PV, AN, PN, AE, PE)SKIP(3);
GO TO ACT1;
FIN2;
END GLOBL;
```

APPENDIX VII

Program BETTY

```

MEMBER NAME   BETTY
BETTY:PROCEDURE *****
/*
/*
/* THIS PROGRAM ACCEPTS AS INPUT HOURLY SAMPLES OF TILTMETER
/* OR GRAVIMETER OBSERVATIONS. THE PROGRAM DOES THE FOLLOWING:
/* (1) A 6-POINT SMOOTHNESS TEST IS MADE AND HOUR BY HOUR
/* RESIDUALS ARE PRINTED OUT. A DISTINCTIVE PATTERN
/* OF RESIDUALS RESULT ACCORDING TO WHETHER THERE IS A
/* SINGLE ISOLATED ERROR OR A GENERAL LEVEL CHANGE.
/* (2) LEVEL CHANGES DETECTED AS ABOVE ARE REMOVED BY INSERT-
/* ING THE APPROPRIATE OFFSET INTO THE DATA WITH AN
/* ASSIGNMENT OF THE FORM: FST(202*23)=+130 ON A
/* HEADER CARD.
/* (3) AVAILABLE DAILY CALIBRATION FACTORS MAY BE ENTERED
/* ON A HEADER CARD IN THE FORM: RM(202)=1.234. THE
/* PROGRAM LINEARLY INTERPOLATES BETWEEN CALIBRATION
/* POINTS. IF NO CALIBRATION FACTORS ARE ENTERED THE
/* VALUE 1.0 IS ASSUMED THROUGHOUT.
/* (4) A LACOLAZET FILTER IS APPLIED TO EACH DAYS RESULTS TO
/* DETERMINE THE NON-TIDAL CONTENT OF THE RECORD. TWO
/* RESULTS ARE GIVEN. THE FIRST CENTERED ON 1200 HOURS
/* THE SECOND CENTERED ON 1800 HOURS.
/* (5) WHEN CARDS=0 IS SPECIFIED CARD OUTPUT IS NOT OBTAINED
/* AND THE CALIBRATION FACTORS ARE NOT APPLIED. WHEN
/* CARDS=1 IS SPECIFIED CARD OUTPUT DESIGNED FOR LST
/* INPUT IS OBTAINED WITH CALIBRATION FACTORS APPLIED
/* TO BOTH CARD OUTPUT AND PRINTER OUTPUT.
/* (6) DAYS FOR WHICH DATA IS COMPLETELY MISSING ARE
/* DETECTED AS MISSING BY THE PROGRAM AND NO OUTPUT
/* CARDS FOR THESE DAYS IS OBTAINED. DAYS WITH PARTIAL
/* DATA ARE NOT SO DETECTED AND MUST BE REMOVED BY OTHER
/* MEANS BEFORE BEING INPUT TO LST.

SYMBOL LIST:
FST(*:*:0:23)
R(*:*:0:23)
RM(*,*)
J1
J2
CRD1
CRD2
TRY(K)

CARDS
ERA
ERA
ERA
AS ABOVE CENTERED ON 1600 HOURS.

CHART DISPLACEMENTS. ASSIGNED VALUES ARE
ACCUMULATED WITHIN PROGRAM.
CHART READING. BOTH INPUT AND OUTPUT.
DIMENSIONS ASSIGNED AT EXECUTION TIME.
DAILY CALIBRATION FACTOR.
FIRST DAY OF DATA
LAST DAY OF DATA
CONTENTS OF FIRST CARDS (TITLE)
CONTENTS OF SECOND CARD (DATA)
DATA FOR THE KTH HOUR DETERMINED BY SMOOTHING
FROM THE THREE PRECEDING HOURS AND THE THREE
FOLLOWING HOURS. LATER USED FOR THE RESIDUAL
FROM THE DATA ACTUALLY OBTAINED.
OPTION ON CRD?. SET EQUAL TO ONE FOR CARD
OUTPUT.
DAILY LINEAR COMBINATION YIELDING NON-TIDAL
CONTENT. CENTERED ON 1200 HOURS.
ERA AS ABOVE CENTERED ON 1600 HOURS.

*****
DECLARE
(X,Y,DEL,CARDS,JAD,YR,ERA,ERR)FLOAT BINARY STATIC,
(J1,J2,K,M)FIXED BINARY STATIC,
TAV(0:23)FLOAT BINARY STATIC.
00000100
00000200
00000300
00000400
00000500
00000600
00000700
00000800
00000900
00001000
00001100
00001200
00001300
00001400
00001500
00001600
00001700
00001800
00001900
00002000
00002100
00002200
00002300
00002400
00002500
00002600
00002700
00002800
00002900
00003000
00003100
00003200
00003300
00003400
00003500
00003600
00003700
00003800
00003900
00004000
00004100
00004200
00004300
00004400
00004500
00004600
00004700
00004800
00004900
00005000
00005100
00005200
00005300
00005400
00005500
00005600
00005700
00005800
00005900
00006000

```

```

MEMBER NAME BETTY
IDENT CHARACTER(2),
EVENT CHARACTER(1),
(CRD1,CRD2)CHARACTER(80);
ON ENDFILE(SYSIN) GO TO TERM;
START;
CARDS=0;
GET EDIT(CRD1)(A(80));
GET EDIT(CRD2)(A(80));
GET STRING(CRD2)DATA;
PUT PAGE;
PUT EDIT(CRD1,DATE)(A,A)SKIP(4);
PUT EDIT(*SMOOTHNESS RESIDUALS FROM 0000 TO 2300 HOURS FOLLOW*)(A)
SKIP(3);
PUT EDIT(* 0 1 2 3 4 5 6 7 8 9 10*)(A)SKIP;
PUT EDIT(* 11 12 13 14 15 16 17 18 19 20 21 22 23*)(A);
/* THIS ADDS EXTRA CARDS TO
J1=J1-1;
J2=J2+1;
/* START AND END TO OVERCOME
/* INDEXING PROBLEM IN SMOOTH.
/* MAIN STORAGE ASSIGNED HERE
TI: BEGIN;
DECLARE
RM(J1:J2) FLOAT BINARY,
(FST(J1:J2,0:23),R(J1:J2,0:23))FLOAT BINARY;
RM=0; FST,R=0; JADE=0;
RM(J1+1)=1; RM(J2-1)=1;
GET DATA;
DO J=J1 TO J2;
DO K=0 TO 23;
JAD=JAD+FST(J,K);
FST(J,K)=JAD;
END;
END;
DATA:
GET EDIT(J,YR,IDENT,EVENT,(R(J,M) DO M=0 TO 23))
(F(3),X(1),F(1),A(2),A(1),24 F(3));
IF(J=J2-1) THEN GO TO FIN;
ELSE GO TO DATA;
(UNORDERFLOW);
FIN:
DO J=J1 TO J2; DO K=0 TO 23;
R(J,K)=R(J,K)+FST(J,K);
END:END;
J1=J1+1; J2=J2-1;
SMOOTH:
DO J=J1 TO J2;
DO K=0 TO 23;
TRY(K)=.75*(R(J+(K=23),(K+1)*(K<23))+R(J-(K<1),23*(K=0)+(K-1)*(K=0)))
-.3*(R(J+(K>21),(K+2)*(K<22)+(K-22)*(K>21))
+R(J-(K<2),(K+22)*(K<2)+(K-2)*(K>1))
+.05*(R(J+(K>20),(K+3)*(K<21)+(K-21)*(K<3)+(K-3)*(K>2)));
END;
TRY(*)=R(J,*)-TRY(*);
/* DETERMINE RESIDUAL FOR EACH
/* HOUR AND PRINT IT.
PUT EDIT(J,(TRY(K) DO K=0 TO 23))(F(3),24 F(4))SKIP;
END SMOOTH;
PUT SKIP;
PUT EDIT(*CORRECTED DATA FOLLOWS*)(A)SKIP;
00005000
00006000
00005100
00006200
00006300
00006400
00006500
00006600
00006700
00006800
00006900
00007000
00007100
00007200
00007300
00007400
00007500
00007600
00007700
00007800
00007900
00008000
00008100
00008200
00008300
00008400
00008500
00008600
00008700
00008800
00008900
00009000
00009100
00009200
00009300
00009400
00009500
00009600
00009700
00009800
00009900
00010000
00010100
00010200
00010300
00010400
00010500
00010600
00010700
00010800
00010900
00011000
00011100
00011200
00011300
00011400
00011500
00011600

```

```

MEMBER NAME BETTY
IF(CARDS=0) THEN DO:
PUT EDIT(' (CALIBRATION FACTORS HAVE BEEN APPLIED--CARD OUTPUT')(A);
END;
ELSE DO:
PUT EDIT(' (CALIBRATION FACTORS NOT USED.')(A); END;
PUT EDIT(' 0/12 1/13 2/14 3/15 4/16 5/17 6/18')(A) SKIP;
PUT EDIT(' 7/19 9/20 9/21 10/22 11/23')(A);
/* ASSIGN DAILY CALIBRATION */
/* FACTORS. INTERPOLATING BETW */
/* BETWEEN GIVEN VALUES WHERE */
/* NECESSARY. */
00012400
00012500
00012600
00012700
00012800
00012900
00013000
00013100
00013200
00013300
00013400
00013500
00013600
00013700
00013800
00013900
00014000
00014100
00014200
00014300
00014400
00014500
00014600
00014700
00014800
00014900
00015000
00015100
00015200
00015300
00015400
00015500
00015600
00015700
00015800
00015900
00016000
00016100
00016200
00016300
00016400
00016500
00016600
00016700
00016800
00016900
00017000

/* CARD OUTPUT
/* CALIBRATION FACTORS HAVE BEEN APPLIED--CARD OUTPUT')(A);
/* NO CARD OUTPUT
/* (CALIBRATION FACTORS NOT USED.')(A); END;
/* 6/18')(A) SKIP;
/* ASSIGN DAILY CALIBRATION
/* FACTORS. INTERPOLATING BETW
/* BETWEEN GIVEN VALUES WHERE
/* NECESSARY.
/* PUNCH TITLE CARD
/* TEST FOR MISSING DAYS
/* PRINT RESULTS WITHOUT APPLY--
/* ING CALIBRATION FACTORS IF
/* NO CARD OUTPUT REQUIRED.
/* DO M=0 TO 11)
/* DO M=12 TO 23)
/* APPLY CALIBRATION FACTORS.
/* PUNCH CARDS AND PRINT
/* DUPLICATE OUTPUT.
/* DO M=0 TO 11)
/* DO M=12 TO 23)
/* DO M=0 TO 11)
/* DO M=12 TO 23)
/* APPLY LINEAR COMBINATIONS
/* 11*(J,3)-10*(J,2)+11*(J,1)-10*(J,0)+5*(J,7)-11*(J,9)+10*(J,8)-5*(J,6)+10*(J,5)-11*(J,4)+10*(J,3)-11*(J,2)+10*(J,1)-11*(J,0)+5*(J,7)-11*(J,9)+10*(J,8)-5*(J,6)+10*(J,5)-11*(J,4)+10*(J,3)-11*(J,2)+10*(J,1)-11*(J,0)
00017100
00017200
00017300
00017400

```

```

MEMBER NAME BETTY
+10*R(J,14)-11*R(J,15)+10*R(J,16)-11*R(J,17)+11*R(J,18)-10*R(J,19)
+11*R(J,20)-10*R(J,21)+5*R(J,22)-R(J,23);
IF(SUM(R(J+1,*))-FST(J+1,*))=0 THEN DO:ERB=999.99;GO TO ZEROS;END;
ERB=-1*R(J,4)+5*R(J,5)-10*R(J,6)+11*R(J,7)-10*R(J,8)+11*R(J,9)
-11*R(J,10)+10*R(J,11)-11*R(J,12)+10*R(J,13)-5*R(J,14)+R(J,15)
+R(J,16)-5*R(J,17)+10*R(J,18)-11*R(J,19)+10*R(J,20)-11*R(J,21)
+11*R(J,22)-10*R(J,23)+11*R(J+1,0)-10*R(J+1,2)-R(J+1,3);
ZEROS: /*PRINT COMBINATIONS RESULTS */
PUT EDIT(ERA,ERB)(2 F(10));
ZER04: /*END OF OUTPUT LOOP
END T2: /*END OF BEGIN BLOCK
END T1: /*LOOK FOR MORE DATA
GO TO START: /*TERMINUS
TERM:
END BETTY:

```

```

00017500
00017600
00017700
00017800
00017900
00018000
00018100
00018200
00018300
00018400
00018500
00018600
00018700
00018800
00018900

```

APPENDIX VIII

World-wide Tidal Data File



no.	amp.	Phase	Long.	Lat.	X100	X100
1	174	150	32.1	33.4	21933	250
2	198	150	32.2	33.5	676	220
3	243	150	32.3	33.6	10290	5080
4	46	150	32.4	33.7	260	70
5	46	150	32.5	33.8	463	70
6	46	150	32.6	33.9	462	70
7	46	150	32.7	34.0	461	70
8	46	150	32.8	34.1	460	70
9	46	150	32.9	34.2	459	70
10	46	150	33.0	34.3	458	70
11	46	150	33.1	34.4	457	70
12	46	150	33.2	34.5	456	70
13	46	150	33.3	34.6	455	70
14	46	150	33.4	34.7	454	70
15	46	150	33.5	34.8	453	70
16	46	150	33.6	34.9	452	70
17	46	150	33.7	35.0	451	70
18	46	150	33.8	35.1	450	70
19	46	150	33.9	35.2	449	70
20	46	150	34.0	35.3	448	70
21	46	150	34.1	35.4	447	70
22	46	150	34.2	35.5	446	70
23	46	150	34.3	35.6	445	70
24	46	150	34.4	35.7	444	70
25	46	150	34.5	35.8	443	70
26	46	150	34.6	35.9	442	70
27	46	150	34.7	36.0	441	70
28	46	150	34.8	36.1	440	70
29	46	150	34.9	36.2	439	70
30	46	150	35.0	36.3	438	70
31	46	150	35.1	36.4	437	70
32	46	150	35.2	36.5	436	70
33	46	150	35.3	36.6	435	70
34	46	150	35.4	36.7	434	70
35	46	150	35.5	36.8	433	70
36	46	150	35.6	36.9	432	70
37	46	150	35.7	37.0	431	70
38	46	150	35.8	37.1	430	70
39	46	150	35.9	37.2	429	70
40	46	150	36.0	37.3	428	70
41	46	150	36.1	37.4	427	70
42	46	150	36.2	37.5	426	70
43	46	150	36.3	37.6	425	70
44	46	150	36.4	37.7	424	70
45	46	150	36.5	37.8	423	70
46	46	150	36.6	37.9	422	70
47	46	150	36.7	38.0	421	70
48	46	150	36.8	38.1	420	70
49	46	150	36.9	38.2	419	70
50	46	150	37.0	38.3	418	70
51	46	150	37.1	38.4	417	70
52	46	150	37.2	38.5	416	70
53	46	150	37.3	38.6	415	70
54	46	150	37.4	38.7	414	70
55	46	150	37.5	38.8	413	70
56	46	150	37.6	38.9	412	70
57	46	150	37.7	39.0	411	70
58	46	150	37.8	39.1	410	70
59	46	150	37.9	39.2	409	70
60	46	150	38.0	39.3	408	70
61	46	150	38.1	39.4	407	70
62	46	150	38.2	39.5	406	70
63	46	150	38.3	39.6	405	70
64	46	150	38.4	39.7	404	70
65	46	150	38.5	39.8	403	70
66	46	150	38.6	39.9	402	70
67	46	150	38.7	40.0	401	70
68	46	150	38.8	40.1	400	70
69	46	150	38.9	40.2	399	70
70	46	150	39.0	40.3	398	70
71	46	150	39.1	40.4	397	70
72	46	150	39.2	40.5	396	70
73	46	150	39.3	40.6	395	70
74	46	150	39.4	40.7	394	70
75	46	150	39.5	40.8	393	70
76	46	150	39.6	40.9	392	70
77	46	150	39.7	41.0	391	70
78	46	150	39.8	41.1	390	70
79	46	150	39.9	41.2	389	70
80	46	150	40.0	41.3	388	70
81	46	150	40.1	41.4	387	70
82	46	150	40.2	41.5	386	70
83	46	150	40.3	41.6	385	70
84	46	150	40.4	41.7	384	70
85	46	150	40.5	41.8	383	70
86	46	150	40.6	41.9	382	70
87	46	150	40.7	42.0	381	70
88	46	150	40.8	42.1	380	70
89	46	150	40.9	42.2	379	70
90	46	150	41.0	42.3	378	70
91	46	150	41.1	42.4	377	70
92	46	150	41.2	42.5	376	70
93	46	150	41.3	42.6	375	70
94	46	150	41.4	42.7	374	70
95	46	150	41.5	42.8	373	70
96	46	150	41.6	42.9	372	70
97	46	150	41.7	43.0	371	70
98	46	150	41.8	43.1	370	70
99	46	150	41.9	43.2	369	70
100	46	150	42.0	43.3	368	70

2540	2541	2542	2543	2544	2545	2546	2547	2548	2549	2550	2551	2552	2553	2554	2555	2556	2557	2558	2559	2560	2561	2562	2563	2564	2565	2566	2567	2568	2569	2570	2571	2572	2573	2574	2575	2576	2577	2578	2579	2580	2581	2582	2583	2584	2585	2586	2587	2588	2589	2590	2591	2592	2593	2594	2595	2596	2597	2598	2599	2600
1000	1001	1002	1003	1004	1005	1006	1007	1008	1009	1010	1011	1012	1013	1014	1015	1016	1017	1018	1019	1020	1021	1022	1023	1024	1025	1026	1027	1028	1029	1030	1031	1032	1033	1034	1035	1036	1037	1038	1039	1040	1041	1042	1043	1044	1045	1046	1047	1048	1049	1050	1051	1052	1053	1054	1055	1056	1057	1058	1059	1060
1060	1061	1062	1063	1064	1065	1066	1067	1068	1069	1070	1071	1072	1073	1074	1075	1076	1077	1078	1079	1080	1081	1082	1083	1084	1085	1086	1087	1088	1089	1090	1091	1092	1093	1094	1095	1096	1097	1098	1099	1100	1101	1102	1103	1104	1105	1106	1107	1108	1109	1110	1111	1112	1113	1114	1115	1116	1117	1118	1119	1120

491	763220	759	5429	55	492	463320	713	5473	493	303220	652	5116	494	1073370	798	5457
492	763370	774	5459	749	496	463370	749	5459	497	303370	699	5130	498	107370	774	5457
493	763520	682	5490	847	500	463520	847	5490	498	303520	729	5160	499	10746	796	5429
494	76370	699	5490	722	503	46370	722	5490	500	30370	722	5160	501	10750	702	5490
495	761520	644	5490	749	506	461520	749	5490	509	301520	699	5160	510	10750	632	5490
496	76220	649	5490	699	510	46220	699	5490	513	30220	699	5160	519	10770	606	5490
497	763370	635	5420	839	514	463370	839	5420	517	303370	722	5160	522	10770	787	5341
498	761520	635	5420	839	514	461520	839	5420	521	301520	722	5160	527	10770	606	5490
499	761520	635	5420	839	514	461520	839	5420	525	301520	722	5160	532	10770	487	5320
500	761520	635	5420	839	514	461520	839	5420	529	301520	722	5160	536	10770	606	5490
501	761520	635	5420	839	514	461520	839	5420	533	301520	722	5160	540	10770	487	5320
502	761520	635	5420	839	514	461520	839	5420	537	301520	722	5160	544	10770	487	5320
503	761520	635	5420	839	514	461520	839	5420	541	301520	722	5160	548	10770	487	5320
504	761520	635	5420	839	514	461520	839	5420	545	301520	722	5160	552	10770	487	5320
505	761520	635	5420	839	514	461520	839	5420	549	301520	722	5160	556	10770	487	5320
506	761520	635	5420	839	514	461520	839	5420	553	301520	722	5160	560	10770	487	5320
507	761520	635	5420	839	514	461520	839	5420	557	301520	722	5160	564	10770	487	5320
508	761520	635	5420	839	514	461520	839	5420	561	301520	722	5160	568	10770	487	5320
509	761520	635	5420	839	514	461520	839	5420	565	301520	722	5160	572	10770	487	5320
510	761520	635	5420	839	514	461520	839	5420	569	301520	722	5160	576	10770	487	5320
511	761520	635	5420	839	514	461520	839	5420	573	301520	722	5160	580	10770	487	5320
512	761520	635	5420	839	514	461520	839	5420	577	301520	722	5160	584	10770	487	5320
513	761520	635	5420	839	514	461520	839	5420	581	301520	722	5160	588	10770	487	5320
514	761520	635	5420	839	514	461520	839	5420	585	301520	722	5160	592	10770	487	5320
515	761520	635	5420	839	514	461520	839	5420	589	301520	722	5160	596	10770	487	5320
516	761520	635	5420	839	514	461520	839	5420	593	301520	722	5160	600	10770	487	5320
517	761520	635	5420	839	514	461520	839	5420	597	301520	722	5160	604	10770	487	5320
518	761520	635	5420	839	514	461520	839	5420	601	301520	722	5160	608	10770	487	5320
519	761520	635	5420	839	514	461520	839	5420	605	301520	722	5160	612	10770	487	5320
520	761520	635	5420	839	514	461520	839	5420	609	301520	722	5160	616	10770	487	5320
521	761520	635	5420	839	514	461520	839	5420	613	301520	722	5160	620	10770	487	5320
522	761520	635	5420	839	514	461520	839	5420	617	301520	722	5160	624	10770	487	5320
523	761520	635	5420	839	514	461520	839	5420	621	301520	722	5160	628	10770	487	5320
524	761520	635	5420	839	514	461520	839	5420	625	301520	722	5160	632	10770	487	5320
525	761520	635	5420	839	514	461520	839	5420	629	301520	722	5160	636	10770	487	5320
526	761520	635	5420	839	514	461520	839	5420	633	301520	722	5160	640	10770	487	5320
527	761520	635	5420	839	514	461520	839	5420	637	301520	722	5160	644	10770	487	5320
528	761520	635	5420	839	514	461520	839	5420	641	301520	722	5160	648	10770	487	5320
529	761520	635	5420	839	514	461520	839	5420	645	301520	722	5160	652	10770	487	5320
530	761520	635	5420	839	514	461520	839	5420	649	301520	722	5160	656	10770	487	5320
531	761520	635	5420	839	514	461520	839	5420	653	301520	722	5160	660	10770	487	5320
532	761520	635	5420	839	514	461520	839	5420	657	301520	722	5160	664	10770	487	5320
533	761520	635	5420	839	514	461520	839	5420	661	301520	722	5160	668	10770	487	5320
534	761520	635	5420	839	514	461520	839	5420	665	301520	722	5160	672	10770	487	5320
535	761520	635	5420	839	514	461520	839	5420	669	301520	722	5160	676	10770	487	5320
536	761520	635	5420	839	514	461520	839	5420	673	301520	722	5160	680	10770	487	5320
537	761520	635	5420	839	514	461520	839	5420	677	301520	722	5160	684	10770	487	5320
538	761520	635	5420	839	514	461520	839	5420	681	301520	722	5160	688	10770	487	5320
539	761520	635	5420	839	514	461520	839	5420	685	301520	722	5160	692	10770	487	5320
540	761520	635	5420	839	514	461520	839	5420	689	301520	722	5160	696	10770	487	5320
541	761520	635	5420	839	514	461520	839	5420	693	301520	722	5160	700	10770	487	5320
542	761520	635	5420	839	514	461520	839	5420	697	301520	722	5160	704	10770	487	5320
543	761520	635	5420	839	514	461520	839	5420	701	301520	722	5160	708	10770	487	5320
544	761520	635	5420	839	514	461520	839	5420	705	301520	722	5160	712	10770	487	5320
545	761520	635	5420	839	514	461520	839	5420	709	301520	722	5160	716	10770	487	5320
546	761520	635	5420	839	514	461520	839	5420	713	301520	722	5160	720	10770	487	5320
547	761520	635	5420	839	514	461520	839	5420	717	301520	722	5160	724	10770	487	5320
548	761520	635	5420	839	514	461520	839	5420	721	301520	722	5160	728	10770	487	5320
549	761520	635	5420	839	514	461520	839	5420	725	301520	722	5160	732	10770	487	5320
550	761520	635	5420	839	514	461520	839	5420	729	301520	722	5160	736	10770	487	5320
551	761520	635	5420	839	514	461520	839	5420	733	301520	722	5160	740	10770	487	5320
552	761520	635	5420	839	514	461520	839	5420	737	301520	722	5160	744	10770	487	5320
553	761520	635	5420	839	514	461520	839	5420	741	301520	722	5160	748	10770	487	5320
554	761520	635	5420	839	514	461520	839	5420	745	301520	722	5160	752	10770	487	5320
555	761520	635	5420	839	514	461520	839	5420	749	301520	722	5160	756	10770	487	5320
556	761520	635	5420	839	514	461520	839	5420	753	301520	722	5160	760	10770	487	5320
557	761520	635	5420	839	514	461520	839	5420	757	301520	722	5160	764	10770	487	5320
558	761520	635	5420	839	514	461520	839	5420	761	301520	722	5160	768	10770	487	5320
559	761520	635	5420	839	514	461520	839	5420	765	301520	722	5160	772	10770	487	5320
560	761520	635	5420	839	514	461520	839	5420	769	301520	722	5160	776	10770	487	5320
561	761520	635	5420	839	514	461520	839	5420	773	301520	722	5160	780	10770	487	5320
562	761520	635	5420	839	514	461520	839	5420	777	301520	722	5160	784	10770	487	5320
563	761520	635	5420	839	514	461520	839	5420	781	301520	722	5160	788	10770	487	5320
564	761520	635	5420	839	514	461520	839	5420	785	301520	722	5160	792	10770	487	5320
565	761520	635	5420	839	514	461520	839	5420	789	301520	722	5160	796	10770	487	5320
566	761520	635	5420	839	514	461520	839	5420	793	301520	722	5160	800	10770	487	5320
567	761520	635	5420	839	514	461520	839	5420	797	301520	722	5160	804	10770	487	5320
568	761520	635	5420	839	514	461520	839	5420	801	301520	722	5160	808	10770	487	5320
569	761520	635	5420	839	514	461520	839	5420	805	301520	722	5160	812	10770	487	5320
570	761520	6														

177	10250314920	-16	179	20240314863	1034	179	25210315617	1170	180	402204429259	5541
181	40180422974	5496	182	401354227017	5874	183	401354228577	4995	184	40154226594	5553
185	40154226608	4529	186	40175422979	5222	187	401054228664	4020	188	40154227306	3530
189	40454228814	3105	190	40245422789	5314	191	402454228058	4020	192	40245422974	2374
193	402254227952	4114	194	402254227952	435	195	402254228058	4675	196	402454228309	1438
197	402354227188	-5	198	402404226326	435	199	402404226995	1357	200	402454228391	1438
201	402354227472	2968	202	402404226326	1910	203	402404226995	1968	204	402454228391	3053
205	4024222546	2060	206	402404226326	4994	207	402404227029	3314	208	402454228391	6073
209	402454227109	5049	210	402454227371	4994	211	402454227029	3314	212	402454228391	4171
213	402454227109	3606	214	402454227371	4994	215	402454227029	3314	216	402454228391	3149
217	402454227336	3606	218	402454227371	4994	219	402454227029	3314	220	402454228391	3149
221	402454227336	4400	222	402454227371	4994	223	402454227029	3314	224	402454228391	3149
225	402454227336	4400	226	402454227371	4994	227	402454227029	3314	228	402454228391	3149
230	402454227336	3400	231	402454227371	4994	232	402454227029	3314	233	402454228391	3149
233	402454227336	3400	234	402454227371	4994	235	402454227029	3314	236	402454228391	3149
239	402454227336	3400	240	402454227371	4994	241	402454227029	3314	242	402454228391	3149
243	402454227336	3400	244	402454227371	4994	245	402454227029	3314	246	402454228391	3149
247	402454227336	3400	248	402454227371	4994	249	402454227029	3314	250	402454228391	3149
251	402454227336	3400	252	402454227371	4994	253	402454227029	3314	254	402454228391	3149
255	402454227336	3400	256	402454227371	4994	257	402454227029	3314	258	402454228391	3149
260	402454227336	3400	261	402454227371	4994	262	402454227029	3314	263	402454228391	3149
269	402454227336	3400	270	402454227371	4994	271	402454227029	3314	272	402454228391	3149
273	402454227336	3400	274	402454227371	4994	275	402454227029	3314	276	402454228391	3149
277	402454227336	3400	278	402454227371	4994	279	402454227029	3314	280	402454228391	3149
283	402454227336	3400	284	402454227371	4994	285	402454227029	3314	286	402454228391	3149
289	402454227336	3400	290	402454227371	4994	291	402454227029	3314	292	402454228391	3149
295	402454227336	3400	296	402454227371	4994	297	402454227029	3314	298	402454228391	3149
300	402454227336	3400	301	402454227371	4994	302	402454227029	3314	303	402454228391	3149
306	402454227336	3400	307	402454227371	4994	308	402454227029	3314	309	402454228391	3149
312	402454227336	3400	313	402454227371	4994	314	402454227029	3314	315	402454228391	3149
319	402454227336	3400	320	402454227371	4994	321	402454227029	3314	322	402454228391	3149
324	402454227336	3400	325	402454227371	4994	326	402454227029	3314	327	402454228391	3149
329	402454227336	3400	330	402454227371	4994	331	402454227029	3314	332	402454228391	3149
334	402454227336	3400	335	402454227371	4994	336	402454227029	3314	337	402454228391	3149
338	402454227336	3400	339	402454227371	4994	340	402454227029	3314	341	402454228391	3149
342	402454227336	3400	343	402454227371	4994	344	402454227029	3314	345	402454228391	3149
346	402454227336	3400	347	402454227371	4994	348	402454227029	3314	349	402454228391	3149
350	402454227336	3400	351	402454227371	4994	352	402454227029	3314	353	402454228391	3149
354	402454227336	3400	355	402454227371	4994	356	402454227029	3314	357	402454228391	3149
358	402454227336	3400	359	402454227371	4994	360	402454227029	3314	361	402454228391	3149
362	402454227336	3400	363	402454227371	4994	364	402454227029	3314	365	402454228391	3149
366	402454227336	3400	367	402454227371	4994	368	402454227029	3314	369	402454228391	3149
370	402454227336	3400	371	402454227371	4994	372	402454227029	3314	373	402454228391	3149
374	402454227336	3400	375	402454227371	4994	376	402454227029	3314	377	402454228391	3149
378	402454227336	3400	379	402454227371	4994	380	402454227029	3314	381	402454228391	3149
382	402454227336	3400	383	402454227371	4994	384	402454227029	3314	385	402454228391	3149
386	402454227336	3400	387	402454227371	4994	388	402454227029	3314	389	402454228391	3149
390	402454227336	3400	391	402454227371	4994	392	402454227029	3314	393	402454228391	3149
394	402454227336	3400	395	402454227371	4994	396	402454227029	3314	397	402454228391	3149
398	402454227336	3400	399	402454227371	4994	400	402454227029	3314	401	402454228391	3149
402	402454227336	3400	403	402454227371	4994	404	402454227029	3314	405	402454228391	3149
406	402454227336	3400	407	402454227371	4994	408	402454227029	3314	409	402454228391	3149
410	402454227336	3400	411	402454227371	4994	412	402454227029	3314	413	402454228391	3149
414	402454227336	3400	415	402454227371	4994	416	402454227029	3314	417	402454228391	3149
418	402454227336	3400	419	402454227371	4994	420	402454227029	3314	421	402454228391	3149
422	402454227336	3400	423	402454227371	4994	424	402454227029	3314	425	402454228391	3149
426	402454227336	3400	427	402454227371	4994	428	402454227029	3314	429	402454228391	3149
430	402454227336	3400	431	402454227371	4994	432	402454227029	3314	433	402454228391	3149
434	402454227336	3400	435	402454227371	4994	436	402454227029	3314	437	402454228391	3149
438	402454227336	3400	439	402454227371	4994	440	402454227029	3314	441	402454228391	3149
442	402454227336	3400	443	402454227371	4994	444	402454227029	3314	445	402454228391	3149
446	402454227336	3400	447	402454227371	4994	448	402454227029	3314	449	402454228391	3149
450	402454227336	3400	451	402454227371	4994	452	402454227029	3314	453	402454228391	3149
454	402454227336	3400	455	402454227371	4994	456	402454227029	3314	457	402454228391	3149
458	402454227336	3400	459	402454227371	4994	460	402454227029	3314	461	402454228391	3149
462	402454227336	3400	463	402454227371	4994	464	402454227029	3314	465	402454228391	3149
466	402454227336	3400	467	402454227371	4994	468	402454227029	3314	469	402454228391	3149
470	402454227336	3400	471	402454227371	4994	472	402454227029	3314	473	402454228391	3149
474	402454227336	3400	475	402454227371	4994	476	402454227029	3314	477	402454228391	3149
478	402454227336	3400	479	402454227371	4994	480	402454227029	3314	481	402454228391	3149
482	402454227336	3400	483	402454227371	4994	484	402454227029	3314	485	402454228391	3149
486	402454227336	3400	487	402454227371	4994	488	402454227029	3314	489	402454228391	3149
490	402454227336	3400	491	402454227371	4994	492	402454227029	3314	493	402454228391	3149
494	402454227336	3400	495	402454227371	4994	496	402454227029	3314	497	402454228391	3149
498	402454227336	3400	499	402454227371	4994	500	402454227029	3314	501	402454228391	3149



181 30300630481 5062 186 30300630491 5063 187 30300630501 5064  
 182 30300630511 5065 188 30300630521 5066 189 30300630531 5067  
 190 30300630541 5068 191 30300630551 5069 192 30300630561 5070  
 193 30300630571 5071 194 30300630581 5072 195 30300630591 5073  
 196 30300630601 5074 197 30300630611 5075 198 30300630621 5076  
 199 30300630631 5077 200 30300630641 5078 201 30300630651 5079  
 202 30300630661 5080 203 30300630671 5081 204 30300630681 5082  
 205 30300630691 5083 206 30300630701 5084 207 30300630711 5085  
 208 30300630721 5086 209 30300630731 5087 210 30300630741 5088  
 211 30300630751 5089 212 30300630761 5090 213 30300630771 5091  
 214 30300630781 5092 215 30300630791 5093 216 30300630801 5094  
 217 30300630811 5095 218 30300630821 5096 219 30300630831 5097  
 220 30300630841 5098 221 30300630851 5099 222 30300630861 5100  
 223 30300630871 5101 224 30300630881 5102 225 30300630891 5103  
 226 30300630901 5104 227 30300630911 5105 228 30300630921 5106  
 229 30300630931 5107 230 30300630941 5108 231 30300630951 5109  
 232 30300630961 5110 233 30300630971 5111 234 30300630981 5112  
 235 30300630991 5113 236 30300631001 5114 237 30300631011 5115  
 238 30300631021 5116 239 30300631031 5117 240 30300631041 5118  
 241 30300631051 5119 242 30300631061 5120 243 30300631071 5121  
 244 30300631081 5122 245 30300631091 5123 246 30300631101 5124  
 247 30300631111 5125 248 30300631121 5126 249 30300631131 5127  
 250 30300631141 5128 251 30300631151 5129 252 30300631161 5130  
 253 30300631171 5131 254 30300631181 5132 255 30300631191 5133  
 256 30300631201 5134 257 30300631211 5135 258 30300631221 5136  
 259 30300631231 5137 260 30300631241 5138 261 30300631251 5139  
 262 30300631261 5140 263 30300631271 5141 264 30300631281 5142  
 265 30300631291 5143 266 30300631301 5144 267 30300631311 5145  
 268 30300631321 5146 269 30300631331 5147 270 30300631341 5148  
 271 30300631351 5149 272 30300631361 5150 273 30300631371 5151  
 274 30300631381 5152 275 30300631391 5153 276 30300631401 5154  
 277 30300631411 5155 278 30300631421 5156 279 30300631431 5157  
 280 30300631441 5158 281 30300631451 5159 282 30300631461 5160  
 283 30300631471 5161 284 30300631481 5162 285 30300631491 5163  
 286 30300631501 5164 287 30300631511 5165 288 30300631521 5166  
 289 30300631531 5167 290 30300631541 5168 291 30300631551 5169  
 292 30300631561 5170 293 30300631571 5171 294 30300631581 5172  
 295 30300631591 5173 296 30300631601 5174 297 30300631611 5175  
 298 30300631621 5176 299 30300631631 5177 300 30300631641 5178  
 301 30300631651 5179 302 30300631661 5180 303 30300631671 5181  
 304 30300631681 5182 305 30300631691 5183 306 30300631701 5184  
 307 30300631711 5185 308 30300631721 5186 309 30300631731 5187  
 310 30300631741 5188 311 30300631751 5189 312 30300631761 5190  
 313 30300631771 5191 314 30300631781 5192 315 30300631791 5193  
 316 30300631801 5194 317 30300631811 5195 318 30300631821 5196  
 319 30300631831 5197 320 30300631841 5198 321 30300631851 5199  
 322 30300631861 5200 323 30300631871 5201 324 30300631881 5202  
 325 30300631891 5203 326 30300631901 5204 327 30300631911 5205  
 328 30300631921 5206 329 30300631931 5207 330 30300631941 5208  
 331 30300631951 5209 332 30300631961 5210 333 30300631971 5211  
 334 30300631981 5212 335 30300631991 5213 336 30300632001 5214  
 337 30300632011 5215 338 30300632021 5216 339 30300632031 5217  
 340 30300632041 5218 341 30300632051 5219 342 30300632061 5220  
 343 30300632071 5221 344 30300632081 5222 345 30300632091 5223  
 346 30300632101 5224 347 30300632111 5225 348 30300632121 5226  
 349 30300632131 5227 350 30300632141 5228 351 30300632151 5229  
 352 30300632161 5230 353 30300632171 5231 354 30300632181 5232  
 355 30300632191 5233 356 30300632201 5234 357 30300632211 5235  
 358 30300632221 5236 359 30300632231 5237 360 30300632241 5238  
 361 30300632251 5239 362 30300632261 5240 363 30300632271 5241  
 364 30300632281 5242 365 30300632291 5243 366 30300632301 5244  
 367 30300632311 5245 368 30300632321 5246 369 30300632331 5247  
 370 30300632341 5248 371 30300632351 5249 372 30300632361 5250  
 373 30300632371 5251 374 30300632381 5252 375 30300632391 5253  
 376 30300632401 5254 377 30300632411 5255 378 30300632421 5256  
 379 30300632431 5257 380 30300632441 5258 381 30300632451 5259  
 382 30300632461 5260 383 30300632471 5261 384 30300632481 5262  
 385 30300632491 5263 386 30300632501 5264 387 30300632511 5265  
 388 30300632521 5266 389 30300632531 5267 390 30300632541 5268  
 391 30300632551 5269 392 30300632561 5270 393 30300632571 5271  
 394 30300632581 5272 395 30300632591 5273 396 30300632601 5274  
 397 30300632611 5275 398 30300632621 5276 399 30300632631 5277  
 400 30300632641 5278 401 30300632651 5279 402 30300632661 5280  
 403 30300632671 5281 404 30300632681 5282 405 30300632691 5283  
 406 30300632701 5284 407 30300632711 5285 408 30300632721 5286  
 409 30300632731 5287 410 30300632741 5288 411 30300632751 5289  
 412 30300632761 5290 413 30300632771 5291 414 30300632781 5292  
 415 30300632791 5293 416 30300632801 5294 417 30300632811 5295  
 418 30300632821 5296 419 30300632831 5297 420 30300632841 5298  
 421 30300632851 5299 422 30300632861 5300 423 30300632871 5301  
 424 30300632881 5302 425 30300632891 5303 426 30300632901 5304  
 427 30300632911 5305 428 30300632921 5306 429 30300632931 5307  
 430 30300632941 5308 431 30300632951 5309 432 30300632961 5310  
 433 30300632971 5311 434 30300632981 5312 435 30300632991 5313  
 436 30300633001 5314 437 30300633011 5315 438 30300633021 5316  
 439 30300633031 5317 440 30300633041 5318 441 30300633051 5319  
 442 30300633061 5320 443 30300633071 5321 444 30300633081 5322  
 445 30300633091 5323 446 30300633101 5324 447 30300633111 5325  
 448 30300633121 5326 449 30300633131 5327 450 30300633141 5328  
 451 30300633151 5329 452 30300633161 5330 453 30300633171 5331  
 454 30300633181 5332 455 30300633191 5333 456 30300633201 5334  
 457 30300633211 5335 458 30300633221 5336 459 30300633231 5337  
 460 30300633241 5338 461 30300633251 5339 462 30300633261 5340  
 463 30300633271 5341 464 30300633281 5342 465 30300633291 5343  
 466 30300633301 5344 467 30300633311 5345 468 30300633321 5346  
 469 30300633331 5347 470 30300633341 5348 471 30300633351 5349  
 472 30300633361 5350 473 30300633371 5351 474 30300633381 5352  
 475 30300633391 5353 476 30300633401 5354 477 30300633411 5355  
 478 30300633421 5356 479 30300633431 5357 480 30300633441 5358  
 481 30300633451 5359 482 30300633461 5360 483 30300633471 5361  
 484 30300633481 5362 485 30300633491 5363 486 30300633501 5364  
 487 30300633511 5365 488 30300633521 5366 489 30300633531 5367  
 490 30300633541 5368 491 30300633551 5369 492 30300633561 5370  
 493 30300633571 5371 494 30300633581 5372 495 30300633591 5373  
 496 30300633601 5374 497 30300633611 5375 498 30300633621 5376  
 499 30300633631 5377 500 30300633641 5378

420	34135629737	4898	426	30465629791	4903	427	611506299607	5010
421	511500629559	5012	425	511875299459	4993	428	611506299399	5046
422	511500629559	4925	429	98200629244	4907	429	611506299135	4863
423	46326296045	4840	430	522220629046	4813	431	611506299135	4782
424	46326296045	4751	431	522220629046	4813	432	611506299135	4720
425	46326296045	4711	432	522220629046	4702	433	611506299135	5297
426	99300630159	5623	433	522220629046	5390	434	611506299135	5521
427	99300630159	5618	434	522220629046	5390	435	611506299135	5690
428	11570629947	5932	435	522220629046	5759	436	611506299135	5933
429	3300630089	6039	436	522220629046	6042	437	611506299135	6000
430	3300630089	6039	437	522220629046	6152	438	611506299135	6000
431	3300630089	6039	438	522220629046	6152	439	611506299135	6405
432	3300630089	6039	439	522220629046	6254	440	611506299135	6428
433	3300630089	6039	440	522220629046	6254	441	611506299135	6428
434	3300630089	6039	441	522220629046	6254	442	611506299135	6428
435	3300630089	6039	442	522220629046	6254	443	611506299135	6428
436	3300630089	6039	443	522220629046	6254	444	611506299135	6428
437	3300630089	6039	444	522220629046	6254	445	611506299135	6428
438	3300630089	6039	445	522220629046	6254	446	611506299135	6428
439	3300630089	6039	446	522220629046	6254	447	611506299135	6428
440	3300630089	6039	447	522220629046	6254	448	611506299135	6428
441	3300630089	6039	448	522220629046	6254	449	611506299135	6428
442	3300630089	6039	449	522220629046	6254	450	611506299135	6428
443	3300630089	6039	450	522220629046	6254	451	611506299135	6428
444	3300630089	6039	451	522220629046	6254	452	611506299135	6428
445	3300630089	6039	452	522220629046	6254	453	611506299135	6428
446	3300630089	6039	453	522220629046	6254	454	611506299135	6428
447	3300630089	6039	454	522220629046	6254	455	611506299135	6428
448	3300630089	6039	455	522220629046	6254	456	611506299135	6428
449	3300630089	6039	456	522220629046	6254	457	611506299135	6428
450	3300630089	6039	457	522220629046	6254	458	611506299135	6428





757	30180627678	2640	758	30180627694	2595	759	30180627873	2559	760	20180627899	2491
1	501307-275	-0	6	751007-192	3549	7	300907 944	4	4120	20180627907	3397
5	20757-398	4037	10	407-284	3281	11	172407 1084	8	0	607 454	3895
12	7207 1006	3746	14	72507 1274	3800	15	102507 1590	12	7	2407 833	3663
17	7607 2221	3645	18	102507 2306	3512	19	7607 1915	20	102307 1501	7607 2691	3100
21	102307 3112	3130	22	102307 3404	3149	23	221807 2934	24	101007 1850	1850 4026	4026
25	61007 1622	4175	26	152907 1572	4114	27	201807 3711	28	171807 2850	2850 2736	2736
29	121807 3948	2080	30	1092507 4063	1949	31	301807 4212	32	201807 4362	4362 1314	1314
31	10010923177	2004	32	5010925004	2001	33	90185924523	34	50185924310	310 3102	3102
35	75195923377	3554	36	75165924050	3201	37	75135923513	38	75105924624	624 2013	2013
39	90240923568	4002	40	90240923305	4007	41	651370023027	42	60270022017	2017 5377	5377
43	6517923325	4008	44	75217923303	3602	45	70233323033	46	70235922551	2551 5279	5279
47	651832423	2008	48	50105924014	2017	49	50125923617	50	50165923422	3422 3960	3960
51	50195923228	3706	52	50179229276	2452	53	50133323024	54	50165922848	2848 3433	3433
55	50175923462	2404	56	50105923229	2452	57	30133323024	58	30165922848	2848 3433	3433
59	50195922644	2713	60	30225522282	2459	61	30165922313	62	30195922653	2653 2797	2797
63	15105922653	2817	64	151335922463	3276	65	10165922313	66	10195922118	2118 3100	3100
67	1510922578	1967									

APPENDIX IX

DEFORMATION DUE TO THE N=1 TERM

Equilibrium of an isotropic elastic solid requires that: (Symbols are those of Caputo [1961])

$$\gamma_{ij,j} = -F_i \quad (1)$$

in the interior of the medium and on the surface bounding the medium:

$$\gamma_{ij} v_j = T_i \quad (2)$$

The stress-strain relation is:

$$\gamma_{ij} = \lambda \delta_{ij} v + 2\mu e_{ij} \quad (3)$$

where  $v = e_{ii}$  is the dilatation or the divergence of the displacement vector,  $e_{ij}$  is the strain. Vanishing of the moments of external forces on the body requires  $\gamma_{ij} = \gamma_{ji}$ .

The displacement  $u_j$  is determined by:

$$u_{i,j} + u_{j,i} = 2e_{ij}$$

Equation 3 can be written also in the form:

$$\gamma_{ij} = \lambda \delta_{ij} u_{k,k} + \mu (u_{i,j} + u_{j,i}) \quad (4)$$

Substituting this equation (1) for the stress gives:

$$\mu u_{i,jj} + (\lambda + \mu) u_{j,ji} + F_i = 0 \quad (5)$$

which can also be written:

$$(\lambda + 2\mu) \text{grad div } u - \mu \text{curl curl } u + F_i = 0 \quad (6)$$

The solution to this equation is found by first finding a particular integral of (6), adding to it the complimentary function of equation (6) with  $F_i = 0$ , then adjusting the arbitrary constants available so that the prescribed boundary conditions are satisfied. (Love, 1892, p 252-253).

Deformation due to mass loading represented by the  $n=1$  term can be found using Caputo's (1961) equations as follows: A particular integral of equation 1 is given by Love (1927) (p253) for a body force which is the gradient of a potential  $V_n$ . Thus a particular integral can be found for each shell. For each shell this particular integral can be added to the complementary function for the same shell and the sum used in Caputo's equations 5 and 6 (and the equations derived from them) to determine the arbitrary constants.

In the special case  $n=1$ , and assuming the single shell case  $m=1$ ,  $A_2$  and  $A_4$  in Caputo's equation 3 must be zero and therefore there are only two arbitrary constants;  $A_1$  and  $A_3$ . When equations 3 are substituted in equations 8 the coefficient of  $A_3$  turns out to be zero and thus we can put  $A_3=0$ . ( $A_3$  corresponds to translation of the earth as a whole). The stresses due to this complementary function now are:

$$P_{rr}(s) = 6\mu r A_1 \cos\theta [1 + (\lambda/\mu) - (\lambda T/2\mu)]$$

$$P_{r\theta}(s) = -\mu A_1 (3/2) r \sin\theta [1+T]$$

where  $T = (2\gamma+3)/(\gamma-1)$  and  $\gamma = \lambda/\mu$

The surface stress due to a uniform pressure  $P_0$  ( $f_r = -P_0$ ) throughout the cap whose semi-angle is  $\omega$  is given by:

$$f_r = \Sigma (P_{n+1}(\cos\omega) - P_{n-1}(\cos\omega)) P_n \cos\theta (P_0/2) - (P_0/2)(1-\cos\omega)$$

thus  $f_{r1} = -(3/4) P_0 \sin^2 \cos\theta$

Finding the potential due to this mass distribution ( $P_0/g$ ) (eqn 20) and substituting the particular integral (eqn. 21)

we obtain:

$$P_{rr}(s) = C_1 r \cos\theta [-(6\mu/5) - \lambda]$$

$$P_{r\theta}(s) = (2/5)\mu C_1 r \sin\theta$$

where  $C_1 = (K\pi d P, \sin^2\omega) / (\lambda + 2\mu) g$

adding the stresses due to both the particular integral and the complementary function and equating to the boundary conditions we obtain:

$$A_1 = 4 C_1 / 15 (1+T)$$

and thus the displacement is: (from Caputo's equations 1 and 2)

$$U_{r1} = -(3aP, \sin^2\omega \cos\theta) / (8\mu(3\gamma+2))$$

Converting to Longman's dimensionless form-  $[u/(am'/m)]$  yields:

$$U_{r1} = -(3g^2 \cos\theta) / [8K\pi\mu(3\gamma+2)]$$

For  $\mu = 1.86 \times 10^{12}$  and  $\gamma = 1.27$  this becomes:

$$U_{r1} = -.159 \cos\theta$$

I have also obtained a solution for the case  $n=1$  assuming an earth consisting of an outer shell enclosing a fluid core. The result for this case is:

$$U_{r1} = -.157 \cos\theta$$

## REFERENCES

- AKSENTIEVA, Z.A., A.E. OSTROVSKII and P.S. MATVEYEV, 1969. Inclinaisons de la surface de la Terre d'apres les observations faites en Union Sovietique de 1957 a 1967. Rapports - Symposium International de Leningrad 1968 Comite de Geophy. d'URSS Moscou, 1969. Trans. to French in: Marees Terrestres Bulletin d'Informations No 55, Assoc. Inter. de Geodesie, Commission Permanente des Marees Terrestres.
- ALSOP, L.E., and J.T. KUO, 1964, The characteristic numbers of semidiurnal earth tidal components for various earth models. Ann. Geophys. 20, 286-300.
- ALTERMAN, Z., H. JAROSCH and C.L. PEKERIS, 1961, Propagation of Rayleigh waves in the earth. Geophys. J., 4 (The Earth Today), 219-241.
- BEAUMONT, C., 1971, Private communication.
- BENDAT, J.S., 1966, Measurement and Analysis of Random Data. Wiley.
- BLUM, P.A., 1969. Etude de la Maree d'Inclinaison dans une station situee au centre du Sahara - Resultats Preliminaires. Sixieme Symposium International sur les Marees Terrestres, Strasbourg 1969. Comm. Serie A, 9, Serie Geophysique 96, Observatoire Royal de Belgique.
- BOGDANOV, C.T., 1962<sup>1</sup>, The tides of the Pacific Ocean. Akademia Nauk SSSR, Trudy Institute Okeanologii, LX.
- BOGDANOV, C.T., 1964, Numerical solution of tide hydrodynamic equations by means of BESM-2 electronic computer for the Pacific area, Akademia Nauk SSSR, Trudy Institute

Okeanologii, 75.

BONCHKORSKIY, V.F. and A.N. SKUR'YAT, 1961, The level variometer. Bull. (Izv) Acad. Sci. USSR, Geophys Ser., No. 1.

BOTT, M.H.P., 1963, Two methods applicable to computers for evaluating magnetic anomalies due to finite three dimensional bodies. Geophysical Prospecting, XI, No. 3. 292-299.

BROWN, I.C., 1968, Groundwater geology, Chapter XIII of Geology and Economic Minerals of Canada, Dept. of Energy, Mines and Resources, Canada.

BÜRMISTER, D.M., 1956, Stress and displacement characteristics of a two-layer rigid base soil system: influence diagrams and practical applications. Proc. of the 35th annual meeting of the Highway Research Board, Washington D.C.

CAPUTO, M., 1961, Deformation of a layered earth by an axially symmetric surface mass distribution. J. Geophys. Res., 66, 5. 1479-1483.

CARTWRIGHT, D.C., 1965, A unified analysis of tides and surges round north and east Britain. Phil. Trans. Roy. Soc. Lon, Series A Math and Physical Sciences, No. 1134, vol 263, 1-55.

DEFANT, A., 1961, Physical Oceanography Vol II, Pergamon Press.

DIETRICH, P., 1944, Die schwingungssysteme der half und eintagigen tiden in den ozeanen, Veroeffentl. Inst.

Meersforsch. Univ. Berlin, A, 41, 1.

DOODSON, A.T., 1922, The harmonic development of the tide-generating potential. Proc. Roy. Soc. Lon. A 100, 305-329.

EATON, J.P., 1959, A portable water-tube tiltmeter. Bull. Seis. Soc. Amer. 49, 4, 301-316.

EMERY, K.O., and E. UCHUPI, 1971, Atlantic Continental Margin of North America, Unpublished manuscript. (In preparation for a book to be published in 1971)

ETO, T., 1966, A recording water-tube tiltmeter, Bull. Disaster Prevention Res. Inst., Vol 15, Part 3, No. 98.

HANSEN, W., 1969, The ocean tide of the N. Atlantic. Mitteilungen des Institute fur Meereskunde der Universitat Hamburg.

HARRISON, J-C | N.F. NESS, I.M. LONGMAN, R.F.S FORBES, E.A. KRAUT and L.B. SLICHTER, 1963, Earth-tide observations made during the international geophysical year, Jour. Geophys. Res., 68, 5.1497-1516.

JEFF<sup>REYS</sup>~~RIES~~, H., 1962, The Earth, 4th Edition Cambridge Univ. Press.

KUO, J.T., and R.C.JACHENS, 1970, Transcontinental tidal gravity profile across the united states, Science, 168, 968-971.

KUO, J.T., and M. EWING, 1966, Spatial variations of tidal gravity in 'The Earth Beneath the Continents, Geophysical Mono No. 10, Am. Geophys. Union.

LAMBERT, A., 1970, The response of the earth to loading by

the ocean tides round Nova Scotia, Geophys. J.R. astr. Soc, 19, 449-477.

LANDAU AND LIFSHITZ, 1959, Fluid Mechanics, Vol 6 of a Course in Theoretical Physics, Pergamon Press, (p303 sound, p236 capillary).

LENNON, G.W., 1964, The deviation of the vertical at Bidston in response to the attraction of the ocean tides, Geophys. J. R. astr. Soc., 6.

LENNON, G.W., and VANICEK, P., 1969, Calibration tests and the comparative performance of horizontal pendulums at a single station. 6th Symposium Int. sur les Marees Terrestres, Observatoire Royal de Belgique, Comm. Serie A No. 9, Serie Geophysique No. 96.

LECOLAZET, R., 1959, Sur l'estimation des erreurs internes affectant les resultats d'une analyse harmonique mensuelle. B.I.M., No. 17, 269-278.

LONGMAN, I.M., 1962, A Green's function for determining the deformation of the earth under surface mass loads, Part I, J. Geophys. Res., 67, 845.

LONGMAN, I.M., 1963, A Green's function for determining the deformation of the earth under surface mass loads, Part II, J. Geophys. Res., 68, 485-496.

LONGMAN, I.M., 1959, Formulas for computing the tidal accelerations due to Moon and the Sun. J. Geophys. Res., 64, 2351-2355.

MELCHIOR, P.J., 1965, The Earth Tides, Pergamon Press (1966).



MELCHIOR, P.J., 1967, Oceanic tidal loads and regional heterogeneity in Western Europe, *Geophys. J. R. astr. Soc.*, 14, 239-244.

MELCHIOR, P.J., and BROUET, J., 1964, Sur les diverses perturbations dans l'enregistrement des marees terrestres, Cinquieme Symposium International sur les marees terrestres. Observatoire Royal de Belgique Communications No 236, Serie Geophysique No 69.

MICHELSON, A.A., and H.G. GALE, 1919, The rigidity of the earth, *Astroph. Jour.* 50, 330-345.

MUNK, W.H., and D.E. CARTWRIGHT, 1966, Tidal spectroscopy and prediction. *Phil. Trans. Roy. Soc. Long.*, a, 259, Nol 1105, 533-581.

MUNK, W.H., and HASSELMAN, K., 1964, Super-resolution of tides, *Studies on Oceanography*, 339-344.

MUNK, W.H., F. SNODGRASS, and M. WIMBUSH, 1970, Tides off-shore: transition from California coastal to deep-sea waters. *Geophysical Fluid Dynamics*, Vol 1, No. 1 and 2, 1-272.

MUNK, W.H., and G.J.F MACDONALD, 1960, *The Rotation of the Earth*. Univ. Press.

MURRAY, M.T., 1964, A general method for the analysis of hourly heights of tide. Vol XLI, No 2. *International Hydrographic Review*. 91-101.

MURRAY, M.T., 1965, Optimisation processes in tidal analysis. *International Hydrographic Review*, Vol XLII, No 1. 73-81.

- NISHIMURA, E., 1950, On earth tides, Am. Geophys. Union. Trans., 31, 357-376.
- PERTSEV, B.P., 1966, On the effect of ocean tides on tidal variations of gravity. Izv. Solid Earth Physics, English Transl, 10, 25-29.
- POULOS, H.G., 1961, Stresses and displacements in an elastic layer underlain by a rough rigid base. Geotechnique, 17, 378-410.
- SCHEEL, G., 1956, Systematische fehler des hydrostatischen nivellements und verfahren zu ihrer ausschaltung. German Geodetic Commission at the Bavarian Academy of Science, Series B: Applied Geodesy Paper No 27.
- SLICHTER, L.B., and M. CAPUTO, 1960, Deformation of an earth model by surface pressures, Jour. Geophys. Res. Vol 65, No 12. 4151-4156.
- SOKOLNIKOFF, I.S., 1956, Mathematical theory of elasticity, McGraw-Hill Publishing Co, 2nd Edition.
- TAKEUCHI, H., 1950, On the earth tide of the compressible earth of variable density and elasticity, Am. Geophys. Un. Trans., 31, 651.
- TIRON, K.D., SERGEEV, Y.N. and A.N. MICHURIN, 1967, Tidal charts of the Pacific, Atlantic and Indian Oceans. Vestnik of Leningrad University, 24, 122-135.
- TOMASCHEK, R., 1953, Non-elastic tilt of the earth's crust due to meteorological pressure distributions, Geofis. pura appl., 25, 17-25.
- UNEO, T., 1964, Theoretical studies on tidal waves

travelling over the rotating globe. The Oceanographical Magazine. Vol 16, No 1-2.

VENEDIKOV, A.P., 1966, Une methode pour l'analyse des marees terrestres a partir d'enregistrements de longueur arbitraire. Marees terrestres bulletin d'informations No. 43. (Assoc. International de Geodesie)

VERBAANDERT, J. and MELCHIOR, P., 1958, Cōnstruction et etalonnage d'un pendule horizontal end quartz. Comm. Obs. Roy. Belg., No 142. S. Geophy., No 47, 114-115.

VERBAANDERT, J., 1959, Etalonnage des pendules horizontaux par crapaudine dilatible etudiee interferometriquement, III'eme Symp. Marees Terr., 81-90, Trieste.

ZIENKIEWICZ, D.C., 1968, The finite element in structural and continuum mechanics McGraw-Hill Publishing Co.

